Characterization of *cis*- and *trans*-acting Elements involved in Ribosome Biogenesis in Archaea

DISSERTATION

ZUR ERLANGUNG DES
DOKTORGRADES DER NATURWISSENSCHAFTEN (DR. RER. NAT.)
DER FAKULTÄT FÜR BIOLOGIE UND VORKLINISCHE MEDIZIN
DER UNIVERSITÄT REGENSBURG

vorgelegt von

Michael Andreas Jüttner

aus Regensburg

im März 2023

Das Promotionsgesuch wurde eingereicht am **06.03.2023**

Die Arbeit wurde angeleitet von:
PD Dr. Sébastien Ferreira-Cerca

Unterschrift:

_____

Michael Jüttner

“If there is one thing the history of evolution has taught us, it’s that Life will not be contained. Life breaks free. It expands to new territories, it crashes through barriers painfully, maybe even dangerously. […] I’m simply saying that Life… finds a way.”

Jeff Goldblum; Jurassic Park 1993

- für meine Eltern -

Table of Contents

1. Abstract

The ribosome is an absolutely fascinating molecule for many reasons. To begin with, it fulfills a universally conserved function in all forms of Life on this planet: the translation of mRNAs into proteins. This universal role is also reflected in the conservation of its building blocks: the ribosomal RNAs (rRNA) and ribosomal proteins (r-protein). The huge ribonucleoparticle consists of a small (SSU) and a large (LSU) subunit. In the past decades, the information contained in the highly conserved sequence and structure of the ribosomal constituents has proven invaluable to answer evolutionary and phylogenetic questions. Archaea, for example, owe their initial recognition as an independent domain of Life next to bacteria and eukaryotes to the tedious analysis of ribosomal RNA sequences. The manufacturing process by which cells make ribosomes is called ribosome biogenesis. It is a complex and tightly controlled task which is highly demanding in terms of cellular energies and machineries. Intriguingly, besides some fundamental, shared common principles, ribosome assembly shows a remarkable variability across the domains of Life. Whereas ribosome biogenesis is relatively well characterized in bacteria and eukaryotes, we still lack a deeper knowledge how ribosomes are assembled in the archaeal domain. Strikingly, at the current state of knowledge archaea seem to combine elements of bacterial and eukaryotic ribosome biogenesis. However, to better comprehend the guiding principles of ribosome biogenesis in all domains of Life, a more detailed understanding of this major, cellular task in archaea is necessary. Therefore, the aim of this work was to characterize key *cis*- and *trans*-acting elements involved in the archaeal ribosome biogenesis pathway. The focus of these studies was on the processing of the SSU precursor rRNA and in particular on the formation of an archaea-specific circular rRNA intermediate. With the implementation of biochemical and genetic tools, these studies could demonstrate the significance of RNA *cis*-acting elements required for this circularization step. Moreover, we could identify a novel, *trans*-acting biogenesis factor in *Haloferax volcanii*. A more comprehensive Nanopore-based sequencing approach allowed us to shed light on rRNA processing pathway in three archaeal model organisms. In addition, other facets like the organization of rRNA genes, intracellular organization of the translation apparatus or the regulation of rRNA synthesis in *H. volcanii* were investigated. Conclusively, the new insights obtained in these investigations were interpreted in the context of current phylogenetic debates, like the placement of the eukaryotic lineage in the tree of Life.

2. Zusammenfassung

Das Ribosom ist aus vielen Gründen ein absolut faszinierendes Molekül. Zunächst erfüllt es eine universell konservierte Funktion in allen, bekannten Lebensformen auf diesem Planeten: die Translation von mRNA in Proteine. Diese universelle Rolle spiegelt sich auch in der Konservierung seiner Bauteile - ribosomale RNA (rRNA) und ribosomale Proteine (r-Proteine), wider. Der riesige Ribonukleopartikel besteht aus einer kleinen (SSU) und großen (LSU) Untereinheit. In den vergangenen Jahrzehnten hat sich die Information, die in der Sequenz und Struktur der ribosomalen Bestandteile enthalten ist, als unschätzbar wertvoll erwiesen, um evolutionäre oder phylogenetische Fragen zu beantworten. Archaeen zum Beispiel, haben ihre ursprüngliche Anerkennung als eigene Domäne des Lebens neben Bakterien und Eukaryoten der mühsamen Analyse von ribosomalen RNA-Sequenzen zu verdanken. Der Herstellungsprozess von Ribosomen wird Ribosomen Biogenese genannt. Es ist eine komplexe, stark kontrollierte Aufgabe, die sehr aufwendig ist, was zelluläre Energie und Maschinerien angeht. Bemerkenswerterweise gibt es neben grundlegenden, gemeinsamen Prinzipien eine auffallende Vielfältigkeit der Ribosomen Assemblierung über alle Domänen des Lebens hinweg. Während die Ribosomen Biogenes in Bakterien und Eukaryoten relativ gut beschrieben ist, fehlt uns immer noch ein tieferes Verständnis darüber, wie Ribosomen in der archaellen Domäne assembliert werden. Zum jetzigen Stand des Wissens scheint es erstaunlicherweise so, als würden Archaeen Elemente der bakteriellen und eukaryotischen Ribosomen Biogenese kombinieren. Dennoch ist ein detaillierteres Wissen dieser wichtigen, zellulären Aufgabe in Archaeen notwendig, um die bestimmenden Prinzipien der Ribosomen Biogenese in allen Domänen des Lebens besser zu verstehen. Deshalb war das Ziel dieser Arbeit *cis*- und *trans*-agierende Schlüsselelemente der archaellen Ribosomen Biogenese zu charakterisieren. Der Fokus dieser Studie lag dabei auf der Prozessierung der SSU-Vorläufer-rRNA und im speziellen auf der Entstehung eines Archaeen-spezifischen, zirkulären Intermediates. Durch die Anwendung von biochemischen und genetischen Werkzeugen konnten die Studien die Bedeutung der *cis*-agierenden RNA-Elemente, die für diesen Zirkularisierungs-Schritt nötig sind, aufzeigen. Des Weiteren konnten wir einen neuen, *trans*-agierenden Biogenese-Faktor in *Haloferax volcanii* identifizieren. Ein umfassenderer Ansatz basierend auf Nanopore-Sequenzierung ermöglichte es den rRNA Prozessierungsweg von drei archaellen Modelorganismen zu beleuchten. Zusätzlich wurden andere Facetten wie die Organisation von rRNA-Genen, die innerzelluläre Organisation des Translationsapparats oder die Regulation der rRNA-Synthese in *H. volcanii* untersucht. Schließlich wurden die in diesen Untersuchungen neugewonnenen Erkenntnisse im Kontext aktueller, phylogenetischer Debatten, wie der Platzierung der eukaryotischen Line, interpretiert.

3. General Introduction

3.1. Archaea – where to put them?

3.1.1. The jungle of phylogenetic trees

The scientific branch of classifying and naming Life on Earth into different groups based on shared traits is called taxonomy. Phylogeny, being cognate to taxonomy, deals with the evolutionary history of species and their lines of descent and relationship (Audesirk, Audesirk, and Byers 2016). The first one, who systematically tried to establish a system of classification was Aristotle, followed by many other famous natural scientists like Carl Linnaeus or Charles Darwin. Their landmark works and legacy are still invaluable today (Paterlini 2007; Reid 2009; Lennox 2021). The progression of taxonomic classification went always hand in hand with the advancement of more sophisticated methods and technologies. Moving from the shear phenotypic characterization to microscopic observations and later molecular biology tools, the tree of Life has been redecorated multiple times.

When Carl Woese, the scientific godfather of the archaeal domain, entered the stage, the current mainstream taxonomic model comprised a five-kingdoms system superseding the Linnaean two-kingdoms system. This long-standing differentiation between plants and animals was mostly made as a metabolic distinction and restricted to the macroscopic world. Yet, the discovery of the unicellular, microscopic world made possible by Antoni van Leeuwenhoek's invention of the microscope caused turmoil for the previous distinction into two kingdoms (Whittaker 1969). Accordingly, the three-kingdom system promoted by Ernst Haeckel appreciated microorganisms as separate group (Whittaker 1969; Kutschera 2016). Another important discrimination at the time was the one of prokaryotes and eukaryotes, although it focused more on the hierarchical nature of biological organization than being a phylogenetic approach (Stanier and Van Niel 1962). To overcome limitations of the Linnaean two-kingdom model or Copeland's four-kingdom model, botanist Robert Whittaker put forward a five-kingdom model in 1969 which also took into account the prokaryote-eukaryote distinction by incorporating the 'Monera' (comprising of bacteria and blue-green algae) next to fungi, animals, plants and protists into the model (Copeland 1956; Whittaker 1969; Sapp 2005). Anyhow, all the above distinctions were still based on biochemical/metabolic or cell morphological characteristics (Escobar-Zepeda, Vera-Ponce de León, and Sanchez-Flores 2015).

Thus, the methanogens analyzed by Carl Woese and George Fox in their revolutionary study were at the time seen as belonging to bacteria (Fox et al. 1977). By comparing the sequences of 16S rRNA genes of 10 methanogens with bacterial and eukaryotic organisms, the authors reported that they "appear[ed] to be only distantly related to typical bacteria" (Fox et al. 1977).

In a follow-up paper published just eight days later Woese and Fox proposed a tripartite line of descent for all life forms. They placed the archaea (originally named archaebacteria) next to bacteria and ‘urkaryotes’ (proto-eukaryotes) resulting in three separate ur-/primary-kingdoms (Carl R. Woese and Fox 1977). Soon after more genera like *Thermoplasma* and *Sulfolobus* or species like *Halobacterium halobium* were declared to belong to the archaea (Magrum, Luehrsen, and Woese 1978; C. R. Woese, Magrum, and Fox 1978). Hence, the notion of the first archaeal representatives was not restricted to methanogens exclusively, yet all of them were thriving in rather extreme environments and the whole group therefore regarded foremost as extremophilic.

Immediately, the discovery sparked even the media‘s interest and most of the scientific community learned about the novel findings from their newspapers (Times 1977; Wolfe 2014). Unfortunately for Woese and co-workers, the first reception within the scientific community was not at all a good one. Woese and his collaborators were debated and attacked, not always in a professional manner by renowned opponents like evolutionary biologist Ernst Mayr or Nobel laureate Salvador Luria (Mayr 1998; Wolfe 2014).

A few years later, James Lake, one of the greatest detractors of Woese, championed the so-called ‘eocyte’ hypothesis. Based on the structural comparison of small and large ribosomal subunits and other data points, Lake and colleges proposed an additional fourth kingdom, the eocytes, next to bacteria, archaea and eukaryotes (Lake et al. 1984). The eocytes comprised thermophilic, sulfur-metabolizing species mostly from the TACK-superphylum. Originally, the TACK superphylum included Thaumarchaeota, Aigarchaeota, Crenarchaeota and Korarchaeota (Guy and Ettema 2011). In the past ten years, the TACK superphylum has been updated by adding more archaeal phyla and renaming others (Castelle and Banfield 2018; De Anda et al. 2021). The halobacteria and methanogens, nowadays part of the ‘Euryarchaeota’ phylum, were categorized as archaea in Lake’s tree (see phylogenetic tree, figure 1 B & 1 C) (Lake 1988). The observed closer relationship between eukaryotes and eocytes led to the proposition of a two domains (2D-) model for the tree of life (Lake et al. 1984). In a follow-up article James Lake even suggested the terms ‘parkaryotes’ (eubacteria & archaeabacteria) and ‘karyotes’ (eocytes & eukaryotes) to obtain two monophyletic superphyla within his 2D-model (Lake 1988). Further evidence for the closer relationship of eocytes and eukaryotes was found in similarities of the translation elongation factor EF-α (Rivera and Lake 1992). However, also Lake’s model faced substantial opposition and after all the 3D-model (see below, see figure 1 A) by Fox & Woese came to be more widely accepted (Gouy and Li 1989; Hasegawa et al. 1990).

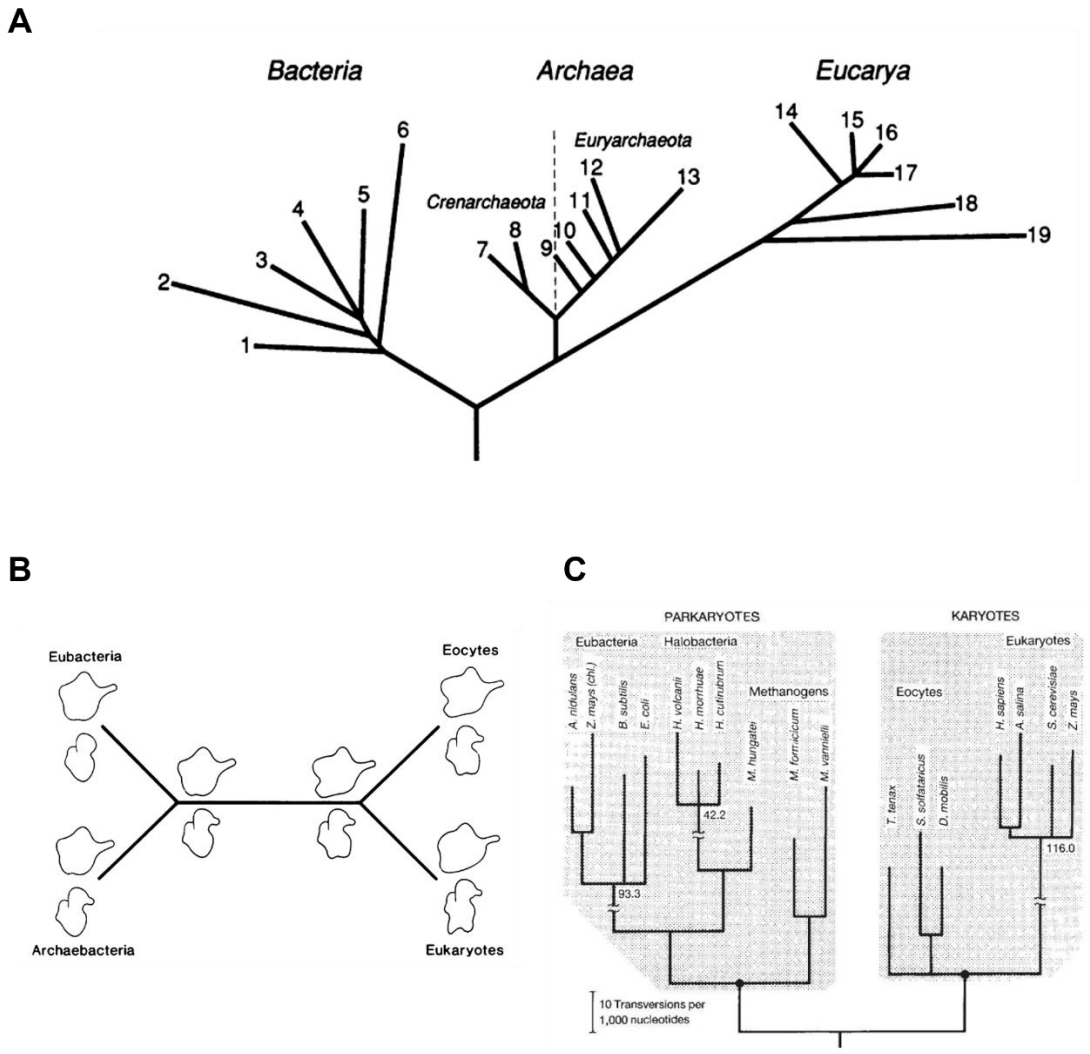

Figure 1: Early 2D and 3D phylogenetic trees. (**A**) Universal phylogenetic tree proposed by Woese and colleagues with three domains (3D) bacteria, archaea and eucarya (C R Woese, Kandler, and Wheelis 1990). (**B**) Universal phylogenetic tree proposed by James Lake and colleagues based on structural similarities of ribosomal subunits. In this tree (2D) eubacteria and archaeabacteria share one line of descent, 'eocytes' and eukaryotes another common line of descent (Lake et al. 1984). (**C**) Universal phylogenetic tree (2D) proposed by James Lake with a separation of two main groups 'parkaryotes' and 'karyotes' (Lake 1988).

Woese's theory and the step-by-step recognition and acceptance of the archaeal kingdom was tremendously facilitated by early pioneers of the field like Wolfram Zillig, Karl Stetter or Otto Kandler. Working on different research topics they all added crucial molecular evidence to the growing body of knowledge. Zillig's group investigated the RNA polymerases of *Halobacterium halobium* and *Sulfolobus acidocaldarius* noticing a lack of analogy regarding subunit composition with the *E. coli* enzyme or from other bacteria. They also observed an *in vitro* resistance to polymerase inhibitors like Rifampicin or Streptolydigin, which usually both block bacterial RNA polymerases (Zillig, Stetter, and Tobien 1978; Zillig, Stetter, and Janeković 1979). Furthermore, immunochemical studies revealed a compositional similarity of the

archaeal RNA polymerases when matched with the eukaryotic RNA polymerases I and II indicating a closer phylogenetic relationship of these two urkingdoms (Huet et al. 1983).

Prior to Woese's first study on the 'archaeabacteria', Otto Kandler had already noted that the cell wall chemistry of two methanogens differed strongly from the typical bacterial cell wall, and was similar to what was reported for *Halococcus* (R. Reistad 1972; Ragnhild Reistad 1975; Otto Kandler and Hippe 1977). In contrast to nearly all bacteria, archaea seemed to lack murein (peptidoglycan) but most possessed cellular envelopes with glycoprotein subunits (O. Kandler 1995).

Karl O. Stetter, another early believer in the 'archaebacteria' was one of the driving forces in the description and cultivation of new archaeal, mostly hyperthermophilic species, which made further studies on their biology tangible (Karl O. Stetter 2006). With the discovery of the novel genera *Pyrodictium* and *Pyrococcus*, Life beyond even 100 °C was shown to be a possibility (Karl O. Stetter 1982; K. O. Stetter, König, and Stackebrandt 1983; Fiala and Stetter 1986).

With the help of these three scientists (and of course others), more and more arguments supporting Carl Woese's idea were piling up. This finally led in 1990 to the proposal of a new phylogenetic system (see figure 1 A) separating the living world in three different domains concomitantly defining 'domain' as new and the highest taxonomic level above kingdoms (C R Woese, Kandler, and Wheelis 1990).

At the time, archaea had been widely acknowledged as a stand-alone domain in the scientific community. However, phylogenetic trees never seem to rest for long, consequently they did not happily live ever after from here on. Back in the day dissenting voices, even though less pronounced did not completely fell silent and especially in recent years, strong debates erupted anew.

3.1.2. New kids on the block – troublemaking Asgardarchaeota

„Every mythology needs a good trickster, and there are few better than the Norse god Loki. He stirs trouble and insults other gods. He is elusive, anarchic and ambiguous. He is, in other words, the perfect namesake for a group of microbes — the Lokiarchaeota — that is rewriting a fundamental story about life's early roots" (Watson 2019). Beautifully put by Traci Watson, this metaphoric description of the Asgardarchaeota's role in modern phylogeny hits the nail perfectly on the head. But what exactly accounts for the explosive potential of the Asgards in the scientific debates?

The discussion is almost as old as the scientific discovery of the archaea. As described in more detail above, the introduction of the archaea as an independent domain of life by Fox and Woese resulted over the years in establishing the widely accepted three domains of life (3D-) model, admittedly not without controversy.

Until the advent of metagenome analysis and new sequencing technologies started to fuel the old debate afresh. For a long time, the investigation of microbial life forms depended heavily on the sometimes-challenging cultivation under laboratory conditions (N. R. Pace 1997; Escobar-Zepeda, Vera-Ponce de León, and Sanchez-Flores 2015). Then, technical improvements allowed first tedious approaches cloning 16S rRNA derived cDNA or isolated DNA fragments into vectors and later whole genome shotgun sequencing which enabled the employment of many more genes as phylogenetic markers (Norman R. Pace et al. 1986; C R Woese, Kandler, and Wheelis 1990; Stein et al. 1996; J. Handelsman et al. 1998; Jo Handelsman 2004; Parks et al. 2018). The possibility to identify all kinds of bacterial and archaeal species in natural environments without the need of cultivation unraveled an unrecognized microbial diversity and the number of available bacterial and archaeal genomes skyrocketed to an unknown magnitude (Barns et al. 1994; Sunagawa et al. 2015; Almeida et al. 2019; Pasolli et al. 2019; Kolter 2021). Thus, it was also possible to speculate about the metabolic potential and many other molecular processes within these Life forms without cultivating them (Adam et al. 2017). The affluence of genomic information about uncultured microorganisms was soon deployed in phylogenetics and resurrected James Lake's eocytes.

Conceptually, an archaeon was suggested to have provided the host cell for a bacterial symbiont which then became the endosymbiont in the most prominent 'eukaryogenesis' scenario. As early as 1883 Andreas Schimper mentioned in a footnote, that plastids in plants might resemble a symbiotic relationship and originate from another organism (Schimper 1883). In the 1950s and 1960s studies provided evidence for a prokaryotic origin of chloroplasts and mitochondria and the presence of extranuclear DNA in eukaryotes (Archibald 2015). Piecing the body of information together Lynn Margulis (Sagan) famously formulated the 'endosymbiotic theory', suggesting a series of endosymbiosis events with free-living cells which would have evolved into chloroplasts or mitochondria (Sagan 1967). The idea that the eukaryotic ancestor might have been the consequence of an archaeal host cell engulfing a bacterial cell was put out early on, but immediately scrutinized by Woese himself (Van Valen and Maiorana 1980; Carl R. Woese and Gupta 1981).

For some time, an origin of the eukaryotic lineage within the Crenarcheota, then the TACK superphylum was discussed, but there were still too many missing links in the prokaryote-eukaryote transition to fully accommodate this idea (Cox et al. 2008; Foster, Cox, and Embley

2009; T. A. Williams et al. 2012; Martijn and Ettema 2013; Guy, Saw, and Ettema 2014; Koonin and Yutin 2014). The huge gap between the eocytes and eukaryotes from a molecular and cell biology perspective could not be bridged satisfyingly (Archibald 2008). For instance, the 'lipid divide', the existence of different types of phospholipids in archaeal and eukaryotic membranes, could not be reconciled at the time (see discussion in chapter 4) (Watson 2019). Anyhow, this hypothesis got more and more popularity. For instance, the very elegant inside-out model centers around the idea that cellular protrusions of an eocyte host could have facilitated the engulfment of a bacterial symbiont. Over time the inward directed protrusions would have formed cytoplasmic organelles of modern-day eukaryotes (Baum and Baum 2014).

As a short parenthesis, Hartman & Fedorov presented a list of 347 so called eukaryotic signature proteins (ESPs), at the time exclusively found in eukaryotes. The ESPs were assigned to functional categories associated with cytoskeleton, ribosome biology, vesicle trafficking or intracellular signaling pathways. Furthermore, the authors put emphasis on characteristics of the endosymbiotic host cell, which was likely not bacterial and must have had actin- and tubulin-based cytoskeleton with an extensive membrane system (Hartman and Fedorov 2002). Surprisingly, some of these signature proteins, like actin and tubulin, were also seen in members of the TACK superphylum, leading back to Lake's eocytes (Ettema, Lindås, and Bernander 2011; Yutin and Koonin 2012).

Then, in 2015 a phylogenetic analysis from Sweden introduced a novel clade of archaea termed 'Lokiarchaeota' after the location where they had been extracted: Loki's Castle, a field of hydrothermal vents in the Atlantic (Spang et al. 2015). Interestingly, there was a substantial number of eukaryotic signature proteins previously found across different TACK lineages united in the Lokiarchaeon's genome, including genes involved in vesicle trafficking and membrane remodeling (Spang et al. 2015). Two years later, the same group even described a whole new phylum of archaea closely related to eukaryotes. Loki-, Odin-, Heimdall- and Thorarchaeota made up the new superphylum of the Asgard archaea, named after the gods of Norse mythology (Zaremba-Niedzwiedzka et al. 2017). And with this discovery, the long standing 2D versus 3D dispute was back with full force, though this time with new advocates on both sides (Cunha et al. 2017; 2018; Da Cunha, Gaïa, and Forterre 2022; Spang et al. 2018; Nasir, Mughal, and Caetano-Anollés 2021). When in 2020, Imachi et al. reported on the first successful cultivation of a Lokiarchaeon, at least the argument that Asgards are purely the result of contaminated samples had been debilitated (Imachi et al. 2020; Albers et al. 2022). Very recently, a second successful cultivation of an Lokiarchaeon was reported (Rodrigues-Oliveira et al. 2022). In both isolated species morphological features like long membrane protrusions or actin-based cytoskeleton could now be visualized, which would support the inside-out hypothesis (Imachi et al. 2020; Rodrigues-Oliveira et al. 2022). In the few years

since the Asgard superphylum has been introduced, the number of newly described members has grown considerably (Y. Liu et al. 2021; Xie et al. 2022) .

Ending her essay Traci Watson writes: “The overall picture is still unclear. In Norse legends, Loki often sows mayhem — and then sets everything right again” (Watson 2019). Time and additional research efforts will tell if the Lokiarchaeota (and the other Asgards) can keep up with the promises of their mythological counterpart.

Although the debates about the placement of the Asgard archaea in relation to the eukaryotic lineage might currently capture most attention, additional phylogenetic debates take place among archaea afficionados. The monophyly of the DPANN cluster (originally: Diapherotrites, Parvarchaeota, Aenigmarchaeota, Nanoarchaeota & Nanohaloarchaeota) (see figure 5) or the origin of halophily are two examples of ongoing discussions in archaeal phylogeny (Rinke et al. 2013; Adam et al. 2017; Dombrowski et al. 2019; Martijn et al. 2020; Feng et al. 2021; Aouad et al. 2022). Combined, it is necessary to expand our current state of knowledge from sequence information towards a greater understanding of archaeal molecular biology to tackle these open questions. Intriguingly, the components of one particular cellular machinery have already been proven in the past to be an almost inexhaustible source of phylogenetic information. Functional aspects and especially the synthesis of this macromolecule is not studied in detail, however deeper insights about these processes might help disentangle the muddle of archaeal phylogeny.

3.2. The ribosome

The machinery mentioned above is of course the ribosome, which is an absolutely astonishing molecular complex. And this is arguably not only the case for the ribosome biogenesis enthusiast. The mere fact that numerous Nobel laurates are linked in one way or another to studying ribosomes and protein synthesis highlights this statement (Rheinberger 2004). One example from the list of celebrated scientists would be Francis Crick. In his central dogma he was the first to entertain the idea, that information travels from nucleic acid sequences to amino acid sequences (protein) in an unidirectional way (Crick 1956; 1958). The highly complex machinery that carries out protein synthesis by translating mRNAs into amino acid chains and therefore taking over a key role in Crick's dogma is the ribosome. The importance of the translation system for all forms of Life is further reflected by some of its unifying attributes greatly compiled by Loren Williams and colleges: Ubiquity (genes for translation dominate the universal gene set of Life), abundance (rRNAs & r-proteins are the most abundant biological macromolecules) or expenditure (translation consumes most cellular energy), just to name a few attributes (Bernier et al. 2018).

Grounded in its imperative function the translation apparatus is also one of the major targets for antimicrobial substances binding to the ribosome and inhibiting its function (Tenson and Mankin 2006; Wilson 2014).

Last but not least, another trademark characteristic that has been capitalized on (and still is) by many scientists over decades is the ribosome's great potential to study phylogenetic relationships. Several intriguing examples specified above in which various ribosomal features like the 16S rRNA gene, the overall structure or characteristics of r-proteins have been used, are demonstrating this (Fox et al. 1977; Lake et al. 1984; Spang et al. 2015; Zaremba-Niedzwiedzka et al. 2017). Noteworthy, research on archaea has historically been linked to ribosome biology by the work of Carl Woese and others after him.

3.2.1. Structure and function

"The ribosome […] is probably the most sophisticated machine ever made" (R. Garrett 1999).

Very briefly, protein synthesis describes the conversion of the nucleic acid code in an amino acid code by which every protein is made. Essentially, mRNAs carrying the genetic information are decoded by the ribosome, which is provided with amino acids by tRNAs and acts as the enzyme forming peptide bonds (Lodish et al. 2021).

To better comprehend Roger Garretts statement about the complexity of the translation apparatus, one has to start looking at the intricate ribosomal architecture. Moreover, the universal functionality of the ribosome in all three domains of Life is highlighted by the conservation of its building blocks (see figure 2).

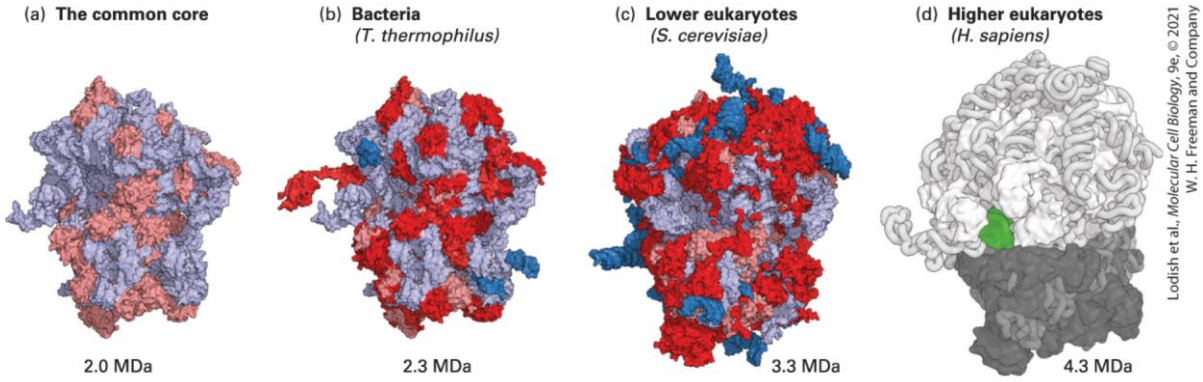

Figure 2: Comparative view on ribosome structures. (**a**) The evolutionary conserved common core of the ribosome is depicted. Ribosomal RNA is shown in light blue, r-proteins in light red. (**b** & **c**) Additions to the common core are shown in red (r-proteins) and blue (rRNA) for the ribosomes of *T. thermophilus* (bacteria) (**b**) and *S. cerevisiae* (eukaryotes) (**c**), respectively. (**d**) Cryo-EM structure of the human ribosome. One tRNA in the E site is shown in green. From: Lodish et al. 2021.

Regarding the composition, the first thing to notice is that every ribosome is a huge and highly complex ribonucleoprotein (RNP) particle divided into a small subunit (SSU) for decoding mRNAs and a larger subunit (LSU) to enable peptide bond formation (Frank 2000). It is usually composed of one-third ribosomal proteins (r-proteins) and two-thirds ribosomal RNAs (rRNAs), even though exceptions can be found for example in some mitochondrial ribosomes (Alberts et al. 2002; Deutscher 2009; Kummer and Ban 2021). Interestingly, the r-proteins occupy more of a scaffolding role, whereas the catalytic activity is provided by the rRNAs (Alberts et al. 2002). In both prokaryotes and eukaryotes, it is built around a large structurally conserved core (Melnikov et al. 2012). Strikingly, 90 % of the rRNA nucleotides which are found in this core warrant the formation of crucial functional elements like e.g. the peptidyl transferase center, the polypeptide exit tunnel, A- & E-site or the subunit interfaces (Bernier et al. 2018). As highly organized and complex structures, the ribosomal RNAs fold into distinct domains. The LSU rRNA domains one to six (I to VI) surround one central domain (0) (Petrov et al. 2013). The SSU rRNA clusters into four domains, a 5', central 3' major and 3' minor domain (Petrov et al. 2014). The secondary rRNA structures of bacteria and eukaryotes are shown in supplementary figure S4. Bacterial and archaeal ribosomes possess 16S rRNA (SSU) and 23S & 5S rRNAs (LSU) resulting in a small subunit of 30S (S=Svedberg, sedimentation coefficient) and a large subunit of 50S and in total a 70S ribosome (G. Blaha and Ivanov 2004). In eukaryotic 80S

ribosomes on the other hand rRNAs are found to be larger with 18S rRNA present in the 40S (SSU) subunit and 25S (28S in human), 5.8S and 5S in the 60S (LSU) subunit (Kressler, Linder, and de la Cruz 1999; D. L. J. Lafontaine and Tollervey 2001; Thomson, Ferreira-Cerca, and Hurt 2013; Lodish et al. 2021). Hence, archaeal rRNAs are resembling the bacterial ones regarding their length. Eukaryotic rRNAs exhibit the greatest species-specific variety but are usually longer (Bowman et al. 2020). Mostly, these size differences are caused by so called 'expansion segments' or 'variable regions' (Venema, Planta, and Raué 1998). Although occurring predominantly in eukaryotes, they are also found in bacterial 5S rRNA and in archaeal rRNAs (Tirumalai et al. 2020; Bowman et al. 2020; Stepanov and Fox 2021). The positions of archaeal expansion segments are also conserved in eukaryotic rRNAs but are excluded from functionally essential regions (Bowman et al. 2020; Penev et al. 2020). Intriguingly, it is reported, that members of the Asgard superphylum feature long expansion segment, atypically vast for archaea (Penev et al. 2020).

a

	Bacteria	Archaea	Eukarya
rDNA repeats numbers [1]	1-16	1-4	150-200 (> 1,000 in plants)
rRNAs	16S, 23S and 5S	16S, 23S and 5S	18S, 25/28S, 5.8S and 5S
rRNA expansion segments [2]	yes (uncommon)	yes (variable - only few)	yes (variable amounts and length)
ribosomal proteins [3]		33 universal r-proteins	
	≈49-59 44 ubiquitous	≈58-68 54 ubiquitous / 71 described	≈78-80 78 ubiquitous
***in vitro* reconstitution** [4]	yes	yes	no*
rRNA modifications [5]	protein-based (≈36 modif)	protein- and sRNP-based	protein- and sRNP-based
2´O-Methylation / Pseudourydilation	4/11	Sso (67/9); Hv (4/2) 7-127 C/D box sRNA	Sc (55/49); Hs (94/95)
additional "stand-alone" base modifications	≈ 20	Hv (7)/Tko (>100)	12
Ribosome biogenesis factors [6]	≈ 50	>40?	>200

b

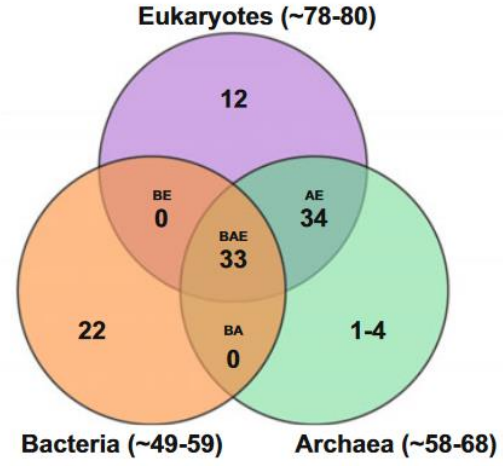

c

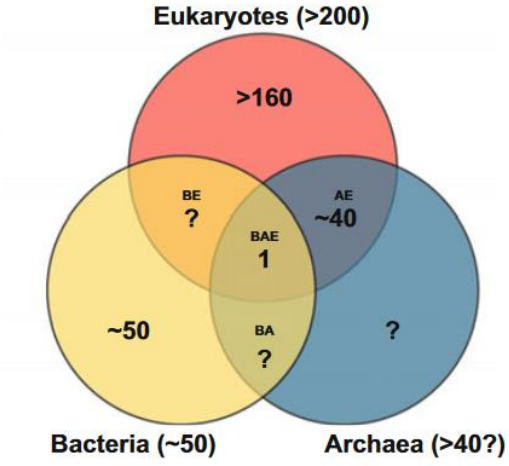

Figure 3: Key ribosome and ribosome biogenesis features in all three domains of Life. (a) Table showing key features of ribosomes and ribosome biogenesis across domains. Comparison of ribosomal proteins **(b)** and ribosome biogenesis factors **(c)** across domains. Adapted from Paola Londei and Ferreira-Cerca 2021.

Regarding the distribution of the r-protein content in the three domains, the picture looks similar. Next to a universally conserved core set of 34 r-protein families, the number of accessory r-proteins is increasing from bacteria to archaea to eukaryotes (Knud H. Nierhaus and Lafontaine 2004). Noteworthy, no r-protein is exclusively shared between bacteria and archaea or bacteria and eukaryotes, whereas a big part of r-proteins is conserved between archaea and eukaryotes besides the universally conserved core (Lecompte et al. 2002; Ferreira-Cerca 2017). These findings highlight the major split between the bacterial and archaeal/eukaryotic lineages. Thus, all archaeal r-proteins are found in the eukaryotic lineage with only a few exceptions (see figure 3 B) (Lecompte et al. 2002; Márquez et al. 2011). Therefore, it has been hypothesized, that the archaeal (and eukaryotic) ancestor possessed a more complex ribosome and some of the archaeal/eukaryotic r-proteins, but not the bacterial ones have been lost (Lecompte et al. 2002; Yutin et al. 2012). Figure 3 shows an overview of ribosome key features in all three domains of Life.

3.3. The process of ribosome biogenesis

The high structural complexity of the ribosome and its essential functional role in every cell demand themselves a highly complex, highly controlled manufacturing procedure that is known as ribosome biogenesis (see figure 4). There are a few fundamental, common principles that underlie this crucial operation in all three domains of life. The ribosomal building blocks must be manufactured, processed, and correctly assembled to obtain translation competent small and large ribosomal subunits. Ribosome biogenesis starts with the transcription of the ribosomal RNA from the rDNA locus as long precursor molecules (pre-rRNAs) and the r-proteins' mRNAs. Usually, the pre-rRNAs contain the mature rRNAs, as well as leader, trailer and internal spacers which are cleaved and trimmed by endo- and exonucleolytic enzyme activities. The rRNAs get chemically modified at different stages during the assembly process (Kaczanowska and Rydén-Aulin 2007; Shajani, Sykes, and Williamson 2011; Woolford and Baserga 2013; Thomson, Ferreira-Cerca, and Hurt 2013). The extent of modifications can vary in a domain- or species-dependent manner (Kaczanowska and Rydén-Aulin 2007; Shajani, Sykes, and Williamson 2011; Sloan et al. 2017; Paola Londei and Ferreira-Cerca 2021). Furthermore, r-proteins must be translated and correctly assembled with the rRNAs at the right place, at the right time. The whole process is facilitated by a diverse set of so-called ribosome biogenesis factors (RBFs). Noteworthy, an important distinction is the characterization of *cis*- and *trans*- acting factors, meaning acting from the same (*cis*) or a different (*trans*) molecule. These would be mainly rRNA structural elements and r-proteins (*cis*) or ribosome biogenesis factors *(trans*) which guide rRNA processing, folding and the overall ribosome assembly (Kressler, Linder, and de la Cruz 1999; Knud H. Nierhaus and Lafontaine 2004). On top of that,

production of new ribosomes must be regulated and adjusted to growth rates or lifestyles. Figure 4 shows a general blueprint of fundamental steps during ribosome assembly.

To understand the key commonalities and differences that guide this cardinal task across the domains, one must take a closer look at the main characteristics of bacterial, eukaryotic and archaeal ribosome biogenesis.

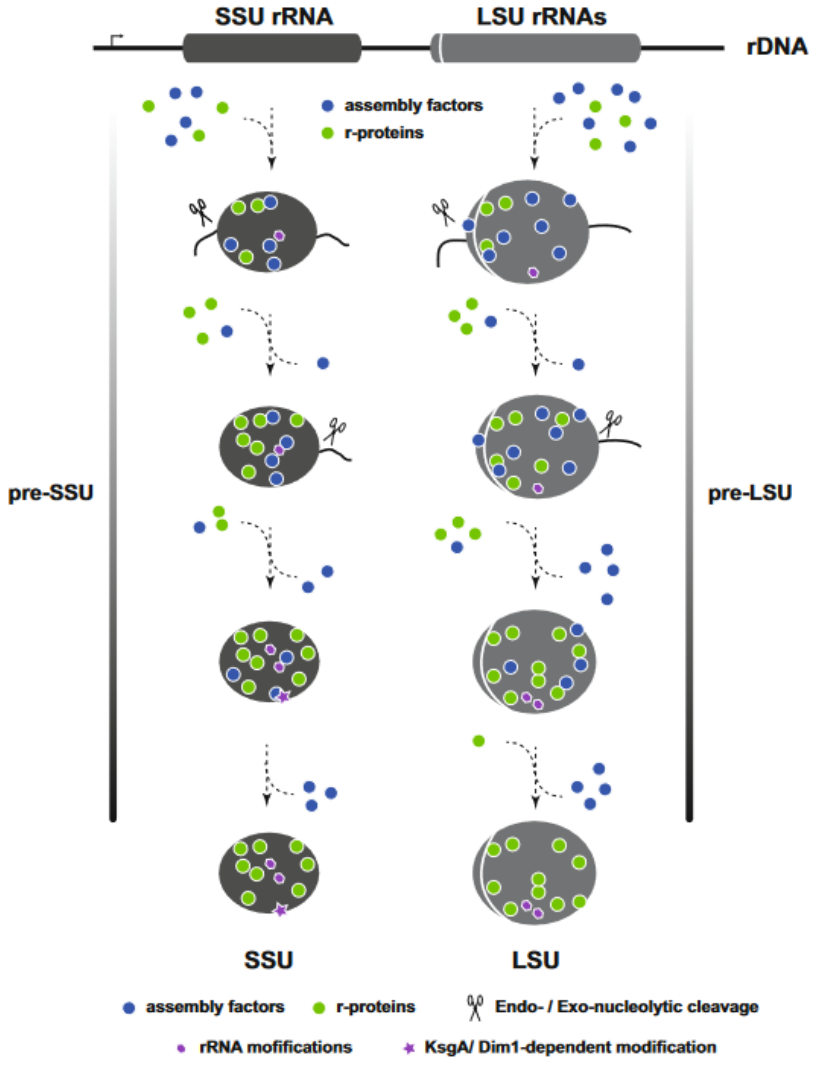

Figure 4: General blueprint of ribosome assembly. Ribosomal DNA gets transcribed, r-proteins (green) assemble to pre-rRNAs, while ribosome assembly factors (blue) and endo-/exonucleases facilitate (scissors) the maturation. Modification of rRNA (violet) are introduced by for example the only conserved ribosome biogenesis factors KsgA/Dim1 (violet star). From Ferreira-Cerca 2017.

3.3.1. Ribosome biogenesis in bacteria

Presumably, the best studied bacterial organism is *Escherichia coli*. Representing a very valuable model system it has been exploited to investigate numerous aspects of bacterial molecular and cellular biology. Accordingly, it has been the main source of knowledge regarding bacterial ribosome biogenesis as well. Many basic concepts and general understandings in the field spring from early work on bacterial ribosomes, especially from *E. coli*.

First of all, it should be noted that ribosome biogenesis is an extremely fast and efficient process. The time required to generate a mature ribosome after completion of the rRNA chain in *E. coli* was estimated to be approximately two minutes *in vivo* at 37 °C and in optimal growth conditions demonstrating the extreme efficiency of the maturation (Lindahl 1975).

One landmark achievement by Traub and Nomura was the first successful reconstitution of functionally active *E. coli* 30S subunits from purified rRNAs and r-proteins *in vitro* (Traub and Nomura 1968). The *in vitro* reconstitution of the 50S subunit in *Bacillus subtilis* or *E. coli* followed soon after (M. Nomura and Erdmann 1970; K. H. Nierhaus and Dohme 1974). The observation, that intermediary particles found *in vivo* in cold-sensitive mutant strains had a similar composition compared to the intermediates forming in the reconstitutions reinforced the experimental validity (Guthrie, Nashimoto, and Nomura 1969). Together, these masterful studies illustrated that the ribosomal building blocks, rRNAs and r-proteins, already carry the entire blueprint for the correct assembly of ribosomal subunits. Put differently, ribosomes seem to possess at least partly self-assembling properties, considerably also acting *in vivo*.

Further work on the order of ribosomal protein binding resulted in so-called assembly maps. They suggested that assembly occurs in big parts in a stepwise, cooperative and hierarchical manner, meaning that r-proteins influence each other's binding (Mizushima and Nomura 1970; Röhl and Nierhaus 1982; Herold and Nierhaus 1987). Based on these studies, r-proteins were categorized in primary (binding to rRNA), secondary (require bound primary r-proteins) and tertiary (require bound secondary r-proteins) binders (Shajani, Sykes, and Williamson 2011).

Contrarily, *in vivo* studies presented evidence questioning the strong binding hierarchies observed in reconstitution experiments. One of the first showed, that the deletion of the gene coding for S15, one of the primary SSU binders, for example, leads to a viable, although compromised, *E. coli* strain. In the mature ribosomes secondary and tertiary r-proteins, depending *in vitro* on S15 could still be detected, hence pointing to alternative maturation pathways *in vivo* circumventing the loss of S15 (Bubunenko et al. 2006). The non-essentiality of a set of bacterial r-proteins indicated as well at least some plasticity in the assembly process

in vivo, even though these non-essential r-proteins still ensure better growth and efficient assembly and translation capabilities (Dabbs 1991; Shoji et al. 2011; Shajani, Sykes, and Williamson 2011; Akanuma et al. 2012). Additional biochemical evidence further hinted to the existence of parallel assembly pathways *in vivo* (Shajani, Sykes, and Williamson 2011; Gupta and Culver 2014).

Moreover, the early reconstitution experiments showed a binding progression with a 5' to 3' polarity, indicating co-transcriptional binding of r-proteins to the nascent transcript, a so-called 'assembly gradient' (Mizushima and Nomura 1970; Herold and Nierhaus 1987; Knud H. Nierhaus and Lafontaine 2004; Kaczanowska and Rydén-Aulin 2007). This notion was supported soon after by additional biochemical evidence and the 'Miller-spreads', which visualized co-transcriptional assembly of bacterial ribosomes using electron microscopy (Miller, Hamkalo, and Thomas 1970; de Narvaez and Schaup 1979). Interestingly, the 5' domain of the 16S rRNA folds very fast independently of the presence of r-proteins *in vitro*. This indicates the early formation of a structural platform allowing the first r-proteins to bind and to enable further RNA folding progression (Adilakshmi, Ramaswamy, and Woodson 2005). State of the art single molecule tracking methods allowed to monitor co-transcriptional assembly thereby corroborating the dynamic and cooperative interplay of rRNA folding and early r-protein binding (Duss et al. 2019; Rodgers and Woodson 2019).

Although the traditional view of bacterial ribosome assembly guided by distinct RNA folding dynamics combined with cooperativity and hierarchy of r-protein binding, is still valid, researchers are yet trying to understand the particularities and details of this process. In the past years, structural biology using cryo-EM has been greatly instrumental and could provide high resolution structures of pre-ribosomal subunits (Mulder et al. 2010; Sashital et al. 2014; Davis et al. 2016; Nikolay et al. 2018; Qin et al. 2023). In this way, many aspects of the early proposed assembly characteristics could be confirmed, but also refined and updated. For instance, the idea of multiple parallel routes of assembly in bacteria *in vivo* in contrast to being strictly sequential is further supported by structural data of intermediary states (Mulder et al. 2010; Davis et al. 2016; Razi, Britton, and Ortega 2017; Qin et al. 2023).

The longer RNA molecules get, the more stable folding alternatives exist, thus rRNA intermediates can presumably get stuck in 'kinetic traps'. This is especially important for the LSU assembly, which is reflected by the more challenging 50S reconstitutions. The self-assembling potential was shown in the early *in vitro* reconstitutions; however, these experiments were performed in non-physiological conditions. Thereby, they suggested the presence of facilitating mechanisms *in vivo* and many enzymes and accessory proteins were later found to support the *in vivo* assembly process. So-called ribosome biogenesis factors

(RBFs), help to avoid kinetic traps, mediate r-protein binding and accelerate the maturation process (Davis and Williamson 2017). A few bacterial RBFs were shown to support *in vitro* the binding kinetics of r-proteins in 30S reconstitution experiments (Bunner et al. 2010). Another role might be the inhibition of pre-mature 30S or 50S subunit interaction to prevent them from entering the translational pool and form non-functional 70S ribosomes (Datta et al. 2007; Guo et al. 2011; Jeganathan et al. 2015). The multitude of ribosome biogenesis factors will not be discussed herein exhaustively. It is however noteworthy, that they comprise a great range of different types of enzymes, ranging from GTPases, RNA helicases, RNases, RNA chaperons or RNA and protein modifying enzymes (Kaczanowska and Rydén-Aulin 2007; Shajani, Sykes, and Williamson 2011; Davis and Williamson 2017). In bacteria there are around 50 of these RBFs known, but, surprisingly, many of these RBFs are also not essential and the reactions they catalyze can be bypassed (Davis and Williamson 2017; Ferreira-Cerca 2017).

In summary, the assembly of a ribosome is basically an RNA folding conundrum. It is solved and guided by r-protein binding in a partly co-transcriptional, to some extent cooperative and hierarchical manner, intrinsic (pre-)rRNA features and the activity of various ribosome biogenesis factors. The processing of the rRNA from the long primary transcripts will be introduced in chapter 5. Regulatory mechanisms, that govern the synthesis of ribosomes in bacteria are outlined in chapter 6.

Notwithstanding, the lessons learned from studying bacterial ribosome biogenesis do not automatically transfer to the much more complex eukaryotic assembly pathway, which will be introduced hereafter.

3.3.2. Ribosome biogenesis in eukaryotes

The eukaryotic equivalent to *E. coli* holding the title ‘best studied model organism’ in the ribosome biogenesis field is supposedly the yeast species *Saccharomyces cerevisiae*. Like bacteria, eukaryotic ribosome construction is a very fast and efficient process, with a huge fraction of major cellular machineries dedicated to this task (Warner 1999). Notably, eukaryotes possess one specialized RNA polymerase, RNAP I, which is exclusively dedicated to the transcription of ribosomal DNA (M. Nomura 2001; Goodfellow and Zomerdijk 2012). Yet, all three cellular RNA-polymerases are involved in the production of ribosomal building blocks. The precursors of ribosomal RNAs are transcribed by RNAP I (precursor transcript of 18S, 25/28S & 5.8S) and RNAP III (pre-5S), whereas RNAP II is engaged in the transcription of mRNAs coding for r-proteins (J. Russell and Zomerdijk 2006; David Alan Schneider 2012; Goodfellow and Zomerdijk 2012). The eukaryotic ‘Miller spreads’, snapshots of a ribosome’s

moment of birth, illustrate the earliest step that is RNAP I transcription. Those recordings even pre-date the bacterial ones (Miller and Beatty 1969).

A hallmark disparity to ribosome biogenesis in prokaryotes is found in the distinctive, eponymous cell biological feature: the eukaryotic nucleus. Eukaryotic ribosome biogenesis takes place in defined cellular compartments, as most of the subunit(s) assembly is centered in the nucleus, and especially the nucleolus, a sub-compartment of the nucleus (Woolford and Baserga 2013). Only after reaching a certain maturation stage pre-ribosomal particles get exported into the cytoplasm and undergo their finalization. On the one hand the synthesis of ribosomes is efficiently, locally concentrated, and early, immature subunits are separated from the cytoplasmic pool of translating ribosomes. Conversely, the spatial repartition of different maturation stages necessitates transport possibilities to import r-proteins and assembly factors, and export pre-ribosomes. The majority of eukaryotic r-proteins bind in the nucleus to pre-ribosomes, yet a few LSU r-proteins bind only very late during the maturation in the cytoplasm (A. K. Henras et al. 2008; Thomson, Ferreira-Cerca, and Hurt 2013; Woolford and Baserga 2013).

Other than bacterial ribosomal subunits, their eukaryotic counterparts could not be reconstituted *in* vitro so far. Only one study claims to have performed this job in *Dictyostelium discoideum*, however the reconstitution was not possible solely from ribosome components and required the nuclear/nucleolar fraction for assembly (Giorgio Mangiarotti and Chiaberge 1997). This speaks for the increased overall complexity of the ribosome and therefore more challenging assembly in eukaryotes.

Most r-proteins are essential in *S. cerevisiae* for growth, whereas in bacteria a substantial fraction is non-essential (Ferreira-Cerca et al. 2005; Pöll et al. 2009; Steffen et al. 2012; Woolford and Baserga 2013). Due to missing *in vitro* reconstitution systems, the order of r-protein association had to be deduced in ambitious *in vivo* studies (Ferreira-Cerca et al. 2005; 2007; Karbstein 2011; Gamalinda et al. 2014; de la Cruz, Karbstein, and Woolford 2015; W. Chen et al. 2017). Excitingly, the order of eukaryotic r-protein assembly *in vivo* appears to parallel the bacterial system. Systematic analyses of SSU r-proteins have shown, that all of these r-proteins are required for proper 18S rRNA production. Upon depletion of individual SSU r-proteins ribosome maturation was affected at distinct stages demonstrating a direct involvement in specific rRNA processing steps. The loss of some r-proteins led to blocking or reducing nuclear export (Ferreira-Cerca et al. 2005). Several homologues of bacterial tertiary binders were found to form a cluster and impaired the same two maturation steps (Ferreira-Cerca et al. 2005). Another commonality seems to be the 5’ to 3’ folding hierarchy of the pre-

rRNA (Anthony K. Henras et al. 2015; Kressler, Hurt, and Baßler 2017). Again, structural biology has contributed immensely to the conformation of certain paradigms by presenting many different nuclear and cytoplasmic intermediary states of pre-ribosomal particles (Kater et al. 2017; Sanghai et al. 2018; Klinge and Woolford 2019; Kater et al. 2020; Ameismeier et al. 2020; Pöll et al. 2021; Cheng et al. 2022). Consequently, interdependent binding behavior of r-proteins or sequential RNA folding can nowadays be visualized at high resolution.

The more complicated assembly is also reflected in the much higher number of ribosome biogenesis factors. Accordingly, the protein content of early yeast pre-ribosomes decreases on their way to becoming mature subunits (Trapman, Retèl, and Planta 1975). Compared to the bacterial system where protein content ever increases during ribosomal maturation, this is diametrically opposed and accentuates the crucial role of the multitude of RBFs. More than 200 proteins attend the coming-of-age tale of a eukaryotic ribosome (Woolford and Baserga 2013). The classes of participating enzymes are akin to the bacterial ones, however more numerous and spatially separated into nuclear- or cytoplasmic-acting proteins. The conservation of RBFs between bacteria and eukaryotes on the other hand is almost non-existent with the only exception of KsgA/Dim1 (Ferreira-Cerca 2017). An inhibition of translation by some eukaryotic SSU binding RBFs has also been speculated (Granneman et al. 2010). In addition, hierarchical and interdependent binding akin to r-proteins is observed for some of these RBFs, like the UTP-complexes or several 60S assembly factors (Woolford and Baserga 2013; Thomson, Ferreira-Cerca, and Hurt 2013). Another clear difference regarding bacterial and eukaryotic ribosome biogenesis is found in the rRNA modification systems. In eukaryotes rRNA modifications are carried out by snoRNP complexes, consisting of a small nucleolar RNA (snoRNA) which acts as guide and multiple proteins, with one of them carrying the enzymatic activity (Hage and Tollervey 2004). Strikingly, the lack of individual modifications has no effect on growth, the depletion of the respective associated protein however disturbs growth and ribosome biogenesis (Woolford and Baserga 2013).

These aforementioned transport requirements for r-proteins, RBFs and pre-ribosomal particles are not matched in a prokaryotic cell, yet they are also used as a quality control facility. Proteins acting as adaptors bind to and thereby label pre-40S or pre-60S particles as competent for export, thereby allowing these subunits to exit the nucleus. Accordingly, depletion of assembly factors or r-proteins can also result in export defects. There might be indirect effects of blocking export factors due to improper pre-ribosome architecture, rapid turnover of erroneous intermediates within the nucleus or alternatively the failure to recycle export factors trapped on misassembled pre-ribosomes in the cytoplasm (Woolford and Baserga 2013). Once exported to the cytoplasm, pre-mature subunits undergo rRNA rearrangements, final maturation steps

and yet missing r-proteins are incorporated. The co-exported RBFs must be released and recycled back to the nucleus. At the same time, it is key for pre-ribosomal subunits to be kept separated from the translational pool. Albeit, this becomes only relevant in the cytoplasm, the mechanism by which this is achieved is similar to bacteria as bound late assembly factors prevent translation initiation (Thomson, Ferreira-Cerca, and Hurt 2013; Woolford and Baserga 2013).

The genomic organization of eukaryotic rRNA genes will be explained in more detail in chapter 4, whereas mechanisms of rRNA processing in eukaryotes are introduced in in 5.2.

Conclusively, eukaryotic ribosome assembly still shares common principles with the bacterial pathway, like 5’ to 3’ RNA folding and stabilization, or cooperative and interactive r-protein incorporation. Likely, these shared properties reflect the intrinsic, self-assembling potential or ancestry rRNA and r-proteins. Nevertheless, the overall picture is more complex in eukaryotes with distinct localization, a specialized RNA polymerase and a great extension of the number of participating ribosome biogenesis factors. Admittedly, this differentiation, presumably after eukaryogenesis, comes with the concomitant loss of self-assembling properties which might have been still present in a proto-eukaryotic ancestor.

3.3.3. The black box - ribosome biogenesis in archaea

In stark contrast to bacteria and eukaryotes, only little of the archaeal ribosome biogenesis chart has been uncovered. Regardless, there are a few known aspects of how ribosomes are made in archaea and interestingly, this fundamental process has been described to be a blend of eukaryotic and bacterial characteristics of ribosome assembly (Ferreira-Cerca 2017; Paola Londei and Ferreira-Cerca 2021).

The nature of this mixture is already reflected in the conservation of ribosomal building blocks, as described above. To what extent do aspects of archaeal ribosome biogenesis compare to the bacterial or eukaryotic assembly process?

Functional small and large subunits from various archaeal species could be reconstituted *in vitro*. Once the conditions of their respective extremophilic lifestyle were taken into account, the assembly was feasible to generate translation competent subunits as was described for bacteria (P. Londei et al. 1986; Sánchez and Amils 1995; Emma Sanchez, Londei, and Amils 1996; Agalarov, Yusupov, and Yusupova 2016). An exciting study on 50S subunits of *Saccharolobus (*formerly *Sulfolobus*) *solfataricus* showed a set of LSU r-proteins behaving like

'primary binders'. Strikingly, the partial binding of these *Sulfolbus* LSU r-proteins to 23S rRNA from a halophilic archaeon or *E. coli*, but not yeast LSU rRNA, was possible, even though these subunits were non-functional (Altamura et al. 1991). Yet, this corroborates the common, simplified principles of prokaryotic ribosome assembly. Alternatively, this notion reminds of ancestral auto-assembly properties of proto-ribosomes that have been lost in eukaryotes through acquiring additional RBFs. Unfortunately, in depth assembly maps revealing r-protein binding hierarchies and interdependencies as present for bacteria are missing in archaea until now.

So far, there are also not many functional investigations about archaeal RBFs. At least, around forty sequence homologues of late-acting yeast RBFs have been found in archaeal genomes (Ebersberger et al. 2014). A follow-up search for orthologues within archaea implemented data from human RBFs to cover a broader eukaryotic RBF perspective. In a nutshell, orthologues of 156 eukaryotic RBFs could be found in archaeal genomes, with the highest number (67) in '*Candidatus* Prometheoarchaeum syntrophicum', the first cultivated Asgard archaeon (Birikmen et al. 2021). The great majority of these proteins awaits a detailed characterization to determine their nature as genuine, *bona-fide* ribosome biogenesis factors. However, a few candidates have been studied more extensively. One example is the almost universally conserved di-methyltransferase KsgA (in bacteria) or Dim1 (in eukaryotes). This enzyme catalyzes the di-methylation of two adjacent adenosines in helix 45 in the SSU rRNA in all three domains of life (Knüppel et al. 2021). Moreover, the methyltransferase Nep1 of *Methanocalducoccus jannaschii* was reported to have a role in 16S rRNA modification (Wurm et al. 2010). Another example would be the Rio kinase/ATPase family, which acts during the late steps of eukaryotic ribosome maturation. It was proposed that the archaeal enzymes play an analogous role and indicate that the late steps of ribosome assembly might be similar in the two domains (Knüppel et al. 2018). Noteworthy, in contrast to their yeast counterparts the archaeal Rio proteins and the archaeal KsgA/Dim1-like turned out to be non-essential for growth (D. Lafontaine et al. 1994; LaRonde-LeBlanc and Wlodawer 2005; Knüppel et al. 2018; 2021). Last but not least, the endonuclease Nob1, conserved in eukaryotes and archaea, was suggested to be involved in pre-rRNA processing in different archaeal species (Veith et al. 2012; Qi et al. 2020). For a more detailed description see chapter 5.

In archaea, rRNA modifications are carried out by stand-alone enzymes as well as by C/D box or H/ACA sRNA guided RNP complexes, thus resembling more the eukaryotic system, as these RNP complexes are absent in bacteria (Paola Londei and Ferreira-Cerca 2021; Czekay and Kothe 2021). The number of rRNA modifications varies greatly among archaeal species. For example, *Haloferax volcanii* shows only very few tRNA and rRNA modifications compared to bacteria or other archaeal species (Grosjean et al. 2008). Conversely, thermophilic and

hyperthermophilic archaea seem to be hypermodified with many C/D box sRNAs encoded genomic (Patrick P. Dennis et al. 2015; Breuer, Gomes-Filho, and Randau 2021). Nevertheless, in average archaea possess less RNA modifications than eukaryotes and accordingly fewer small guide RNAs are found (Ferreira-Cerca 2017).

Several other principles of archaeal ribosome biogenesis like rRNA genes organization, the processing of ribosomal RNA or the regulation of ribosome synthesis will be introduced in the chapters 4, 5 and 6.

In summary, as many other aspects of ribosome synthesis in archaea the regulatory mechanism governing the cell's need for ribosomes and enabling adaptations to environmental changes have to be illuminated.

3.4. Goals of this work

Historically, a strong bond originally forged by Carl Woese ties the discovery of the archaeal domain and ribosome biology perennially together. Afterwards, many others have further corroborated this entanglement with their invaluable work. To this day, there are ongoing, phylogenetic discussions where to put archaea as a domain in the phylogenetic tree or how individual subgroups should be placed in relation to each other.

The ribosome has proven to be an inexhaustible treasure chest for evolutionary biology for the past decades. Numerous aspects like for example structure or sequence of the ribosomal building blocks have been exploited to reconstruct whole forests of trees of Life and sparked to say the least lively debates. Besides structure and sequence of components, understanding their respective function should not be neglected as it might help to unravel molecular constraints and direction of evolutionary selection pressure. Given that, the translation apparatus is such an essential and universal part, studying the synthesis of these molecules is of great interest. What is more, similar to its conserved function, ribosome assembly might be guided by common key principles but has also evolved different pathways in the three domains of Life. In both bacteria and eukaryotes, the process of ribosome biogenesis has been characterized in detail, especially in the model organisms *E. coli* and *S. cerevisiae*. In archaea on the other hand, this fundamental process has been studied only very poorly.

To reach a more holistic picture of ribosome biogenesis spanning across the whole tree of Life it appears instrumental to learn more about how ribosomes are made in archaea. Our main goals for this purpose are therefore to:

i) Define key *cis*- and *trans*-acting elements of ribosome biogenesis in archaea
ii) Compare our new insights with attributes of bacterial and eukaryotic ribosomes biogenesis
iii) Draw possible phylogenetic and evolutionary conclusions
iv) Identify common or specific principles of ribosomes biogenesis across all three domains of Life

In this thesis various aspects that constitute the whole process of ribosome synthesis in archaea were investigated. The model organisms of choice in the lab were the halophilic archaeon *Haloferax volcanii* and the thermoacidophilic *Sulfolobus acidocaldarius*. First, we were looking at the organization of archaeal rRNA genes and phylogenetic implications. After transcription from the rRNA genes, pre-rRNAs get cleaved by various nucleases. The processing of the SSU pre-rRNA has been the major focus of the present work. Researching the role of *cis*-acting elements in rRNA precursors required the previous establishment of a

reporter assay to circumvent potential lethality of (pre-)rRNA mutations. As the assay proved to be effective, different structural RNA elements were analyzed regarding their involvement in pre-rRNA maturation. Furthermore, within a scientific collaboration we determined the function and structure of a *trans*-acting factor, a yet unidentified *H. volcanii* ribonuclease and analyzed its role in 16S pre-rRNA processing. For a broader and more comprehensive overview of rRNA processing events, long-read RNA sequencing of three archaeal representatives using Oxford Nanopore technology was performed in a second collaboration project. Using previously established tools, we asked about the regulatory mechanisms of ribosome production. Precisely, we increased the copy number of rRNA genes to test for gene dosage effects in *H. volcanii*. Finally, we developed RNA-FISH microscopy to follow the localization of distinct steps of ribosome biogenesis in archaea.

Collectively, we hope our work can contribute to deepen the knowledge first about ribosome biogenesis in archaea, and in a more general context to identify common and specific principles of this astonishing process in all domains of Life.

4. Organization of rRNA genes across domains

4.1. Introduction

At the very beginning of every ribosome stands the transcription of the rRNA genes, an essential duty carried out by the respective RNA-polymerases. Typically, the SSU (16S or 18S) and LSU (23S or 25S/28S, 5.8S) rRNAs are found in one transcriptional unit across all domains, whereas the 5S rRNA gene is more often located elsewhere (Hadjiolov 1985; Srivastava and Schlessinger 1990; Torres-Machorro et al. 2010). Interestingly, the arrangement of these genes is not unitarily the same everywhere and differs across the tree of Life. Presumably, there are functionally important characteristics at the basis of the genomic organization which might be relevant for transcription and ribosome assembly. For one, a polycistronic nature of rRNA operons could enable means to ensure balanced, stochiometric synthesis of all rRNAs, i.e., both subunits. In contrast, separate transcriptional units might underlie diverse constraints overcome by auxiliary mechanisms granting equal transcriptional output. Furthermore, rRNA processing and subunit assembly overall could be different between pre-rRNAs which are individually transcribed or pre-rRNAs confined in one long precursor, with the latter potentially facing a more interdependent, coupled maturation pathway. On this account, the genomic organization of rRNA genes could exhibit strong functional relevance for the production of new ribosomes and resemble a slow evolving trait, valuable for phylogenetic analyses. Intriguingly, the ribosomal RNA operon structure was already used early on by James Lake to argue in favor of his idea of the ‘karyote’ – ‘parkaryote’ bifurcation (see general introduction 3.1.1; Lake 1988).

The prokaryotic rRNA genes (*rrn)* operons are relatively similar in terms of organization and copy number. In archaeal species the 16S rRNA gene count is one to four per haploid genome, whereas the copy number in bacteria ranges from one to fifteen according to the *rrn* database (*rrn*DB) (R. A. Garrett et al. 1991; Z. M.-P. Lee, Bussema, and Schmidt 2009). The varying number of rDNA copies might give an indication of growth strategies and resemble adaptations to diverse ecological niches as has been reported for phylogenetically distant bacteria (Klappenbach, Dunbar, and Schmidt 2000; Roller, Stoddard, and Schmidt 2016). In eukaryotes there is a great copy number variation of the rRNA genes. It can reach up to several thousand copies and changes in rDNA copies are even seen in different tissues or during ontogenesis (Hadjiolov 1985; Symonová 2019; Salim and Gerton 2019). In *S. cerevisiae* the rDNA array is found on chromosome XII and comprises typically around 150 copies arranged in tandem repeats (Hadjiolov 1985; Warner 1999).

Now, what about the genomic arrangement? The *rrn* genes of prokaryotes are predominantly grouped in one operon with the structure 16S-23S-5S. In some cases, an internal tRNA is interspersed between the 16S and 23S rRNA genes, in others an additional tRNA might be located downstream of the 5S rRNA gene (Brown et al. 1989; R. A. Garrett et al. 1991; Thomm and Hausner 1993; Yip, Vincent, and Baserga 2013). Both of these types (with and without downstream tRNA) are seen in the two rDNA operons of *Haloferax volcanii*, the main model organism of this work (Hartman et al. 2010). Another notable feature is the separation of 5S rRNA genes from the 16S-23S unit or individual 5S rRNA genes elsewhere in the genome besides present 16S-23S-5S operons (Brown et al. 1989; R. A. Garrett et al. 1991; Thomm and Hausner 1993). This 5S rRNA gene separation is mostly observed in members of the TACK (see general introduction 3.1.1) superphylum (Thomm and Hausner 1993; Clouet-d'Orval et al. 2018).

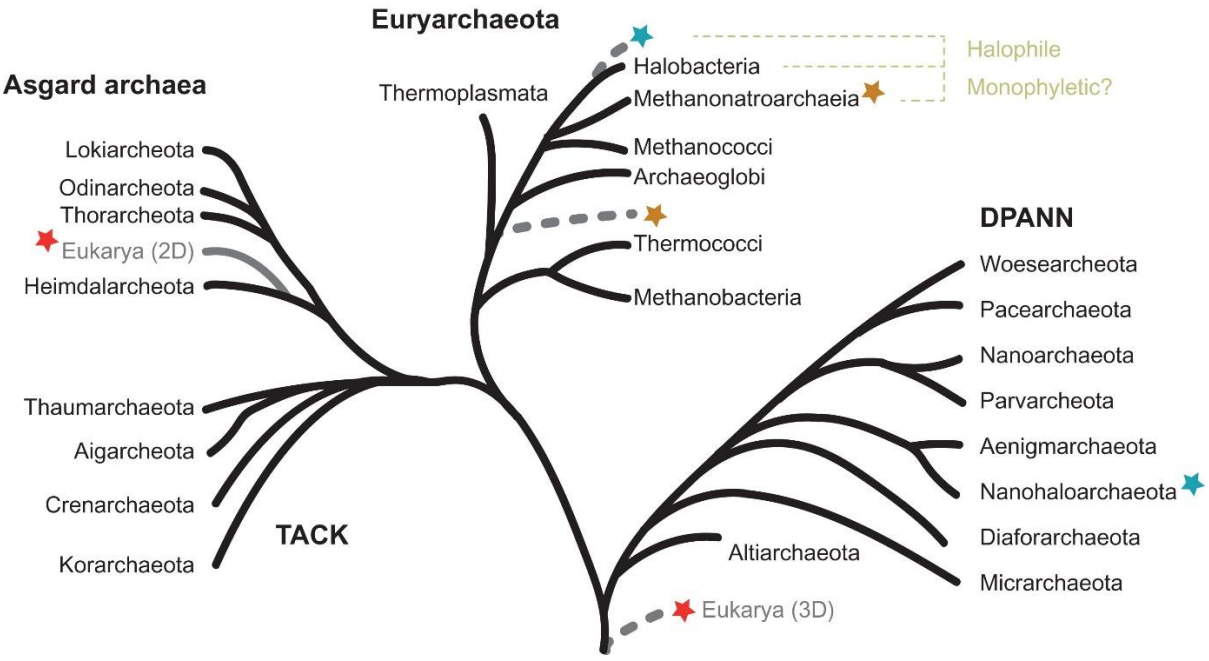

Figure 5: Current view on archaeal diversity and phylogeny. Archaea are divided into the Euryarchaeota phylum and the DPANN, TACK and the Asgard archaea superphyla. Note that the positioning of the eukaryotic lineage (see red star) within the archaeal phylogeny is subject to debate. The placement of several halophiles remains controversial as well (see orange and blue stars). Phylogenetic/evolutionary distance is not reflected by the branch length. From Jüttner and Ferreira-Cerca 2022.

Usually, the eukaryotic 18S, 25/28S and 5.8S rRNA genes are transcribed as one transcriptional unit by RNA-polymerase I, resulting in the 35S-47S precursor (*S. cerevisiae* – mammals) (Hori, Engel, and Kobayashi 2023). Notably, the 5.8S rRNA corresponds to the 5' end of prokaryotic 23S rRNA and has been separated over the course of evolution in almost

all eukaryotes (Torres-Machorro et al. 2010). The 5S rRNA is transcribed by RNA-polymerase III and either located within the rDNA array like in yeast or scattered across the genome (Hori, Engel, and Kobayashi 2023). Altogether, there are some variations and peculiarities seen in the eukaryotic rDNA organization like the localization of the 5S rRNA gene, split 5.8S rRNA gene in some Diptera or the 5.8S as an integral part of the 25S in microsporidia (Charles R. Vossbrinck and Woese 1986; Shimada 1992; Peyretaillade et al. 1998; Torres-Machorro et al. 2010). Nonetheless, in all known eukaryotic rDNA the transcriptional unit of 18S and 25S/28S is conserved (Torres-Machorro et al. 2010; Hori, Engel, and Kobayashi 2023).

Strikingly, not all prokaryotes show an organization with linked 16S and 23S rRNA genes as one transcriptional unit. In four to five percent of analyzed genomes unlinked *rrn* operons, i.e. 16S and 23S rRNA genes with a distance of at least 1.5 kb, were found (J. Tu and Zillig 1982; Ahn et al. 2020; Brewer et al. 2020). Remarkably, the disjuncture of 16S and 23S rRNA genes is strongly conserved at the species and genus level, more common in slow-growing species and most notably associated with a symbiotic lifestyle (Ahn et al. 2020; Brewer et al. 2020). The archaeon *Thermoplasma acidophilum* was one of the earliest examples in which a complete partition of all three rRNA genes was realized (J. Tu and Zillig 1982). *Nanoarchaeum equitans* is another example, notably it thrives symbiotically with its host *Ignococcus hospitalis* (Waters et al. 2003). Figure 6 shows the different organizational types of *rrn* operons in all three domains.

4.2. Results & discussion

Very intriguingly, the presence of unlinked rRNA genes has been noticed in one analyzed member of Asgard archaea (Brewer et al. 2020). This observation appears difficult to reconcile with the notion of Asgard archaea representing the cradle of the eukaryotic lineage, as there is no separation of 18S-25S/28S rRNA genes seen in eukaryotes. We became curious by this apparent discrepancy and (re-)analyzed selected archaeal genomes, especially from members of the Asgard superphylum (see figure 5).

To our surprise, almost all available Asgard genomes revealed an unlinked rRNA gene organization (Brewer et al. 2020; Jüttner and Ferreira-Cerca 2022). Lokiarchaeota, Heimdallarchaeota, Thorarchaeoa, Njordarchaeota, Wukongarchaeota and other lately described representatives of the Asgard superphylum were falling into this category (Jüttner and Ferreira-Cerca 2022). In addition, the recently presented, first cultivated '*Candidatus* Prometheoarchaeum syntrophicum' showed an unlinked rDNA arrangement (Imachi et al. 2020; Jüttner and Ferreira-Cerca 2022).

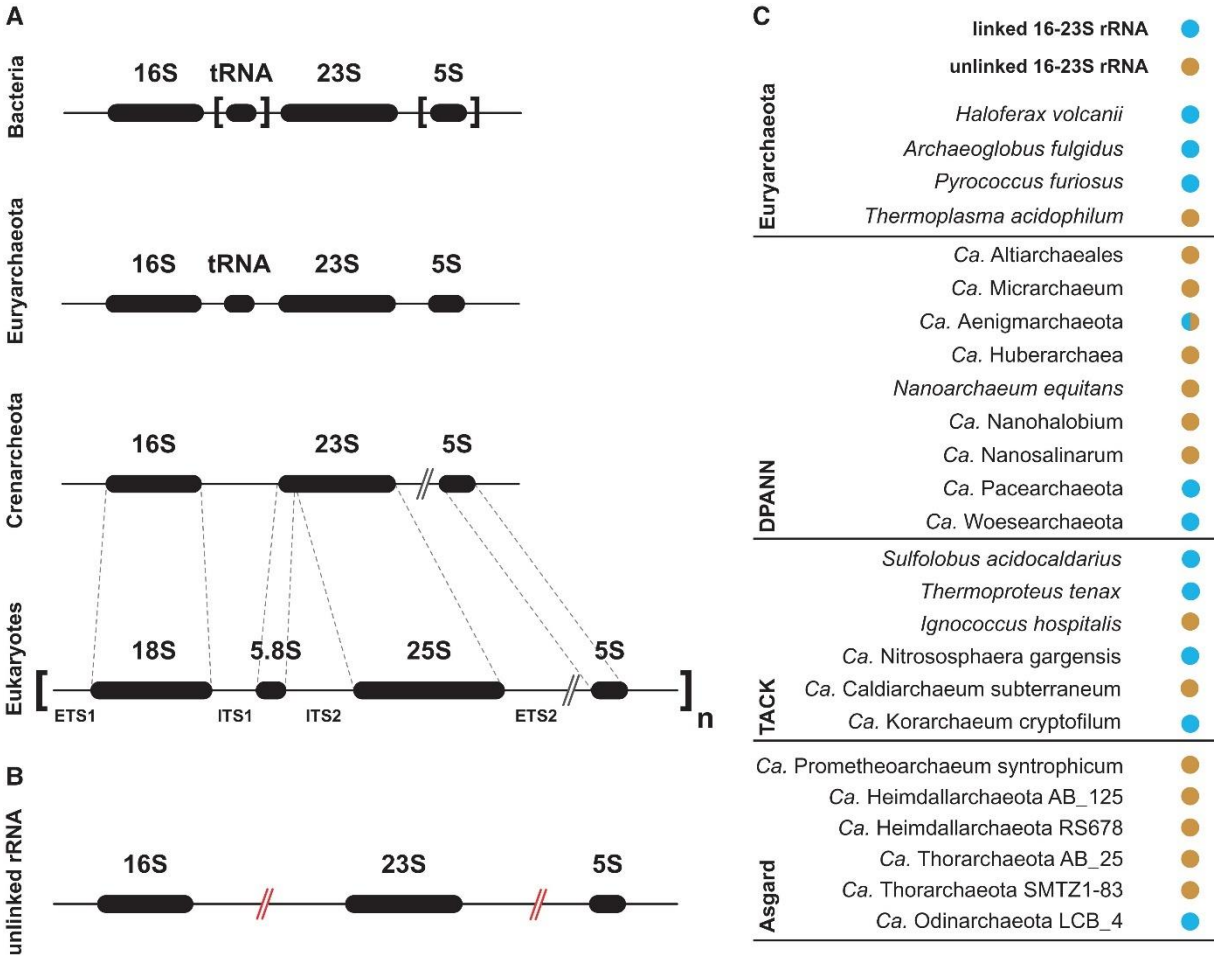

Figure 6: The organization of rRNA genes across all three domains of Life. (**A**) The most common, linked rDNA arrangement in bacteria, archaea, or eukaryotes is depicted. Note that the eukaryotic 5.8S is reminiscent of the prokaryotic 23S rRNA's 5' end. (**B**) Unlinked rDNA arrangement with 16S and 23S rRNAs as transcriptionally separated units (indicated by red //). (**C**) Distribution of linked and unlinked rDNA organization types across selected archaeal species. Blue dot indicates linked, orange dot indicates linked rDNA arrangement. From Jüttner and Ferreira-Cerca 2022.

It must be noted, that many of the Asgard genomes originate from metagenomic analysis and rRNA genes assembly is notoriously difficult in these circumstances (Yuan et al. 2015; Gruber-Vodicka, Seah, and Pruesse 2020). Hence, the available datasets and conclusions regarding rRNA genes organization should be taken with some caution. The only exception within the Asgard superphylum the Odinarchaeota (Odinarchaeum LCB_4) with a linked rRNA genes arrangement (Jüttner and Ferreira-Cerca 2022). The validity of the genomic data of Odinarchaeum LCB_4 was corroborated by long-read sequencing analysis (Tamarit et al. 2022).

Moreover, many species of the DPANN phylum (see general introduction 3.1.2; see figure 5), as well as few Euryarchaeota and members of the TACK superphylum (see general introduction 3.1.1; see figure 5) showed an unlinked rDNA organization type (Brewer et al.

2020; Jüttner and Ferreira-Cerca 2022). Figure 6 C shows the distribution of linked and unlinked rDNA organization in archaea.

A correlation of symbiotic lifestyle and unlinked rRNA genes has already been described in bacteria (Brewer et al. 2020; Ahn et al. 2020). Accordingly, the few cultivated DPANN and Asgard archaea members were grown in co-cultures with other bacterial or archaeal species and genomic analyses have also suggested DPANN archaea to thrive as obligate symbionts (Huber et al. 2002; Podar et al. 2008; Dombrowski et al. 2019; Hamm et al. 2019; Schwank et al. 2019; Dombrowski et al. 2020; Imachi et al. 2020; Sakai et al. 2022; Krause et al. 2022; Rodrigues-Oliveira et al. 2022). One study reported on enriching a member of the Microarcheota together with its Thermoplasmatales host and both organisms share the trait of unlinked rRNA genes (Krause et al. 2022). A functional connection of rRNA genes organization and symbiotic lifestyle remains currently elusive. It is striking, however, that the compositional and structural appearance of ribosomes is much more diverse in endosymbionts, parasites, or intracellular organelles. Mitochondrial ribosomes are remarkably different in their architecture in comparison with their cytosolic counterparts and display an enormous species-dependent variety (Kummer and Ban 2021). Furthermore, mitochondrial ribosomes from *Plasmodium falciparum* or some algae are even built from fragmented rRNA segments (Feagin et al. 2012; Waltz et al. 2021; Tobiasson, Berzina, and Amunts 2022). Intriguingly, the rRNAs of the eukaryotic, human pathogen *Giardia lamblia* are even shorter than typical bacterial rRNAs and lack most eukaryote-specific expansion segments (Edlind and Chakraborty 1987; Hiregange et al. 2022). In microsporidia, a group of unicellular, parasitic fungi, the 5.8S rRNA is fused to the 25S rRNA, resembling the prokaryotic 23S rRNA (C. R. Vossbrinck et al. 1987; Torres-Machorro et al. 2010). Nevertheless, microsporidia are not thought to represent an ancient link to the prokaryotic domains at the root of the eukaryotic lineage, but rather reflect reductive evolutionary traits (B. A. P. Williams et al. 2002; T. A. Williams et al. 2021). Accordingly, ribosomes appear simplified due to a reduction of r-protein numbers in bacterial organisms with very small genomes, typically associated with symbiotic or parasitic life styles (Nikolaeva, Gelfand, and Garushyants 2021). These studies are only selected examples indicating that in stable host environments the diversification of the ribosomal components and architecture has a much greater latitude. The evolutionary selection pressure in these conditions might cause ribosomal gene re-arrangements, mutations in rRNAs or r-proteins or deletions to be more often neutral or only slightly deleterious. Hence, taking lifestyles into consideration could be a trait worth incorporating into the interpretation of phylogenetic information based on ribosome-biology.

Our notion of the Asgardarchaeotas' rRNA genes organization being almost exclusively unlinked led us to deduce evolutionary implications for the Asgards – eukaryotes relationship from this perspective. Assuming eukaryotes emerged from the Asgard lineage or shared a common ancestor as current hypotheses suggest, several scenarios are imaginable and outlined in figure 7. First, the eukaryotic ancestor emerged from an Asgard archaeon with unlinked rRNA genes, implying later re-linkage of these genes (see figure 7, scenario 1). This possibility seems in our opinion the least likely, as massive co-adaptations might be required in the 'reversing' scenario. The three other suggestions suppose a eukaryotic emergence from an Asgard member with linked rRNA genes. Hence, option two and three presumes linked rRNA genes in the last Asgard-eukaryotic common ancestor (LAsgECA) and one or multiple split events in the ancestor of Asgardarchaeota with unlinked rDNA organization after an early split of the eukaryotic lineage (see figure 7, scenario 2 & 3).

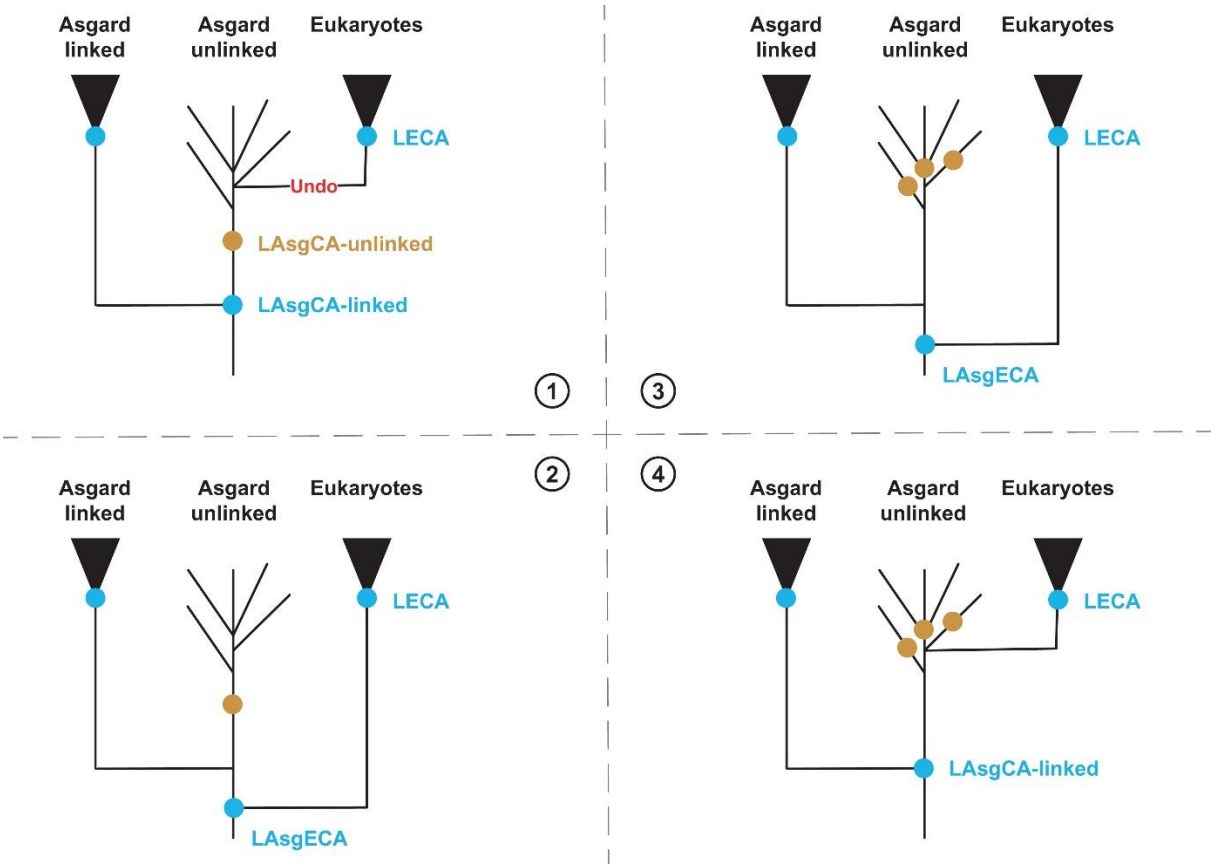

Figure 7: Evolutionary implications for the Asgard-eukaryotes relationship from the perspective of rDNA organization. Different scenarios based on linked/unlinked rRNA genes are depicted. The presence of linked or unlinked rRNA genes is indicated by blue or brown dots, respectively. The first scenario implies an 'undo' event in which the eukaryotic ancestor with an unlinked arrangement re-linked its rRNA genes. Possibilities two to four suggest a unlinked rDNA organization evolved later in Asgard archaea, after the split of the eukaryotic lineage. Note, that linked rDNA organization was only found in Odinarchaea LCB_4 (see main text). LAsgECA, last Asgard-eukaryotic common ancestor; LAsgCA, last Asgard common ancestor; LECA, last eukaryotic common ancestor. From Jüttner and Ferreira-Cerca 2022.

The fourth and final scenario puts the branching of the eukaryotic lineage close to Asgards with an unliked rDNA type (see figure 7, scenario 4). Current phylogenetic trees based on concatenated protein sequence of universally conserved genes place eukaryotes as emerging from within the Asgardarchaeaota close to Njordarchaeota (Xie et al.) or Heimdall-Wukongarchaeota branch (Liu et al.) (Y. Liu et al. 2021; Xie et al. 2022). These trees would correspond to the fourth scenario presented in figure 7. Alternatively, trees with a deeper branching of eukaryotes within archaea (close to the TACK and Asgard superphyla) were also considered and reflect scenarios two and three in figure 7 (Y. Liu et al. 2021).

To our knowledge there was no evidence suggesting a re-linkage scenario like for example a 23S-16S-5S or 23S-5S-16S organization. However, as already noted in the introduction, Lokiarchaeota are famous for causing trouble by mixing up things. The very recently published genome of another isolated Asgard species '*Candidatus* Lokiarchaeum ossiferum' disclosed three slightly different rDNA copies in its genome. Stunningly, one shows an unlinked rDNA organization, but the remaining two operons are annotated with a 23S-16S arrangement. This type of organization would be the exceptional genomic evidence, one would look for in a re-linkage scenario. However, this organization is a reverse linkage and different from the classical eukaryotic rDNA operon structure. Whether the 23S and 16S rRNA genes are linked as one transcriptionally unit resulting in an unprecedented 23S-16S rRNA precursor must be investigated in the future. In this case, the dataset was also obtained by Nanopore-based long-read sequencing, consolidating its credibility (Rodrigues-Oliveira et al. 2022). Moreover, it is crucial to increase the number of Asgard genome assemblies of high quality to further understand the frequency of such a peculiar scenario.

Lastly, there is not much known regarding a potential co-evolution of rDNA organization and rRNA processing machineries. Yet, Brewer et al. noticed that in bacteria with unlinked rRNA genes RNase III genes were significantly less frequently encoded (Brewer et al. 2020). In *E. coli* RNase III separates 16S, 23S and 5S pre-rRNAs from the long rRNA precursor molecule but is not an essential gene and not required for 16S rRNA maturation (see 5.1.1). Hence, loss of RNase III could be regarded as easier than loss of the archaeal endA, which is crucial for both tRNA and rRNA processing (see 5.3). Genomes of archaea with unlinked rRNA genes have not yet been analyzed in regard of potential loss of rRNA processing enzymes.

Here we presented our efforts to demonstrate how studying features of ribosome biogenesis might contribute to a better understanding of phylogenetic relationships or for the least initiate thought-provoking impulses. Doubtless, the displayed trees reflect only one singular aspect of binary nature which of course cannot be utilized to establish whole phylogenetic trees. Nevertheless, understanding the functional relevance of ribosome biogenesis characteristics

and using this information, might help to refine already existing phylogenetic trees. In our view, assessment of evolutionary hypotheses should either use established, functionally validated knowledge or propose scenarios that can be experimentally tested. A success story of such an approach is found in the attempts to explain the 'lipid divide'. Archaea use a different set of membrane lipids than bacteria and eukaryotes, which has always been a soft spot for proponents of a 2D scenario (i.e., an archaeal ancestry of eukaryotes). Now, researchers could show, that bacterial cells are in principle able to simultaneously possess a combination of ester and ether lipids in their membranes (Caforio et al. 2018; Villanueva et al. 2021; Sahonero-Canavesi et al. 2022). These experiments suggest a putative existence of mixed membranes in ancestral organisms and bridge 'the lipid divide'. As another example and potential future avenue, the evolutionary trajectories of an rDNA genes split event could be simulated and analyzed as we generated split 16S and 23S rDNA plasmids for *H. volcanii* (see chapter 6). Similarly, the remarkable 23S-16S rRNA gene arrangement of '*Candidatus* Lokiarchaeum ossiferum' could be mimicked in a distantly related archaeon like *H. volcanii*. Conclusively, this function-aware, evolutionary perspective might spark thought processes or challenge dogmatic views. This idea was recently introduced under the 'functional phylogenetics' label (Knüppel et al. 2021; Jüttner and Ferreira-Cerca 2022). Certainly, this approach implies a deep functional understanding of the molecular principles of ribosome biogenesis in all three domains of Life. In our view, it is therefore essential to learn more about this fascinating, yet poorly understood process in archaea. The following chapters illustrate our attempts to shed light on how ribosomes are made in archaea.

5. Ribosomal RNA Processing in Archaea

This work was focused in large parts on the maturation of the 16S rRNA in archaea. Hence, the key aspects of SSU pre-rRNA processing in bacteria, eukaryotes and archaea will be introduced hereafter. As described above, the rDNA gets usually transcribed as a long precursor molecule comprising all rRNAs. From these pre-rRNAs the mature rRNAs must be excised by removing leader, trailer, and internal sequences (see figure 8).

5.1. Ribosomal RNA processing in bacteria

5.1.1. Trans-acting elements involved in pre-rRNA processing in *E. coli*

The seven *rrn* operons in *E. coli* contain the 16S rDNA, one to two internal tRNA genes, the 23S, 5S rDNAs and none to two tRNA genes downstream of the 23S rRNA gene (Srivastava and Schlessinger 1990; Deutscher 2009). All these individual rRNAs (and tRNAs) must be excised from the long precursor molecule. During transcription the regions flanking the 16S rRNA and 23S rRNA, respectively, form double helical stem structures. Subsequently, the first cleavage reaction is carried out by RNase III which recognizes the double-stranded stem structures and thus separates 16S, 23S and 5S rRNA precursors as well as internal tRNA precursor(s), as depicted in figure 8 A (Srivastava and Schlessinger 1990; Kaczanowska and Rydén-Aulin 2007; Deutscher 2009). The resulting 16S rRNA precursor has 115 nucleotides remaining at the 5’ end and 33 nucleotides at its 3’ end. The processing of the 3’ terminus involves the activity of the 3’-5’ exonucleases RNase II, R, PH, the polynucleotide phosphorylase PNP and the endonuclease YbeY (Davies et al. 2010; Jacob et al. 2013; Sulthana and Deutscher 2013; Vercruysse et al. 2016). After removal of the extra 3’ nucleotides, the 5’ residues become single-stranded. Only then, RNase E is able to generate the 66 nucleotide long overhang at the 5’ end which gets eventually processed by RNase G (Zhongwei Li, Pandit, and Deutscher 1999). This implies, that the order of the processing events results from the built-in structure of the precursor rRNA and the specificity of the respective RNases, in other words an intriguing interplay of *trans*- and *cis*-acting elements (Deutscher 2015). Interestingly, the processing pathway of the 16S rRNA shows some degree of redundancy as the maturation can also occur in absence of RNase III, RNase E or with an incomplete subset of the 3’ exonucleases (Arraiano et al. 2010; Sulthana and Deutscher 2013). In contrast, RNase III is strictly required to form mature 23S rRNA, even though RNase III deficient strains are viable (King and Schlessinger 1983). The 23S rRNA is liberated from the long precursor transcript by RNase III with only several extra nucleotides on both 5’ and 3’ end.

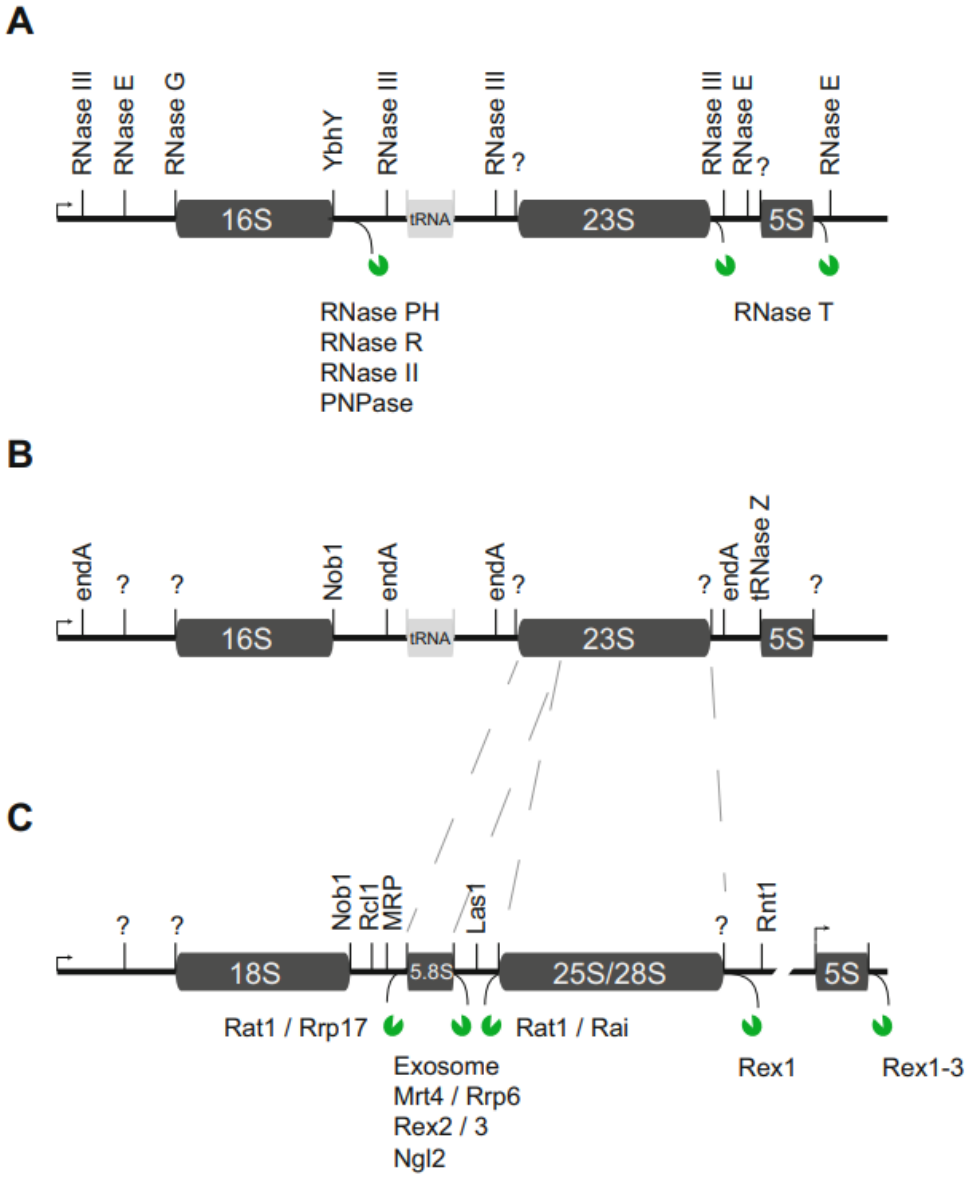

Figure 8. The processing of rRNA across all three domains of Life. Long, primary rRNA precursors containing all rRNAs, leader, internal spacer and trailer sequences are depicted. Note that 5S rRNA is transcribed separately in eukaryotes (**C**). Endo- (black vertical line) and exonucleases (green pacman) involved in pre-rRNA processing in bacteria (**A**), archaea (**B**) and eukaryotes (**C**) are illustrated. The bacterial pathway in (**A**) shows the participating enzymes known in *E. coli*. From Ferreira-Cerca 2017.

The final maturation of the 5’ end is still not known, the 3’ end is finalized by RNase T (Kaczanowska and Rydén-Aulin 2007; Deutscher 2009; Shajani, Sykes, and Williamson 2011). Eventually, the maturation of the 5S rRNA precursor occurs by the joint action of RNase E, RNase T and one unidentified enzyme (Deutscher 2009).

Albeit *E. coli* was mainly used to introduce the bacterial rRNA processing, it should be briefly noted, that not all bacteria employ the same RNA maturation pathways. *Bacillus subtilis* utilizes in part a different set of RNases, especially for the final 5’ end maturation of the 16S rRNA.

After the conserved RNase III cleavage, the two-step reaction catalyzed by RNase E and G in *E. coli* is for example carried out by the endo-/exoribonuclease RNaseJ1 in *B. subtilis* (Britton et al. 2007; Deutscher 2015). The final maturation of the 23S rRNA in *B. subtilis* occurs by an RNase III-like nuclease called Mini-III (Redko, Bechhofer, and Condon 2008).

5.1.2. Swiss army knife of RNA metabolism in *E. coli* - the RNase E/G family

A section of this work has investigated the role of an archaeal RNase E/G-like protein. Thus, the ensuing paragraphs illuminate in greater detail the importance of RNases E and G for rRNA maturation in *E. coli*. As mentioned above, the two endonucleases RNase E and its paralogue RNase G are involved in the two-step sequential processing of the 16S rRNA 5' end after the RNase III cleavage. What is more, they also take part in pre-5S rRNA and tRNA processing or mRNA metabolism and decay (Zhongwei Li, Pandit, and Deutscher 1999; Arraiano et al. 2010; Mackie 2013). RNase E is encoded by two alleles, *rne* and *ams,* and mutants of both were found to result in temperature-sensitive strains with increased mRNA stability and defects in ribosomal RNA processing (Apirion and Lassar 1978; Ono and Kuwano 1979; Mudd, Krisch, and Higgins 1990; Babitzke and Kushner 1991). Complete lack of the RNase E protein leads to nonviability, RNase G on the other hand is dispensable for cell growth (Apirion and Lassar 1978; Zhongwei Li, Pandit, and Deutscher 1999; Carpousis, Luisi, and McDowall 2009). The two enzymes belong to the same RNase E/G family and the N-terminal part of RNase E shows a considerable level of sequence identity (~34 %) and similarity (~50 %) with the RNase G gene (McDowall et al. 1993; Aït-Bara and Carpousis 2015). Accordingly, overexpression of RNase G could enable viability in a RNase E deletion strain (K. Lee, Bernstein, and Cohen 2002). However, their functional overlap remains limited as RNase G cannot sufficiently complement the role of RNase E in the different aspects of RNA metabolism (K. Lee, Bernstein, and Cohen 2002; Ow, Perwez, and Kushner 2003).

Distinctively, RNase E/G endonucleases prefer 5'-monophosphorylated RNAs but cleave the RNA substrate distant from the free 5' terminus (Koslover et al. 2008). *In vitro* work has shown, that RNase E or G cut the phosphate backbone with an optimal spacing of 8 or 6 nucleotides from the 5' RNA end, respectively, however both are able to cut within a greater distance (Richards and Belasco 2016). These features are best explained by taking a more detailed look at the structure of the enzyme. RNase E can be divided in two functionally distinct regions. The N-terminal part enharbours the catalytic domain with a relatively high level of conservation among bacteria and plants possessing this enzyme (Marcaida et al. 2006; Arraiano et al. 2010). The C-terminal half, which is absent in RNase G, is non-catalytic, rather unstructured

and not very well conserved. It helps coordinating interactions of a multienzyme complex, the RNA degradosome, which is a central player of mRNA decay (Callaghan et al. 2004; Carpousis 2007; Arraiano et al. 2010). Segment A, midway of the N- and C-terminal part, is located between the residues 565 and 582 and acts as an anchor to the inner cytoplasmic membrane, which was also shown to be important for normal growth (Khemici et al. 2008). The crystal structure of RNase E reveals that the catalytic part forms a homo-tetramer and contains a subdomain resembling the RNase H endoribonuclease family, which seems not be active (Callaghan et al. 2005). Within this RNase H subdomain reside two folds which are both important for RNA binding and orientation: a S1 domain and a 5' end recognition motif, (Callaghan et al. 2005). This mirrors the preferential cleavage of 5'-monophosphorylated RNAs, even though some structured RNAs can be processed as well (Mackie 1998; Arraiano et al. 2010). Lastly, at the surface of a DNase I-like subdomain a magnesium ion is coordinated by two aspartate residues and is critical for the cleavage reaction and conserved in the RNase E/G family (Callaghan et al. 2005). Mechanistically, the mediation of substrate binding and distant catalytic activity was described in a 'mouse-trap' model (Callaghan et al. 2005). First, the 5' end recognition motif/S1 domain are highly exposed to the solvent, thereby also allowing the binding of large and structured RNAs (Koslover et al. 2008). Upon binding of the 5' terminus of a monophosphorylated RNA the enzyme presumably switches from an open to a closed state (Callaghan et al. 2005; Grossmann et al. 2008; Koslover et al. 2008). This conformational change brings the substrate in close proximity to the active center and enables a nucleophilic attack on the scissile phosphate (Callaghan et al. 2005; Koslover et al. 2008).

Regarding the high similarity of the N-terminal part of RNase E enharbouring the catalytic sites and RNase G supported by *in vitro* and *in vivo* studies the mode of action is likely to be similar (Jiang and Belasco 2004; Callaghan et al. 2005; Jourdan and McDowall 2008; Richards and Belasco 2016).

5.2. Ribosomal RNA processing in eukaryotes

In yeast, the primary 35S rRNA transcript contains the 18S, 5.8S and 25S rRNAs which are separated by two internal transcribed spacers (ITS1 & ITS2) and 5' and 3' external transcribed spacers (5'-ETS & 3'-ETS) (Venema and Tollervey 1995). Similar to the bacterial system the 35S precursor in yeast has to undergo a complex series of endo- and exonucleolytic cleavage events (Venema and Tollervey 1995; Anthony K. Henras et al. 2015; Fernández-Pevida, Kressler, and de la Cruz 2015; Kressler, Hurt, and Baßler 2017). These can occur either co-transcriptionally or post-transcriptionally, though the participating enzymes differ from the bacterial counterparts (see figure 8 C). One exception would be the endonuclease Rnt1, which is homologous to bacterial RNase III but acts different than in bacteria by generating the 3' end of the 35S precursor in yeast (Elela, Igel, and Ares 1996; Kufel, Dichtl, and Tollervey 1999). Overall, most of the eukaryotic rRNA processing takes place in the nucleolus, some parts in the nucleoplasm and only the final maturation in the cytoplasm (Thomson, Ferreira-Cerca, and Hurt 2013; Anthony K. Henras et al. 2015).

First cleavages take place within the 90S pre-ribosome/SSU processome, a huge RNP enharbouring the entire 35S transcript. Notably, nucleolar processing does not happen on isolated RNA molecules, but the RNP context is crucial for productivity. A whole army of *trans*-acting factors of the 90S/SSU processome is described to be required for these reactions, although the participating nucleases are not unambiguously identified (Anthony K. Henras et al. 2015; Baßler and Hurt 2019; Kressler, Hurt, and Baßler 2017). Amongst the components are above all SSU r-proteins, several RBFs and many snoRNPs (small nucleolar ribonucleoparticles) (Venema and Tollervey 1995; Kressler, Hurt, and Baßler 2017). Cleavages at sites A_0 and A_1 are needed to generate the mature 5' terminus of the 18S rRNA (Fernández-Pevida, Kressler, and de la Cruz 2015). A_2 cleavage in the ITS1 allocates pre-ribosomal SSU and LSU into two independent maturation pathways (Fernández-Pevida, Kressler, and de la Cruz 2015). One central player in the SSU processome which is involved in the early steps of the RNA processing must be highlighted in particular: the U3 snoRNP. For one, U3 binds upstream of the 18S rRNA 5' terminus and coordinates A_0, A_1, and A_2 cleavages (J. m. Hughes and Ares Jr 1991; Beltrame and Tollervey 1992; Beltrame, Henry, and Tollervey 1994; Beltrame and Tollervey 1995; Venema and Tollervey 1995; Woolford and Baserga 2013). Secondly, U3 snoRNA makes extensive base pairing with sequences in the 18S rRNA. This interaction is thought to chaperone RNA folding and to prevent a premature formation of the central pseudoknot (CPK), a hallmark structural feature in the SSU (see figure 12 A) (J. m. Hughes and Ares Jr 1991; Kudla et al. 2011; Woolford and Baserga 2013). After the separation through A_2 cleavage the pre-40S particle gets rapidly exported to the cytoplasm together with the already associated endonuclease Nob1, which then catalyzes the final 3' end (Fatica et al.

2003; Lamanna and Karbstein 2009; Pertschy et al. 2009; Fernández-Pevida, Kressler, and de la Cruz 2015).

Compared to the straightforward maturation of the SSU after separation at A_2, the pre-60S ribosomes have a more sophisticated and complex route ahead of them. A series of complex endo- and exonucleolytic processing events within the 27S pre-rRNA (pre-25S & pre-5.8S) eventually yield the mature 25S and 5.8S rRNAs (Venema and Tollervey 1995; Fernández-Pevida, Kressler, and de la Cruz 2015; Kressler, Hurt, and Baßler 2017). Some steps, like for example the formation of the 5' terminus of the 5.8S pre-rRNAs and the 3' terminus of the 25S rRNA, by cleavages in the ITS1 and 3'-ETS, seem to be coordinated (Venema and Tollervey 1995; Anthony K. Henras et al. 2015). In contrast to the pre-18S rRNA, the pre-25S rRNA is completely matured in the nucleus before it gets exported to the cytoplasm (Venema and Tollervey 1995; Anthony K. Henras et al. 2015). Remarkably, two separate pathways produce two different 5' ends of the 5.8S rRNA, resulting in a shorter and a longer form ($5.8S_S$ & $5.8S_L$). The 3' terminus of the 5.8S rRNA is finalized by a multi-step process involving several exonucleases (Fernández-Pevida, Kressler, and de la Cruz 2015).

The pre-5S rRNA is transcribed by RNAP III and independently matured by exonucleolytic trimming by Rex1. Nevertheless, 5S rRNA associated with the ribosomal protein L5, was found in both the pre-60S and the 90S particles, and accompanies the 60S pre-ribosomes (Ciganda and Williams 2011; Fernández-Pevida, Kressler, and de la Cruz 2015).

Just as *E. coli* is clearly not entirely representative for all bacteria, the yeast way of rRNA processing is not transferable to every other eukaryotic organism. For instance, the finalization of the 18S rRNA 3' end necessitates a combination of endo- and exonucleolytic activities in human cells, different from the two endonucleolytic cleavage reactions required in yeast (Anthony K. Henras et al. 2015). The processing scheme of the LSU rRNAs yet appears to be more conserved across eukaryotes (Anthony K. Henras et al. 2015).

5.3. Ribosomal RNA processing in archaea

Concerning the current knowledge about archaeal pre-rRNA processing the general theme is, not surprisingly once more - largely unexplored. However, some studies have enabled us to start contemplating the maturation pathways of rRNAs in archaea. So, what do we actually know about the significant *cis*- and *trans*-acting factors so far?

As described above and comparable to bacteria and eukaryotes, the three archaeal rRNAs get usually transcribed from one polycistronic rDNA operon. The regions flanking the 16S and 23S rRNAs at their respective 5' and 3' ends form long processing stems akin to *E. coli* pre-rRNAs. Usually, both of these processing stems contain a typical RNA structural motif, the so-called bulge-helix-bulge motif (bhb). The archaeal bhb motif, in its canonical form a four base-pairs central helix flanked by two juxtaposed bulges of three nucleotides, was initially noticed for its role in the splicing of intron containing tRNAs (L. D. Thompson and Daniels 1990; Lykke-Andersen et al. 1997; Marck and Grosjean 2003). The multimeric splicing endonuclease endA is highly conserved, recognizes this structural element and cleaves within RNA stem structures (Clouet-d'Orval et al. 2018). Much later the corresponding tRNA ligase RtcB was discovered to be the enzyme catalyzing a subsequent ligation step of the 5' and 3' ends of excised introns generating circular RNA molecules (Englert et al. 2011; Clouet-d'Orval et al. 2018).

The presence of the bulge-helix-bulge motifs in the 16S and 23S rRNA processing stems of most archaea was recognized early on. Hence, a contribution to the rRNA maturation pathway in a tRNA-like processing mechanism was suspected (R. A. Garrett et al. 1991). Various investigations confirmed indeed cleavage events at the bhb motifs in the processing stems of different archaeal species, but processing sites upstream in the 5' leader region were also reported in *Sulfolobus acidocaldarius* (J. Chant and Dennis 1986; Durovic and Dennis 1994; P. P. Dennis, Ziesche, and Mylvaganam 1998; A. G. Russell, Ebhardt, and Dennis 1999). Furthermore, later studies confirmed indirectly the presence of circular 16S and 23S rRNA precursor molecules in archaea (Tang et al. 2002; Danan et al. 2012). Interestingly, the before mentioned, earlier studies using S1 protection assays observed intermediates relating to circularization and re-opening of pre-rRNAs (J. Chant and Dennis 1986; P. P. Dennis, Ziesche, and Mylvaganam 1998). At the time these molecules could not be assigned correctly, and some processing sites might be misinterpreted as cleavages within the 5' leader. Overall, the first steps of archaeal pre-rRNA processing seem to resemble initial RNase III cleavages in the processing stems of bacteria. However, archaea use the processing machinery of intron containing tRNAs instead. Noteworthy, the occurrence of the circular pre-16S and circular pre-23S intermediates is according to the current knowledge a unique feature in the archaeal

domain. Covalent ligations of the pre-rRNAs' 5' and 3' termini have not been suggested in bacteria, nor in eukaryotes (Ferreira-Cerca 2017).

How 16S and 23S pre-rRNA maturation continues from this point on remains so far enigmatic. The dynamics and required *cis*- and *trans*-acting players for the formation of linear, mature rRNAs are not known. Regarding the final maturation of the 16S 3' end an old acquaintance from the eukaryotic rRNA processing arouses suspicion: the endonuclease Nob1, which is also found in the genomes of many archaeal species. *In vitro* cleavage experiments with archaeal Nob1 from *Pyrococcus horikoshii* revealed a potential involvement in 3' end processing of 16S pre-rRNA (Veith et al. 2012). One investigation studying a a methanogenic archaeon claimed that Nob1 could be the endonuclease to open and linearize the circular 16S pre-rRNA by cleavage at the 3' end (Qi et al. 2020).

Another well conserved archaeal nuclease, RNase Z is not only associated with the formation of 3' ends of tRNAs but also the generation of the 5' end of 5S rRNA (Hölzle et al. 2008; Clouet-d'Orval et al. 2018). The enzyme required for 3' end maturation of the 5S rRNA is still unknown (Paola Londei and Ferreira-Cerca 2021). *In vitro* experiments with cell extracts from three different halophiles indicated a RNase E-like activity in archaea and suggested a participation in 5S pre-rRNA processing (Franzetti et al. 1997). Later, functional analysis of the *fau-1* gene in Thermococcales also indicated an involvement in rRNA maturation and/or degradation. The product of the *fau-1* gene is a potential orthologue of RNase E/G enharbouring a S1 and 5' sensor domain (see 5.1) (Ikeda et al. 2017). The putative pre-rRNA processing pathway is depicted in figure 8 B.

5.4. Analysis of *cis*-acting RNA elements in *H. volcanii*

5.4.1. Towards a *cis*-acting elements rDNA reporter system

When we began investigating the archaeal rRNA maturation by mainly using *Haloferax volcanii* as a model system several open questions seemed for us most valuable to address:

i) What are the key *cis*-acting structural RNA elements important for (pre-)rRNA processing?
ii) What are the missing *trans*-acting factors involved to mature archaeal pre-rRNAs?
iii) How can we methodologically approach these issues *in vivo*?

In particular, we were curious about the relevance and contribution of the circular pre-rRNA intermediates. Yet, tackling this problem needed some considerations. Deletion or mutation of the tRNA splicing machinery components i.e., endA or RtcB may critically affect rRNA and tRNA metabolism. Moreover, rRNA mutations in other model systems turned out to be lethal *in vivo*, thus potentially making genetic manipulation and follow-up analysis of *cis*-acting RNA structural elements challenging (Stark, Gourse, and Dahlberg 1982). To circumvent these problems a couple of students in our group started developing a rDNA *cis*-acting reporter assay system for *H. volcanii* and I was myself joining this project during my Master thesis. Reporter systems based on rDNA plasmids were already successfully employed in bacteria and eukaryotes to study ribosome maturation or degradation (Musters et al. 1989; 1990; Mori et al. 1990; Youngman and Green 2005; Piir et al. 2011; Burman and Mauro 2012; Paier et al. 2015). The basic idea of the approach was to introduce slightly altered rDNA plasmids carrying four point mutations, two in the mature 16S and 23S, respectively. These changes (*Haloferax volcanii* numbering) were expected to confer for one (partial) antibiotic resistance against Pactamycin ($16S^{A633G}$ & $16S^{C734T}$) or Chloramphenicol ($23S^{C2479T}$) to examine functionality of ribosomal subunits *in vivo*. Secondly, mutations at positions $16S^{C734T}$ and $23S^{A2496C}$ created two new restriction sites for EcoRV and BssS1α, respectively. These additional restriction sites provided the possibility to follow (pre-)rRNA mutations *in vivo* regarding their relative expression level. The basis of the rDNA constructs was the plasmid pTA1228, which encodes the *pyrE2* gene required for growth in selective casamino medium of uracil auxotrophic h26 cells and possess an Ampicillin resistance (Amp^R) gene to be amplified in *E. coli* (Allers et al. 2010; Brendel et al. 2014).

A detailed depiction of how both the functional analysis and the relative expression analysis of the assay function, is shown in figures 9 and 10 C and described in more detail in the corresponding publication (Jüttner et al. 2020)**.** In short, rDNA reporter plasmids with and without carrying desired mutations are transformed into *H. volcanii* h26 cells. Note that the

genomic rDNA background is always present in these cells. Now, cell growth can be analyzed in the presence of different antibiotics to see whether functional, i.e., resistant ribosomal subunits, are made from mutation carrying rDNA loci. The relative expression analysis exploits the EcoRV or BssS1α restriction sites to distinguish between the genomic and plasmid derived rRNA populations. Total RNA gets extracted, cDNA synthesis with subsequent PCR using fluorescently labeled oligos is performed, and samples analyzed after restriction digest with the respective enzyme on a PAGE-gel. Use of specific cDNA primers enables the analysis of different (pre-)rRNA species. Even though a PCR-step is involved, a semi-quantitative read-out of fluorescent signals corresponding to either genomic or plasmid born rRNAs is possible.

5.4.2. Analyzing the contributions of the bhb motif

Having this tool available we set out to on the one hand proof the applicability of this assay and at the same time address biological questions. First, we wanted to shed light on the functional relevance of circular pre-rRNA intermediates during the maturation pathway in archaea. Therefore, we generated a collection of mutations of the bhb motifs in the 16S or 23S processing stems or combinations affecting bhb motifs in bhb stems (see figure 10 B). The summary of the bhb mutant analysis is depicted in figure 10 D. All 16S bhb mutants had a detrimental effect on the output of circular 16S pre-rRNA and total 16S rRNA amounts. In the same way, every alteration of the 23S bhb motif led to a strong decrease of circular 23S pre-rRNA and total 23S rRNA. Surprisingly, changes in the 16S bhb motif had also a deleterious effect on the production of 23S rRNA species, indicating a certain level of coordination or order of the 16S and 23S pre-rRNA processing (see figure 10 D; Jüttner et al. 2020). Another study in *H. volcanii* focused on one of the two corresponding *trans*-acting factors for this step, endA. The evaluation of a *endA* CRISPRi strain via qPCR experiments demonstrated a clear reduction of circular pre-rRNAs compared to the wild type, thereby confirming the crucial interplay of bhb motif and nuclease in the formation of circular pre-rRNAs (Schwarz et al. 2020).

To begin with, the investigation of the bhb motif mutants demonstrated the applicability and merit of the established *cis*-acting elements reporter assay. Furthermore, we illuminated the functional relevance of these structural elements for the formation of circular pre-rRNAs and total RNAs. We and others provided evidence, that the first steps of pre-rRNA processing in archaea resemble the processing of intron containing tRNAs and the same machineries are employed (Jüttner et al. 2020; Schwarz et al. 2020).

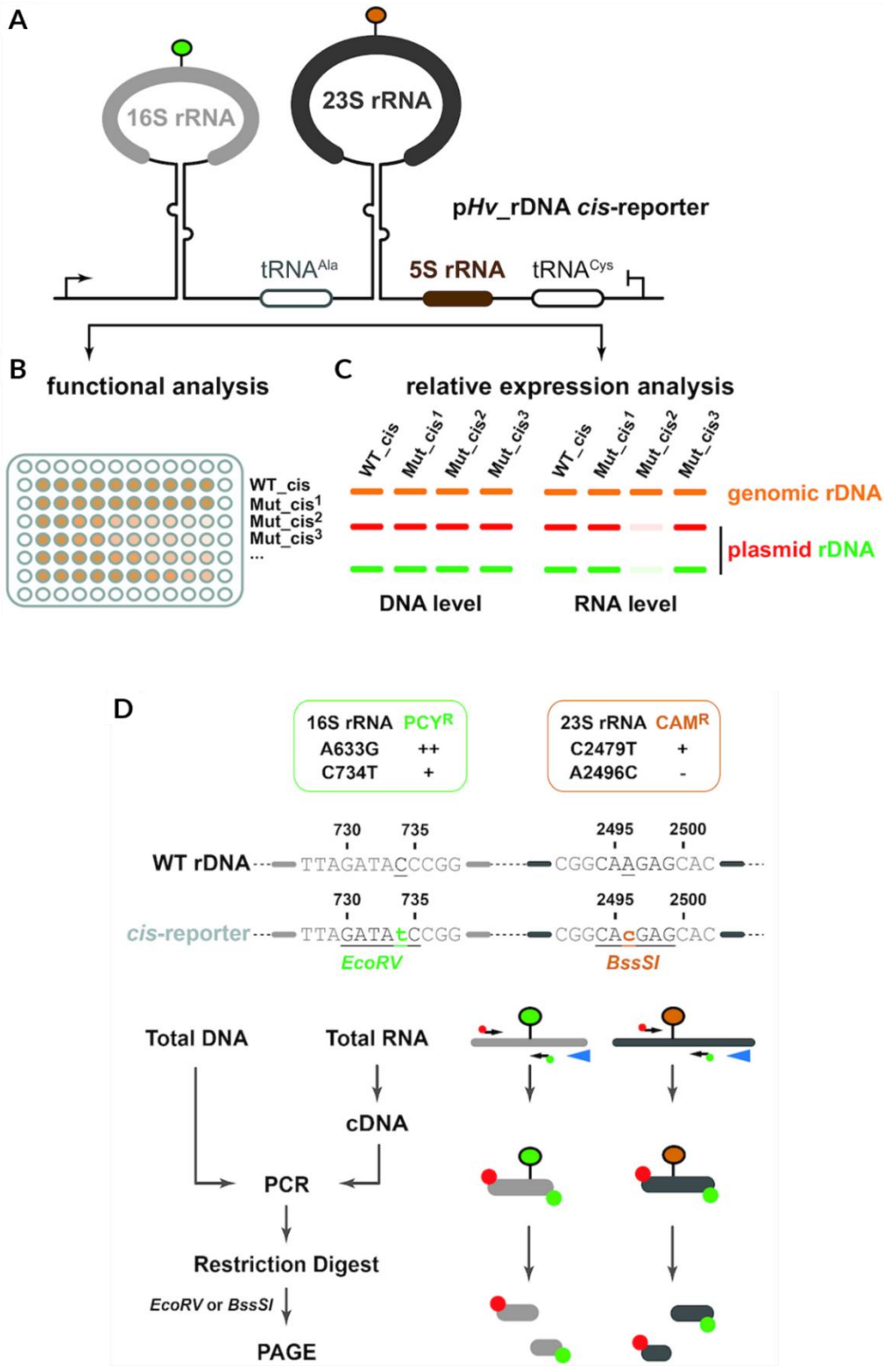

Figure 9: General principle of the *cis*-acting rDNA reporter system. (**A**) rDNA reporter plasmid containing the complete rDNA operon A of *H. volcanii* with additional point mutations in the 16S rDNA (green dot) and the 23S rDNA (orange dot). (**B**) Functional read-out is possible by testing antibiotic resistance to Pactamycin (SSU) and Chloramphenicol (LSU). (**C**) Relative rDNA levels and rRNA expression from reporter plasmids can be examined by exploiting additional restriction sites for EcoRV and BssSI in a PCR-based approach with fluorescently labeled oligos. (**D**) General workflow of the relative expression analysis is depicted. After transformation of rDNA reporter plasmids into *H. volcanii* cells, DNA or RNA extraction followed by cDNA synthesis, a PCR-based approach with fluorescent oligos is performed. Subsequent restriction digest and polyacrylamide gel electrophoresis enables the differentiation between rRNA derived from genomic loci or rDNA reporter plasmids. From Jüttner et al. 2020.

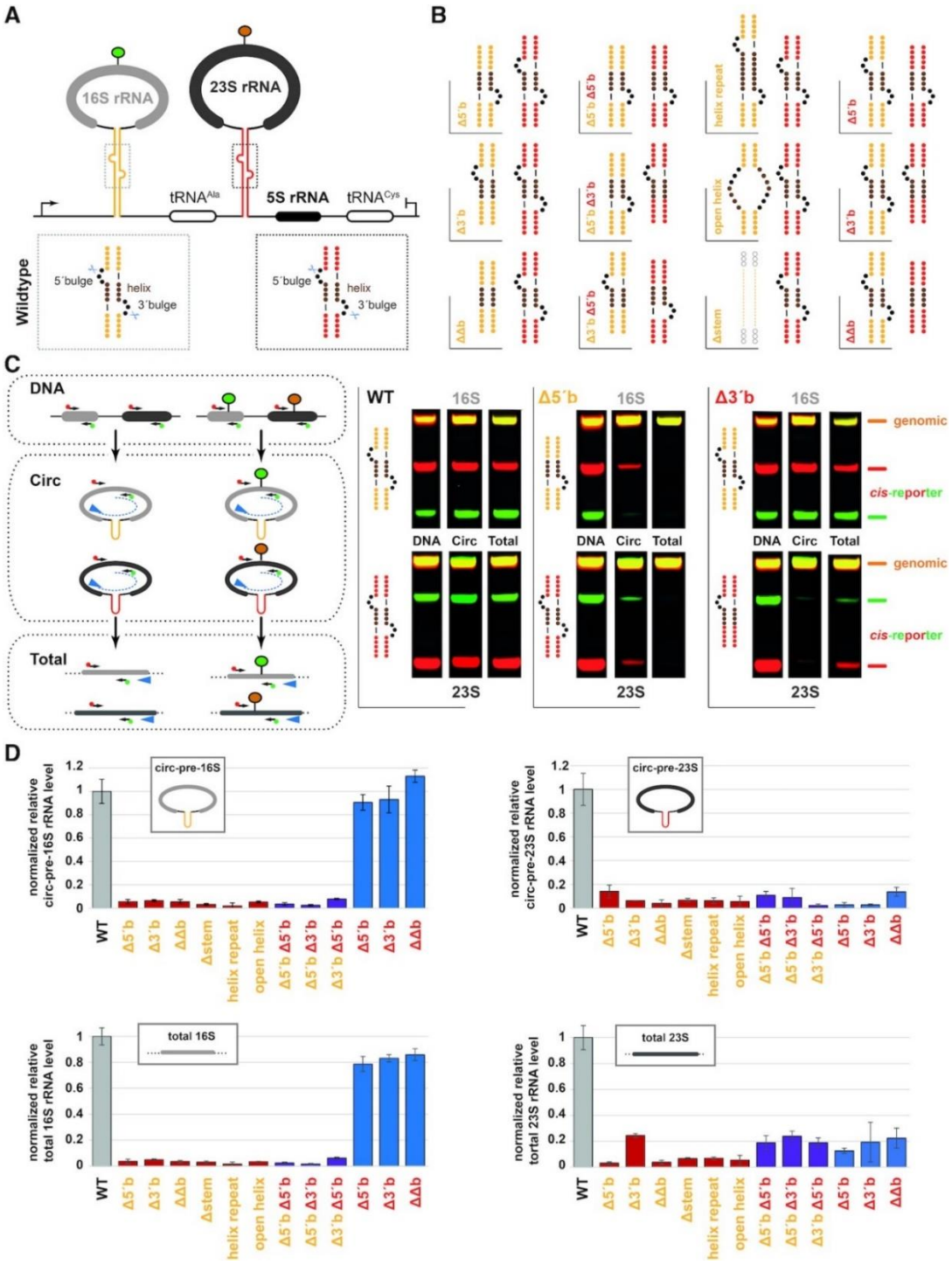

Figure 10: Relative rRNA expression analysis of bhb mutant analysis. (**A**) Schematic depiction of the rDNA reporter plasmid containing the bhb motifs within the pre-rRNA processing stems in yellow (16S pre-rRNA) and red (23S pre-rRNA). (**B**) Overview of all tested bhb mutations with deletions or alteration of the 16S and 23S pre-rRNA processing stems. (**C**) Exemplary analysis of 16S bhb or 23S bhb mutations in comparison with the wild type. Left panel briefly shows the workflow of the rDNA reporter system. Selection of different RT primers (blue arrow) allows for analysis of circular pre-rRNA or total rRNA amounts after a subsequent PCR with fluorescently labeled oligos (red and green dots on black arrow). Right panel depicts PAGE-gel readout after restriction digest of exemplary bhb mutants. Relative rDNA, circular pre-rRNA and total rRNA amounts were analyzed. Yellow bands represent genomic origin (uncut), green and red bands represent plasmid-born rRNAs (cut). Note that relative rDNA amounts are similar in wild type and mutants. (**D**) The bhb motif is required for efficient pre-RNA processing of early maturation steps. Summary of results for all tested bhb mutants from (**B**). 16S bhb mutations (red bars) negatively affected production of 16S and 23S circular pre-rRNA and total rRNA. 23S bhb mutations (blue bars) interfered with 23S circular pre-rRNA and total rRNA maturation. Combinations of 16S and 23S bhb mutations (purple bars) behaved similarly as the 16S bhb mutants. From Jüttner et al. 2020.

The multimeric, highly conserved endA occurs in different subunit compositions in archaea and most of them, like the α2 subtype, cleave only canonical bhb motifs (Clouet-d'Orval et al. 2018). Accordingly, the strong effects on pre-rRNA maturation in all bhb motif mutants is good agreement with the endA α2 subtype found in *H. volcanii*.

Circular pre-rRNA formation is an archaea-specific intermediate which does not occur during bacterial and eukaryotic ribosome assembly. Yet, the initial pre-rRNA processing steps resemble the bacterial RNase III dependent cleavage events to some extent. The mode of action, i.e., cleavage within stem structures formed by inverted repeats is comparable in the two systems, however RNase III is not required for production of mature 16S rRNAs. Intriguingly, we observed a putative coordination of the first pre-rRNA processing steps in *H. volcanii*. The integrity of the 16S rRNA processing stem was necessary for the efficient production of circular and total (pre-)rRNAs of both subunits. The reverse effect of the 23S bhb motif on the production of 16S (pre-)rRNAs was not seen. In addition, this impact was only affecting plasmid-born, non-endogenous rRNAs, suggesting a *cis*-acting activity of the apparent coordination. Conceptually, prior cleavage at the bhb motif in the 16S rRNA processing stem, subsequent ligation, and removal of the circular 16S pre-rRNA from the primary transcript seems to be required to allow further processing of the 23S pre-rRNA. The exact molecular mechanisms of this coupling are yet unknown. Potentially, steric hinderance preventing 23S processing stem formation or blocking accessibility for the tRNA intron splicing machinery could be one option necessitating this processing order. Alternatively, in the case of co-transcriptional cleavage, removing pre-16S rRNA might also be demanded to ensure transcription elongation of the primary transcript. Interestingly, the presence of the corresponding intermediate with ligated the 5' leader/3 'trailer of the 16S rRNA flaking regions joint to the nascent 23S rRNA has been detected in *Saccharolobus (*formerly *Sulfolobus*) *solfataricus* and *Archaeoglobus fulgidus* (Tang et al. 2002). The specific structural features of this newly emerging precursor after 16S pre-rRNA excision could also serve as a recruitment platform for certain ribosome biogenesis factors, support the assembly of LSU r-proteins or assist in RNA folding dynamics. In support of this idea comes the notion that the ligated region might adopt C/D-box snoRNA like structures, which typically guide 2'-O-methylations (Tang et al. 2002). The *in vivo* role of the potential newly emerging *cis*-acting structural RNA element remains to be elucidated. To our knowledge, this level of coordinating rRNA processing is not reported in bacteria and eukaryotes. For instance, eukaryotic SSU and LSU pre-rRNAs are separated relatively early and experience different rRNA processing pathways. Accordingly, deletions in the 5'-ETS or ITS1 regions were shown to affect SSU pre-rRNA processing, but allowed normal maturation of LSU pre-rRNAs (Musters et al. 1990). Moreover, deletion of U3 snoRNA or mutations of the 5'-ETS region base-pairing with U3 snoRNA affected 18S rRNA,

but not 25S/5.8S rRNA processing (Beltrame and Tollervey 1992; Beltrame, Henry, and Tollervey 1994). Conversely, large deletions of ITS2 greatly reduced 25S/5.8S processing but left 18S rRNA processing unaffected (van der Sande et al. 1992). Moreover, only a few eukaryotic RBFs are presumably involved in the maturation of pre-40S and pre-60S subunits (Lebaron et al. 2005; 2013; Khoshnevis et al. 2019).

Besides the observed coordination, the functional relevance of the circular pre-rRNAs and the biological context in which these intermediates originated remains a puzzling issue. One possible explanation is that ligation of free 5' and 3' ends during ribosome biogenesis, delivers protection against unspecific exonucleolytic degradation. Moreover, processing stem formation enables the close proximity of future mature 5' and 3' ends in a protected, defined RNP environment during ribosome biogenesis. These structurally confined constraints might facilitate r-protein assembly or govern rRNA folding dynamics. A role in safeguarding a certain processing order through distinct timing of ligation and re-opening of circular intermediates is conceivable as well. It is also considerable, that the circular pre-rRNAs originated in an ancient biological context in which circularization was required, however the functional necessity has been lost, in contrast to the still present intermediates (see 8.2 for detailed discussion).

5.4.3. Analyzing the contributions of the 5' leader helices

Additional structural elements in the rRNA precursor of *H. volcanii* are found in the 5' leader region (5'-ETS in eukaryotes) with four helices termed helix A', B', A and B. Helices A and B have been described to be conserved in halophiles, helices A' and B' were named by us (P. P. Dennis, Russell, and Moniz De Sá 1997). Moreover, the conserved stem structure of helix A and B has been used to support a monophyletic nature of extreme halophiles, thermophiles, and methanogens in the early days of archaeal research, especially helix B was proposed to be of high functional relevance (Kjems and Garrett 1990). However, a functional link to archaeal ribosome biogenesis has not yet been provided so far.

Thus, we generated rDNA reporter plasmids carrying deletions of the helices A', A and B and analyzed the effects with our *cis*-acting elements reporter assay. Investigations of helix B' have not yet been performed but will be carried out in the future. The sequence and predicted secondary structure of the respective helices is given in figure 11 A. Helix A' and A deletions did not show any rRNA processing defect compared to the wild type when levels of circular 16S pre-rRNA and total 16S rRNA amounts were tested. In contrast, deletion of helix B led to

a very strong reduction of circular 16S pre-rRNA and total 16S rRNA production. The results are shown in figure 11 B.

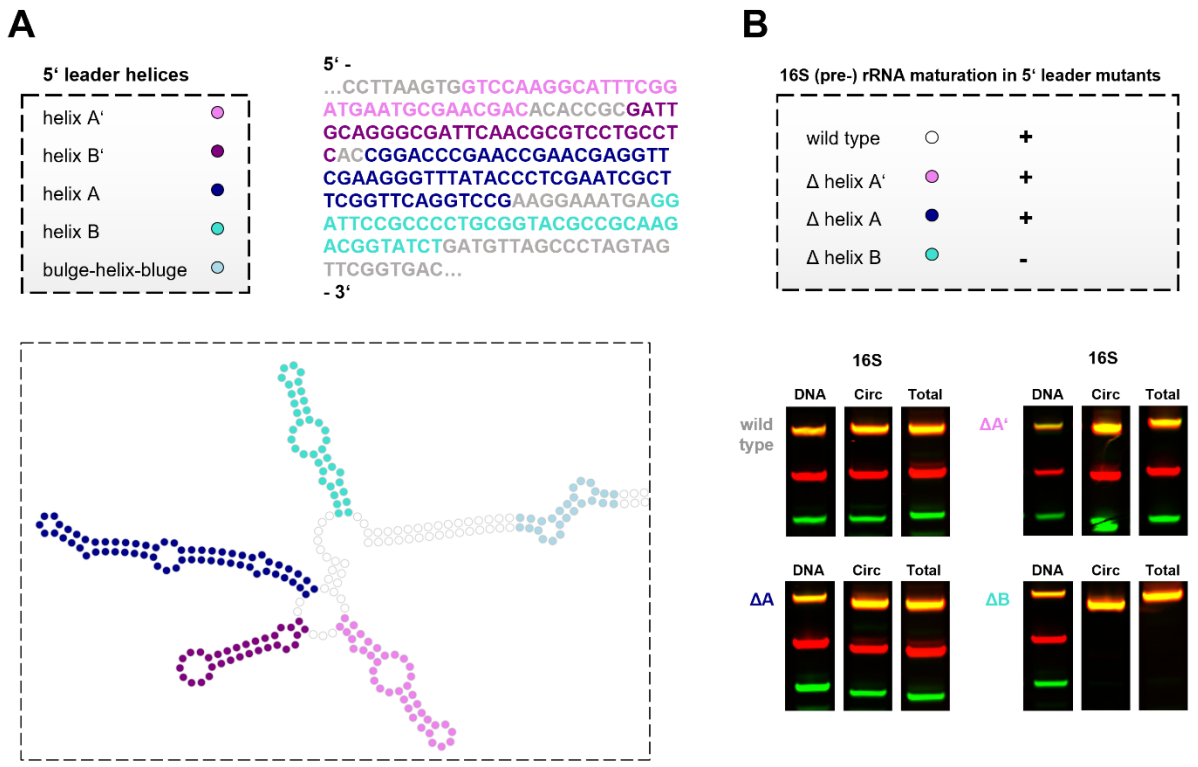

Figure 11: Effects of 5‘ leader helices on 16S pre-rRNA maturation. (**A**) Nucleotide sequence and predicted secondary structure of 5’ leader helices A’ (pink), B’ (purple), A (darkblue) and B (cyan) is depicted. The predicted secondary structure also shows the bhb motif. (**B**) Analysis of 5’ leader mutants. Helix A’, A and B were individually deleted and analyzed with the *cis*-acting reporter assay. Helix B had a strong effect on circular pre-rRNA and total rRNA production. Helix A’ and A behaved like the wild type. Exemplary PAGE-gels are shown in the lower panel of **B**. RNA secondary structures have been calculated with the ViennaRNA Web Services website (Gruber et al. 2008).

Interestingly, helix B seems to be quite conserved in several halophilic archaea and was suggested to have a similar role as eukaryotic U3 snoRNA (P. P. Dennis, Russell, and Moniz De Sá 1997). U3 snoRNA is required in *S. cerevisiae* for the promotion of early cleavage events by binding to complementary 5’-ETS sequences (J. m. Hughes and Ares Jr 1991; Beltrame and Tollervey 1995). Furthermore, U3 snoRNA possess an RNA chaperone function for the folding of the central pseudoknot (CPK) in the SSU rRNA through long-range base pairing interactions (see figure 12 B) (J. M. X. Hughes 1996; Dutca, Gallagher, and Baserga 2011; Kudla et al. 2011; Woolford and Baserga 2013; Kressler, Hurt, and Baßler 2017). The universally conserved central pseudoknot connects the 5’ domain with the central and 3’ major domains and is shown in figure 12 A in the mature SSU rRNA of *E. coli*.

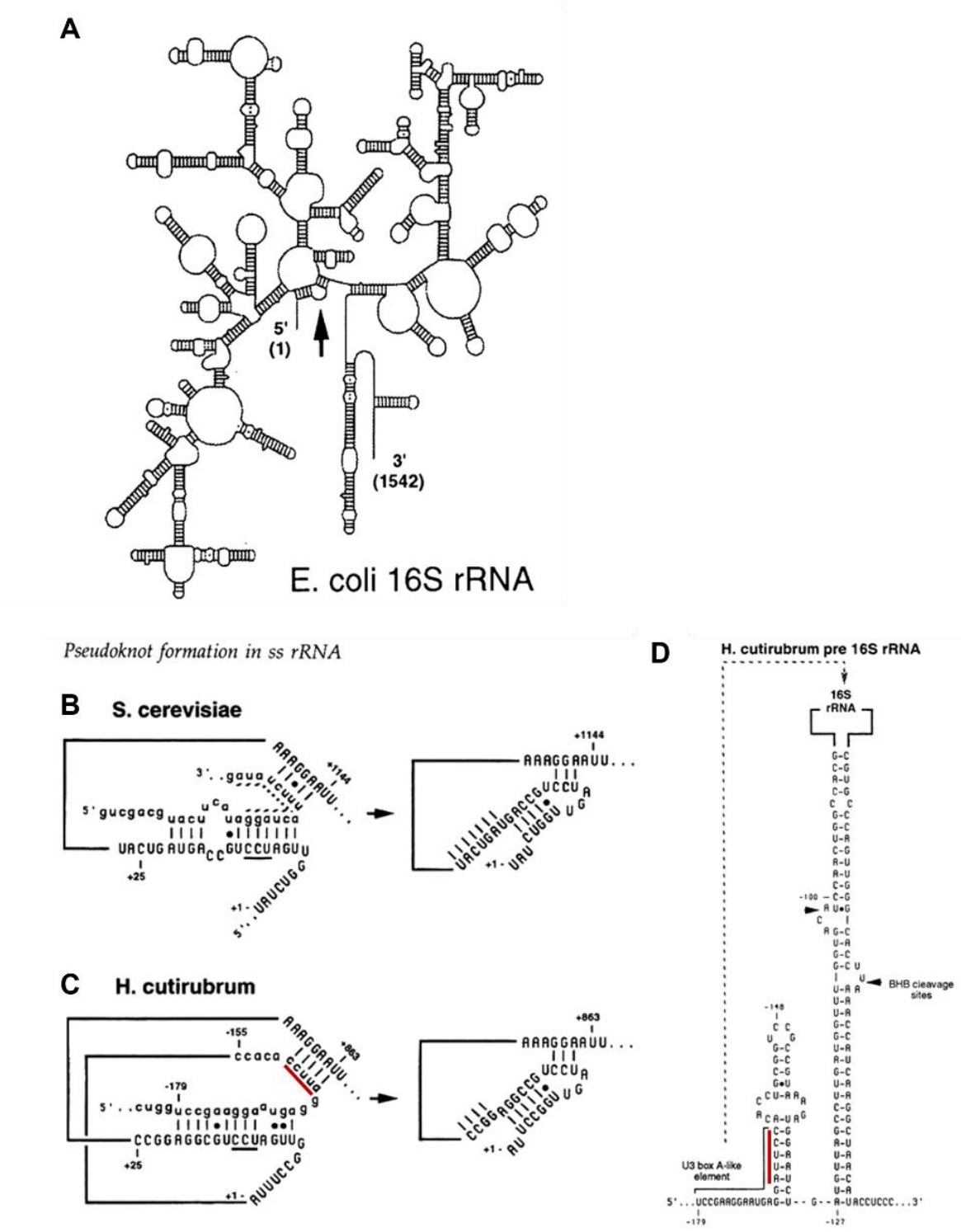

Figure 12: Model for central pseudoknot formation by U3 snoRNA or 5' leader regions. (**A**) Secondary structure of mature 16S rRNA in *E. coli*. The universally conserved central pseudoknot (CPK), indicated by a black arrow, is a hallmark structure connecting the 5' terminus with central and 3'-terminal domains. (**B**) Interaction of U3 snoRNA (lower case) with 5'-terminal regions (upper case) of 18S rRNA prevents premature formation of CPK in *S. cerevisiae*. Rearrangement and displacement of U3 snoRNA during ribosome biogenesis allows proper folding of CPK. (**C**) Proposed interaction of 5' leader region with 5'-terminal regions of 16S rRNA in *H. cutirubrum*. 5' leader sequence base pairs and blocks pseudoknot region, indicated by a red line. Rearrangement and displacement of interacting 5' leader sequence to allow proper folding of CPK. (**D**) Secondary structure of *H. cutirubrum* 16S pre-rRNA. Helix B is depicted in front of the long 16S pre-rRNA processing stem and contains a U3 box A-like element. The sequence potentially base pairing with the CPK region is highlighted by the red line. Adapted from P. P. Dennis, Russell, and Moniz De Sá 1997.

Importantly, the essentiality of the central pseudoknot in the mature SSU for translation functionality was demonstrated previously (Poot et al. 1998). It is a critical step during the assembly of the small subunit and occurs late in the SSU assembly pathway (Powers, Daubresse, and Noller 1993; Besançon and Wagner 1999; Holmes and Culver 2004; Sashital et al. 2014). Since U3 snoRNA is missing in prokaryotes, the question arose, how the CPK is properly formed in bacteria and archaea. Previous studies in *E. coli* could provide evidence for an interaction of the 5' leader sequence with central helices forming the CPK in the 16S rRNA (Dammel and Noller 1993; Pardon and Wagner 1995). Thereby, it putatively competes for the base-paring with helix 1 and blocks the premature CPK formation. Remarkably, the RNA secondary structure 5' leader core region from the rDNA operon B in *E. coli* looks stunningly similar to the RNA structure seen in figure 11 A (Pardon and Wagner 1995). Correspondingly, based on sequence and structure analyses in several bacteria and halophilic archaea, Dennis et al. suggested interactions of helix B with the CPK sequences in the SSU pre-rRNAs, thereby guiding the proper folding dynamics during assembly. They proposed a *cis*-acting U3 snoRNA-like mechanism provided by the pre-rRNA leader sequence in prokaryotes, as they lack U3 snoRNA (see figure 12 C & D; P. P. Dennis, Russell, and Moniz De Sá 1997). To address this issue *in vivo* and learn more about the function of helix B in rRNA maturation we engineered an additional set of targeted helix B mutations. Mutations were either changing the secondary structure of the helix, altering nucleotides potentially interacting with the CPK region (see helix B wild type in figure 13 A) or an insertion of six adenosines to increase the distance between helices. The predicted secondary structures of the designed mutants and the results of the *cis*-acting elements reporter assay are shown in figure 13. The relative expression analysis of these mutants revealed a reduction of 16S total rRNA amounts compared to the wild type, however, to varying degrees. The T37C substitution resulted in a more stable G-C bond compared to G·U at the base of the stem and had the smallest effect with a moderate reduction to around 40 % of total 16S rRNA production. In this mutant, the sequence AUUCC which putatively interacts with the CPK region (see figure 12 A) is not changed and the structure presumably resembling wild type helix B (see 13 A). The predicted secondary structure of G2A mutation showed a disruption of the base pairing at the base of helix B and had a stronger effect than T37C. Exchanging the first four and the last four nucleotides kept the stem structure and led to a reduction to 15-20 % of 16S total rRNA production compared to the wild type. Changing the upper part of helix B but keeping the same structure, deletion of the middle part or introducing a leader sequence of six adenosine had a detrimental effect on 16S total rRNA output. Noteworthy, already single nucleotide substitutions had a moderate (T37C) to strong (G2A) effect and integrity of sequence and structure might both be required for the physiological function of helix B. Introduction of a 6A leader sequence had also drastic effects, even though helix B itself was not altered.

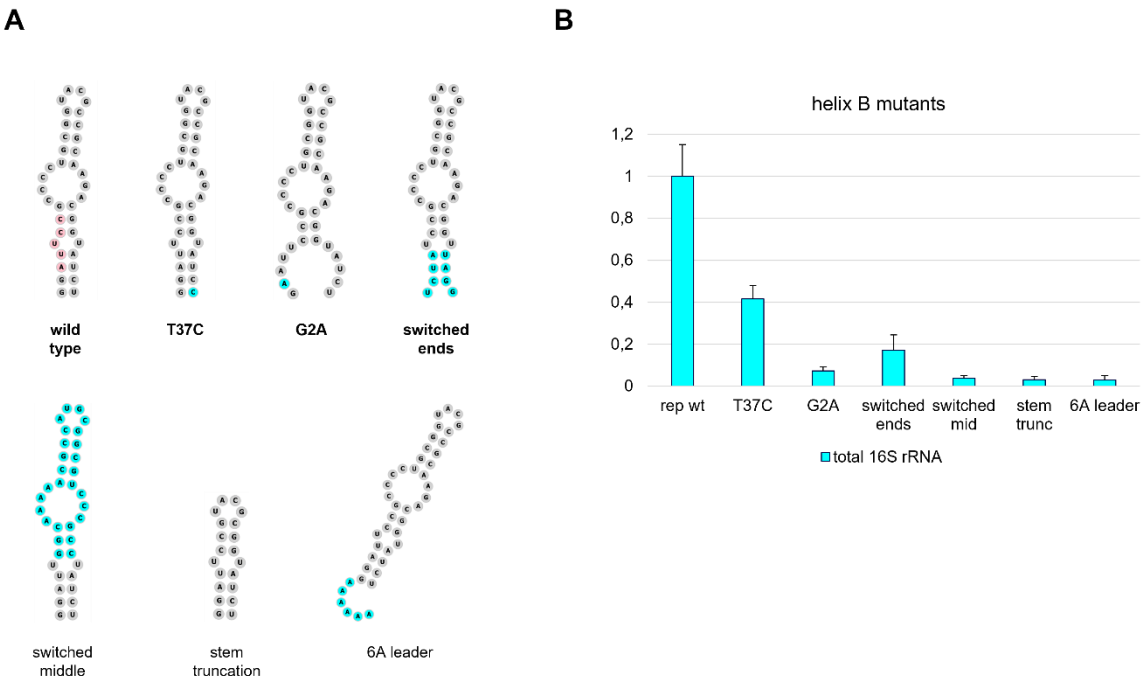

Figure 13: Helix B mutations affect total 16S rRNA production. (**A**) The predicted secondary structures of helix B wild type and introduced mutations are shown. Nucleotides potentially interacting with CPK sequences are highlighted in pink in the helix B wild type structure. Alterations from helix B wild type are given in cyan. (**B**) Effects of the helix B mutations of the relative total 16S rRNA production are depicted. Two to three biological replicates were analyzed. RNA secondary structures have been calculated with the ViennaRNA Web Services website (Gruber et al. 2008).

In summary, we could show that helix B has a particular role in 16S pre-rRNA maturation and is important for total 16S rRNA production. Nevertheless, the question of what makes up for the functional significance of helix B in detail remains open and awaits further investigation. An additional set of mutants for the reporter assay or supplementary methods would be required to better understand the molecular functional basis of this structural pre-rRNA element (see also discussion in 8.2). In addition, large-scale bioinformatical analysis of 5' leader secondary structures could greatly benefit an understanding how widespread the functional relevance of helix B might be in archaea. Out of curiosity, we predicted the secondary structures in one selected, intriguing example: *Haloarcula marismortui* (see supplementary figure S2). This organism has three different rDNA operons with remarkable sequence variability and a bhb motif is only found in one of three 16S processing stems (Mylvaganam and Dennis 1992; Baliga et al. 2004). Noteworthy, helix B is in its sequence and structure very conserved in all three operons. This might suggest a similar role in the same task during ribosome biogenesis. The function seems to be independent from the respective rRNA variant and the presence of a 16S bhb motif, indicating a role not directly linked to circularization of 16S pre-rRNAs.

5.5. Insights into archaeal rRNA processing using Nanopore-based RNA sequencing

5.5.1. Introduction

So far, we and others could provide evidence how early pre-rRNA steps occur and which *cis*- and *trans*-acting elements are involved in the formation of circular pre-rRNAs (Jüttner et al. 2020; Schwarz et al. 2020; Qi et al. 2020). A big part of this work was done in *Haloferax volcanii*. At this point we wanted to for one gain insights into the pre-rRNA processing post-circularization, secondly, confirm previous findings and lastly, expand our knowledge how rRNA maturation functions in other archaeal species.

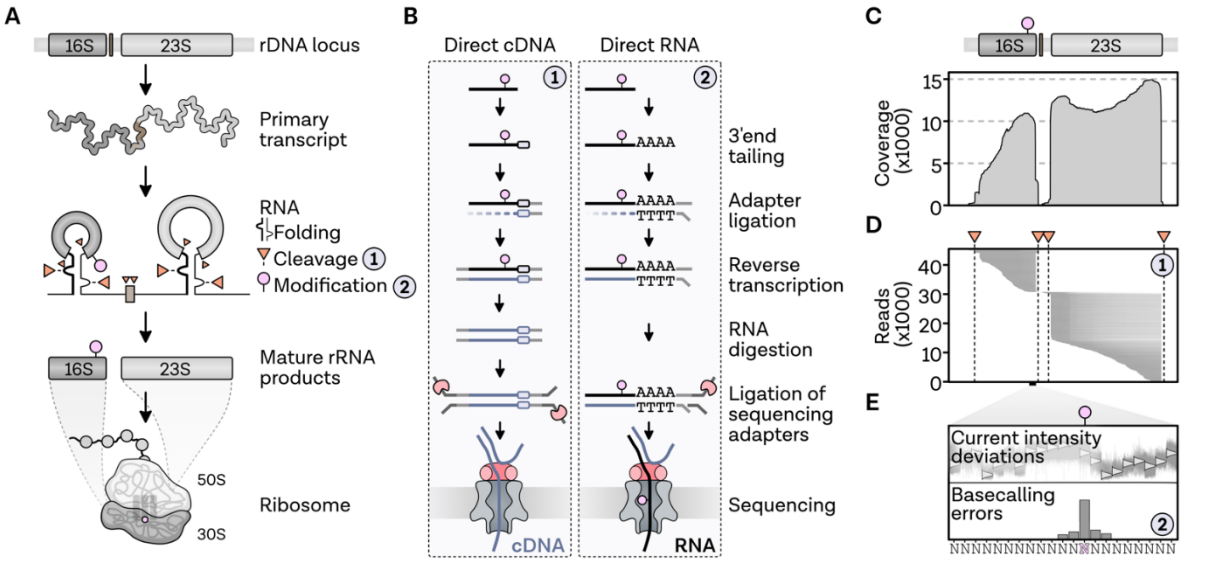

Figure 14: Investigating rRNA maturation using Nanopore-based RNA-seq. (**A**) Simplified depiction of archaeal rRNA maturation beginning with the primary transcript containing all rRNA species. Orange triangles represent endonucleolytic cleavage events, whereas pink dots represent rRNA modifications. (**B**) Workflow for direct cDNA or direct RNA sequencing approaches. (**C-E**) Exemplary readout and data analysis after Nanopore sequencing of archaeal rRNAs. (**C**) Exemplary direct cDNA read coverage profile (**D**), exemplary single-read plot of *H. volcanii* rDNA locus I with cleavage events indicated (orange triangles) (**E**) and detection of RNA base modification by base calling errors is shown. From Grünberger et al. 2022.

Typically, the illumination of rRNA maturation pathways requires intricate, challenging biochemical studies and/or genetically tractable model organisms. In our case, we established the *cis*-acting elements reporter assay for *H. volcanii*. Notwithstanding that it is a very useful tool to answer specific questions about the role of certain structural RNA elements, this method lacks a broader, more general perspective, and so far, is restricted to one model organism. In

contrast, state of the art RNA-seq technologies combine more general applicability with great explanatory power and can represent valuable alternatives. As such, Oxford Nanopore Technology (ONT) provides a long-read sequencing platform which allows to study full-length transcripts at single-molecule resolution. In principle, nucleic acids move through a protein nanopore sitting on a membrane and changes in current are detected and translated into sequence information. Recently, this technique was used to compare different RNA sequencing protocols in *E. coli*. Direct RNA-seq suffered from lower yields and accuracy compared to direct cDNA or PCR amplified cDNA sequencing, on the other hand some RNA modifications can be read-out in direct RNA-seq approaches (Grünberger, Ferreira-Cerca, and Grohmann 2022). The great advantage of such technologies lies in the potential to investigate very long transcripts at single-molecule resolution and retain 5' and 3' end information. Hence, these features potentially make ONT a viable means to obtain a comprehensive overview about the rRNA processing pathway. We started a collaboration with Dr. Felix Grünberger and Prof. Dina Grohmann from the microbiology department (University Regensburg) and used ONT to examine rRNA maturation in archaea. Therefore, we chose three exemplary, phylogenetically distant archaeal species: the Euryarchaeota *Haloferax volcanii* and *Pyrococcus furiosus* and the Crenarchaeon *Sulfolobus acidocaldarius*. This exploration used both direct cDNA and direct RNA sequencing approaches. Figure 14 shows the basic workflow of this analysis.

5.5.2. Results

The following results are the outcome of a collaborative study with Dr. Felix Grünberger, Prof. Dina Grohman and our group. ONT sequencing including library preparation and bioinformatical data evaluation was performed by Felix Grünberger. Cultivation of *S. acidocaldarius* and *H. volcanii* strains and biochemical work like primer extension, RNase H cleavage assays and Northern blots were performed by Robert Knüppel and me. The main findings of this study will be outlined in the ensuing paragraphs and refer to the submitted preprint (Grünberger et al. 2022).

5.5.2.1. Direct cDNA sequencing of *Haloferax volcanii*

Amplification free, (i.e., no PCR step) direct cDNA Nanopore sequencing was performed to identify various pre-rRNA maturation stages. Instead of 3'-poly(A)-tailing a custom 3' adaptor

was used to improve the detection quality of 3' ends. For the classification of potentially new rRNA processing intermediates it is crucial to exclude sequencing artifacts and confidently identify genuine full-length transcripts. To avoid misinterpretation of terminal ends, reads were filtered according to having simultaneously 5' and 3' adaptors in the right orientation. After quality control and reads filtering the first striking observation was that the terminal positions of mature rRNAs in *H. volcanii* did not match the available annotations at the NCBI. To validate our data, we performed primer extension analysis which confirmed the Nanopore sequencing results (data not shown, see preprint). Hence, the corrected annotation was used for the subsequent analysis.

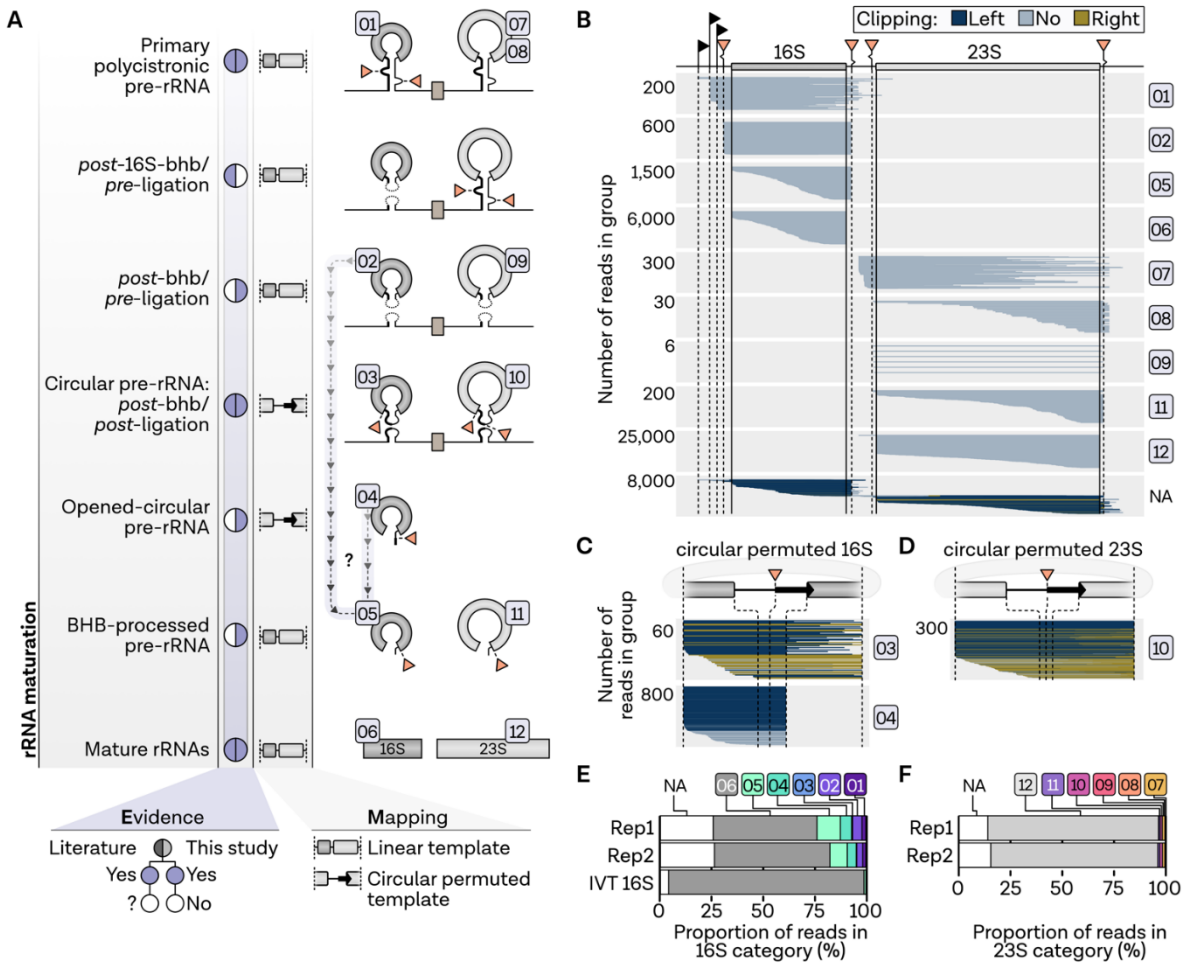

Figure 15: Ribosomal RNA processing in *H. volcanii*. (**A**) Proposed rRNA maturation in *H. volcanii* based on ONT direct cDNA sequencing results. Distinct classes of rRNA precursors were detected. Classes 1 to 5 represent 16S pre-rRNA maturation, classes 7 to 11 represent 23S pre-rRNA maturation. Some of these intermediates were previously described elsewhere. Processing sites are indicated by orange triangles (**B**) Individual reads mapping to genomic linear template (x-axis), sorted according to read start position. Y-axis is showing the relative number of reads. (**C** & **D**) Individual reads mapping to 16S and 23S circular permuted templates. (**E** & **F**) Read proportion of detected 16S and 23S (pre-)rRNA intermediates is shown as stacked bar charts. From Grünberger et al. 2022.

First, the start of rDNA transcription at the three promoters in *H. volcanii* could be visualized. A full-length primary transcript comprising 5'-leader-16S-tRNA-23S-5S-(tRNA)-trailer-3' could not be seen with this analysis, indicating co-transcriptional or very fast first cleavage events. In comparison, in *E. coli* only 1 % to 2 % of total rRNA account for long precursor species whereas later processing intermediates are more abundant (King and Schlessinger 1983). Figure 15 shows the unambiguous identification of several pre-rRNA species. Primary pre-rRNAs were indirectly observed as either 5'- (class 8) or 3'- (class 1 and 7) processed reads. The next noticeable maturation stages were post-bhb-cleavage/pre-ligation intermediates (class 2 and 9).

The second class of precursors corresponded to circular pre-rRNAs, in other words post-bhb-cleavage/post-ligation. Yet, it must be stated, that these molecules cannot be directly read-out with ONT sequencing as no free ends are available for adapter ligation. Thus, the reads most likely originate from random nicking of circular pre-rRNAs during sample preparation. This observation was validated by re-mapping Nanopore reads to an artificially designed, permuted sequence in which 3' and 5' processing sites of the bulges are joined. Previous findings with our *cis*-acting elements reporter assay indicated a distinct order of 16S bhb and 23S bhb processing Supposedly, it would imply the presence of a precursor containing the ligated 5′ leader/3′ trailer sequences of the cleaved 16S pre-rRNA flanking regions joint to the nascent 23S pre-rRNA (Jüttner et al. 2020). However, this particular intermediate could not be detected in the direct cDNA approach in *H. volcanii*.

The third main class corresponded to a putative 16S pre-rRNA species (class 4) with an extended, immature 3' end which maps to permuted spacer sequences found in the circular 16S pre-rRNA. Possibly, this intermediate results from an endonucleolytic linearization of circular 16S pre-rRNAs at the mature 5' terminus. The last observable class was defined by a mature 5' end and an accurate 3' end at the bhb cleavage site and seen in 16S and 23S processing pathways (class 5 and 11). Two mutually exclusive options are considerable for the generation of this class and cannot be further dissolved with our current knowledge. The first possibility depends on previous circularization and further endo- or exonucleolytic trimming of re-opened class 4 intermediates. On the other hand, an alternative, circularization-independent pathway following class 2 or 9 with prior processing of the mature 5' to the 3' terminus could account for class 5 and 11 intermediates (see figure 15 A & 15 B). Considerably, different pathways could guide 16S and 23S pre-rRNA processing post-circularization or alternative, circularization independent ways for rRNA maturation could take place.

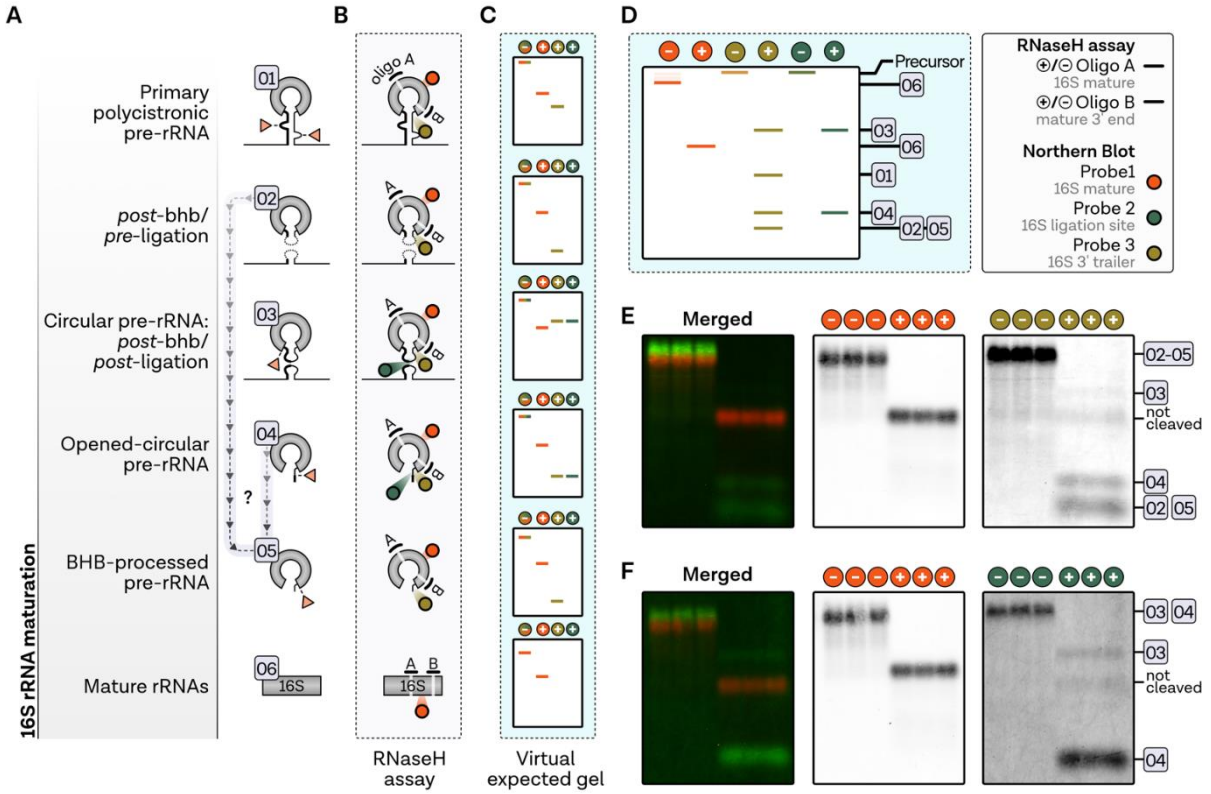

Figure 16: Validation of 16S pre-rRNA species with RNase H cleavage assay and Northern blot. (**A**) Proposed 16S maturation pathway with pre-rRNA species determined by Nanopore-based sequencing is depicted and suggested cleavage sites are indicated by orange triangle. (**B**) Workflow of RNase H assay. Oligo A and B are annealed to the mature 16S rRNA and RNase H cleaves DNA-RNA hybrids at the indicated sites. Red, green and yellow ocher dots represent the binding sites of Northern blot probes 1 to 3. (**C**) Expected virtual gel for all found 16S (pre-) rRNA species after RNase H cleavage assay is shown with (+) and without (-) RNase H. Colours correspond to the respective Northern blot probes. (**D**) Overview of expected cleavage products of all 16S (pre-) rRNA species with and without RNase H and the respective Northern blot probes. Right panel shows positions of the used oligos and probes for RNase H cleavage assay or Northern blot. (**E**) Northern blot after RNase H cleavage assay of *H. volcanii* h26 total RNA with (+) and without (-) RNase H. Probe 1 (red) and probe 3 (yellow ocher) were used for hybridization. Note that total RNA was not cleaved a 100 % by RNase H. (**F**) Similar to **E**. Probe 1 (red) and 2 (green) were used for hybridization. From Grünberger et al. 2022.

As confirmation of the observed 16S pre-rRNA intermediates we performed RNase H cleavage assays with subsequent Northern blot analysis, which are described in material & methods 9.2.7.5 and 9.2.7.6. One major advantage of this assay is the differentiation of circular and 5' end opened circular intermediates which are similar in size and sequence. In brief, total RNA was extracted and specific DNA oligos annealed. RNase H cleaves these RNA/DNA hybrids and differently sized cleavage products can be analyzed with fluorescent Northern blot oligos. Thus, rRNA processing intermediates can be identified, as seen in figure 16 E and 16 F. With these experiments 16S pre-rRNA classes 2, 3, 4 and 5 were readily detectable in *H. volcanii* and confirmed the ONT results.

Overall, we could identify several new maturation stages, confirm already described precursors and propose a pre-rRNA processing pathway for *H. volcanii* (see figure 15 A). Based on the

observation of defined 3’ ends in pre-rRNAs one can speculate that this pathway is mostly governed by endonucleases. However, rapid exonucleolytic activities resulting in distinct 3’ termini cannot not be excluded at this point.

5.5.2.2. Direct cDNA sequencing of *Pyrococcus furiosus*

The second euryarchaeal model organism analyzed in this project was the hyperthermophilic organism *Pyrococcus furiosus*. By and large, the observed pre-rRNA processing pathway resembled the one from *H. volcanii* (see figure 17 A). Yet, a few differences must be highlighted. First, post-bhb-cleavage/pre-ligation intermediates (class 2 and 9) could not be detected. The 3’ ends of 16S pre-rRNAs (class 4 and 5) were less precisely defined potentially hinting towards exonucleolytic trimming of these pre-rRNAs in *P. furiosus*. Another peculiarity concerns the mature 23S rRNA, which was described to be circularly permuted through the excision of RNA helix 98 (H98) after circularization (Birkedal et al. 2020). Hence, reads of the mature 23S rRNA had to be re-mapped to specifically designed permuted sequences. Circular pre-rRNAs were detected similarly to the workflow performed in the analysis of *H. volcanii*. Indeed, the excision of H98 requires previous circularization of pre-rRNAs and provides evidence for the necessity of this archaea-specific maturation event in *P. furiosus* (see figure 17 A & 17 C).

5.5.2.3. Direct cDNA sequencing of *Sulfolobus acidocaldarius*

The third member on board of this enterprise, *Sulfolobus acidocaldarius* represents the Crenarchaeota. Durovic and Dennis investigated the pre-rRNA maturation of this hyperthermophlic organism almost 30 years ago and reported 11 separate processing sites (Durovic and Dennis 1994). The terminal positions from this study combined with the ones observed so far in *H. volcanii* and *P. furiosus* were taken into consideration for (pre-)rRNA stage classification in *S. acidocaldarius* (see figure 17 D and 17 E). Primary rRNA transcripts were again not detectable, only indirectly via classes 1, 7 and 8. Like *P. furiosus* post-bhb-cleavage/pre-ligation intermediates (class 2 and 9) could not be detected. Also different from *H. volcanii* and resembling more *P. furiosus* was the observation, that 3’ termini of class 4 and 5 intermediates did not seem to be generated by distinct endonucleolytic processing events at defined positions, rather by exonucleolytic trimming. On the other hand, several distinct 23S pre-rRNA processing sites were revealed.

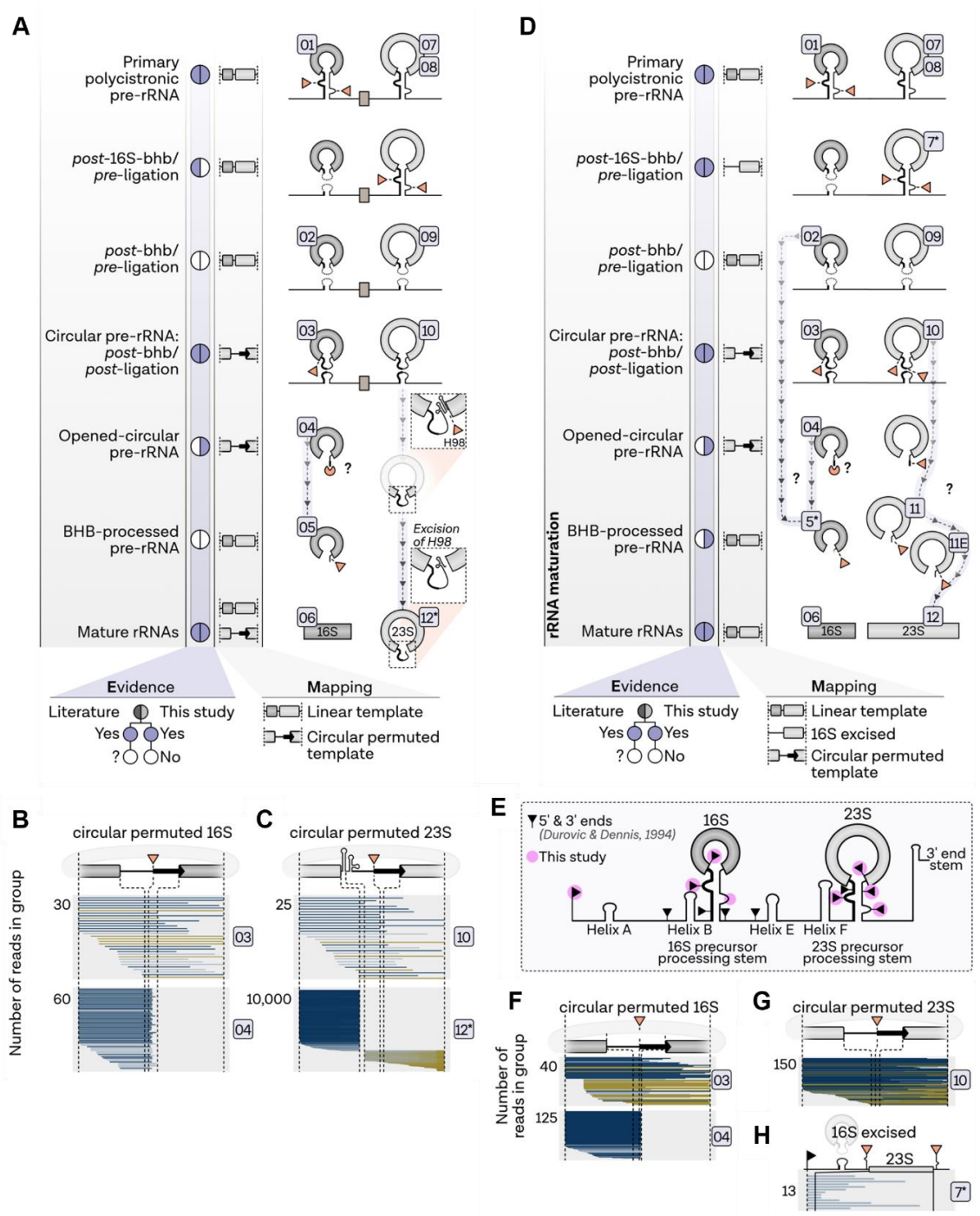

Figure 17: Ribosomal RNA processing in *Pyrococcus furiosus* (A-C) and *Sulfolobus acidocaldarius* (D-H) (**A**) Proposed rRNA maturation in *P. furiosus* based on ONT direct cDNA sequencing results. Distinct classes of rRNA precursors were detected. Classes 1 to 5 represent 16S pre-rRNA maturation, classes 7 to 10 represent 23S pre-rRNA maturation. Some intermediates were previously described elsewhere. Note that mature 23S rRNA (class 12*) is circularly permuted and results from excision of H98. Processing sites are indicated by orange triangles. (**B** & **C**) Individual reads mapping to *P. furiosus* 16S and 23S circular permuted templates. (**D**) Proposed rRNA maturation in *S. acidocaldarius* based on ONT direct cDNA sequencing results. Distinct classes of rRNA precursors were detected. Classes 1 to 5 represent 16S pre-rRNA maturation, classes 7 to 11 represent 23S pre-rRNA maturation. Some intermediates were previously described elsewhere. Processing sites are indicated by orange triangles. (**E**) Detection of 5'- and 3'- terminal positions in Durovic & Dennis (1994) in comparison with ONT data analysis. Several positions could be confirmed, one new processing site was found, whereas some previously reported positions could not be verified. (**F** & **G**) Individual reads mapping to *S. acidocaldarius* 16S and 23S circular permuted templates. (**H**) Detection of maturation stage class 7* with excised 16S pre-rRNA. This intermediate results from prior 16S bhb prior to 23S bhb cleavage and contains joint 5′ leader/3′ trailer sequences of the cleaved 16S pre-rRNA flanking regions with the nascent 23S pre-rRNA. Adapted from Grünberger et al. 2022.

Interestingly, another, yet unseen intermediate was found. This precursor species (class 7*) results from prior 16S bhb to 23S bhb cleavage and contains joint 5′ leader/3′ trailer sequences of the cleaved 16S pre-rRNA flanking regions with the nascent 23S pre-rRNA. Reads were re-mapped to a 16S rRNA excised sequence as validation of this intermediate. The results were convenient with what was hypothesized from the *cis*-acting elements reporter assay in *H. volcanii* and previously detected in *Archaeoglobus fulgidus* and *Saccharolobus (*formerly *Sulfolobus*) *solfataricus* (Tang et al. 2002; Jüttner et al. 2020). Presumably, processing dynamics are too rapid to see this pre-rRNA species in *H. volcanii* and/or higher sequencing depth would be necessary.

5.5.2.4. Detection of stage-specific rRNA modification

As mentioned before, a superb advantage of Nanopore-based RNA-seq technology is the capacity to detect RNA modifications. After classifying the archaeal rRNA maturation pathways with various pre-rRNA intermediates by cDNA sequencing, we aimed to explore the possibility to assign RNA modifications to distinct maturation stages. Therefore, we turned to direct RNA-sequencing in *H. volcanii*, which is outlined in figure 14 B and 14 E. Since the chemical nature of some RNA modifications causes a notable increase in base calling errors, these aberrations can be bioinformatically interpreted as the presence of the respective RNA modification. As our testing ground we were focusing on the KsgA/Dim1-dependent di-methylation of two adjacent adenosines in helix 45 of the SSU rRNA. A *H. volcanii* knockout strain for this RBF was readily available in our lab and served as control. After direct RNA sequencing, reads were first sorted according to the described pre-rRNA classes in *H. volcanii*. Then, base calling errors were examined by the in Eligos2 implemented algorithm to determine stage-dependent installation of the KsgA/Dim1 introduced methylation. Strikingly, early 16S rRNA precursors (class 1 and 2) did not show statistically significant modification in helix 45. The earliest time point KsgA/Dim1-dependent methylations can be assigned with statistical confidence concerns precursors after circularization (data not shown, see preprint). To this end, we can conclude, that stage-specific detection of rRNA modifications is in principle feasible with Nanopore-based direct RNA-sequencing. Still, it must be stated, that this kind of analysis relies on the chemical nature and size of the respective RNA modification. Knockout strains lacking the respective RNA modification might be also very helpful to establish the protocols. Furthermore, additional archaeal species should be analyzed in the same way to show the reproducibility of the technique. Likely, *P. furiosus* and *S. acidocaldarius* would be the most suited model organisms to begin with, as direct cDNA sequencing has already been performed and KsgA/Dim1 knockout strains are available (Knüppel et al. 2021).

5.5.3. Discussion

To summarize, in this collaborative work we have explored the capacity of Nanopore-based sequencing to study features of rRNA maturation in archaea. Three model organisms which represent the euryarchaeal and crenarchaeal phyla had been selected. For stage-specific classification of pre-rRNA intermediates amplification-free direct cDNA sequencing was performed and rRNA processing pathways were proposed for each examined archaeon after bioinformatical data analysis. As to the limitations of this investigation circular pre-rRNAs can only be identified indirectly through random nicking during library preparation, which makes absolute quantification of pre-rRNAs difficult. Additionally, the primary full-length transcript could not be directly observed in any of the three organisms due to either 3' RT (reverse transcriptase) bias, (i.e., insufficient, aberrant reverse transcription) or fast and/or co-transcriptional cleavage events. In general, it seems that short-lived or low abundant pre-rRNAs might escape the detection, presumably due to rapid rRNA processing *in vivo*. The classes 2 and 9, for example could only be seen in *H. volcanii*, not in the other two archaea, although based on our current knowledge these intermediates should exist. Hence, in depth comparison of species-specific rRNA maturation might be difficult as half-life of precursor and general rRNA processing dynamics appear to differ from organism to organism, potentially also in varying growth conditions. For instance, the intermediate originating from post-16S-bhb-cleavage/pre-23S-bhb-cleavage and ligation of 16S 5' leader and 3' tailer sequences was only found in *S. acidocaldarius*. Although cDNA sequencing could not demonstrate this intermediate in *P. furiosus*, we could show its existence in an earlier analysis using a direct RNA sequencing approach (Grünberger et al. 2020). We hypothesized the existence of this precursor in a previous study in *H. volcanii*, however it might be too short-lived to be detectable with the ONT approach (Jüttner et al. 2020). Still, the same processing order starting at the 16S bhb motif, seems to apply in the distantly related *S. acidocaldarius* as well. To circumvent detection issues, sequencing depth could be increased, even though it might be difficult to establish a generally applicable standard. On the other hand, commonalities found in the individual maturation processes can be regarded as more robust findings and furthermore as universal principles underlying rRNA maturation in archaea. Accordingly, the presence of circular pre-rRNAs was indirectly shown in all three model systems, as well as some other common precursors. Remarkably, a recent study claimed, that mature 23S rRNA in *P. furiosus* lacks H98 and may also be a circular molecule (Birkedal et al. 2020). Our analysis in *P. furiosus* could confirm the observed excision of H98, however we could not find any evidence supporting the existence of circular, mature 23S rRNA. An investigation in a methanogenic archaeon proposed an opening of circular 16S pre-rRNA by the endonuclease Nob1 at the mature 3' end (Qi et al. 2020). Our findings clearly contradict this notion since we could show

in all three archaeal representatives an endonucleolytic cleavage near the mature 5’ end prior to final 3’ end maturation.

We used the KsgA/Dim1-dependent di-methylations in h45 of the 16S rRNA as a benchmark to explore the possibility of assigning precursor stage-specific rRNA modification patterns. We were able to show that the modification in h45 occurs rather late during ribosome biogenesis. Nevertheless, there are still technical limitations and further improvements of the technology must be done to achieve a more global investigation of (pre-)rRNA modifications.

In conclusion, we regard Nanopore-based sequencing as very valuable tool to study rRNA processing in archaea. Although the technology comprises some limitations, its broad applicability is a huge advantage. It relies only on the cultivation of the model organism but does not require any genetic tools to study ribosome biogenesis in archaea. This is especially precious in the archaeal domain where genetics are not widely applicable and in general challenging. Therefore, future studies focusing on different growth conditions, knockouts of RBFs or additional representatives of the archaeal community are feasible and of great interest.

5.6. Structural and functional analysis of archaeal RNase E/G-like

5.6.1. Phenotypical and functional analysis of archaeal RNase E/G-like

Besides a few exceptions, RNases participating in archaeal rRNA processing are still very poorly identified and characterized. As described above, RNase E and G are important players for rRNA processing in *E. coli* (see 5.1.2). RNase E/G-like activity has been described *in vivo* in Thermococcales and *in vitro* in several halophiles, among them *Haloferax volcanii* (Franzetti et al. 1997; Ikeda et al. 2017). The corresponding enzyme in *T. kodakarensis* FAU-1 was reported to be involved in rRNA processing (Ikeda et al. 2017). Now, we wanted to investigate this potential ribonuclease in *H. volcanii* and check for a possible contribution to rRNA processing. Our collaboration partners from the group of Prof. Anita Marchfelder at the university of Ulm generated a viable *H. volcanii* RNase E/G-like deletion strain which was phenotypically analyzed (PhD thesis Karina Haas 2017). The RNase E/G-like knockout had almost no detectable growth phenotype, also in different stress conditions like salt or temperature stress (PhD thesis Karina Haas). A subtle discrepancy was observed in the final OD_{600nm} cells reached during heat stress. Spot assays in similar conditions were performed in our lab and confirmed the previous observations (data not shown). Light microscopy of wild type and ΔRNase E/G-like cells revealed no striking differences in the overall cellular morphology, even though ΔRNase E/G-like cells were slightly smaller (PhD thesis Karina Haas).

After characterization of growth behavior and cell morphology, we wanted to examine whether rRNA processing is affected in the RNase E/G-like knockout. Therefore, we transformed *H. volcanii* RNase E/G-like knockout cells with either an empty control plasmid or a complementation plasmid encoding the full-length protein. Total RNA was extracted from these cells, and we performed RNase H cleavage assays, as described above (see 5.5.2 or in material & methods 9.2.7.6). The readout was achieved by subsequent Northern blot analysis with fluorescent probes targeting different 16S pre-rRNA species, as depicted in figure 18 A & B. The control reactions without RNase H in the colored image in the upper panel in figure 18 C reveal a clear accumulation of intermediates visualized by the 16S pre-rRNA ligation site probe in the knockout compared to the complementation strain. Fluorescent signals in green represent a mixture of 16S pre-rRNA classes 3 and 4 (referring to Nanopore sequencing results), which are illustrated in figure 18 A. RNase H cleavage assay enables the further differentiation of the intermediates class 3 and 4 as seen in the black and white image at the bottom in figure 18 C. Accordingly, the greatest fraction of the signal (class 3 and 4) stems

from an accumulation of opened circular, 3'-extended 16S pre-rRNAs (class 4) and only a minor fraction represents circular 16S pre-rRNAs (class 3).

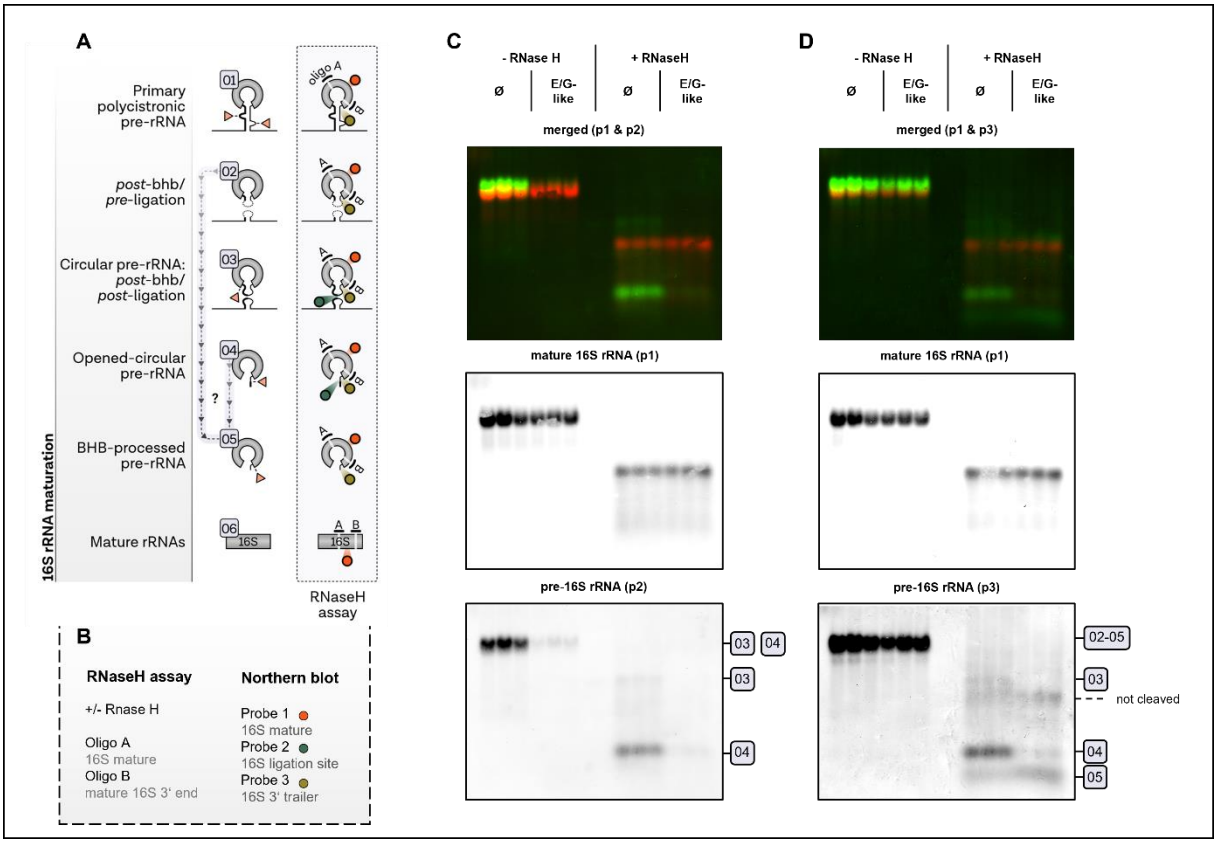

Figure 18: *H. volcanii* RNase E/G-like is involved in 16S pre-rRNA maturation. (**A**) 16S pre-rRNA maturation pathway derived from Nanopore sequencing analysis with cleavage events indicated by orange triangles. Oligo A and B were used for RNase H cleavage assay. The target regions for Northern blot probes 1 to 3 are represented by red, green, and yellow ocher, respectively. (**B**) Oligos and probes from (**A**) listed showing their purpose and target region. RNase H cleavage pattern is presented in figure 16 D. (**C & D**) Accumulation of distinct 16S pre-rRNA species in RNase E/G-like deficient *H. volcanii* strain. RNase E/G-like KO was transformed with a RNase E/G-like complementation plasmid and an empty control plasmid (Ø). After RNase H cleavage assay with oligos A and B Northern blot analysis with probes 1 and 2 (**C**) and 1 and 3 (**D**) was performed. RNase H cleavage allows to differentiate between pre-rRNA species 3 and 4, as both are detected with probe 2, but have varying length. Note, that the major fraction of the accumulation seen with probe 2 stems from an accumulation of pre-rRNA species 4. Panels **A** and **B** are adapted from Grünberger et al. 2022.

The second fluorescent oligo we applied on the same Northern blot detected a broader range of 16S pre-rRNA intermediates (classes 2 to 5) upstream and downstream in the processing pathway (see figure 18 A & B). Conversely, no strong accumulation of precursors could be demonstrated in this experiment, even though an accumulation of 16S pre-rRNA species 3 and 4 was detectable after RNase H cleavage in the knockout background. Hence, an overall accumulation of 16S pre-rRNAs does not occur in the absence of RNase E/G-like arguing for alternative or complementary processing events downstream of RNase E/G-like cleavage. At

this point, we could provide evidence for an active participation of archaeal RNase E/G-like in 16S pre-rRNA processing and thus identify a novel ribosome biogenesis factor in *H. volcanii*. Strikingly, RNase E/G-like does not seem to be required for efficient rRNA production, as for one no growth phenotype could be registered in the tested conditions and secondly, no strong overall accumulation of 16S pre-rRNAs was observed. In absence of the nuclease only specific intermediates accumulated. This speaks either for some redundancy due to other enzymes overtaking important functions or the possibility to bypass certain rRNA processing events in *H. volcanii* through downstream acting RBFs/nucleases.

Next, we wanted to gain insights in the molecular characteristics and mechanisms of archaeal RNase E/G-like. Hence, we collaborated with Prof. Nicolas Leulliot's group (University of Paris) to obtain a crystal structure of the protein. Biological molecules from halophilic organisms are notoriously ill-suited for structural analysis. In addition, the expression of recombinant *H. volcanii* RNase E/G caused issues and we switched gears to continue the work with RNase E/G-like from two old acquaintances: *Pyrococcus furiosus* and *Sulfolobus acidocaldarius*.

5.6.2. Structure analysis of archaeal RNase E/G-like

Briefly, RNase E/G-like from *P. furiosus* and *S. acidocaldarius* (hereafter pfAU-1 and saAU-1) were recombinantly expressed in *E. coli* BL21 cells and purified according to crystallography (see protocol in PhD thesis Marlene Vayssieres). *In vitro* RNase activity assays were performed with the purified PfAU-1 protein and after some optimization RNase activity was detected (data not shown). Strikingly, the cleavage reactions were dependent on the presence of manganese not on magnesium. *In vitro* assays using *E. coli* RNase E showed that both divalent ions promote RNA cleavage, however Mg^{2+} is likely the physiological metal ion supporting RNase E (K. J. Thompson, Zong, and Mackie 2015). Then, protein crystallization was prepared, and it was possible to obtain diffracting crystals for both organisms resulting in high resolution structures at 2.6 A (pfAU-1) and 2.0 A (saAU-1) (see figure 19). The structures revealed an interesting domain architecture. Features typical for *E. coli* RNase E like the 5' sensor domain, a S1 domain and the RNase active sites were identified by analyzing structural homology. Remarkably, another domain of unknown function was found which is not present in the *E. coli* counterpart. A predicted diphosphatase domain comprising structural homology to a *Streptomyces coelicolor* diphosphatase (SCO5041) characterizes the C-terminal part of the archaeal RNase E/G-like, thereby making it a chimeric fusion protein. The function of this diphosphatase domain is at the moment completely unknown. Strikingly, one study presented another bifunctional protein in *S. coelicolor* (SCO2299) which consists of a phosphatase and

RNase H domain (Ohtani et al. 2005). Both domains were enzymatically active even though the physiological role of this protein is unknown (Ohtani et al. 2005). Nevertheless, the fusion of a phosphatase with a RNase domain reminds of the chimeric protein we were observing.

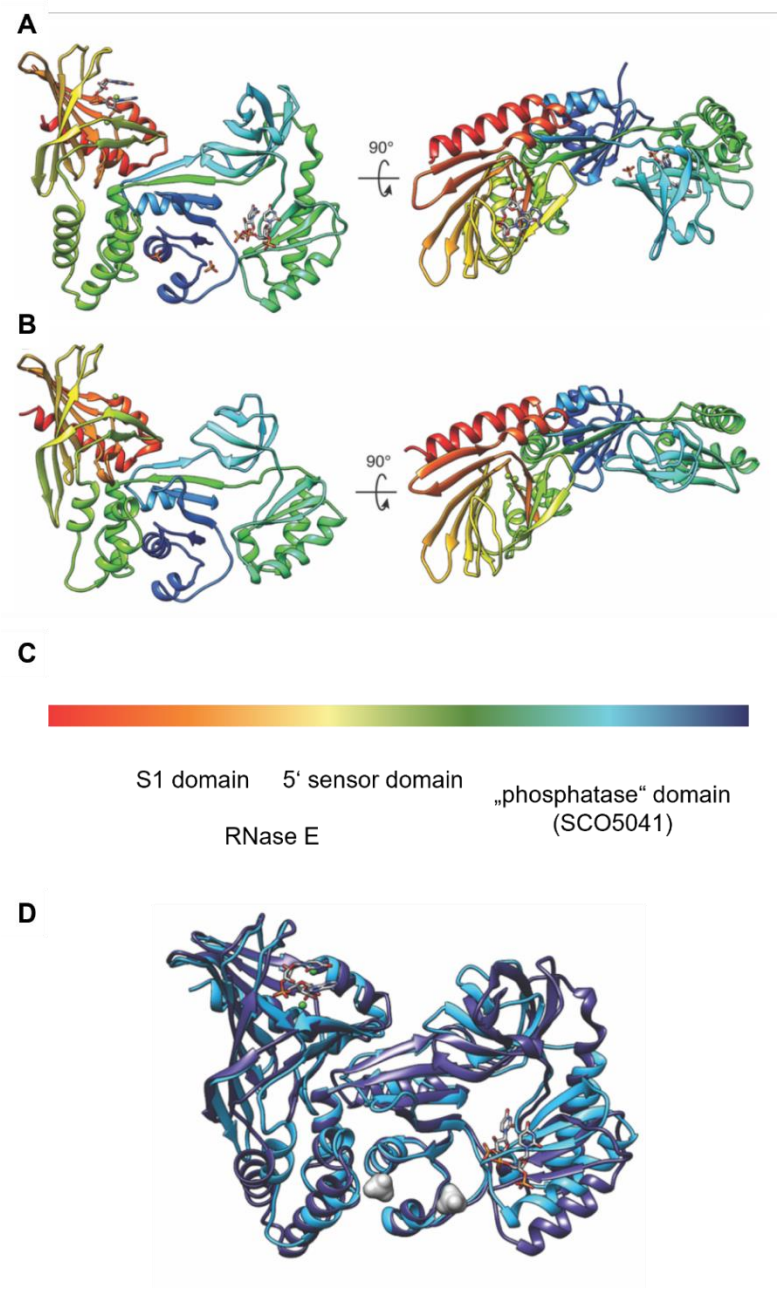

Figure 19: Crystal structures of *P. furiosus* (A) and *S. acidocaldarius* (B) RNase E/G-like protein. (**A** & **B**) Enzyme is colored in red (N-terminus) to blue (C-terminus). Nucleotides are represented in grey, two single phosphates in orange, two magnesium ions as green dots. (**C**) Domain architecture of **A** and **B** crystal structures based on structural homology with *E. coli* RNase E with S1 and 5’ sensor domain or *S. coelicolor* phosphatase SCO5041. (**D**) Superposition of structures from *P. furiosus* and *S. acidocaldarius* shows the high similarity of both proteins. Densities corresponding to phosphates are represented in grey. Adapted from PhD thesis Marlene Vayssieres.

Based on the new structural insights about the domain architecture of the protein, we designed targeted amino acid changes located in different domains and N- & C-terminal deletions. Then, we analyzed the effects of these mutations *in vivo* in *H. volcanii* (see figure 20).

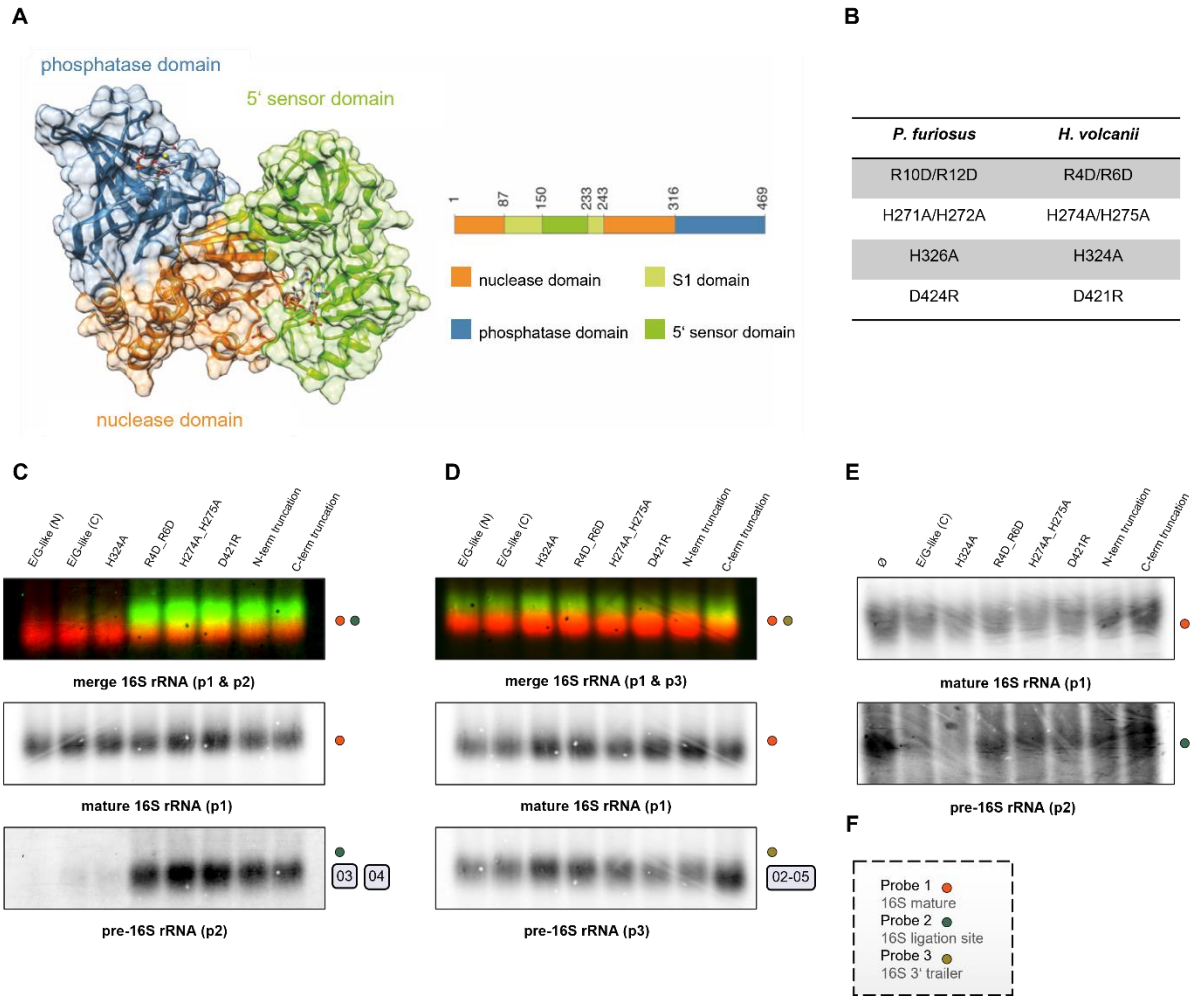

Figure 20: Specific amino acid substitutions in different domains of *H. volcanii* RNase E/G-like lead to loss of function. Based on the obtained crystal structure several mutations were introduced in different domains of *H. volcanii* RNase E/G-like. (**A**) Domain architecture of pfAU1 is represented. (**B**) Amino acid changes are translated from *P. furiosus* numbering to *H. volcanii* numbering. (**C**-**E**) Plasmids carrying mutations were either transformed into RNase E/G-like *H. volcanii* knockout cells (**C & D**) or h26 cells (**E**) and compared with complementation plasmid carrying wild type RNase E/G-like. Northern blots shown in **C** and **D** were performed with biological triplicates. Same Northern blot probes as described in figure 18. (**C**) Northern blot analysis of total RNA from RNase E/G-like knockout with wild type and mutant plasmids. Two differently tagged versions (C- or N-terminal tag) of RNase E/G-like were transformed. Probes 1 and 2 were used for hybridization. 16S pre-rRNA species #3 and #4, determined from Nanopore sequencing (see figure 15) are accumulating in five mutants compared to the wild type (lane 4 to 8). (**D**) Similar to **C**. Probes 1 and 3 were used for hybridization. No clear accumulation of pre-rRNA species was detectable with probe 3. (**E**) Northern blot analysis of total RNA from h26 transformed with an empty plasmid (Ø), wild type RNase E/G-like or mutant plasmids. Note that the endogenic version of RNase E/G-like is also present in these cells. (**F**) List of Northern blot probes with respective hybridization sites. **A** was adapted from PhD thesis Marlene Vayssieres.

Plasmids carrying wild type or mutated versions of *H. volcanii* RNase E/G-like were transformed into *H. volcanii* ΔRNase E/G-like strains and total RNA was extracted from these cells. We performed Northern blot analyses comparing full-length complementation with altered variants of the protein. The fluorescent probes for Northern blot hybridization (figure 20 F) were the same oligos used before (hybridization sites in figure 18 A). Except for one amino acid substitution (H324A), all RNase E/G-like mutations presented a strong accumulation of fluorescent signals representing 16S pre-rRNA ligation site in comparison to the wild type complementation (figure 20 C). In contrast, the oligo hybridizing to the 3' trailer sequence of 16S rRNA showed no overall accumulation of 16S pre-rRNA species in the mutants compared to the wild type (figure 20 D). Lastly, we aimed to examine if non-functional mutant proteins can interfere with rRNA processing in wild type *H. volcanii* cells, while endogenous wild type copies are also active. Accordingly, we transformed an empty plasmid, or plasmids carrying wild type or altered versions of *H. volcanii* RNase E/G-like in h26 cells. We extracted total RNA and performed Northern blot analyses. Unfortunately, the quality of the Northern blot was rather poor, and the experiment should be replicated. Anyhow, the application of the oligo targeting the 16S pre-rRNA ligation site revealed a slight accumulation of 16S pre-rRNA in the empty control or the mutant proteins suspected to be non-functional (see figure 20 E). Carefully interpreted, this would suggest that defective RNase E/G-like proteins might interfere with 16S pre-RNA processing, even if functional wild type copies are present.

5.6.3. Discussion

In summary, we could demonstrate that RNase E/G-like is involved in 16S pre-rRNA processing in *H. volcanii*. Presumably, it catalyzes rRNA processing steps after circular 16S pre-rRNA has been opened at the 5' end. Combining our results from Nanopore-based sequencing and the study of archaeal RNase E/G-like we can now provide an updated 16S rRNA processing pathway in *H. volcanii*. It was possible to identify specific maturation stages and place a new ribosome biogenesis factor at the transition of these classes (4 to 5). A proposed rRNA processing scheme including RNase E/G-like is illustrated in figure 21. Nevertheless, its function does not seem to be crucial for effective production of mature 16S rRNA. Potentially, other nucleases can (partly) take over its role comparable to the maturation of the 16S rRNA 3' end in *E. coli*. Any one of four exonucleases is sufficient for this exonucleolytic activity (Sulthana and Deutscher 2013). Alternatively, cleavage events further downstream can finalize the mature 16S rRNA 3' end without prior RNase E/G-like activity. Analysis of a set of mutations indicated that the different domains of the protein seem to be equally important for its *in vivo* function. Even though the mode of action remains yet elusive,

an interesting hypothesis can be formulated. The 5' sensor domain of bacterial RNase E binds to the 5' phosphate of its RNA substrate and thereby positions the catalytically active part in proper distance. An analogous mechanism of binding to the 5' end of opened circular pre-rRNA could help stabilize the pre-rRNA architecture by retaining a circular-like structure after re-opening. The fusion domain of unknown function, resembling a diphosphatase, might depict an exciting backstory of a chimeric protein emerging during evolutionary history and might be worth further investigations. Another open question regards the processing of other RNAs. The study in *T. kodakarensis* suggested also a participation of FAU-1 in the formation of mature 5S and 23S rRNAs (Ikeda et al. 2017). In addition, RNase E is well-studied for its role in general RNA degradation in *E. coli*. Finally, the cellular localization of this archaeal protein should be determined, since the *E. coli* enzyme was shown to be anchored to the inner cytoplasmic membrane (Khemici et al. 2008). Although, we made substantial progress in deciphering the puzzle of 16S rRNA maturation in archaea, it is not yet entirely solved. How could the final maturation of the 3' end 16S rRNA processing look like? In comparison with the eukaryotic system several shared, late acting ribosome biogenesis factors like Nob1, Pno1, Fap7 or RioK1 stand out. Strikingly, the endonuclease Nob1 which catalyzes the cleavage step at the 3' end of 20S pre-rRNA to generate the mature 18S rRNA in the cytoplasm, is already bound to pre-40S subunits in the nucleus, but not yet catalytically active (Fatica et al. 2003; Lamanna and Karbstein 2009; Pertschy et al. 2009). After the pre-40S particles get exported the interplay of Fap7, Pno1, RioK1 and Nob1 with concomitant rRNA conformational rearrangements are thought to enable

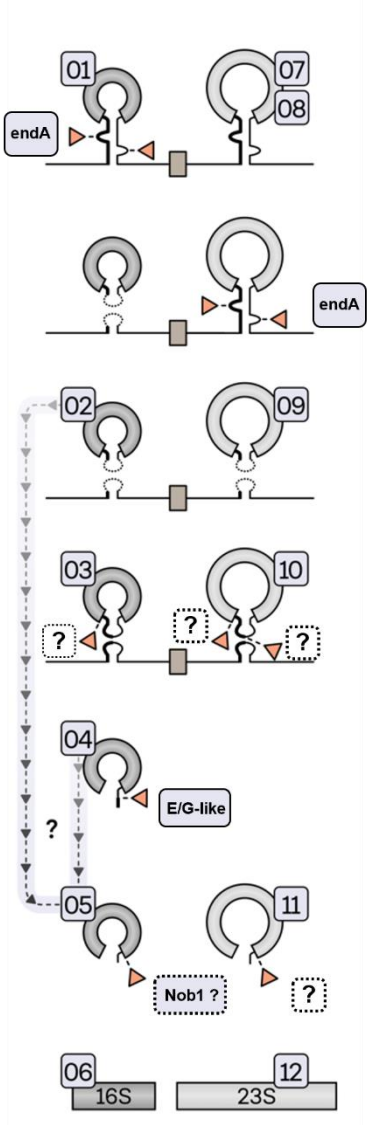

Figure 21: Updated pre-rRNA maturation in *H. volcanii* with participating endonucleases. Different pre-rRNA classes were determined by Nanopore-based long read sequencing (see 5.5). Known cleavage sites are indicated by orange triangles. EndA initiates maturation by cleaving at the bhb motif in the 16S and 23S rRNA processing stems. After circularization by RtcB circular 16S and 23S pre-rRNAs are re-opened at the mature 5' end by yet unknown endonucleases, represented by '?'. RNase E/G-like was characterized in this study and cleaves after re-opening of the 16S pre-rRNA. Nob1 would be a potential candidate to carry out final 16S rRNA processing at the 3' end (see discussion 5.6.3). Final 3' end maturation of the 23S pre-rRNA is achieved by a yet unknown enzyme. Adapted from Grünberger et al 2022.

Nob1 to do its catalytic duty (Granneman, Nandineni, and Baserga 2005; Hellmich et al. 2013; Turowski et al. 2014; Ameismeier et al. 2020). There is some indication that in archaea the final maturation of the 16S rRNA 3' end might also occur in a comparable fashion to the eukaryotic system. Nob1, Pno1, Fap7 or RioK1 are also found in archaeal genomes and supposedly function in a similar manner (Veith et al. 2012; Hellmich et al. 2013; Ebersberger et al. 2014; Knüppel et al. 2018). Mechanistically, 16S pre-rRNA substrate preparation could also be important for the last cleavage at the 16S rRNA 3' end in archaea. This might conceivably happen by the interplay of archaeal Pno1 and RioK1 homologues. What is more, RNase E/G-like could have a role in producing Nob1 cleavage-competent pre-16S rRNAs. On the other hand, in the RNase E/G-like knockout cells the processing of the 3' end was still possible, but potentially slowed-down in absence of RNase E/G-like. Further studies focusing on Nob1 or Pno1 will be necessary to illuminate the very last steps of archaeal 16S pre-rRNA processing.

In bacteria, on the other hand, RNase R has been proposed to be involved in the final 3' maturation of 16S rRNA (Purusharth, Madhuri, and Ray 2007; Davies et al. 2010). Interestingly, a RNase R homologue was described in *H. volcanii* and would represent another intriguing study object to examine a putative participation in rRNA processing (Portnoy and Schuster 2006).

5.7. Exceptions prove the rule - circular pre-rRNA distribution in archaea

The presence of circular pre-rRNAs in archaea is now a well-known fact and the underlying mechanisms involving the bhb motif, splicing endonuclease endA and RNA ligase RtcB have been characterized (Tang et al. 2002; Danan et al. 2012; Jüttner et al. 2020; Qi et al. 2020; Schwarz et al. 2020; Paola Londei and Ferreira-Cerca 2021). The issue of the universality of this intermediate in the rRNA maturation of all archaeal species and the concomitant question of potential alternative rRNA processing pathways is yet unresolved. A few outliers characterized by the absence of a bhb motif contained in the 16S rRNA processing stem have been reported (R. A. Garrett et al. 1991; P. P. Dennis, Ziesche, and Mylvaganam 1998; Qi et al. 2020). Amongst them is *Thermoplasma acidophilum* which was already described above as exceptional example due to its widely separated rRNA genes (see chapter 4; R. A. Garrett et al. 1991). Another astonishing case is the model organism that rose to fame by facilitating the Nobel prize winning first crystal structure of a large ribosomal subunit: *Haloarcula marismortui* (Ramakrishnan and Moore 2001). In this archaeon, three different rDNA operons A (*rrnA*), B (*rrnB*) and C (*rrnC*) are found with operon A being remarkably different than the operons B and C that share a high level of similarity at the sequence level (Baliga et al. 2004). It should be noted that the nomenclature of the three different rDNA operons is ambiguous in the corresponding literature (P. P. Dennis, Ziesche, and Mylvaganam 1998; Baliga et al. 2004). In our analysis 16S rRNA genes of *rrnA*, *rrnB* and *rrnC* refer to the genbank ncRNA names rrs-1 (chr. I 2634211-2633826), rrs-2 (chr. II 3949-5420) and rrs-3 (chr. I 1106973-1108444), respectively (UCSC Archaeal Genome Browser). Several other *Haloarcula* species have been described which also possess three divergent rDNA operons (H. Liu et al. 2011; Ding et al. 2014; Yun et al. 2015). Interestingly, not only the mature rRNA of *H. marismortui* differs but also the leader and trailer sequences of the 16S rRNA as only the processing stem of operon A contains a bhb motif (P. P. Dennis, Ziesche, and Mylvaganam 1998; Baliga et al. 2004). Given that this organism is easy to cultivate, it represents a promising model to study potential intraspecies variation of rRNA processing.

After studying the bhb motif in *H. volcanii* in detail, we now wanted to gain a broader view of how prevalent circular pre-rRNAs are in archaea. Moreover, we aimed to understand how the presence of circular pre-rRNAs correlates with the presence of the bhb motif and if circularization can occur in archaeal organisms without this structural element. Therefore, we developed a PCR-based approach which allowed us to detect circular 16S pre-rRNAs in archaea in a species independent manner.

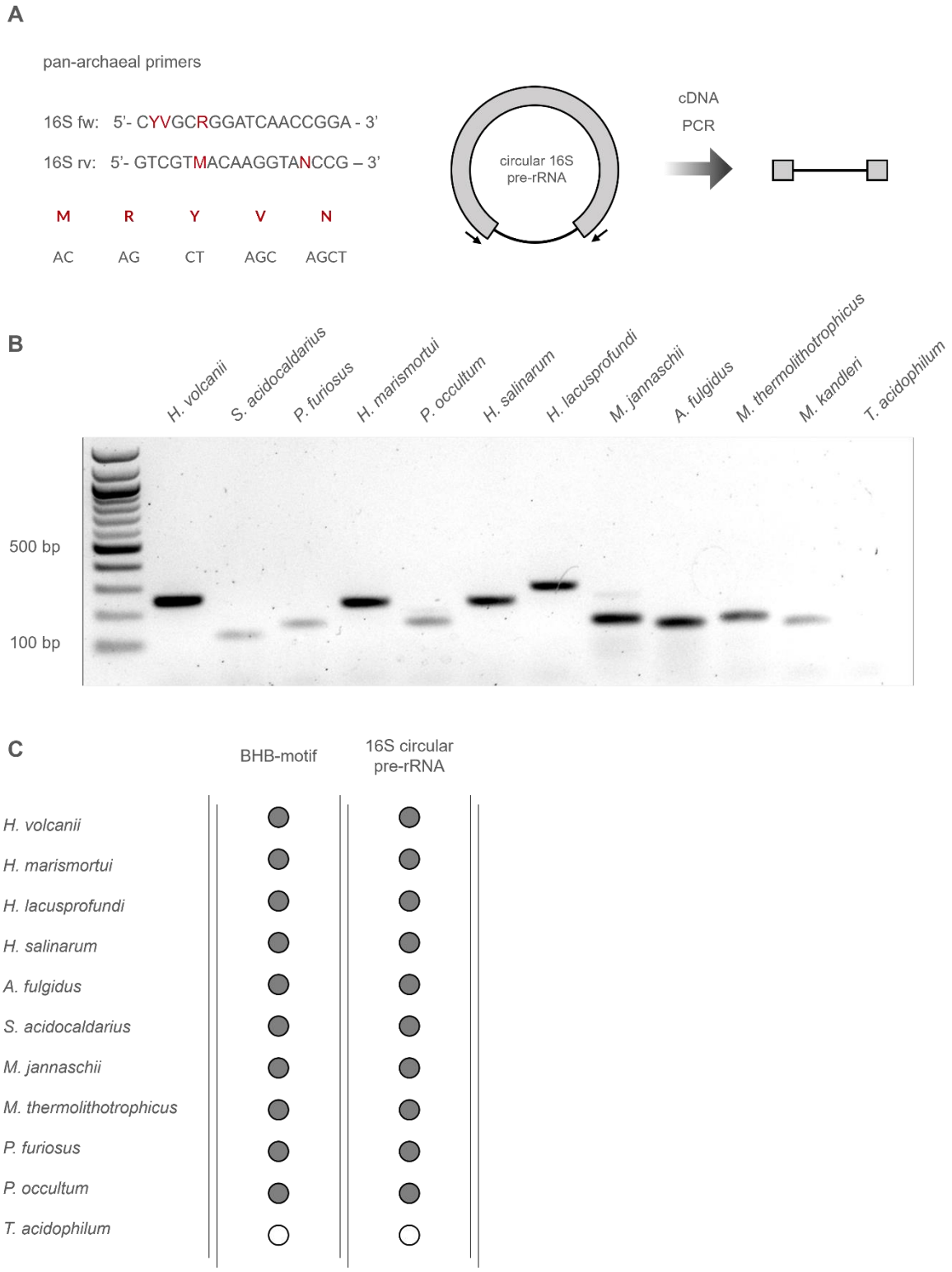

Figure 22: Detection of circular 16S pre-rRNAs in various archaeal species. (**A**) The workflow of the 'pan-archaea' primer approach is depicted. Degenerate oligos are shown with variable nucleotides in red. RT and PCR was performed to detect circular 16S pre-rRNAs. (**B**) Agarose gel showing PCR products from PCR-based assay to detect circular 16S pre-rRNA. Except *T. acidophilum* all analyzed archaea showed a PCR product which was further verified by Sanger sequencing. (**B**) Correlation between successful secondary structure prediction of bhb motif in the 16S rRNA processing stems and detection of circular 16S pre-rRNA from **A**. Adapted from Master thesis Maximilian Liebl.

A recent study used degenerate ‘universal’ primer sets specifically designed to detect archaeal rRNA genes for metagenomic analyses and provided the basis for our assay (Bahram et al. 2019). These degenerate oligos exploit the high sequence similarity of the 5’ and 3’ ends of 16S rRNAs and are shown in figure 22 A. After total RNA extraction from cell pellets cDNA synthesis with and without reverse transcriptase (RT) and a ‘pan-archaea’ RT primer hybridizing to the mature 5’ end of the 16S rRNA was carried out. Subsequently, PCR with ‘pan-archaea’ primers was performed and read-out on an agarose gel. PCR products confirmed the presence of circular 16S pre-rRNA and comprised the complete ligation site spanning from the mature 5’ to the mature 3’ end. The general principle is outlined in figure 22 A. For further validation, PCR products were sent for Sanger sequencing and aligned with expected *in silico* designed circular 16S pre-rRNAs. The technical implementation of this work was mostly done by Maximilian Liebl, a Master student in our lab. As proof of principle the approach was first verified by applying it to *H. volcanii* and *S. acidocaldarius*, which we had analyzed previously with species-specific oligos (Jüttner et al. 2020). It was possible to detect circular 16S pre-rRNA with specific and ‘pan-archaea’ oligos (data not shown, Master thesis Maximilian Lieb). Then, several archaeal species were tested regarding the occurrence of circular 16S pre-rRNAs. Cell pellets and total RNA for most of the examined archaeal organisms were kindly provided by the microbiology department and the Archaea Center Regensburg or were obtained by us. As seen in figure 22 B almost all the examined archaeal species exhibited a PCR product representing the presence of circular 16S pre-rRNA. Except for *M. kandleri* and *P. occultum*, all PCR products were sent for Sanger sequencing as confirmation. The only exception was *Thermoplasma acidophilum*, which does not contain a bhb motif in its 16S rRNA processing stem. To reassure this observation oligos specific for *T. acidophilum* were used and generated the same result (data not shown, Master thesis Maximilian Lieb). Conclusively, in the case of *T. acidophilum* no circular 16S pre-rRNA could be detected. The evaluation of the universal primer approach yielded in a perfect correlation between the presence of circular 16S pre-rRNA and the possibility to predict a bhb motif (see figure 22 C, Master thesis Maximilian Liebl).

What is more, we investigated the particular case of *Haloarcula marismortui* with specifically designed primers to differentiate 16S pre-rRNA intermediates derived from the three different rDNA operons. Figure 23 A gives an overview of all the oligos used for RT and PCR. Again, Maximilian Liebl was mainly responsible for the execution of these experiments. Control reactions without reverse transcriptase were always added to identify unspecific PCR products. First, we employed PCR primers (oHv373/oHv539) that bind to sequences in the mature 16S rRNA of all three operons and hypothetically generate PCR products representing circular 16S pre-rRNAs. As shown in figure 23 B, one distinct band was visible on the agarose

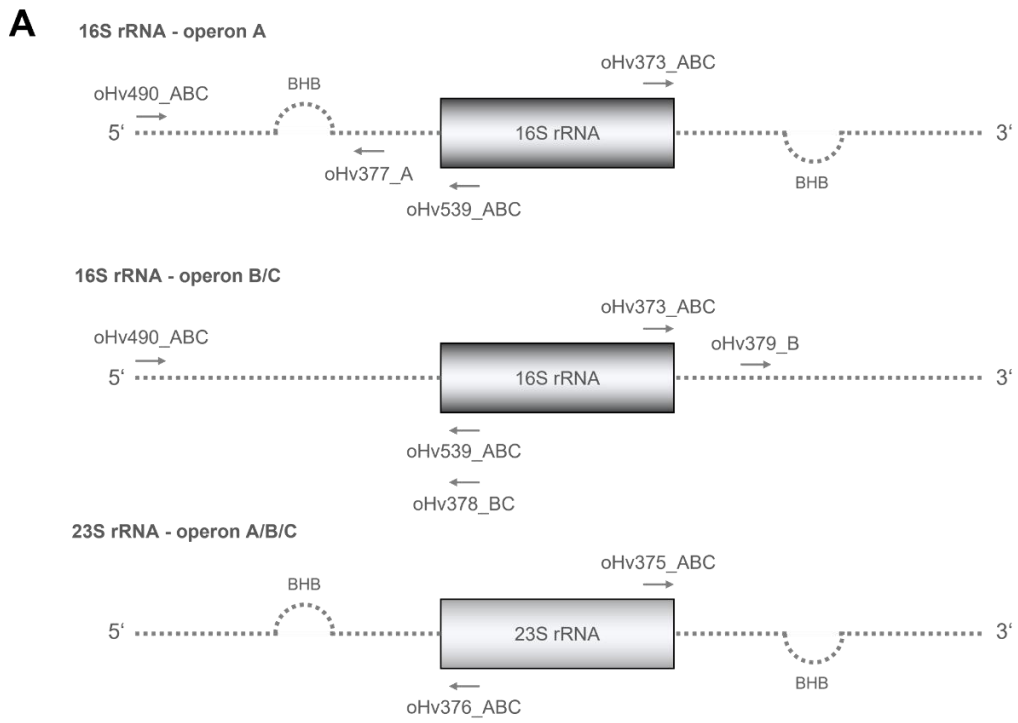
A
16S rRNA - operon A
oHv490_ABC
BHB
oHv373_ABC
5'
16S rRNA
3'
oHv377_A
BHB
oHv539_ABC
16S rRNA - operon B/C
oHv490_ABC
oHv373_ABC
oHv379_B
5'
16S rRNA
3'
oHv539_ABC
oHv378_BC
23S rRNA - operon A/B/C
BHB
oHv375_ABC
5'
23S rRNA
3'
BHB
oHv376_ABC

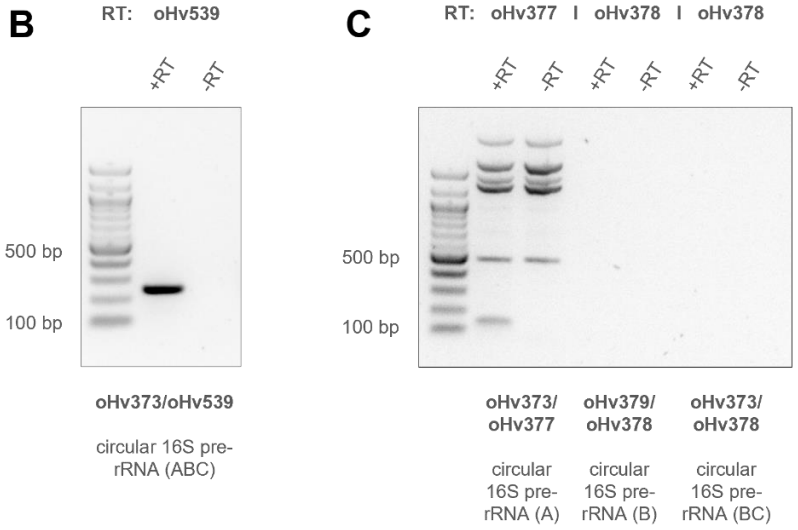
B
RT: oHv539
+RT
-RT
500 bp
100 bp
oHv373/oHv539
circular 16S pre-rRNA (ABC)
C
RT: oHv377 I oHv378 I oHv378
+RT
-RT
+RT
-RT
+RT
-RT
500 bp
100 bp
oHv373/ oHv377
circular 16S pre-rRNA (A)
oHv379/ oHv378
circular 16S pre-rRNA (B)
oHv373/ oHv378
circular 16S pre-rRNA (BC)

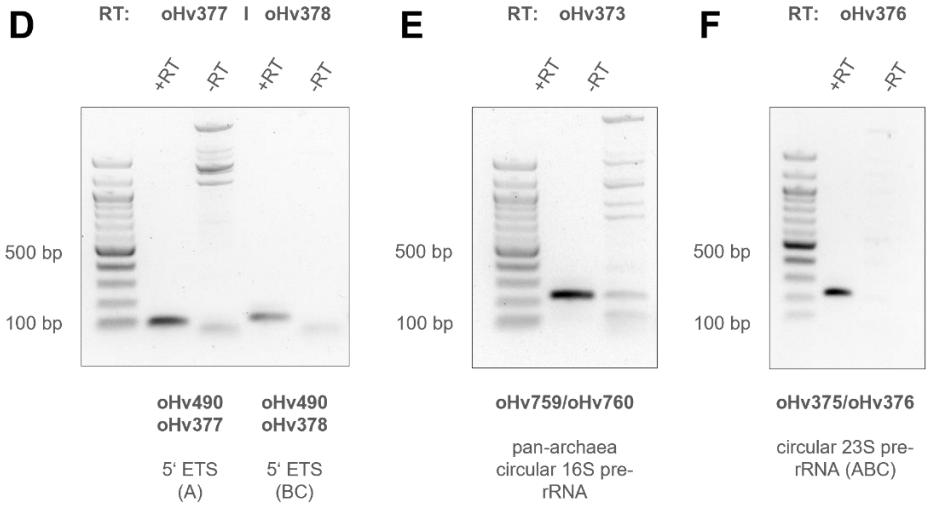
D
RT: oHv377 I oHv378
+RT
-RT
+RT
-RT
500 bp
100 bp
oHv490 oHv377
5' ETS (A)
oHv490 oHv378
5' ETS (BC)
E
RT: oHv373
+RT
-RT
500 bp
100 bp
oHv759/oHv760
pan-archaea circular 16S pre-rRNA
F
RT: oHv376
+RT
-RT
500 bp
100 bp
oHv375/oHv376
circular 23S pre-rRNA (ABC)

Figure 23: PCR-based analysis of rRNA expression in *Haloarcula marismortui*. (**A**) Depiction of the three rDNA operons A, B and C from *H. marismortui* with only operon A containing a bhb motif in the 16S rRNA processing stem. Note that the 23S pre-rRNA contains a bhb motif in all 23S rRNA processing stems. All the oligos used in the PCR reactions (**B**-**F**) are depicted with their respective binding sites. (**B**-**F**) Agarose gels with PCR products representing different pre-rRNA species. Oligos used for RT are indicated above agarose gel images. A control without reverse transcriptase (-RT) was performed in same conditions as the +RT reaction. Oligos used for PCR are indicated below agarose gel images. (**B**) Detection of circular 16S pre-rRNAs from rDNA operon A, B or C in *H. marismortui*. (**C**) Detection of circular 16S pre-rRNAs from rDNA operon A, B or B/C in *H. marismortui*. (**D**) Detection of 5' leader sequences from rDNA operon A or B/C. (**E**) Detection of circular 16S pre-rRNAs from rDNA operon A, B or C in *H. marismortui* with 'pan-archaea' oligos (see figure 22). (**F**) Detection of circular 23S pre-rRNAs from rDNA operon A, B or C in *H. marismortui*. Adapted from Master thesis Maximilian Liebl.

gel and Sanger sequencing of this PCR product confirmed the derivation from rDNA operon A. We performed PCRs with oligos specific for rDNA operon A, B or B and C to disentangle this result. Figure 23 C presents the according PCR products analyzed on an agarose gel and again only rDNA operon A was found to yield circular 16S pre-rRNA, whereas PCRs testing rDNA operon B and C showed no product. To eliminate problems during cDNA synthesis as the cause of failed PCR, we wanted to amplify the 16S leader sequence using the same RT primer, which was successfully done as portrayed in figure 23 D. As additional validation we applied our 'pan-archaea' degenerate oligos in this case and obtained the same result as before with one distinct band representing circular 16S pre-rRNA originating from rDNA operon A (figure 23 E). Finally, we aimed to check for the presence of circular 23S pre-rRNA in *H. marismortui*. The bhb motif is contained in the 23S rRNA processing stems of all three rDNA operons, even though it should be mentioned that the mature 23S rRNA sequence also differs in all operons. Expectedly, we could provide evidence for circular 23S pre-rRNA *H. marismortui* as depicted in figure 23 F.

Summing up, we could establish a PCR based assay to detect circular 16S pre-rRNAs in various archaeal species. We tried to apply a similar assay to detect circular 23S pre-rRNAs, which was unfortunately not working yet as conveniently. Presumably, degenerate 23S rRNA primers must be further optimized. Whereas circular pre-rRNAs are of great interest to us, the scope of this assay could go beyond the mere detection of these intermediates. Metagenomic studies determine microbiological communities based on DNA sequencing, however this kind of investigation cannot give any insights about transcriptional activity of the examined species. Conversely, detecting pre-rRNAs could hint to transcriptional activity and clarify which species are actively dividing opposed to dormant or dead organisms. For instance, this information could be of valuable for diagnostic investigation of the human gut microbiome. Few archaeal species have been found in the human gut and are putatively linked to medical conditions (Mohammadzadeh et al. 2022). The feasibility of such an application has of course to be tested with mixed samples or environmental probes.

The presence of circular 16S pre-rRNA intermediates correlates perfectly with the presence of a bhb motif in the 16S processing stems. *T. acidophilum* seems to be the exception proving the rule as no bhb motif can be found in its 16S processing stem and no circular 16S pre-rRNA could be detected with the assay. In this case, alternative, circularization-independent maturation pathways are likely acting in this organism. No 16S pre-rRNA processing intermediates were found by S1 nuclease protection assays. In contrast, the presence of partially processed 23S pre-rRNA could be demonstrated (Ree and Zimmermann 1990). The authors of this study drew an interesting parallel with rRNA maturation of *E. coli* where RNase III is not required to form mature 16S rRNA, but crucial for final 23S rRNA maturation (Ree and Zimmermann 1990). Strikingly, *T. acidophilum* is not only an outlier due to its missing bhb motif in the 16S rRNA processing stem, but also represents the unlinked rDNA organization type with all three rRNA genes scattered across the genome (see chapter 4). Hence, the question arises if these two observations cluster more frequently together indicating a functional link or are independent occurrences. One counter witness in this case is *Nanoarchaeum equitans*. In this organism the rRNA genes are unlinked, however a secondary structure of a canonical bhb motif in the 16S rRNA processing stem could be predicted (Qi et al. 2020).

Like in *T. acidophilum*, additional, yet unknown rRNA processing mechanisms might be in place in *Haloarcula marismortui*. Circular 16S pre-rRNA and circularization-independent maturation occurs both, depending on the operon. EndA and RtcB are found in the two organisms, but as the two enzymes are also required for tRNA metabolism or rRNA processing from operon A in *H. marismortui* this would be to expect (Qi et al. 2020). Available genomic data from different *Haloarcula* species could be compared with other halophilic archaea and examined for the presence of uncommon RNases, which might be involved in rRNA processing. Alternatively, *Haloarcula* species used the already existing RNA processing machinery for circularization independent rRNA maturation. Interestingly, the concurrent presence of mature rRNAs in *H. marismortui* cells derived from all three rDNA operons was detected by fluorescence in situ hybridization microscopy and qPCR analyses (Amann et al. 2000; López-López et al. 2007). In addition, rDNA deletion strains without operon B or operon B and C were viable and grew like the wild type in rich medium (D. Tu et al. 2005). The heterogeneity of ribosomal RNA naturally involves the question of functional adaptation of the translation apparatus to either answer different environmental challenges or provide two distinct protein synthesis platforms with altered translational features. So far, it has been speculated, that the rRNA divergence in *H. marismortui* is an adaptation to temperature changes, which could be explained with differential RNA stability at higher temperatures (López-López et al. 2007). Furthermore, variations in *H. marismortui* rRNA sequences are mostly found in paired complementary sites and leave thereby the overall subunit structure

intact (Baliga et al. 2004). This observation speaks against altered characteristics of translation. The notion that the basis of this heterogeneity could be an adaptation to varying temperatures in their natural habitats was further corroborated by similar results from examinations of a couple other *Haloarcula* species (Sato, Fujiwara, and Kimura 2017; Sato and Kimura 2019).

How could the expression of such crucial genes be regulated? A closer look at the promotor sequences of rDNA operon A or B/C revealed differences that might enharbour the regulatory potential (López-López et al. 2007). Next to transcription regulation, another way to control varying levels of divergent ribosomal RNA within the same organism could take place at the level of rRNA processing with different mechanisms and nucleases involved. Remarkably, structure prediction of the aforementioned helix B in the 5' leader shows that it is structurally quite conserved in three pre-rRNAs (see chapter 5.4.3). Accordingly, this indicates a crucial role in rRNA maturation for this structural element independent from the circularization of 16S pre-rRNA (see supplementary figure S2).

To learn more about the rRNA processing of these out of the ordinary archaeal representatives the above described Nanopore-base sequencing approach (see 5.5) could be a very promising option. Various pre-rRNA species might be observable in *H. marismortui* and *T. acidophilum* and the already established rRNA maturation pathways in *H. volcanii*, *P. furiosus* and *S. acidocaldarius* can serve as comparison.

6. Regulation of Ribosome Biogenesis in Archaea

6.1. Introduction

6.1.1. Regulation of ribosome synthesis in *E. coli*

Basically, a cell is a ribosome's way to make new ribosomes. Massive amounts of cellular machineries and energy are dedicated to the task of ribosome biogenesis in bacterial and eukaryotic species (Warner 1999; Iskakova, Connell, and Nierhaus 2004; T. Moss et al. 2007). Accordingly, ribosome biosynthesis requires elaborate regulatory mechanisms and adjustments to varying growth conditions.

The relationship between cellular concentration of ribosomes and growth rate as a linear function in fast growing enterobacteria was noticed several decades ago (Schaechter, MaalØe, and Kjeldgaard 1958; Neidhardt and Magasanik 1960). Ever since, investigators were trying to answer the question how ribosome synthesis is regulated globally. This is especially important when considering the many involved ribosome biogenesis factors and different building blocks, whose production must be precisely tailored. Consequently, the regulatory principles that constitute the synthesis of stable RNAs (rRNAs & tRNAs) and the production of r-proteins have been extensively studied (Masayasu Nomura 1999).

Two main regulatory principles have been described in *E. coli*: growth rate regulation and stringent response. Stringent response (or control) represents a key bacterial stress answer. It is initiated upon starvation or other stress conditions, causing reduced translational capabilities, and relies on the intracellular level of the small molecule (p)ppGpp (Irving, Choudhury, and Corrigan 2021; Bange et al. 2021). An increasing concentration of (p)ppGpp affects general metabolism, replication, or translation and leads to an immediate transcriptional shutdown of rRNA and tRNA genes (Cashel et al. 1996; Kaczanowska and Rydén-Aulin 2007; Bange et al. 2021). In addition, the expression of ribosomal proteins was also found to be under stringent control in *E. coli* (Patrick P. Dennis and Nomura 1974; Cole and Nomura 1986). Two key enzymes, SpotA & RelA, are responsible for the metabolism of (p)ppGpp in *E. coli*. Both proteins possess a (p)ppGpp synthetase and a hydrolase domain and are therefore both involved in generation and degradation of the effector molecule (Potrykus and Cashel 2008; Bange et al. 2021). Conversely, a 'relaxed' phenotype was attributed to SpoT/RelA *E. coli* mutants without a stringent response (A. Martin 2009).

In rapidly growing bacterial cells, a higher translation rate can only be achieved by a higher number of ribosomes, as translation kinetics remain constant. To adjust for that, growth rate regulation has to account for a balanced, coordinated neo synthesis of r-proteins and rRNAs. Intriguingly, the amounts of most r-proteins are not regulated on the transcriptional, but on the translational level (Masayasu Nomura 1999). By a very elegant, autogenous feedback mechanism, surplus r-proteins (i.e., not being incorporated into assembling ribosomes) bind to their own mRNAs, often organized in operons, block further translation and in some cases even induce mRNA degradation (Fallon et al. 1979; Yates, Arfsten, and Nomura 1980; Kaczanowska and Rydén-Aulin 2007). Thereby, r-protein output is also indirectly coupled to rRNA synthesis as free r-proteins would preferentially bind to pre-rRNAs.

On the other hand, the ratio of stable RNAs to other cellular components (DNA, protein, etc.) increases faster in exponential growth (Cashel et al. 1996; Kaczanowska and Rydén-Aulin 2007). The following issue was then, how rRNA synthesis is controlled. One way to address this problem was to test the influence of rRNA gene dosage in *E. coli*. In general, gene dosage describes the number a particular gene is present in the genome (Hartwell et al. 2010). In *E. coli* the ribosomal RNA is transcribed from seven, almost identical rRNA operons with two promotors P1 & P2 (David A Schneider, Ross, and Gourse 2003). Early experiments increasing rRNA gene dosage by adding rDNA plasmids did not lead to a concomitant raise in rDNA transcription (Jinks-Robertson, Gourse, and Nomura 1983). Strikingly, deletions in the rDNA leading to non-functional rRNA caused higher transcription rates of rRNA and tRNAs genes encoded in the rDNA operons (Jinks-Robertson, Gourse, and Nomura 1983). The authors concluded that rRNA synthesis rate must therefore not be regulated by gene copy number, but functional rRNA contained in free, non-translating ribosomal subunits (Jinks-Robertson, Gourse, and Nomura 1983; Gourse and Nomura 1984; Yamagishi, de Boer, and Nomura 1987). This model was further supported by work using a conditional rDNA plasmid overexpression system, which resulted in an overproduction of free 30S and 50S ribosomal subunits. In this analysis the transcription of chromosomal rRNA genes was reduced, suggesting a negative feedback effect by the non-translating subunits (Gourse et al. 1985). Notably, the constructs used carried the strong phage promotor λ P_L and significantly higher (p)ppGpp levels were registered (Gourse et al. 1985). Interestingly, the synthesis rate of rRNA and tRNAs was also increased in a mutant strain with defective rDNA transcription antitermination (Sharrock, Gourse, and Nomura 1985). In addition, the P1 promotor, which is also under stringent control, seemed to be involved in the feedback control mechanisms (Sarmientos and Cashel 1983; Gourse, de Boer, and Nomura 1986). In contrast to the idea of regulation by non-translating subunits stood the observation that an accumulation of free ribosomal subunits by limiting translation initiation factor 2 led to an increase of rRNA

transcription (Cole et al. 1987). Hans Bremer's group advocated for a (p)ppGpp controlled rDNA transcription model involving translating ribosomes rather than free subunits (Baracchini and Bremer 1988). To test competing hypotheses Hans Bremer's group repeated the initial experiments from Jinks-Robertson et al. and included pp(G)pp measurements (Baracchini and Bremer 1991). Through meticulous calculations the authors arrived in parts at dissenting conclusions. Preeminently, upon adding intact or defective rDNA copies they detected an increase in the rRNA/tRNA ratio by using different normalization methods than Nomura's group. Moreover, extra wild type copies of *rrn* genes resulted in raising (p)ppGpp concentrations. Lastly, the addition of intact or defective rDNA copies negatively affected bacterial growth and a reduced rRNA synthesis rate per *rrn* gene was observed (Baracchini and Bremer 1991). Later electron microscopy studies could confirm a lower RNA polymerase occupancy per operon in *E. coli* cells with increased rRNA gene dosage (Voulgaris et al. 1999). Another study found that in non-optimal media addition rDNA plasmids caused a drastic increase (~100 %) of total RNA and reduced growth of *E. coli* (Stevenson and Schmidt 1998).

In an unifying attempt Bremer and Dennis suggested a feedback regulation for growth rate dependencies, stringent control and *rrn* gene dosage effects including ribosome function and (p)ppGpp as signal molecule (Bremer and Dennis 2008). In exponentially growing *E. coli* cells, cellular amino acid (AA) and energy levels must be monitored in a balanced supply-meets-demand fashion. Strikingly, both are reflected in the translation elongation rate of the ribosome. Insufficient amino acid or energy (ATP or GTP) levels cause deviations from the optimal elongation rate of 22 amino acids per second at 37 °C. Likewise, changes in rDNA gene dosage were suspected to alter rRNA/tRNA levels and influence translation functionality. Subsequently, SpoT (p)ppGpp synthetase is activated by an unknown regulatory mechanisms and ribosome neo synthesis repressed by elevated levels of (p)ppGpp (Bremer and Dennis 2008). Still, growth rate-dependent control of ribosome synthesis was also observed in strains, that do not produce any (p)ppGpp (T. Gaal and Gourse 1990; Hernandez and Bremer 1993). Moreover, P1 mutations suggested partly independent mechanisms for the feedback regulation of rRNA synthesis and growth rate control (Voulgaris et al. 2000) .

Increasing or decreasing the number of chromosomal *rrn* gene copies also resulted in adjustments of transcriptional activity by RNAP allocation (Condon et al. 1993; 1995; Asai et al. 1999; Gyorfy et al. 2015; Fan et al. 2022). Even though *E. coli* cells were still viable with fewer rDNA copies, it was suggested that the number of seven operons reflects an optimal adaptation to a 'feast and famine' lifestyle (Condon et al. 1995; Gyorfy et al. 2015). Noteworthy, one report showed that (p)ppGpp levels did not change after inactivation of several *rrn* operons (Condon et al. 1993). In general, the number of rDNA copies was proposed to be indicative for

ecological strategies in bacteria (Klappenbach, Dunbar, and Schmidt 2000; Roller, Stoddard, and Schmidt 2016).

In a nutshell, it can be stated that other than the well-understood stringent control the feedback mechanisms of rRNA synthesis is not comprehended in every detail. Unequivocally, there is feedback control on rRNA production in dependency of growth rate and *rrn* gene dosage. However, the competing hypotheses around free or translating ribosomal subunits as indicator for adjusting rRNA gene expression or the participation of (p)ppGpp could so far not be entangled completely. Furthermore, if increased gene dosage leads to elevated rRNA synthesis rates, it is not entirely clear to what extent and how this is reflected for example on the level of pre-rRNAs. It seems likely that, the P1 promotor and the signal molecule (p)ppGpp have a role in the regulatory mechanisms.

6.1.2. Regulation of ribosome synthesis in eukaryotes

Direct but also coordinated regulation of r-protein and rRNA levels occurs in eukaryotes in response to nutrient changes (Kief and Warner 1981). In amino acid starvation conditions similar responses as in *E. coli* on the production of rRNA and r-proteins have been described in eukaryotes. Such a stringent-like behavior is seen not only in eukaryotic microorganisms but mammalian cells alike, however, these mechanisms do not seem to rely on (p)ppGpp (Warner 1989; Masayasu Nomura 1999; T. Moss et al. 2007). Another difference to *E coli* is the absence of a global, autoregulatory feedback mechanism of r-protein synthesis in yeast (Masayasu Nomura 1999). Whereas in *E. coli* the regulation of ribosome biogenesis takes presumably place at the level of rRNA synthesis, the situation is more complex in eukaryotes (T. Moss et al. 2007; Grummt 2010; Albert et al. 2012; Hori, Engel, and Kobayashi 2023).

Stunningly, the number of rDNA copies in eukaryotes ranges from few to tens of thousands (Torres-Machorro et al. 2010). In exponentially growing cells rRNA synthesis can make up to 80 % of all transcription in the cell, but even in these circumstances only up to half of the rRNA gene copies are actively transcribed (Tom Moss and Stefanovsky 2002; Grummt and Pikaard 2003). These findings indicated first an excess of rRNA genes in relation to the cell's actual need of rRNAs and secondly, the presence of systems to effectively regulate the dosage of their rRNA genes (Neves, Viegas, and Pikaard 2005).

Two main regulatory principles of eukaryotic rRNA synthesis have been established. The first one concerns the chromatin status of the individual rDNA gene copy, which can be found in an 'open', active or 'closed', inactive form. This status is even heritable by the implication of

DNA methylation and post-translational modifications of histones (Grummt and Pikaard 2003). Secondly and most importantly, fine-tuning of RNA-polymerase I initiation and elongation enables response to different growth conditions (Grummt and Pikaard 2003; T. Moss et al. 2007; Tucker, Vitins, and Pikaard 2010; Albert et al. 2012).

Studies on rRNA gene dosage in eukaryotes have been mostly performed by altering chromosomal rDNA numbers and confirmed the notion, that rRNA gene dosage does not influence overall rRNA production in eukaryotes (Ide et al. 2010; Lopez et al. 2021). Surprisingly, yeast strains with only twenty chromosomal rDNA copies left grew normally and produced similar levels of rRNA, but were susceptible to DNA damage and had exclusively open (active) rRNA genes (Ide et al. 2010). As recently shown, drastic gene copy reduction by Cas9-mediated gene editing in *Arabidopsis thaliana* did not lead to altered transcriptional rates and steady-state RNA levels compared to the wild type (Lopez et al. 2021). The high number of rDNA copies is rather believed to be important for DNA repair, aging and genome maintenance (Kobayashi 2011). The introduction of rDNA plasmids into a yeast strain with a complete deletion of chromosomal rDNA slightly reduced growth, which was suspected to stem from a disruption of nucleolar structures (Wai et al. 2000). The localization of rDNA plasmids in the nuclear periphery might cause reduced capability to recruit the Pol I machinery, especially in strains with chromosomal rRNA genes left (Oakes et al. 1998; Wai et al. 2000; M. Nomura 2001). Interestingly, after perturbations of chromosomal rDNA copy numbers, yeast strains returned to around 150 rDNA copies, indicating a maintenance system to retain rRNA gene dosage (Kobayashi et al. 1998). It has even been demonstrated, how yeast cells can mechanistically ‘count’ and adjust rDNA copy numbers in a feedback mechanism involving the RNAP I transcription initiation factor UAF and the histone deacetylase Sir2 (Iida and Kobayashi 2019a; 2019b). What is the molecular basis for such an apparently tight control of excess rDNA copies?

In summary, rRNA gene dosage control in eukaryotes is achieved by adjusting rDNA copies, chromatin status and presumably to the greatest extent by the availability of polymerase I initiation factors.

6.1.3. Regulation of ribosome synthesis in archaea

Very few insights about the regulation of ribosome synthesis have been gained in archaea. Some archaeal organisms were determined to be stringent, others seemed to have a ‘relaxed’ phenotype (Beauclerk et al. 1985; Cimmino, Scoarughi, and Donini 1993; Cellini et al. 2004;

Müller et al. 2021). The synthesis of stable RNAs of *H. volcanii,* the main model organism of this study, was found to be under stringent control (Cimmino, Scoarughi, and Donini 1993). Homologues of RelA/SpotA, which are involved in bacterial pp(G)pp metabolism, have been found in the genomes of several Euryarchaeota (Atkinson, Tenson, and Hauryliuk 2011). Interestingly, catabolic formate or anabolic phosphate limitations caused different growth rate-dependent cellular responses on ribosome synthesis regulation in *Methanococcus maripaludi* (Müller et al. 2021; Gu et al. 2022). The increase of ribosomal RNA in dependency of growth rate in *Pyrococcus furiosus* was not described by a linear function (DiRuggiero et al. 1993). In contrast, it was shown in *Halobacterium cutirubrum* that rRNA synthesis is regulated proportionally with growth rate (John Chant et al. 1986). Remarkably, bioinformatic analyses predicted in archaea four r-leader motifs in the untranslated regions (UTR) of r-protein mRNAs. These UTRs are typically bound by r-proteins to inhibit translation in the autogenous regulation described in bacteria, potentially indicating the presence of such a feedback mechanism in archaea (Eckert and Weinberg 2020). Nevertheless, this has still to be experimentally verified *in vivo*. At which level the production of ribosomal building blocks is controlled in archaea is currently almost completely uncharted territory. Not merely mechanisms of cellular responses to varying environmental conditions or growth rate dependencies, but also rRNA gene dosage effects or the co-regulation of individually transcribed rRNA genes from split rDNA operons (see chapter 4) are mainly unidentified so far. For starters, we wanted to study therefore the effects of increased rDNA gene dosage in *H. volcanii*.

6.2. Results

We realized that in our before established rDNA reporter assay, we potentially already created a rRNA overexpression system by introducing additional rDNA copies. Now we wondered, how excess rDNA copies would influence the overall production of rRNAs. We used rDNA plasmids encoding the complete rDNA operon A of *H. volcanii* or split variants encoding either 16S rDNA or 23S rDNA (see figure 24). These split constructs included respective 5’ leader and 3’ trailer sequences to enable transcription initiation, processing stem formation and correct rRNA processing. Moreover, the plasmids did not carry the point mutations described above to compare as accurately as possible with the wild type rDNA copies. After transformation of wild type h26 cells with the three rDNA variants and the empty plasmid pTA1228 used as a control, colonies were picked from plates, grown in selective casamino acids medium, and harvested at an OD_{600nm} around 0.5. Cell pellets were used for DNA or RNA extraction. First, we aimed to determine rDNA and plasmid copy numbers by Southern blot analysis.

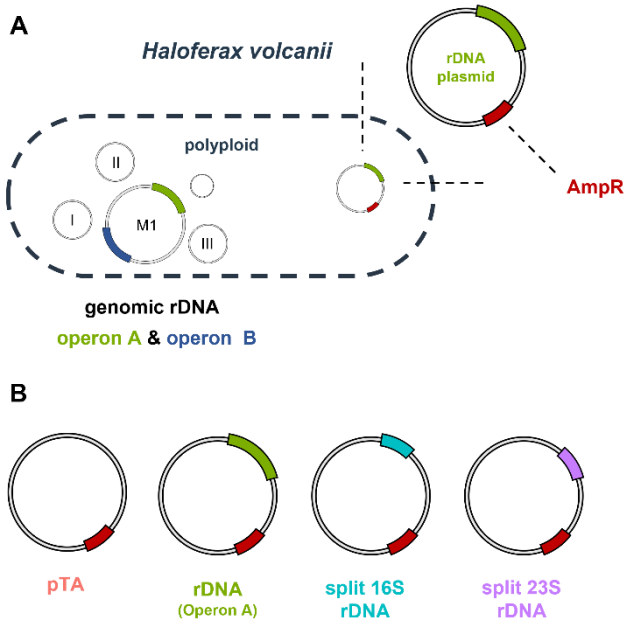

Figure 24: Outline of rRNA gene dosage experiments. (**A**) The polyploid archaeon *H. volcanii* is shown with its genome on one main chromosome (M1) and three additional plasmids (I, II and III). The two rDNA operons A (green) and B (blue) are found on M1. Additional copies of rDNA carrying plasmids with an Ampicillin resistance gene (red) were transformed into *H. volcanii* h26 cells. (**B**) Constructs used for gene dosage analysis are depicted. An empty pTA1228 plasmid (red), rDNA plasmid (green) or rDNA split constructs carrying either 16S rDNA (turquoise) or 23S rDNA (violet) were used.

Therefore, extracted h26 DNA and rDNA plasmid as control was digested with HindIII and XhoI and digestion products loaded on an 1.3 % agarose gel, which was run over night. Restriction enzymes were specifically chosen to cleave at different positions within or next to the 23S rRNA gene to generate three different sized restriction products depending on the origin from rDNA plasmid, operon A or B. Southern blot analysis was performed as described in material & methods 9.2.6.13 and radioactively labeled PCR probes hybridizing to the 23S rDNA or Amp^R gene were applied (see figure 25 A). The results of the two hybridizations are depicted in figure 25 B & C. The three anticipated restriction fragments representing operon A, B or plasmid encoded 23S rRNA genes are clearly distinguishable. As expected, plasmid 23S rDNA copies are only detectable in cells transformed with the rDNA and split 23S rDNA constructs or in the control digest of the rDNA plasmid seen in the last lane (figure 25 B). Detection of Amp^R gene was possible for all cells transformed with the four constructs and for the control digest of the rDNA plasmid in the last lane (figure 25 C). In eukaryotes, rDNA copy number can be regulated upon environmental changes and vary in a large range. To estimate potential changes in chromosomal rDNA copy numbers by introducing plasmid rDNA copies we calculated the relative copy number of detected genomic 23S rDNA fragments from figure 25 B compared to cells transformed with the empty pTA1228 plasmid. The mean of the two operons was calculated for each replicate and one pTA1228 value arbitrarily set to one as a

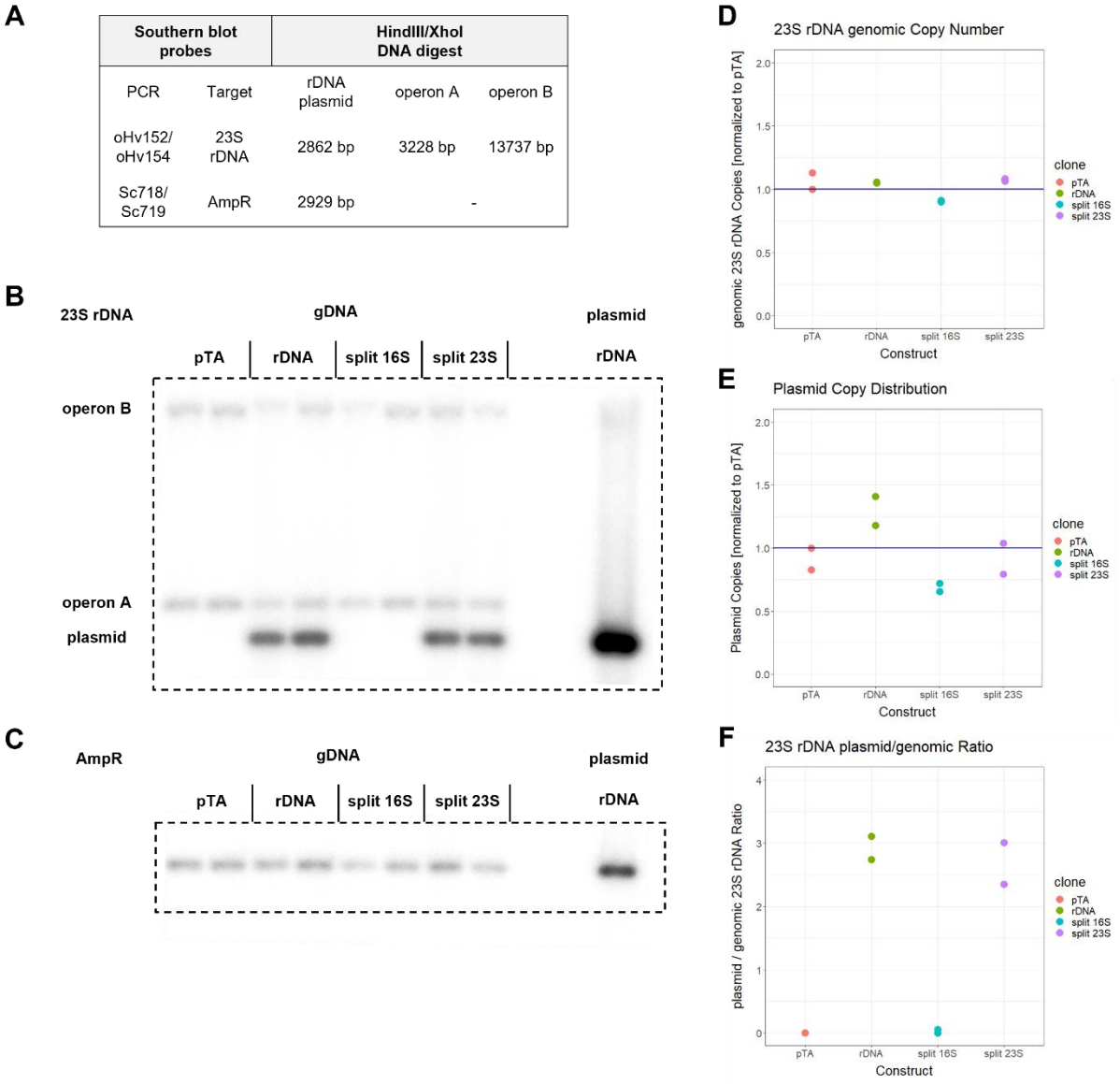

Figure 25: Estimation of rDNA copy number in *H. volcanii* strains transformed with rDNA plasmids. (**A**) Table showing Southern blot outline. Extracted total DNA from *H. volcanii* cells was digested with HindIII/XhoI. Endonucleolytic cleavage within the 23S rDNA sequence generated three differently sized fragments depending on their origin from genomic rDNA operon A, B, or the transformed rDNA plasmids. Digested DNA fragments which could be detected with probes hybridizing to 23S rDNA or the gene coding for Ampicillin resistance. (**B**) Quantification of 23S rDNA gene numbers with additional plasmid encoded rDNA copies by Southern blot analysis. Experiments were performed in biological duplicates. DNA was extracted from h26 cells transformed with empty control (pTA), rDNA, split 16S rDNA or split 23S rDNA plasmids. As an additional control a rDNA plasmid was digested. After HindIII/XhoI digest samples were loaded on an agarose gel and Southern blot analysis performed. Signals were normalized to overall load on syber safe stained agarose gel. Digestion products from genomic rDNA copies (operon A & B) can be visualized in all strains. Fragments originating from the rDNA, or split 23S rDNA plasmids are represented by the band at the bottom. The last lane shows a control rDNA plasmid which was digested likewise. (**C**) Quantification of plasmid copy numbers in relation to additional plasmid encoded rDNA copies by Southern blot analysis. A radioactively labeled probe detecting the Amp resistance gene was hybridized with the same blot as in **B**. (**D**) Evaluation of Southern blot from **B**. The genomic 23S rDNA remains relatively constant independent of the additional plasmid encoded rDNA copies. The result for pTA #1 was arbitrarily set to 1 and used as reference. (**E**) Evaluation of Southern blot from **C**. The plasmid copy number is slightly higher in cells transformed with the rDNA plasmid. The plasmid copy number is slightly lower in cells transformed with the split 16S rDNA plasmid. The result for pTA #1 was arbitrarily set to 1 and used as reference. (**F**) Plasmid derived 23S rDNA copy number in relation to genomic copies from **B**. The mean ratios from plasmid to operon A and plasmid to operon B signals were calculated. In cells transformed with rDNA or split 23S rDNA plasmids 2 to 3 23S rDNA copies on plasmids were present for every genomic copy. This signifies an overall increase of 23S rDNA copies of 2 to 2.5 compared to the wild type (pTA) situation.

reference. As overall normalization total DNA load was used based on signals from imaging the SYBR Safe stained agarose gel. Figure 25 D shows, that the genomic rDNA copy number remained quite constant in this analysis regardless of the respective transformed rDNA constructs. Similarly, plasmid copy number was estimated based on the Amp^R gene detection from figure 25 C. A slight increase in plasmid copy number was observed in the two rDNA plasmids transformed replicates, whereas plasmid copy number decreased slightly in the split 16S rDNA transformed clones (see figure 25 E). Lastly, we aimed to get an estimation of the total increase of rDNA copies in the cells after transformation with plasmid variants. For this purpose, we first calculated the ratio of plasmid encoded 23S rDNA copies compared to the genomic copies. The cells transformed with rDNA, or split 23S rDNA constructs exhibited a ratio of around 2 to 3 plasmid encoded copies per one genomic copy (see figure 25 F). Adding the 2 to 3 plasmid copies to the two genomic copies results in a 2- to 2.5-fold total increase of the rDNA copy number. Hence, we could demonstrate, that the introduction of rDNA plasmids or variants thereof lead to increased rRNA gene dosage.

Next, we wanted to examine the consequences of higher rRNA gene dosage in *H. volcanii* cells. Does a higher copy number signify a concomitant increase in rDNA transcription or maybe even higher production of mature ribosomal subunits? Total RNA was extracted from transformed h26 cells with classical phenol/chloroform extraction or RNA extraction kit as described in material & methods 9.2.7.1 and 9.2.7.3. Subsequently, Northern blot analysis or Agilent 4200 TapeStation runs were performed to check mature and precursor rRNA levels. Figure 26 B and C show the detection of different 16S pre-rRNA species by Northern blot analysis. Strikingly, there was a strong accumulation of 16S pre-rRNAs observed when the rDNA or split 16S rDNA plasmids were transformed in h26 cells (see figure 26 B & C). In contrast, the 16S pre-rRNAs signal almost disappeared in the cells transformed with split 23S rDNA construct if compared to the pTA1228 control. The effects were reproducibly noted in all three biological replicates.

As an alternative method to analyze total RNAs we were using the Agilent 4200 TapeStation system. This instrument can separate nucleic acids by means of electrophoresis and gives very sensitive and precise measurements. The provided software offers valuable information and helps with data analysis. As seen in figure 27 B, the electrophoresis run produces an image in the format of an agarose gel as readout, which can be further transformed into individual profiles representing the signal intensity throughout each whole lane (figure 27 C – F**)**. In the rDNA and split 16S rDNA plasmid RNA samples the 16S rRNA peak in these profiles was notably broader and showed a little shoulder on the right-hand side (see figure 27 D and E).

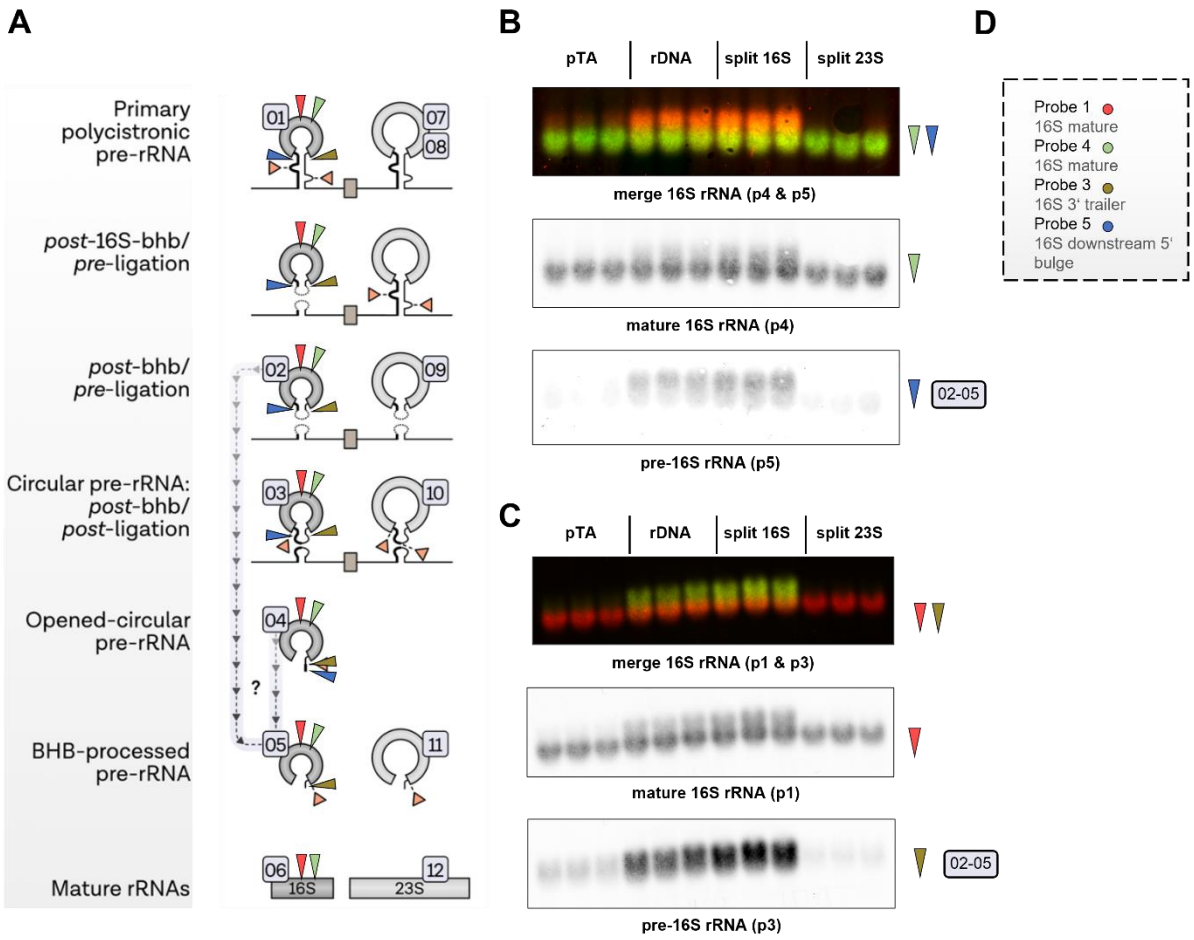

Figure 26: Extra copies of rDNA genes result in increased pre-rRNA levels analyzed by Northern blot. (**A**) Maturation parthway of 16S rRNA (dark grey) and 23S rRNA (grey) is depicted. Fluorescent oligos used for Nothern blot analysis detecting mature 16S (red or green arrow) or different maturation species like 16S pre-rRNA downstream 5' bulge (blue arrow) or 16S 3' trailer (yellow ocher arrow) and their respective hybridization sites are indicated. (**B** & **C**) Northern blot analysis of total RNA extracted from cells transformed with rDNA constructs (see figure 24). Experiments were performed with biological triplicates. Mature and precursor 16S rRNAs were detected with probes 4 and 5 (**B**) and probes 1 and 3 (**C**). Both Northern blots showed a strong accumulation of 16S pre-rRNAs in the cells transformed with additional 16S rDNA copies (rDNA & split 16S). The accumulation appeared strongest in cells transformed with split 16S rDNA constructs. The signal of 16S pre-rRNAs in the cells transformed with split 23S rDNA constructs was slightly reduced compared to the pTA control (**B**). (**D**) Fluorescent probes used for Northern blot anaylsis are listed. Panel **A** is adapted from Grünberger et al. 2022.

The observation correlates with the Northern blot results from the same cells and could also pose an accumulation of 16S pre-rRNAs. It must be mentioned however, that the exact identity of the RNA species cannot be defined in these profiles based on sequence length only. Another helpful characteristic of the technique on the other hand is the computation of molarities by integration of individual peaks and normalization to the overall concentration. Thereby, a table including a set of parameters for every profile is created (shown in figure 27 B). To get an estimation of changes in (pre-)rRNA amounts we calculated the ratio of 16S peak to 23S peak molarities in all conditions. Figure 27 G illustrates the ratios in two plots done for each RNA extraction method.

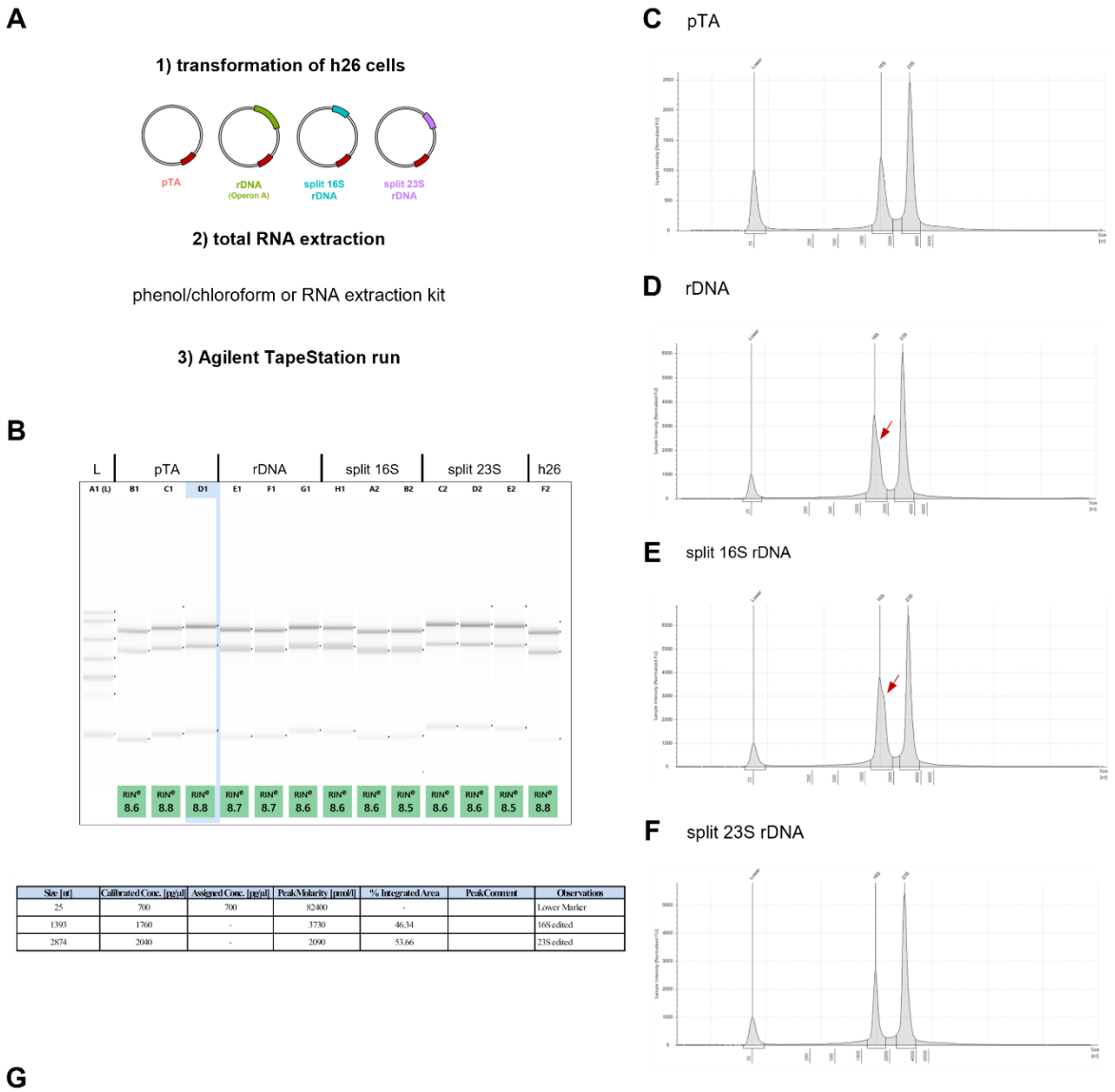

Size [nt]	Calibrated Conc. [pg/µl]	Assigned Conc. [pg/µl]	Peak Molarity [pmol/l]	% Integrated Area	Peak Comment	Observations
25	700	700	82400	-		Lower Marker
1393	1760	-	3730	46.34		16S edited
2874	2040	-	2090	53.66		23S edited

Figure 27: Extra copies of rDNA genes result in increased pre-rRNA levels analyzed by Agilent TapeStation analysis. (**A**) General workflow is depicted. *H. volcanii* h26 cells were transformed with pTA1228, rDNA**,** split 16S rDNA or split 23S rDNA constructs. Subsequently, total RNA was extracted with either classical phenol/chloroform extraction or RNA extraction kit form MACHEREY-NAGEL and RNA was analyzed on Agilent 4200 TapeStation system according to manufacturer's protocol. As an additional control h26 grown in YPC was analyzed. (**B**) Provided ladder (L), RNA from the four different constructs in biological triplicates were loaded on high sensitivity RNA Screen tape. TapeStation readout is shown in the form of an agarose gel image. RINs (RNA integrity numbers) in green indicate good RNA quality. Agilent TapeStation software calculates features like concentrations or peak molarity via integration of signal peaks seen in (**C**-**F**). Table below depicts exemplary results. (**C**-**F**) Profiles of selected

(figure 27 continued) TapeStation runs are illustrated (peaks from left to right: ladder, 16S, 23S,). The 16S peaks of the 16S split rDNA and rDNA constructs appeared broader with a shoulder (red arrow) at the right edge of the peak, indicating higher molarity. (**G**) Two plots showing rRNA ratios computed based on peak molarity calculations. RNAs extracted with RNA extraction kit or classical phenol/chloroform extraction were analyzed in this way. The value of one pTA replicate was arbitrarily set to 1 and used as respective reference.

As a reference the 16S to 23S ratio of one pTA1228 clone was arbitrarily set to one. The 16S to 23S (pre-)rRNA ratios increased in the cells transformed with rDNA (up to around 1.25-fold) and split 16S rDNA (up to around 1.5- fold) constructs. In the split 23S rDNA transformed cells on the other hand, the ratio decreased, indicating more 23S(pre-)rRNAs compared to 16S (pre-)rRNAs. The results for the two RNA extraction methods were conclusive and the overall picture confirmed the apparent increase of (pre-)rRNA previously observed in the Northern blot analysis.

To shortly sum up, we could detect a 2- to 2.5-fold increase of rDNA copies in h26 cells after transformation of respective rDNA plasmids. Furthermore, we could demonstrate a higher rate of up to 1.5-fold of (pre-)rRNAs present in the cells with increased rRNA gene dosage by Northern blot and Agilent TapeStation analysis.

6.3. Discussion

Which conclusions can be drawn from the cumulated findings? First, the introduction of additional rDNA copies does not seem to change the genomic rDNA copy number. This would oppose a global regulatory mechanism of genome copy number solely based on total rDNA copies present in the polyploid organism *H. volcanii*. Another observation was the slight increase of rDNA plasmid copy number compared to the other constructs. Potentially, high transcription rates of the rRNA gene would favor transcription-induced replication of the plasmids and thereby elevate their numbers. High transcription from rDNA loci was suggested to support replication in absence of DNA replication origins in *H. volcanii* (Hawkins et al. 2013). Still, as a caveat it should be noted, that using the SYBR Safe signals to normalize the Southern blot signals is not the most accurate method and results should be interpreted cautiously. Alternatively, using genes which are not involved in ribosome biology and are encoded on the *H. volcanii* wild type plasmid pHV2 would be better suited for internal normalization to determine copy numbers of the main chromosome or transformed plasmids (Hartman et al. 2010). The estimation of genomic versus plasmid encoded rDNA copies is more reliable as the ratios are calculated from the same Southern blot experiment.

Gene dosage increased 2- to 2.5-fold and the ensuing question was whether the higher copy number is also reflected in a simultaneous raise of precursor and mature rRNA production. Northern blot experiments clearly showed an accumulation of 16S pre-rRNAs in the rDNA and split 16S rDNA construct transformed cells. Most likely, this effect originates from higher rDNA transcription rates in cells with increased rRNA gene dosage in combination with a decelerated or even arrested maturation of excess pre-rRNAs. At which stage a slowdown of the maturation occurs, can only be speculated about. The disposability of r-proteins could be one limiting factor. Conversely, it is conceivable that 'naked' pre-rRNAs completely devoid of r-proteins would be rapidly degraded. Therefore, a certain pre-ribosomal assembly stage might be reached before particular r-proteins are missing and affecting progression of the maturation. Another possibility would be a limitation of ribosome biogenesis factors to sufficiently keep up with the higher transcriptional output generating more pre-rRNAs. In this scenario r-proteins would already be available in excess in the wild type situation, or their level is co-regulated with the rDNA transcription rate. A third possibility could be the intracellular localization of rDNA plasmids. There is at least some evidence that functional compartmentalization might be a means to streamline ribosome biogenesis in bacteria (see chapter 7; Scholz et al. 2019). Nucleolar-like ribosome assembly factories close to genomic rRNA genes could be disrupted by transcription from elsewhere located, cytoplasmic rDNA plasmids, that might recruit and disperse RBFs. Localization studies of RNAP in *E. coli* revealed that cytoplasmic rDNA plasmids were able to physically relocate polymerases away from the chromosomal, nucleoid-located *rrn* loci, which was associated with the observed, reduced growth (Cabrera and Jin 2006).

Eventually, in all the scenarios listed above this would mean that the availability and/or capability of molecular components required for rDNA transcription like RNAPs, or transcription factors is higher than those required for either adequate RNA degradation or ribosome maturation like r-proteins or RBFs. In other words, ribosome maturation rather than rDNA transcription would be the bottleneck and rate limiting capacity of ribosome assembly in the described scenario of increased rRNA gene dosage.

Notwithstanding, the more quantitative results of the Agilent TapeStation analysis suggested that increased gene dosage is not reflected in a one-to-one increase in transcriptional activity. The 2-to-2.5-fold higher number of rDNA copies was accompanied by an at most 1.5-fold increase of 16S (pre-)rRNAs production. This contradicts the initial *E. coli* model in which no significantly higher transcription rate was detected concomitantly with a similar 2 to 3 fold increase of total rDNA copies (Jinks-Robertson, Gourse, and Nomura 1983). Another study reported a 1.5-fold and 2.5-fold increase of rRNA transcription when introducing intact or

defective rDNA plasmids, respectively (Baracchini and Bremer 1991). Increasing *rrn* gene dosage in non-optimal media had an even more drastic effect on rRNA transcription (Stevenson and Schmidt 1998). Three options appear considerable. For one, rDNA transcription is faster than ribosome maturation can occur, yet it is limited by the availability of RNAPs, transcription factors or other components. Secondly, rDNA transcription is in parts restricted by active regulatory mechanisms of e.g., transcription factors as opposed to the first indirect limitation. It is also questionable if all present rDNA copies are always actively transcribed or whether there are molecular mechanisms to shut-down active gene copies similar to eukaryotic 'open' or 'closed' chromatin states. In case such mechanisms are in place in *H. volcanii*, rDNA copies on plasmids might escape this shutdown and still be excessively transcribed. Lastly, transcription rates might be even higher than calculated, however a fraction of excess (pre-)rRNAs gets rapidly degraded due to the lack of decorating, thereby protecting r-proteins or RBFs.

What is more, the balance of 16S and 23S (pre-)rRNA generation can be investigated with the expression of 16S split and 23S split rDNA constructs in *H. volcanii*. Northern blot analysis revealed a slight decrease of 16S pre-rRNAs in the 23S split rDNA plasmid transformed cells. This observation was supported by the Agilent TapeStation experiment which showed a decreased 16S/23S (pre-)rRNA ratio in 23S split rDNA plasmid transformed cells. Remarkably, a higher 16S to 23S (pre-)rRNA ratio in cells transformed with rDNA plasmid was observed in the two different analyses even though a one-to-one ratio would be expected. This imbalance could be explained with either an aberrant rDNA transcription or higher degradation of LSU (pre-)rRNAs. The notion of decreased 16S pre-rRNAs, likely indicating faster maturation, at presumably higher 23S rDNA transcription rates, however, cannot reconcile either one of the above-described scenarios. Nevertheless, it can be stated, that there is some crosstalk and coordination regarding the production of the two ribosomal subunits. Yet, it is so far completely unknown at which level regulation might occur and further experiments must be performed to illuminate this issue. In *E. coli*, the effects of such an unbalanced rRNA gene dosage have been studied by introducing plasmids with large deletions in the 16S and 23S rRNA genes. Although the deletions affecting both 16S and 23S rDNA or only 23S rDNA resulted in imbalanced rRNA synthesis, excess rRNAs were not stable and rapidly degraded (Siehnel and Morgan 1985). Moreover, small, and large subunit ratios have been determined in this study by sucrose gradient centrifugation. Except in one deletion construct, no variations could be detected. Interestingly, the only notable outlier, a large deletion in the 23S rRNA gene caused a subunit imbalance which was suggested to originate from the accumulation of an unprocessed precursor (Siehnel and Morgan 1985). Interestingly, transfection of split 18S rDNA plasmids in mammalian cells also caused an accumulation of pre-rRNAs (Burman and

Mauro 2012). To test subunit imbalances sucrose gradient centrifugation analyses were performed one time in our lab to reveal the subunits ratio (supplementary figure S3). The outcome reflected roughly the results observed with the Agilent TapeStation and further supports an expected stabilization of excess (pre-)rRNAs. The ratio of 30S and 50S peaks changed in dependency of the respective transformed construct. Nevertheless, these experiments have only been performed once with only one biological replicate and should therefore be repeated and validated.

The present work revealed several insights into the effects of increased rRNA gene dosage in *H. volcanii*. By identifying rate-limiting steps it can also provide the basis for future avenues inquiring general regulation of ribosome biogenesis in archaea. Still, the significance of the obtained results could benefit from reproduction of some experiments. For example, Southern blot analyses were only performed in biological duplicates. Moreover, many questions remain open and further experiments are required to answer them. A more accurate Southern blot normalization method to determine plasmid copy numbers could potentially consolidate the observed trend. Along those lines, we also tried to use qPCR analysis as alternative, however, unidentified issues led to inconclusive results (data not shown).

Classical biochemistry work has utilized psoralen accessibility assays to analyze the ratio of open and closed, i.e., actively transcribed vs inactive rDNA genes in yeast and changes thereof in varying growth conditions (Dammann et al. 1993). In the past years, it became clear, that structural genome organization in the form of DNA packaging by nucleosomes in a chromatin-like organization is a common feature in archaea (Sanders, Marshall, and Santangelo 2019). More specifically, genome-wide nucleosome occupancy maps have been created by MNase-seq in *H. volcanii* (Ammar et al. 2012). Both techniques, psoralen accessibility assays and MNase-seq, could be tested to investigate the rDNA packaging status in the described rRNA gene dosage settings. Furthermore, DNA-FISH microscopy at sufficiently high resolution could indicate the localization of rDNA plasmids in relation to genomic rDNA copies and even assign plasmid copy numbers at single-cell level. Practical DNA-FISH protocols for *H. volcanii* are not yet available in our lab, however we are working on establishing such methodologies (see chapter 7). Similarly, it would be interesting to check the localization of RNAPs in the presence of rDNA plasmids in comparison to the observed effects in *E. coli* (Cabrera and Jin 2006). Single molecule tracking of RNAPs is feasible in living in *H. volcanii* cells and was recently described (Turkowyd et al. 2020).

Analogous to Nomura's studies in *E. coli*, gene dosage effects with defective rDNA plasmids producing non-functional ribosomal subunits could be analyzed to test some of the hypothesis above regarding the stage of regulation (Gourse et al. 1985; Yamagishi, de Boer, and Nomura

1987). Aside from that it would be important to identify nascent transcription rate, independent from potential degradation of excess (pre-)rRNAs. In the experiments performed so far, transcription and degradation cannot be distinguished. For this purpose, pulse-chase experiments might be valuable to follow nascent transcripts *in vivo*. Protocols for 4-thiouracil labeling of nascent RNAs in archaea have been established in our lab and are perfectly suited for this kind of analysis (Knüppel, Kuttenberger, and Ferreira-Cerca 2017). Similarly, protocols to perform BONCAT (biorthogonal noncanonical amino acid tagging) in archaea have been developed for *H. volcanii* and could be used to analyze changes of bulk translation (Kern and Ferreira-Cerca 2022). In addition, the localization of excess mature ribosomal subunits or pre-ribosomes in single cells could be of investigated by applying already available RNA-FISH microscopy protocols as described in chapter 7.

The study of rRNA gene dosage in archaea could benefit from a broader phenotypic investigation of the different transformants. Growth behavior and general traits like e.g., cell morphology could easily be analyzed, as many protocols are available and in use in the lab. It would also be interesting to know if the increased rRNA gene dosage and concomitant higher transcriptional rate comes with a cost of being less adaptive in certain stress conditions. Introducing intact and defective rDNA plasmids in *E. coli* negatively affected growth (Baracchini and Bremer 1991). As the picture of rRNA gene dosage effects in *E. coli* was not entirely unambiguous, it might also be worth to consider re-evaluating nascent rRNA synthesis rates and checking the accumulation of pre-rRNAs in *E. coli* with similar analyses as described herein.

Lastly, the rDNA and split constructs could themselves be exploited as tools to study other aspects of ribosome biogenesis in archaea. Certain analyses suffer from detection limit issues and a relative increase of pre-rRNA levels might be helpful to overcome problems in some biochemical protocols. Examples could be the purification of pre-ribosomal particles or detection of scarcely abundant rRNA precursors.

7. Functional Compartmentalization in Archaea

7.1. Introduction

Yet another aspect of ribosome biology concerns the intracellular localization of the translation apparatus and its manufacturing machineries. The nucleus and within it especially the nucleolus is the hotspot for most of ribosomal gene transcription and maturation of ribosomal subunits in eukaryotes (Boisvert et al. 2007). Emphasizing its key role, the nucleolus architecture is directly linked to its functional status i.e., active ribosome assembly, since it disassembles when ribosomal gene transcription is repressed (Misteli 2001). By definition, almost all prokaryotes lack such a defined, membrane-engulfed compartment governing transcription and ribosome assembly as the eukaryotic nucleus (Fuchs et al. 2014). Nonetheless, the view of bacterial cell biology as solely being homogeneous and static has changed over the years (Gitai 2005). Cytoskeletal elements, cellular polarity or the aggregation of chromosomal DNA in a formation called the nucleoid is commonly found in bacteria (Gitai 2005). In *E. coli*, *B. subtilis* or *B. bacteriovorus* ribosomes are mostly excluded from the DNA containing nucleoid (Lewis, Thaker, and Errington 2000; Borgnia, Subramaniam, and Milne 2008; Bakshi et al. 2012; Chai et al. 2014). Conversely, ribosomes and DNA spread equally throughout the cell in *Caulobacter crescentus* (Montero Llopis et al. 2010). Interestingly, studies with GFP-tagged RNA polymerases (RNAP) in *E. coli* indicated a role of stable RNA genes transcription for the condensation of the nucleoid (Cabrera and Jin 2003; Cabrera et al. 2009). Moreover, in fast-growing cells RNAP concentrated in transcription foci, likely transcribing predominantly stable RNAs (Cabrera and Jin 2003; Cabrera et al. 2009). Additionally, six of seven rDNA operons in *E. coli* were found to colocalize in the nucleoid in dependency of the rDNA promotor P1 (Tamas Gaal et al. 2016). High resolution mapping of transcriptional activity on the *E. coli* chromosome revealed, highly transcribed *rrn* operons partly in clusters (Scholz et al. 2019). Furthermore, RNAP accumulations were detected to colocalize with rRNA precursors, however these clusters were also forming independently of high levels of rRNA transcription (Weng et al. 2019). Analogous experiments were performed in *B. subtilis* and a spatial separation of ribosomes and RNAP as well as growth-rate dependent RNAP foci were observed (Lewis, Thaker, and Errington 2000). Selected antibiotics were used to reassure the correlation of active transcription and translation with functional compartmentalization (Cabrera et al. 2009). Altogether, these lines of evidence indicate a potential functional compartmentalization in bacteria resembling the eukaryotic nucleolus. Correspondingly, intriguing RNA-FISH experiments visualized early pre-rRNA species associated with the nucleoid and correlated rRNA processing events with their sub-cellular localization (Malagon 2013).

How about the intracellular organization of archaea? Microscopy technologies have demonstrated that archaeal cells come in all shapes and forms (Bisson-Filho, Zheng, and Garner 2018). The picture of the inner cellular organization of archaea is not yet very well defined, nevertheless in the past years it became somewhat clearer. For one, nucleoid structures like in bacteria were also seen in various archaeal species (Popławski and Bernander 1997; Malandrin, Huber, and Bernander 1999; Pelve et al. 2011; Delmas, Duggin, and Allers 2013). Furthermore, recent technological advancements have enabled archaea researchers to study cellular characteristics like cell division proteins, components of the chemotaxis machinery or the dynamics of RNAP (Zhengqun Li et al. 2019; Pulschen et al. 2020; Turkowyd et al. 2020; Nußbaum et al. 2021; Liao et al. 2021). Remarkably, experiments on *Sulfolobus* species revealed higher-ordered chromatin architecture typically found in eukaryotes and more complex than in bacteria (Cremer and Cremer 2001; Takemata, Samson, and Bell 2019; Takemata and Bell 2021). Notably, loop structures brought genes encoding ribosomal genes into close proximity, pointing to a spatial coordination of ribosome assembly (Takemata and Bell 2021). In contrast, euryarchaeal representatives did not exhibit this level of compartment-like structure (Cockram et al. 2021). Intriguingly, Islas-Morales et al. provided evidence for a nucleolus-like structure in *Saccharolobus (*formerly *Sulfolobus*) *solfataricus* cells using electron microscopy and proteomic analyses (Islas-Morales et al. 2023). With the application of a staining protocol, typically used to visualize eukaryotic nucleolar organizer regions, similar structures could be detected in the archaeal cells (Islas-Morales et al. 2023).

Unfortunately, there is not much known about the distribution of gene expression machineries in archaeal cells. Yet, in the marine *Crenarchaeum symbiosum* a polar distribution of rRNA and DAPI stained DNA was detected (Preston et al. 1996; Könneke et al. 2005). Another study, ironically from the usually very inaccessible Asgard archaea, reported on a spatial separation of genetic material and ribosomes in Loki- and Heimdallarchaeota (Avcı et al. 2022). Conversely, cryo-tomograms of the recently isolated '*Ca.* L. ossiferum' showed a relatively homogenous distribution of ribosomes in the cell, however genetic material was not simultaneously visualized (Rodrigues-Oliveira et al. 2022). Still, our understanding of archaeal cell biology is far from being comprehensive and future investigations are required.

Therefore, we wanted to address the issue of how archaeal cell biology compares to what was seen in some bacteria regarding the spatial separation of transcription and translation machineries. What is more, we aimed to investigate putative functional compartmentalization in archaeal cells in regards of ribosome biology and biogenesis. To this end, we started to establish RNA-fluorescence *in situ* hybridization (RNA-FISH) microscopy methodologies applicable in *Haloferax volcanii* and *Sulfolobus acidocaldarius*. Greatly instrumental for this

project was a Master student I was fortunate enough to supervise, Maximilian Liebl, who was engaged in the development of protocols and image collection. Our goals were to first visualize mature ribosomal subunits and their sub-cellular localization. Secondly, we set out to investigate whether compartmentalization is dependent on transcriptional or translational activity by applying different antibiotic drugs. Finally, we were aiming to detect pre-rRNA species to potentially determine the location of distinct rRNA maturation steps in the cell.

7.2. Results

The first hurdle to overcome in this regard was to establish applicable RNA-FISH protocols for *H. volcanii* and *S. sulfolobus*. Robert Knüppel, Maximilian Liebl and I worked on the adaptation of protocols used for RNA-FISH microscopy in yeast or mammals to study various facets of eukaryotic RNA biology (Long et al. 1995; Bertrand et al. 1998; Darzacq et al. 2002; Ferreira-Cerca et al. 2014). The final workflow is described in material & methods 9.2.8.2. In brief, *H. volcanii* or *S. sulfolobus* cultures were grown in full media at 42 °C or 65 °C, respectively and crosslinked with formaldehyde. Nucleoid staining was achieved by adding Hoechst 33342 to the cultures during crosslinking. Cells were then transferred onto poly-L-lysine coated glass slides. After pre-hybridization fluorescently labeled RNA-FISH probes were incubated for 3 hours directly on slides, which were washed and eventually imaged on a microscope. Applied oligos were labeled with fluorescent dyes Atto488, Cy3, Cy5 or Alexa647 and are listed in material & methods 9.1.3 in table 14.

7.2.1. RNA-FISH in *Haloferax volcanii*

As a start and appropriate validation for our RNA-FISH protocol we were looking at the cellular repartition of the translation apparatus and its location relative to the nucleoid in *H. volcanii*. Ribosomal subunits were successfully visualized with RNA-FISH probes hybridizing to mature 16S rRNA and 23S rRNA as shown in figure 28. Interestingly, mature rRNAs were predominantly detected in the cytoplasm excluded from the nucleoid. Apparently, ribosomes surrounded the nucleoid, suggesting a functional separation of genetic material and translation machinery, i.e., transcription and translation. Similar compartmentalization has been observed in *E. coli* and *B. subtilis* (Lewis, Thaker, and Errington 2000; Bakshi et al. 2012; Chai et al. 2014). To examine whether this intracellular partition is the result of the activity of important gene expression functions like active transcription and translation we were testing different

antibiotics and performed RNA-FISH experiments. Actinomycin D, Rifampicin or Thiostrepton were used for this purpose affecting transcription by intercalating into the DNA, inhibiting RNAP or inhibiting translation, respectively (Hartmann et al. 1967; Sobell 1985; Walter et al. 2012). After 1 hour of treatment with either one of these drugs a slight mixture of ribosomal subunits with the nucleoid could be observed, especially in the case of Actinomycin D, as seen in figure 29. Furthermore, in the latter case cells appeared to be uniformly round, whereas untreated cells exhibited the two typical morphotypes for *H. volcanii*, that is to say rod shaped and discoid-shaped cells. These two main morphologies of *H. volcanii* cells are dependent on growth phase or medium composition (Mullakhanbhai and Larsen 1975; de Silva et al. 2021). It was also reported elsewhere that DNA damage induced by UV radiation or Actinomycin D

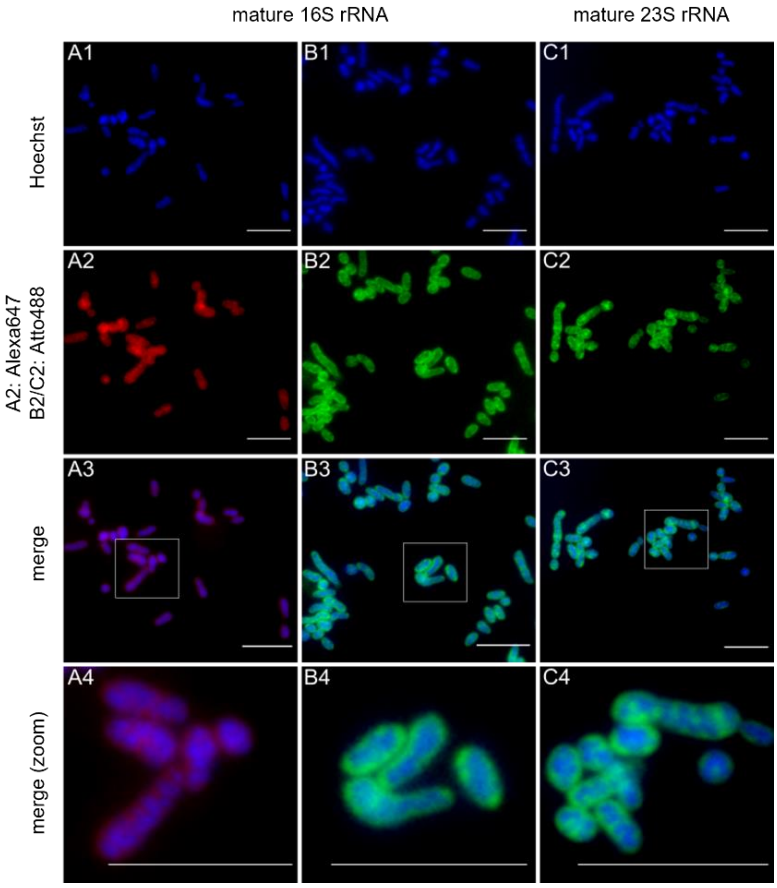

Figure 28: Partial separation of genetic material and translation machinery in *Haloferax volcanii* visualized by RNA-FISH fluoresence microscopy. Visualization of nucleoid was performed with Hoechst staining (A1-C1). Oligos labeled with fluorescent dyes Alexa647 (A2) or Atto488 (B2/C2) hybridized to mature 16S and 23S rRNA and were used to track small and large ribosomal subunits (for hybridization sites see figure 30 B). Images A3-C3 show the overlapping fluorescent signals of stained nucleoid and RNA-FISH, which is magnified in images A4-C4. Exclusion of ribsomal subunits from the nucleoid was detectable in round and rod-shaped *H. volcanii* cells. Exposure times: Hoechst: 1/20 s; Alexa647: 1.2 s; Atto488: 1.0 s. Scalebar: 10 µm. Adapted from Master thesis Maximilian Liebl.

leads to nucleoid compaction as part of the DNA damage response in *H. volcanii* (Delmas, Duggin, and Allers 2013). Accordingly, active transcription and translation might participate in the intracellular organization of genetic material and translation machinery in mechanisms depending on active gene expression. In comparison, translation inhibiting drugs also induced the nucleoid to collapse into a compact, central mass in *E. coli* or *B. subtilis* (Dworsky and Schaechter 1973; Mascarenhas, Weber, and Graumann 2001; Zimmerman 2002; Chai et al. 2014). Noteworthy, bacterial, and archaeal cells after certain antibiotic treatment resemble cells in stationary phase in which less gene expression would be expected. Anyhow, antibiotic treatment at the given concentrations for one hour could be too short to cause a complete disruption. On the other hand, apart from active gene expression other aspects might influence the repartition in *H. volcanii*.

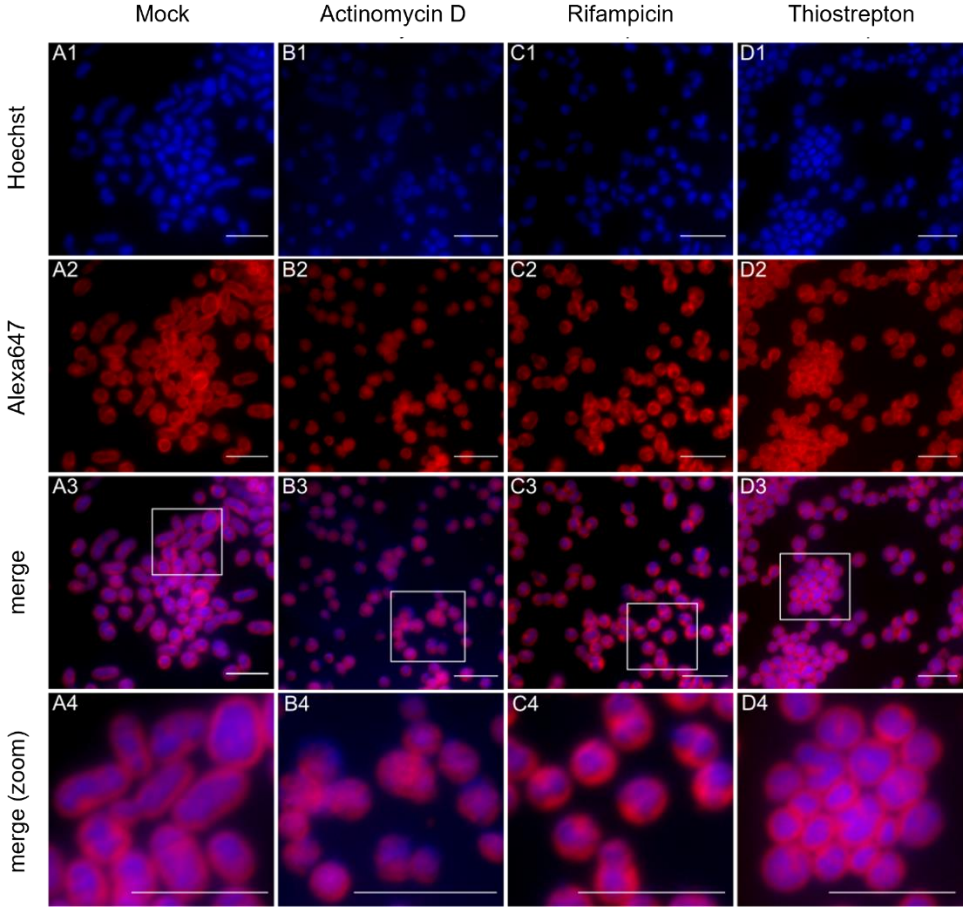

Figure 29: Active transcription or translation are participating in intracellular, spatial organization of the nucleoid and ribosomes in *H. volcanii*. *H. volcanii* cells were treated without (Mock) or with antibiotic drugs inhibiting transcription (Actinomycin D or Rifampicin) or translation (Thiostrepton) for 1 hour and RNA-FISH fluorescence microscopy was performed. Visualization of nucleoid was performed with Hoechst staining. Mature 16S rRNA was targeted with RNA-FISH oligos (A2-D2). Images A3-D3 show the overlapping fluorescent signals of stained nucleoid and RNA-FISH, which is magnified in images A4-D4. The exclusion of small ribosomal subunits in A4 is clearly visible, whereas the signals seem to become more mixed after antibiotic treatment, especially in the case of Actinomycin D. Exposure times: Hoechst: 1/20 s; Alexa647: 1.2 s Scalebar: 10 µm. Adapted from Master thesis Maximilian Liebl.

Next, we started to explore the feasibility of detecting rRNA precursors representing distinct rRNA maturation steps and their subcellular localization. To this end, we tested several pre-rRNA probes, which are depicted in figure 30 B. Fortunately, it was possible to employ RNA-FISH oligos binding to 16S rRNA precursors, upstream of the 5' bulge (very early), downstream of the 5' bulge (intermediate) or the 16S pre-rRNA ligation site (intermediate), representing circular and re-opened 16S pre-rRNA (see figure 30 A; for more details on pre-rRNA species see also 5.5). Furthermore, we could detect the 23S pre-rRNA ligation site, representing circular or re-opened 23S pre-rRNA. Small foci mostly co-localizing with the nucleoid were detected with the RNA-FISH oligo binding to 16S pre-rRNA upstream of the 5' bulge. As this pre-rRNA species represents very early intermediates right after or even during transcription the co-localization with the DNA would make sense. Probes hybridizing to the 16S pre-rRNA region downstream of the 5' bulge could also be visualized.

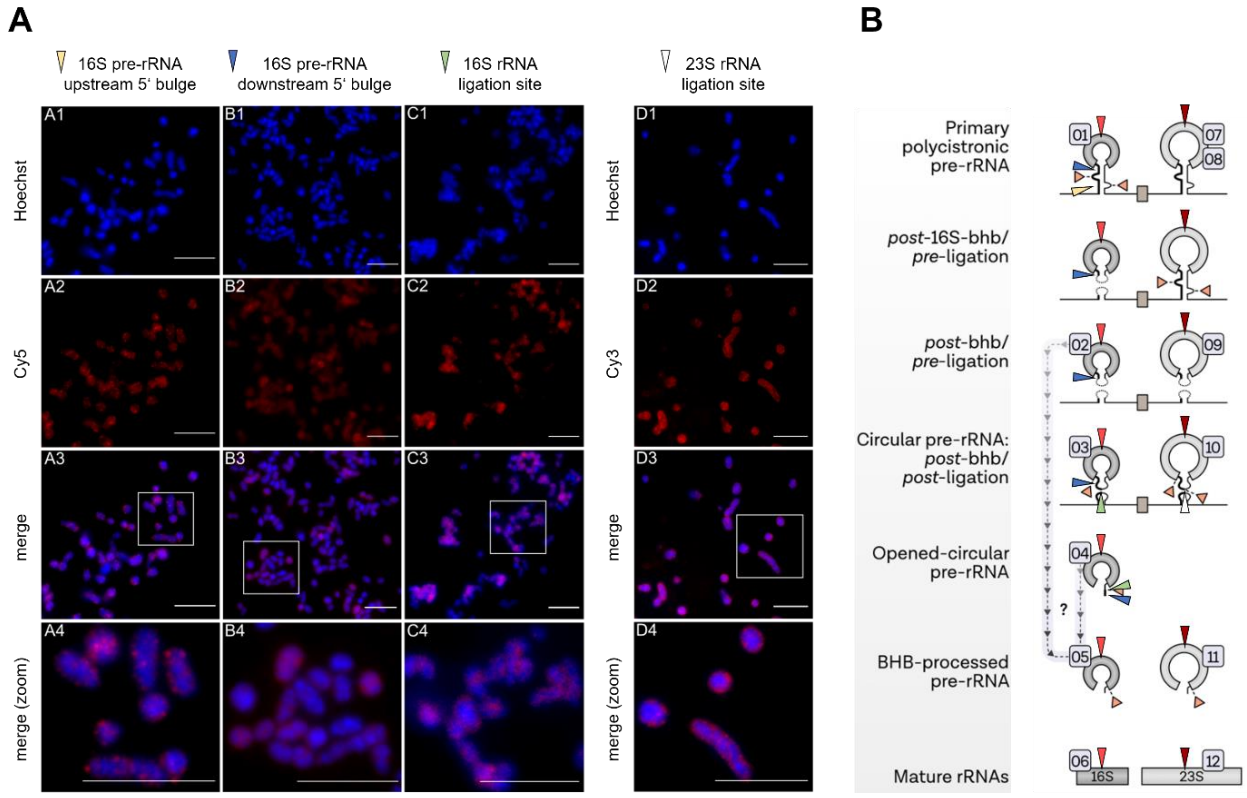

Figure 30: Localization of rRNA precursors in *H. volcanii* visualized by RNA-FISH fluoresence microscopy. (**A**) Visualization of DNA was performed with Hoechst staining (A1-D1). RNA-FISH oligos labeled with fluorescent dyes Cy5 (A2-C2) or Cy3 (D2) were used to track 16S and 23S pre-rRNAs (shown in B) with RNA-FISH microscopy. Images A3-D3 show the overlapping fluorescent signals of stained nucleoid and RNA-FISH, which is magnified in images A4-D4. Exposure times: Hoechst: 1/20 s; Cy5: 1.2 s (A2; B2, D2); Cy3: 2.5 s (C2); Scalebar: 10 µm. Adapted from Master thesis Maximilian Liebl (**B**) Maturation pathway of 16S rRNA (dark grey) and 23S rRNA (grey). RNA-FISH oligos used to detect mature 16S rRNA (red arrow), 23S rRNA (dark red arrow) or different maturation species like 16S pre-RNA upstream 5' bulge (yellow arrow), 16S pre-rRNA downstream 5' bulge (blue arrow), 16S pre-rRNA ligation site (green arrow) and 23S rRNA ligation site (white arrow) and their respective hybridization sites are indicated. Panel **B a**dapted from Grünberger et al. 2022.

Note that this probe targets various maturation intermediates (see figure 30 B). In this case the RNA-FISH signal still co-localizes with the nucleoid but becomes more blurry and less defined, in comparison with the defined foci observed with the previously described probe. Another oligo targeting the 16S pre-rRNA ligation site, binding to two different intermediates (see figure 30 B) was also successfully used. Here, the fluorescent signal appeared to be similar to the 16S pre-rRNA upstream of the 5' bulge probe and was found either co-localizing with or in close proximity to the nucleoid. The last RNA-FISH oligo of this set was employed to track the localization of the 23S pre-rRNA ligation site. Based on results from Nanopore sequencing, the probe likely detects mostly circular 23S pre-rRNAs. The signals clustered in many small

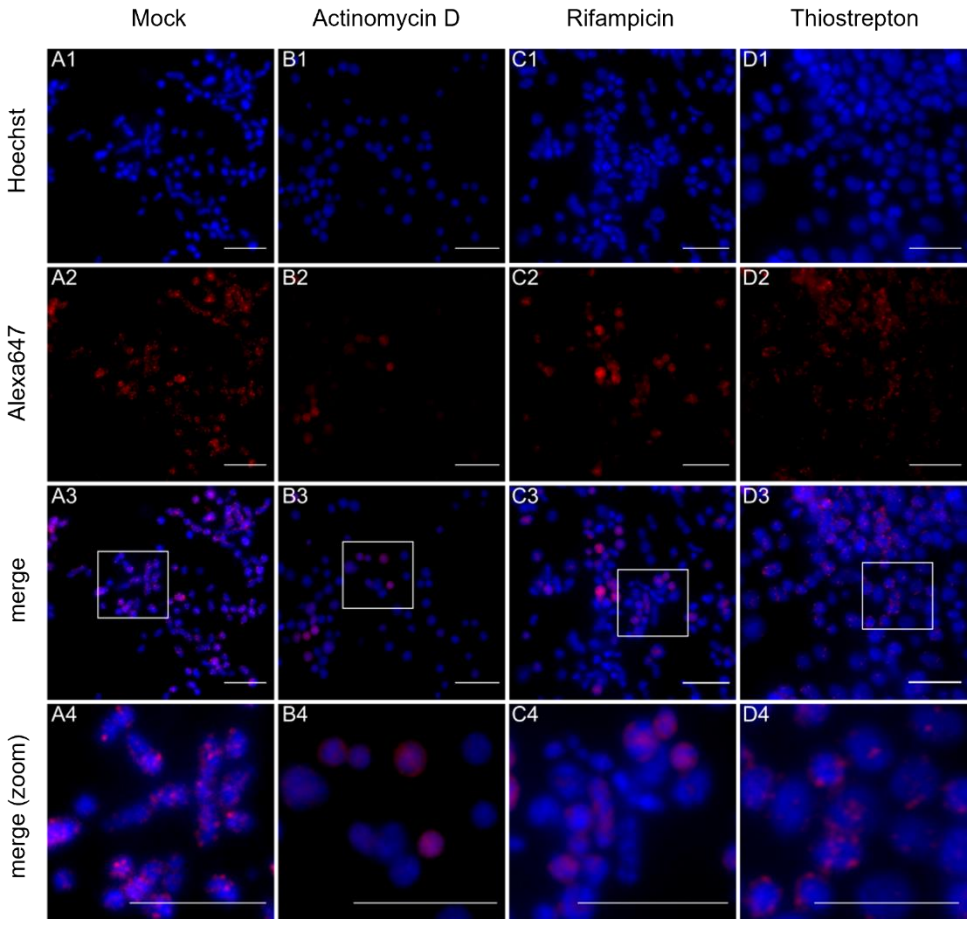

Figure 31: Transcription, but not translation inhibiting drugs affect localization of early 16S rRNA precursors in *H. volcanii*. *H. volcanii* cells were treated without (Mock) or with antibiotic drugs inhibiting transcription (Actinomycin D or Rifampicin) or translation (Thiostrepton) for 1 hour and RNA-FISH fluorescence microscopy was performed. Visualization of DNA was performed with Hoechst staining (A1-D1). Alexa647 labeled RNA-FISH oligos were used to show the localization of 16S pre-rRNA upstream 5' bulge (A2-D2), representing very early intermediates. See figure 30 B for hybridization target site. Images A3-D3 show the overlapping fluorescent signals of stained nucleoid and RNA-FISH, which is magnified in images A4-D4. RNA-FISH signal is co-localizing with the nucleoid in small dots in untreated cells (A4). The signal becomes more diffuse in Actinomycin D (B4) or Rifampicin (C4) treated cells, whereas Thiostrepton (D4) has no clear effect. Exposure times: Hoechst: 1/20 s; Alexa647: 1.2 s Scalebar: 10 µm. Adapted from Master thesis Maximilian Liebl.

foci and co-localized in some cases with the nucleoid but were more often found at the border of the nucleoid surrounding the genetic material. Hence, it was possible to detect a variety of pre-rRNA intermediates indicative of distinct pre-rRNA maturation steps with our RNA-FISH protocol.

The next question we were asking was how active transcription or translation inhibiting drugs affect the respective subcellular localization of pre- rRNAs. For this purpose, we treated *H. volcanii* cells with the same antibiotics as before (see figure 29 & 31). Then, we performed RNA-FISH with the oligos targeting 16S pre-rRNA upstream (see figure 31) and downstream of the 5' bulge (see figure 31). In comparison with the foci co-localizing with the nucleoid in the untreated cells (Mock) the RNA-FISH signal became slightly weaker, more diffuse and mixed with the nucleoid after Actinomycin D and Rifampicin treatment. Noteworthy, the translation inhibiting drug Thiostrepton led to a mild reduction of signal intensity but had no clear effect on the distribution of the 16S pre-rRNA upstream of the 5' bulge intermediate (see figure 31). The results for the RNA-FISH experiment targeting 16S pre-rRNAs downstream of the 5' bulge looked slightly different. Compared to the untreated cells, Actinomycin D treated cells showed a similar picture as before with fluorescent signals becoming more diffuse and mixed with the nucleoid. In the case of Rifampicin, no great difference to the untreated *H. volcanii* cells was visible. Interestingly, the RNA-FISH signal became notably more intense after Thiostrepton treatment with relatively steady distribution of signals compared to the mock control (see figure 32). The previously observed phenotype of uniformly round cells after Actinomycin D treatment could be confirmed in the two experimental setups focusing on 16S pre-rRNAs. Overall, transcription and translation inhibiting drugs were shown to alter the subcellular localization of certain 16S pre-rRNAs. The RNA-FISH signal intensity was also reduced in some cases, indicating less pre-rRNA production or increased degradation. Yet, this observation should be further reassured, for example by using more powerful microscopy techniques with higher quantitative validity.

Lastly, we explored the possibility to visualize the RNA base methylation status of 16S rRNA by using special RNA-FISH oligos, so called molecular beacons. These particular single-stranded probes contain a fluorescent dye on one end, a quencher attached on the other end of the molecule which are brought closely together by an internal stem-loop structure. Upon hybridization to target RNA or DNA a conformational change occurs that forces the two arms with fluorophore and quenching moiety apart, allowing the dye to emit a fluorescent signal (Tyagi and Kramer 1996). Molecular beacons can also be utilized to detect RNA modifications as described before with a method called methylation-sensitive RNA fluorescence *in situ* hybridization (MR-FISH) (Ranasinghe et al. 2018). The methodology exploits altered base-

pairing features of methylated RNA bases. In this study, a knockout of the bacterial di-methyltransferase and ribosome biogenesis factor KsgA was used as proof of principle for MR-FISH technique by exhibiting clearly different intensity of fluorescent signal upon hybridization of molecular beacons (Ranasinghe et al. 2018). Fortunately, a previous study from our lab investigated the role of archaeal KsgA-like protein and we used the existing *H. volcanii* ΔKsgA strain likewise as a control to test MR-FISH in our setup (Knüppel et al. 2021). Intriguingly, a clear difference of fluorescent signal intensity between wild type and ΔKsgA was observed (data not shown; Master thesis Maximilian Liebl). Conclusively, we could demonstrate that the methylation status of selected RNA bases can be monitored with our RNA-FISH setup, using specific molecular beacons.

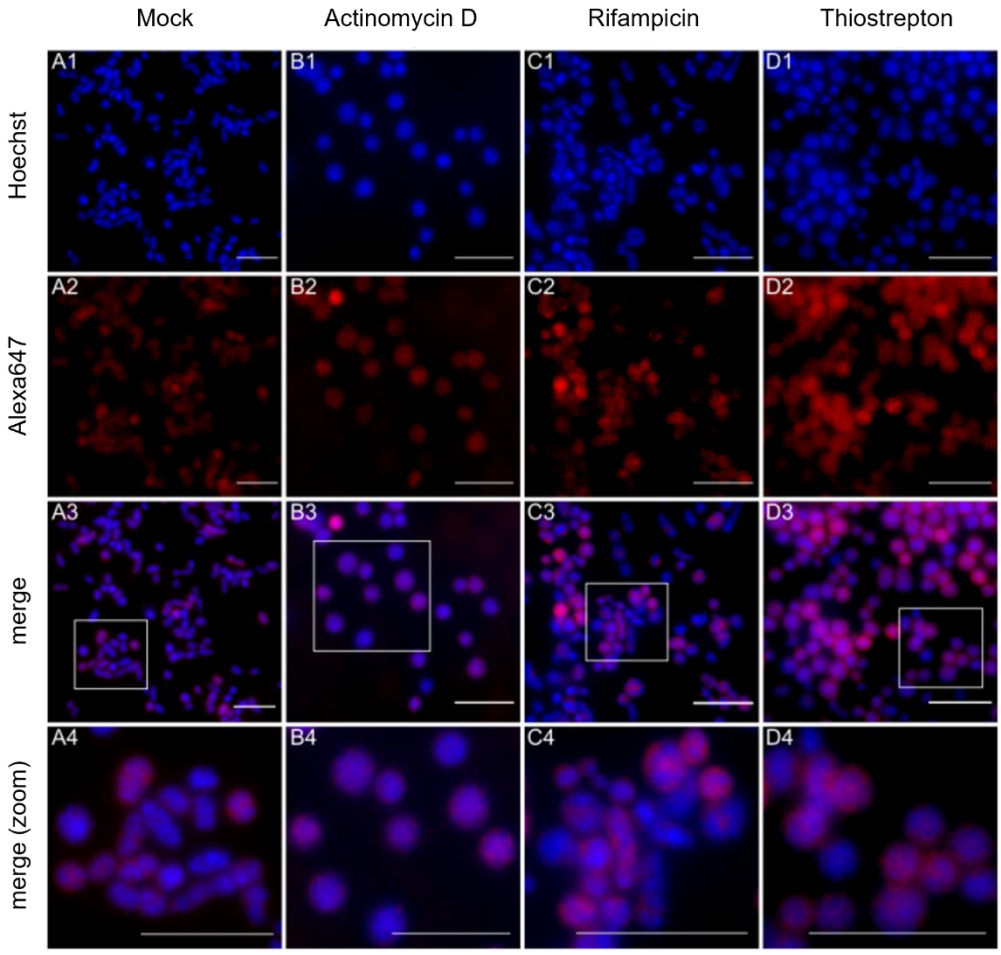

Figure 32: Transcription and translation inhibiting drugs moderately affect localization of 16S rRNA precursors in *H. volcanii*. *H. volcanii* cells were treated without (Mock) or with antibiotic drugs inhibiting transcription (Actinomycin D or Rifampicin) or translation (Thiostrepton) for 1 hour and RNA-FISH fluorescence microscopy was performed. Visualization of DNA was performed with Hoechst staining (A1-D1). Alexa647 labeled RNA-FISH oligos were used to show the localization of 16S pre-rRNA downstream 5' bulge (A2-D2), representing early to late intermediates. See figure 30 B for hybridization target sites. Images A3-D3 show the overlapping fluorescent signals of stained nucleoid and RNA-FISH, which is magnified in images A4-D4. RNA-FISH signal is co-localizing with the nucleoid in untreated cells (A4). The signal becomes slightly more diffuse in Actinomycin D (B4) or Rifampicin (C4) treated cells. The RNA-FISH signals seem to become stronger in Thiostrepton (D4) treated cells. Exposure times: Hoechst: 1/20 s; Alexa647: 1.2 s Scalebar: 10 µm. Adapted from Master thesis Maximilian Liebl.

7.2.2. RNA-FISH in *Sulfolobus acidocaldarius*

After we successfully established a feasible RNA-FISH protocol for *H. volcanii*, we wanted to gain a broader insight into the localization of ribosomal components in archaea. Accordingly, we were using the model system *Sulfolobus acidocaldarius*, a crenarchaeal representative thriving at low pH and at an optimal growth temperature of 75 °C. Except from different cultivation conditions, RNA-FISH experiments were performed similarly to *H. volcanii*.

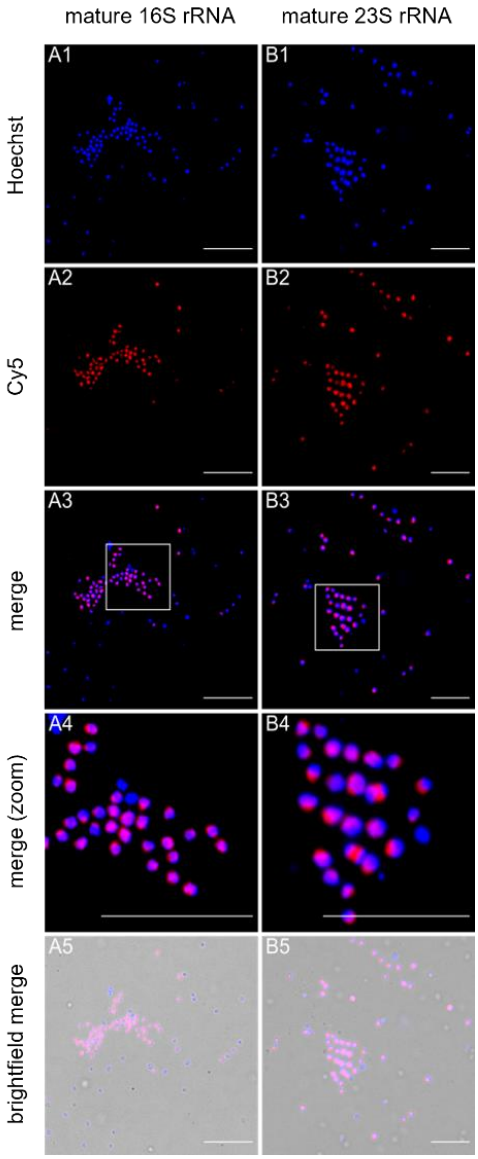

Figure 33: Clear separation of genetic material and translation machinery in *Sulfolobus acdidoladarius* cells visualized by RNA-FISH fluorescent microscopy. Visualization of nucleoid was performed with Hoechst staining (A1 and B1). RNA-FISH oligos labeled with fluorescent dye Cy5 hybridized to mature 16S and 23S rRNA and were used to track small and large ribosomal subunits (A2 and B2). Images A3 and B3 show the overlapping fluorescent signals of stained nucleoid and RNA-FISH, which is magnified in images A4 and B4. Images A5 and B5 additionally show overlap with brightfield picture. A clear separation of mature rRNAs and nucleoid was detectable indicating a polar distribution of ribosomes. Exposure times: Hoechst: 1/20 s; Cy5: 1.2 s; Scalebar: 10 µm. Adapted from Master thesis Maximmilian Liebl.

First, we were looking at the distribution of mature small and large ribosomal subunits with RNA-FISH oligos targeting mature 16S rRNA and 23S rRNA. As illustrated in figure 33 a very strong segregation of both ribosomal subunits from the Hoechst-stained nucleoid was visible. Remarkably, it looked quite different from the results observed in *H. volcanii*, where ribosomes mostly surrounded the nucleoid. In *S. acidocaldarius* however, there was almost no mixing of the RNA-FISH signal with the Hoechst signal, suggesting a polar distribution of the translation apparatus.

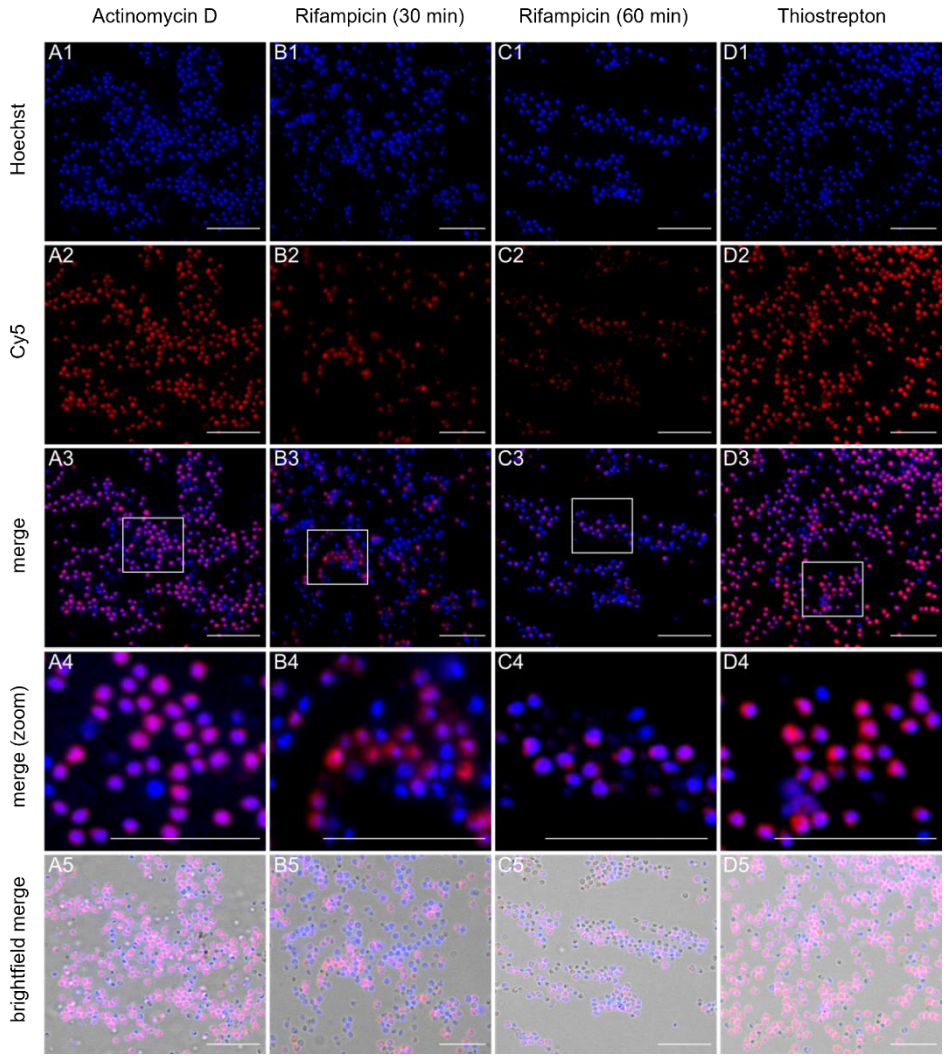

Figure 34: Active transcritpion or translation are participating in strong separation of genetic material and translation machinery in *Sulfolobus acidocaldarius* cells visualized by RNA-FISH fluorescent microscopy. *S. acidocaldarius* cells were treated with antibiotic drugs inhibiting transcription (Actinomycin D or Rifampicin) or translation (Thiostrepton) for 30 to 60 minutes (Rifampicin) or one hour (Actinomycin D and Thiostrepton) and RNA-FISH fluorescence microscopy was performed. Visualization of nucleoid was performed with Hoechst staining (A1 to D1). RNA-FISH oligos labeled with fluorescent dye Cy5 hybridized to mature 16S rRNA and were used to track small ribosomal subunits (A2 to D2). Images A3-D3 show the overlapping fluorescent signals of stained nucleoid and RNA-FISH, which is magnified in images A4 to D4. Images A5 to D5 additionally show overlap with brightfield picture. Polar distribution of ribosomes and separation from the nucleoid disappeared after Actiomycin D and Thiostrepon treatment. Rifampicin treatment reduced the RNA-FISH signal over time. The RNA-FISH signals seem to become stronger in Thiostrepton (D4) treated cells Exposure times: Hoechst: 1/20 s; Cy5: 1.2 s; Scalebar: 10 µm. Adapted from Master thesis Maximmilian Liebl.

In the same manner as performed in *H. volcanii* we wanted to examine the influence of active gene expression i.e., active transcription and translation, on the cellular distribution of ribosomes. Hence, we treated *S. acidocaldarius* cells for one hour with the antibiotics Actinomycin D, Thiostrepton or with Rifampicin for 30 or 60 minutes and performed RNA-FISH with oligos hybridizing to mature 16S rRNA. Strikingly, all three drugs had strong, although diverse effects on the distribution of the translation machinery in relation to the genetic material. Figure 34 shows a strong and very strong mixing of the RNA-FISH signal with the Hoechst signal after Thiostrepton or Actinomycin D treatment, respectively. The polar distribution of ribosomes is almost completely lost in the case of Actinomycin D and strongly reduced after Thiostrepton treatment. Rifampicin treatment induced a mixing of the RNA-FISH and Hoechst signals. Even more pronounced was the overall reduction of the RNA-FISH signal intensity over time. Presumably, this indicates a fast degradation of mature ribosomal RNA after transcription arrest by RNAP inhibition. Anyhow, this observation must be further examined by alternative methods like for example Northern blot, qPCR or quantitative RNA-seq technologies. All three antibiotic drugs induced a stark alteration of the translation apparatus' localization in relation to the DNA. These results suggest that active transcription and translation participate in the maintenance of the subcellular organization in *S. acidocaldarius*.

In summary, we could successfully establish applicable RNA-FISH protocols for archaeal species that enable us to:

i) Visualize the subcellular distribution of mature ribosomes
ii) Explore the effects of drugs or differential environmental circumstances
iii) Follow distinct pre-rRNA species indicative of certain rRNA maturation events
iv) Track specific RNA modifications in ribosomal rRNA

7.3. Discussion

Revealing the subcellular localization of distinct pre-rRNA maturation intermediates is one approach to comprehend the spatial progression of distinct ribosome biogenesis events in archaea. We showed the distribution of several pre-rRNA species in *H. volcanii*, mostly 16S pre-rRNAs, hence additional probes targeting 23S pre-rRNAs should also be examined. Unfortunately, it was not yet possible to detect pre-rRNAs in *S. acidocaldarius* with RNA-FISH or Northern blot (data not shown). This would indicate a different ratio of mature to precursor rRNAs in *Sulfolobus* compared to *Haloferax* or other technical issues. Indeed, our Nanopore-based sequencing analysis also suggests a much higher precursor to mature rRNA ratio in *H. volcanii* compared to *S. acdiocaldarius* (Grünberger et al. 2022). Very early pre-rRNAs have

been visualized by RNA-FISH microscopy in *E. coli*. The signal distribution co-localizes with the nucleoid and looks remarkably similar to our results with RNA-FISH probes detecting early pre-rRNA species in *H. volcanii* (see figure 30; Malagon 2013). Moreover, we observed an effect of transcription, but not translation inhibiting drugs on the localization of early pre-rRNAs. Later rRNA precursors seemed less affected, presumably indicating more stable intermediates with longer half-lives. In contrast, a partial exclusion of pre-ribosomes was reported in *E. coli* cells after translation inhibition (Sanamrad et al. 2014).

Tracking mature small and large ribosomal subunits was working well in both model organisms. One conspicuous notion was the apparent degradation of mature 16S rRNA after Rifampicin treatment in *S. acidocaldarius*, but not in *H. volcanii*. Noteworthy, Rifampicin treatment induced fast reduction of mature 16S and 23S rRNA in *E. coli* by degradation mechanisms likely involving RNase E (Hamouche, Poljak, and Carpousis 2021). It was also stated, however, that stable degradation after Rifampicin treatment might be different in rich or minimal medium (Lindahl 1975). *Sulfolobus* was reported to possess stringent control of stable RNA accumulation but apart from that there is no current idea how rRNA steady-state levels are reacting to changing nutrient or stress conditions, like antibiotic drugs (Cellini et al. 2004). At this point, complementary methods should be applied to first validate the observed rRNA degradation in *Sulfolobus* and then better understand the molecular basis of this effect.

It was previously reported that the conformation of the nucleoid was different in exponentially growing or stationary *Sulfolobus* cells (Popławski and Bernander 1997). Hence, the effect of growth conditions or environmental influences like for example varying temperature, salt concentration or nutrient content on intracellular distribution of either mature or precursor rRNAs should be closer investigated in *H. volcanii* and *S. acidocaldarius*. Having two phylogenetically distant representatives at hand, enables us to draw a more comprehensive and broader picture of archaeal intracellular ribosome biology. Moreover, as a technical expansion, super resolution microscopy might be a promising pursuit to obtain more precise and robust datasets and study allocation of pre-rRNAs in archaea. A scientific collaboration currently explores this possibility using our RNA-FISH protocols with the established oligos for mature rRNAs and pre-rRNAs.

Regarding the particular repartition of ribosomes in both analyzed archaeal species with a partial exclusion of ribosomes from the nucleoid in the case of *H. volcanii* and the polar distribution in *S. acidocaldarius* alternative methods could be employed to refine and reassure these results. In an ongoing collaboration project, we started to establish a cryo-ET workflow for *S. acidocaldarius* cells. Cryo-ET is an high resolution imaging technique which can generate three-dimensional views of samples like biological macromolecules or cells (Lučić, Leis, and

Baumeister 2008). With this kind of technology, ribosomes and their cellular repartition could be illustrated in great detail. Some preliminary, promising results were obtained, but workflows still have to be refined and better cryo-ET datasets generated.

The separation of ribosomes and the nucleoid has been observed in some bacterial species, yet not in all studied organisms (Lewis, Thaker, and Errington 2000; Borgnia, Subramaniam, and Milne 2008; Montero Llopis et al. 2010; Bakshi et al. 2012; Chai et al. 2014). A certain degree of variability concerning the intracellular organization of archaeal cells seems therefore plausible. The functional implications for gene expressions of the observed organization types in bacteria go along with the issue of transcription-translation coupling. The existence of co-transcriptional translation of mRNAs in bacteria has been determined decades ago by Miller and co-workers, the proportion to which this event occurs is however an open question and is probably species-specific (Miller, Hamkalo, and Thomas 1970; Montero Llopis et al. 2010; Bakshi et al. 2012; Castellana, Hsin-Jung Li, and Wingreen 2016). Different types like temporal coupling or an actual physical link of RNAP and pioneering ribosome as well as species specific differences have been discussed (Irastortza-Olaziregi and Amster-Choder 2021; G. M. Blaha and Wade 2022). Conclusively, the intracellular organization confines the possibilities of transcription machinery and translation apparatus to interact. In bacteria this coupling is spatially expected at the boundaries of the nucleoid and ribosome-rich regions or at the remaining fraction of ribosomes that co-localizes with the nucleoid (Bakshi et al. 2012; Sanamrad et al. 2014; Irastortza-Olaziregi and Amster-Choder 2021). Since *H. volcanii* and *S. acidocaldarius* displayed both a non-random distribution of ribosomes and nucleoid, similar underlying features might concern transcription-translation coupling in archaeal cells. Even if there might be some hints, there is still no direct evidence yet that this phenomenon occurs in archaea and future work will be needed (Weixlbaumer et al. 2021).

In addition, an interesting comparison that can be made between *S. acidocaldarius* and the few analyzed examples from the Asgard- or Crenarchaeota lineages. In *Crenarchaeum symbiosum* ribosomes showed a polar distribution and seemed to be excluded from the nucleoid (Preston et al. 1996; Könneke et al. 2005). A segregation of ribosomes and DNA was also observed in Heimdall- and Lokiarchaeota (Avcı et al. 2022). It should be stated, however, that the big gap between DNA and riboplasm is unusual at this magnitude and attempts to detect a separating membrane in the form of a nuclear envelope failed (Avcı et al. 2022). On the other hand, cryo-ET data from another Asgardarchaeon indicated a more regular distribution of ribosomes (Rodrigues-Oliveira et al. 2022). Hence, a strong separation of translation machinery and genetic material is probably not an exclusive characteristic of

Asgardarchaeota. It should therefore be treated with caution as an argument in the phylogenetic Asgard-eukaryotes debates.

What is more, as a complementary approach to RNA-FISH, ribosomal proteins could be tagged with fluorescent proteins, as demonstrated for many other proteins in *H. volcanii* and *S. acidocaldarius* (Zhengqun Li et al. 2019; Turkowyd et al. 2020; Nußbaum et al. 2021; Liao et al. 2021). Tagged versions of the SSU r-proteins S4 and S7 are readily available in our lab and could prove useful in this respect. Along those lines, another valuable tool, however not yet at hand would be GFP (or other fluorescent proteins)-tagged versions of ribosome biogenesis factors. These would potentially provide spatial insights into specific events of ribosome maturation and its progression, as some of them can be roughly classified as earlier or later acting factors during ribosome assembly. Live-cell imaging is technically possible in *H. volcanii* and dynamics of archaeal RBFs including binding and dissociation to pre-ribosomal subunits could be followed (Turkowyd et al. 2020).

Another general feature of rRNA maturation deals with the modification of rRNA. Hence, rRNA modification status may be corresponding to particular maturation stages. Molecular beacons could probably represent a practical tool to detect rRNA modification, as was demonstrated in the case of the KsgA-dependent di-methylation of 16S rRNA in *H. volcanii*. In the same manner, molecular beacons targeting other rRNA modifications could be tested in the future, bearing in mind the necessity for appropriate controls, most likely in the form of corresponding knockout strains of RNA modifying enzymes.

In terms of studying spatial organization of ribosome biogenesis in archaeal cells, it might also be helpful to visualize rRNA genes within the nucleoid by rDNA-FISH microscopy. The potential co-localization of rRNA genes with early rRNA precursors or early acting ribosome biogenesis factors could provide interesting insights in the spatial and even chronological progression of ribosome assembly steps. Furthermore, the presence of rRNA gene transcription hotspots could be investigated with GFP-tagged RNA-polymerases and rDNA-FISH. Tagged versions of RNAP already exist for the model system *H. volcanii* and have been successfully utilized to track RNAP dynamics in living cells at single molecule resolution (Turkowyd et al. 2020). Therefore, Maximilian Liebl tried to establish rDNA-FISH in *H. volcanii* and generated a first data set, however this protocol still needs some improvement and better validation.

In a nutshell, there is still a plethora of unexplored avenues to continue the study of functional compartmentalization and spatial organization of ribosome biogenesis in archaea. With the establishment of easily applicable RNA-FISH protocols in two archaeal species we provided first tools and insights in this field of study. As to the limitations of this approach, we could not

detect pre-rRNAs in *S. acidocaldarius*. It must also be mentioned that interpretation of signal intensity is not perfectly suited to make quantitative statements and supplementary methods should be applied to confirm observations.

8. General Discussion

Studying and characterizing the immensely complex process of ribosome biogenesis with all its specific nuances across the domains of Life has been and remains to this day a Herculean task. We have dedicated our interest to the particularities of how ribosomes are made in the archaeal domain. In contrast to the much better understood ribosome assembly process in eukaryotes or bacteria, only very little is known in archaea so far.

The present work aimed to illuminate several aspects of this fundamental cellular task in archaea, even though it can only be a drop in the ocean and numerous puzzles remain to be solved. We were starting out with the aim to characterize key *cis*- and *trans*-acting elements of archaeal ribosome biogenesis. Moreover, we try to compare gained insights with bacteria and eukaryotes to identify common and specific principles of this process in all domains of Life. We also reflect on our claim, that studying ribosome biogenesis can help to refine phylogenetic trees. Hereafter, the main findings of this work are summarized and discussed regarding the reconciliation of our initial goals.

8.1. Key findings

We were investigating a variety of aspects governing the ribosome assembly in archaea. To begin with, we took a closer look at the organization of the rDNA genes in archaea. As described in chapter 4, rDNA genes are in most organisms found in a linked form and transcribed as one polycistronic unit. However, in some archaeal and bacterial species, the SSU and LSU rRNA genes are separated and individually transcribed. Presumably, rDNA organization might be important for rRNA processing steps and enable stochiometric balance of both ribosomal subunits. For example, some evidence points to a distinct order of pre-rRNA processing steps in *H. volcanii*, which could potentially require a linked rDNA organization (see 5.4 and 5.5). Hence, certain functional necessities might be incorporated already in the organization of the rDNA and concomitantly some evolutionary pressure on retaining these features. On the other hand, we introduced split rDNA plasmids in *H. volcanii* and caused a one-sided overproduction of pre-rRNAs which likely mature into ribosomal subunits. At least in this plasmid-based approach linkage of rRNA genes was not a prerequisite for pre-rRNA production and putatively ribosomal subunit assembly. Interestingly, there are some prokaryotic outliers without a linked organization of the rDNA genes (Ahn et al. 2020; Brewer et al. 2020; Jüttner and Ferreira-Cerca 2022). A separation of the SSU and LSU rRNA genes

seems to be evolutionary conserved and there was until very recently no evidence for reversing a once unlinked rDNA organization. Eukaryotic rDNA organization appears to be exclusively linked, whereas in the Asgard superphylum, there were almost exclusively unlinked rRNA genes observed, aside from two exceptions (see chapter 4; Brewer et al. 2020; Jüttner and Ferreira-Cerca 2022; Rodrigues-Oliveira et al. 2022). This apparent discrepancy draws some attention since Asgards are handled as the prime candidate for being the cradle of the eukaryotic lineage. We argued therefore that the evolutionary trajectories of this feature of ribosome biogenesis must be taken into consideration for phylogenetic conjectures about the Asgard-eukaryotes relationship. Most notably, in the genome of the latest, isolated Asgard representative, a striking 23S-16S rRNA gene organization was found (Rodrigues-Oliveira et al. 2022). Although it is unclear at the moment if the rRNA genes are transcriptionally linked, this arrangement could indeed display an inverted re-linkage scenario of once separated rRNA genes.

After and/or while rDNA transcription produces the primary rRNA precursor transcript, ribosome maturation begins. Our favorite organism to examine archaeal ribosome biogenesis in the lab is *Haloferax volcanii*. Adjusted for this model organism, we developed our main methodology to effectively study the contribution of *cis*-acting rRNA elements to (pre-)rRNA processing: the *cis*-acting elements reporter assay. This tool allows us to follow (pre-)rRNA mutations and their effects on the maturation *in vivo*. So far, we demonstrated the significance of the bhb motif for efficient rRNA maturation and the circularization of pre-rRNAs (see 5.4.2; Jüttner et al. 2020). The presence of circular pre-rRNAs is an archaea-specific feature and has not been observed in the rRNA processing pathways of eukaryotes or bacteria.

We also used this method to study the importance of several stem structures in the 5’ leader sequence of the pre-rRNA in *H. volcanii*. One of the helices stood out noticeably since deletion of this helix completely impaired circular 16S pre-rRNA and total 16S rRNA production (see figure 11 in 5.4.3). The so-called helix B causing this effect does not attract researchers’ attention for the first time. In a previous study, it was already speculated that this helix might contribute to ribosomal RNA folding dynamics and adopt the role of the eukaryotic U3 snoRNA (P. P. Dennis, Russell, and Moniz De Sá 1997). Eukaryotic U3 snoRNA is thought to prevent the premature formation of the central pseudoknot, a hallmark RNA structure in the small subunit (J. M. X. Hughes 1996; Kudla et al. 2011; Woolford and Baserga 2013). The study from Dennis et al. based their proposition on the high conservation of this helix and sequence information. With our new insights, we could now provide *in vivo* evidence to demonstrate the functional significance of helix B in archaea. Intriguingly, presuming the aforementioned hypothesis would indicate the evolution of a *cis*-acting element, helix B in archaea, towards a

trans-acting element, U3 snoRNA in eukaryotes. Nevertheless, it is yet unknown which molecular mechanisms underlie the importance of helix B in *H. volcanii*. To gain more information and investigate a possible role in preventing premature central pseudoknot formation, we designed some mutants of helix B and analyzed their effects with the *cis*-acting elements reporter assay (see figure 13 in 5.4.3). To this end, the results can unfortunately not be interpreted conclusively, and follow-up experiments are still necessary. For instance, nucleotide exchanges in helix B could be combined with compensatory mutations in the potential base pairing sequence of the CPK on the rDNA reporter plasmids. Similar compensatory mutations have been analyzed in yeast to rescue U3 snoRNA mutations (Beltrame and Tollervey 1995). Additionally, implementing methodologies to identify RNA-RNA interactions like CLASH (cross-linking, ligation, and sequencing of hybrid), which has been employed to investigate snoRNA-rRNA binding, would be greatly instrumental (Kudla et al. 2011).

Still, several other possibilities for the role of helix B are conceivable based on compiled investigations in different model systems. Broadly speaking, the physiological role of rRNA precursors for ribosome generation is scrutinized already for a long time and has been an object of speculations as early as 1969 (Adesnik and Levtnthal 1969). Soon after, one report showed that *in vitro* reconstitutions of 30S subunits from *E. coli* require a lower activation energy if precursor 16S rRNA is used instead of mature 16S rRNA, underlying their facilitating function for assembly (G. Mangiarotti et al. 1975). More specifically, the 5'-external transcribed spacer sequences in bacteria and eukaryotes have been extensively studied. Just to name a few examples, the rRNA leader sequence in *E. coli* has been proposed to be important for antitermination to facilitate *rrn* operon transcription (Holben and Morgan 1984; Berg, Squires, and Squires 1989; Squires et al. 1993). Single nucleotide changes in the 5' leader sequence of *E. coli* rRNA caused temperature sensitive mutants presumably due to altered RNA folding properties (Mori et al. 1990). Deletions in the 5'-ETS sequence, not only in the region base pairing with U3 snoRNA, were shown to prevent maturation of 40S subunits in yeast (Musters et al. 1990). In contrast, large deletions of 5' ETS regions outside the U3 snoRNA interacting sequences did not affect 18S pre-rRNA processing (Burman and Mauro 2012). This observation could correspond to the deletions of helices A' and A in *H. volcanii*, which showed no 16S rRNA processing defect (see figure 11). In conclusion, further studies will be needed to disentangle the physiological role of helix B and the rRNA spacer regions in *H. volcanii*.

Next, we wanted to explore the archaeal rRNA processing pathway with a broader and more comparative approach. Thus, we employed Oxford Nanopore-base sequencing in a collaboration with Dr. Felix Grünberger and Prof. Dina Grohmann. We chose three archaeal

model organisms representing two different archaeal phyla. Overall, our analysis identified several new pre-rRNA intermediates and could confirm the presence of already known or hypothesized precursors (see 5.5). Additionally, we could show the capacity to assign rRNA di-methylation to stage-specific intermediates, thereby suggesting a timeline for this modification during the assembly process (see 5.5.2.4). Still, there are some technical limitations of this method and complementary biochemical analysis might be necessary to answer certain biological questions. Oxford Nanopore technology has not been used before to study archaeal rRNA processing. However, in our case study the technology proved to be a useful tool for this kind of analysis. Now, the established workflows can be applied to study for example particular growth conditions or deletion strains of selected, *trans*-acting ribosome biogenesis factors (Grünberger et al. 2022).

One of these *trans*-acting factors is the ribonuclease characterized in the present work. RNase E/G-like was identified as a novel ribosome biogenesis factor and is involved in the processing of 16S pre-rRNAs in *H. volcanii*. The contributions of RNase E and G to rRNA maturation are well characterized in *E. coli.* Hence this part of archaeal ribosome biogenesis could resemble more the bacterial rRNA processing type. We could show that archaeal RNase E/G-like is participating in the processing of a 16S pre-rRNA class after opening of the circular 16S pre-rRNA. This intermediate was previously observed in the Nanopore-based sequencing approach (see 5.5.2.1). Remarkably, deletion of RNase E/G-like did not show a strong growth phenotype and mature rRNA was readily produced, indicating a non-essential role in the final 3’ end maturation of the 16S rRNA (see 5.6.1). Moreover, structural analysis revealed an interesting domain architecture of this protein, which contains a proposed diphosphatase domain fused to some part of the typical RNase E/G domains (see 5.6.2). It is yet unknown if this ribonuclease is restricted in its activity to 16S pre-rRNAs or also involved in the maturation of 23S or 5S rRNAs. In addition, as *E. coli* RNase E is also degrading mRNAs, non-ribosomal RNAs could be a target. Extending the work until now, established Nanopore-based sequencing might be a valuable alternative to further define the role of RNase E/G-like in archaea. Nevertheless, our combined, newly gained insights allowed us to propose an updated 16S pre-rRNA processing pathway in *H. volcanii* (see figure 21 in 5.6.3). The nucleases involved in the opening of the circular 16S pre-rRNA at the 5’ end, the finalization of the 16S rRNA 3’ end or the downstream processing of circular 23S pre-rRNAs await their characterization.

Next, we investigated the general distribution of circular 16S pre-rRNA in archaea and asked whether circularization is an occurrence strictly linked to the presence of a bhb motif. Few archaeal species without a bhb motif in their 16S processing stem have been reported (Ree

and Zimmermann 1990; P. P. Dennis, Ziesche, and Mylvaganam 1998). Therefore, we developed a PCR-based ‘pan-archaea’ primer approach to detect circular 16S pre-rRNAs without the requirement for species-specific primers. Thus far, we analyzed around 10 archaeal species and found a perfect correlation between the presence of circular 16S pre-rRNA and a 16S bhb motif. The only organism without detectable circular 16S pre-rRNA was *Thermoplasma acidophilum*, in which no bhb motif is predictable in the 16S processing stem (see 5.7). Another interesting study subject was *Haloarcula marismortui*. In this halophilic archaeon three different rDNA operons are present. Remarkably, only one of the three different 16S rRNAs undergoes circularization during its maturation (see 5.7). Thus, some aspects of rRNA maturation appear to vary depending on the rDNA operon and moreover it seems that in this organism a heterogenous population of ribosomal subunits is present (Amann et al. 2000). Hence, the two species would be very intriguing model organisms to study atypical rRNA processing pathways in archaea as well as ribosome heterogeneity. Fortunately, cultivation of these model systems is relatively easy and some genetic tools are available for both organisms (D. Tu et al. 2005; Baka et al. 2013). Strikingly, knocking out individual rDNA loci has already been achieved previously in *H. marismortui* (D. Tu et al. 2005). In addition, the two organisms would be very exciting candidates for the established Nanopore-based sequencing approach.

The regulation of ribosome synthesis was yet another feature of ribosome biology in archaea we focused on. Accordingly, we used rDNA plasmid variants to analyze the effects of increased rRNA gene dosage in *H. volcanii*. We could indeed detect increased transcriptional activity upon higher copy number of rRNA genes, however this effect does not seem to reflect a linear function between copy number and transcription rate. Since the effects of increased rRNA gene dosage in *E. coli* appear not to be completely unambiguous, no definite comparisons can be drawn. At this point there is much room for speculation at which level regulation in *H. volcanii* could occur. Various possibilities how to continue this work are proposed in the discussion of chapter 6. Anyhow, we could describe rRNA gene dosage effects in archaea for the first time. The results shown in the present work can be the foundation to further study the regulation of archaeal ribosome synthesis and we presented valuable tools to approach this goal.

Last but not least, we were looking at the intracellular organization of the translation apparatus and ribosome biogenesis steps in archaea. We first needed suitable tools and started with the development of RNA-FISH microscopy in *H. volcanii* and *S. acidocaldarius*. After successfully implementing this technology, we showed the non-homogenous distribution of mature ribosomal subunits in the two model organisms (see chapter 7). Remarkably, the repartition was partly dependent on active gene expression since drugs affecting transcription or

translation were effectively disrupting the intracellular organization to some extent. In *E. coli* comparable effects were seen, suggesting the influence of active gene expression on intracellular organization is a more widespread trend in prokaryotes (Cabrera et al. 2009). Moreover, RNA-FISH microscopy allowed us to visualize the localization of various pre-rRNAs in *H. volcanii*. Again, we could lay the foundation for an unexplored field of study: the functional relevance of intracellular architecture for ribosome biology and synthesis in archaea. High resolution microscopy technologies in combination with the development of rDNA-FISH and the visualization of ribosome biogenesis factors tagged with fluorescent proteins will help to illuminate the intricate intracellular organization of this processes in archaea (see 7.2.3 for detailed discussion).

In summary, we shed light on a wide range of issues concerning ribosome biogenesis in archaea. As the genetic and molecular biological tools available for archaeal model systems are not as advanced as in bacteria or eukaryotes, method development was an important aspect of this work. Therefore, methodological advancements like the development of the *cis*-acting elements reporter assay, the ‘pan-archaea’ primer approach or the implementation of ONT-based sequencing and RNA-FISH microscopy have been invaluable to enable us to study our favorite research topic: the synthesis of ribosomes in archaea.

8.2. Functional relevance of circular pre-rRNAs

Circular RNAs are not exclusively restricted to the archaeal domain. Early descriptions are found in the reports about circular genomes of RNA viruses (Pettersson and von Bonsdorff 1975; Kolakofsky 1976; Sanger et al. 1976; Hewlett, Pettersson, and Baltimore 1977). Soon after, electron microscopy experiments showed the presence of circular RNAs in eukaryotic cytoplasm (Hsu and Coca-Prados 1979). Nowadays, the biological diversity, function, and biogenesis of these molecules has been explored in much greater detail. Circular RNAs have been suggested to act as microRNA or protein sponges, enhance protein function or facilitate enzyme-substrate complex formation in the eukaryotic system (Kristensen et al. 2019). Exciting possibilities for biotechnological applications of circular RNAs as enhanced protein production platforms or even RNA vaccines have been considered very recently (R. Chen et al. 2022; Qu et al. 2022).

Coming back to archaeal ribosome biogenesis, one major question remains unanswered: what is the functional relevance of the circularization of pre-rRNAs in archaea?

Several scenarios are conceivable, and their respective implications outlined. First, the covalent ligations of free 5’ and 3’ ends provide general protection against unspecific exonuclease activity. Misassembled or non-functional ribosomal subunits are rapidly degraded in bacteria and eukaryotes (Dez, Houseley, and Tollervey 2006; D. L. J. Lafontaine 2010; Piir et al. 2011; Maiväli, Paier, and Tenson 2013; Paier et al. 2015; Luidalepp et al. 2016; Sulthana, Basturea, and Deutscher 2016). Thus, circularization could act as an early ribosome assembly quality control step. The presence of a couple of exonucleases, which could be involved in the decay of ribosomal RNA has been described in archaea (Clouet-d’Orval et al. 2018). However, it appears obvious that alternative protective measures are amply functioning in bacteria, eukaryotes, or archaeal species without circular pre-rRNA intermediates. For instance, the rapid assembly of r-proteins decorating the rRNA precursors might offer sufficient protection. Besides, it was recently argued that the distinct cellular localization of RNase E prevents unspecific degradation of early pre-rRNAs (Hadjeras et al. 2023). RNase E is a major component of *E. coli* degradation machinery and anchored to the inner cytoplasmic membrane (Carpousis 2007; Khemici et al. 2008). In *B. subtilis*, which lacks RNase E, RNase Y fulfills a similar function and is membrane-bound as well (Hui, Foley, and Belasco 2014; Redder 2016). If the sub-cellular localization of RNA degrading enzymes is important to prevent pre-rRNA decay in bacteria what about the localization of such enzymes in archaea? In *S. solfataricus* the majority of the exosome, another RNA degradation complex, is also localized to the membrane (Roppelt et al. 2010; Witharana et al. 2012). Contrarily, the localization of other archaeal RNA degrading nucleases like for example the 3’-5’ exonuclease RNase R in

H. volcanii is not known (Clouet-d'Orval et al. 2018). It remains to be determined whether circular pre-rRNAs emerged in a cellular context in which protection from (freely floating) RNase activities was crucial.

Next, these unique, archaea specific intermediates might provide molecular constraints, which are important for efficient rRNA maturation. For example, particular folding properties of circular pre-rRNAs could form recruitment platforms for designated ribosome biogenesis factors, determine dynamics of ribosomal subunit assembly and facilitate distinct maturation steps. According to this, 23S rRNA maturation in Thermococcales critically depends on circularization and subsequent excision of H98 (see 5.5.2.2; Birkedal et al. 2020; Grünberger et al. 2022). Moreover, the observed opening of the circular 16S pre-rRNA next to the mature 5' end at a position different from the ligation site might assure a certain pre-rRNA processing order (i.e., 5' prior to 3' maturation). In *E. coli* some rRNA processing events do not follow a certain order whereas others necessitate a distinct 5'-/3'-processing order, which is already built in the rRNA precursor (Deutscher 2015). An open question is however, if in archaea with circular pre-rRNAs, circularization is an obligatory event for all pre-rRNAs, or alternative pathways are in place. The *cis*-acting reporter assay could not unambiguously distinguish the essentiality of the bhb motif from the circularization itself for further pre-rRNA processing. Nevertheless, Nanopore-based sequencing analysis and RNase H cleavage assays clearly showed, that a substantial amount of pre-rRNA intermediates experiences circularization (see 5.5). Another interesting observation is, that even though the 16S bhb motif and thus circular 16S pre-rRNA have been lost in few archaea, the 23S processing stems in these species seemed unchanged, i.e., still contain a bhb motif (Ree and Zimmermann 1990; P. P. Dennis, Ziesche, and Mylvaganam 1998). Consequently, one assumes a greater evolutionary pressure on keeping circular 23S pre-rRNAs, implying a key functional relevance during LSU assembly. This notion is further supported by the above mentioned circularly permuted mature 23S rRNA in Thermococcales.

The third hypothesis for the functional relevance of circular pre-rRNAs picks up a general, widespread concept of ribosome assembly: bringing the 5' and 3' termini into proximity, which resembles their conformation in mature ribosomal subunits (Ferreira-Cerca 2017; Bohnsack et al. 2023). Different mechanistic examples how this might be facilitated have been studied. For one, the formation of rRNA processing stems in bacteria ensures a close arrangement of the 5' and 3' ends (Srivastava and Schlessinger 1990; Deutscher 2009). Likewise, this is true for the processing stems found in archaea, independently of the presence of a bhb motif (Ree and Zimmermann 1990; R. A. Garrett et al. 1991; P. P. Dennis, Ziesche, and Mylvaganam 1998; Qi et al. 2020). Interestingly, the Nus elongation factors have been proposed to facilitate the

emergence of the 16S rRNA processing stem in *E. coli* by binding to the 5' leader and the transcribing RNA polymerase. A looped structure is thereby formed until the 3'-terminal part of the processing stem has been transcribed and correctly base-paired (Bubunenko et al. 2013).

What is more, the universally conserved uL3 binds to the 5' region of the 5.8S rRNA and the 3' end of the 25S rRNA in the eukaryotic mature LSU (Ben-Shem et al. 2011; Gamalinda et al. 2014). Thereby, it presumably contributes to the stabilization of the topology of 5' and 3' domains in the LSU and is unique in its binding behavior compared to other LSU r-proteins. Furthermore, it has significant relevance for assembly of the large subunit. It was reported to be one of two assembly initiator r-proteins of the 50S subunit in bacteria (Nowotny and Nierhaus 1982). In pre-50S ribosomes of *B. subtilis* uL3 is located very close to Mini-III (RNase III family) and stimulates its pre-rRNA cleavage activity (Redko, Bechhofer, and Condon 2008; Oerum et al. 2020). Moreover, it is required for the first steps of eukaryotic rRNA processing (Gamalinda et al. 2014). Interestingly, cryo-EM structures of bacterial pre-50S subunits revealed that domains I, II, III and VI stably assemble prior to domains IV and V which is consistent with the binding behavior of LSU r-proteins in the eukaryotic system (N. Li et al. 2013; Gamalinda et al. 2014). LSU rRNA domains are depicted in supplementary figure S4. All these findings strongly suggest an important role of uL3 in the early steps of LSU assembly, potentially by holding 5' and 3' ends of the rRNA in place. In addition, the importance and possibly the contributions of uL3 to ribosome assembly seem to be conserved in bacteria and eukaryotes.

The other way round, the pre-rRNA topology with the RNA termini in vicinity might be required for the proper activity of certain ribosome biogenesis factors. For instance, Npa1p is required for optimal pre-rRNA processing and the recruitment of other early acting assembly factors during the very first steps of eukaryotic ribosome assembly (Dez et al. 2004). Cross-linking analyses determined binding sites of this protein in the 5.8S rRNA as well as near the 3' end regions of the 25S rRNA, indicating long-range interactions between 5' and 3' regions (Joret et al. 2018). As a short reminder, the 5.8S rRNA is reminiscent of the prokaryotic 5' end of the prokaryotic 23S rRNA (Hadjiolov 1985). Similarly, an interaction partner of Npa1p, the snoRNA snR190 has been suggested to potentially contact the 5' end and 3' domains of the 25S rRNA (Joret et al. 2018; Jaafar et al. 2021). The long-range interactions within different rRNA domains occur already during the early steps of ribosome assembly, might have important functions, and could rely on a certain pre-rRNA topology. Hence, ensuring close proximity of the two rRNA termini might facilitate ribosome assembly steps from the very beginning.

Furthermore, eukaryotic 5.8S pre-rRNA has been proposed to establish base pairing with the 25S rRNA 5' terminus and ITS2 (Veldman et al. 1981). Correspondingly, cryo-EM structures

showed that the 5.8S pre-rRNA is incorporated already in very early LSU pre-ribosomal particles with the domains I, II and VI being completely or at least partly folded and stabilized (Kater et al. 2017; Klinge and Woolford 2019). Likewise, base pairing interactions between the 5’ end of 18S rRNA and the 3’-flanking spacer sequence, ITS1, were suggested in yeast (Veldman et al. 1981). The secondary structures of bacterial and eukaryotic SSU and LSU rRNAs are illustrated in supplementary figure S4.

In addition, the previously mentioned U3 snoRNA is a key structural organizer during SSU assembly (see also figure 12). It forms extensive base pairing with 5’ and central regions of the 18S pre-rRNA with the 5’-ETS, thereby providing topological constraints required for proper RNA folding and processing (Beltrame and Tollervey 1992; 1995; Dutca, Gallagher, and Baserga 2011; Woolford and Baserga 2013; Kressler, Hurt, and Baßler 2017).

Lastly, our functional and structural study of archaeal RNase E/G-like led us to hypothesize a mode of action in which the enzyme holds free 5’ and 3’ ends of 16S pre-rRNA together (see detailed discussion in 5.6.3). In this way, a circular-like architecture would still be retained after opening the circular 16S pre-rRNA.

In summary, the common feature of the universally conserved uL3, eukaryotic 5.8S pre-rRNA and U3 snoRNA or prokaryotic processing stems seems to support the pre-rRNAs topological organization in bringing the 5’ and 3’ ends in close vicinity. Furthermore, this conformation is stabilized and retained in the mature ribosomal subunits. In other words, pseudo-circularization of pre-rRNA appears to be a general mechanism and may be crucial for efficient ribosome assembly in all three domains of Life. Recently, these concepts were also discussed elsewhere (Ferreira-Cerca 2017; Bohnsack et al. 2023). In archaea, the most prevalent way of achieving this might be covalent circularization of pre-rRNAs. Nonetheless, exceptions from this rule were discussed (see 5.7) and potential mechanisms of pseudo-circularization in archaea should be studied in this regard.

Putting the above-mentioned possibilities for the functional relevance of circular pre-rRNAs in archaea aside, one final option should be mentioned. The necessity of circularization might stem from an ancient cellular context in which this step has been crucial during ribosome biogenesis. In this ancestral archaeon, the molecular constraints, perhaps resembling the ones discussed here, might have been lost in modern-day archaea. Regardless, the rRNA processing machinery required for circularization (endA & RtcB) could have piggybacked on the essentiality of tRNA intron splicing during evolution. On the other hand, one selected counterargument here would again be the necessity to circularize 23S pre-rRNA in Thermococcales (see 5.5.2.2; Birkedal et al. 2020; Grünberger et al. 2022). Alternatively,

circularization of pre-rRNA is an even older mechanism present in the last common ancestor. However, over the course of evolution, it has been lost in bacteria, eukaryotes and some archaea.

Concerning the last point, it is worth considering the evolutionary trajectories of forming circular pre-rRNAs and tRNA intron splicing in archaea. Both pathways share some enzymatic activities, and the question arises, whether rRNA processing used already existing enzymes involved in tRNA metabolism or the other way round.

Another interesting question strikes the reported outliers *Thermoplasma acidophilum* and *Haloarcula marismortui* (see 5.7). How might the functional requirements linked to circular pre-rRNAs have been overcome in these organisms? And what would be the necessary co-adaptations to compensate for this change? S1 nuclease mapping and primer extension experiments performed in *T. acidophilum* could not detect any 16S rRNA processing intermediates (Ree and Zimmermann 1990). Hence, on these grounds, it is impossible to speculate about its 16S rRNA maturation. *T. acidophilum* and *H. marismortui* can both be grown in the lab and would be very interesting candidates for Nanopore-based sequencing. Thereby, one could detect maturation intermediates, identify the particularities of their pre-rRNA processing and broaden our perspective of this process in archaea in general.

Along those lines, a yet neglected, however very exciting issue concerns the existence of circular pre-rRNAs in the Asgard superphylum. One way to approach this, would be to first predict bioinformatically the secondary structures of pre-rRNA processing stems and check for the presence of a bhb motif in the available genomes of Asgardarchaeota. Furthermore, the respective enzymes, endA and RtcB, would likely have to be present, if one expects circular pre-rRNAs. As only two, slow-growing Asgard representatives are known, biochemical analyses might still be difficult (Imachi et al. 2020; Rodrigues-Oliveira et al. 2022). Nevertheless, if enough cell material can be obtained, the ‘pan-archaea’ primer approach would be an option to check for circularpre-rRNA intermediates in Asgardarchaeota. Intriguingly, this knowledge could putatively help us to further understand the Asgard-eukaryotes relationship from a ribosome biogenesis perspective.

Usually, answering one scientific question immediately poses five new ones. Accordingly, there is much more to learn about the archaea-specific circular intermediates and reason to investigate additional aspects of these fascinating molecules. For instance, how exactly does the rRNA topology and folding look like in the circular precursors? Which rRNA domains and regions are already stabilized, and which r-proteins or biogenesis factors have been bound to these intermediates? Is the central pseudoknot in the 16S pre-rRNA already properly folded?

Regarding the circular 23S pre-rRNA, it would be interesting to know if uL3 has yet been incorporated. Does it maybe stabilize the 5’ and 3’ ends after opening of the circular 23S pre-rRNA? At which step does RNase E/G-like enter the stage? Are there additional important *cis*-acting RNA elements in the flanking regions that are involved in the formation of the circular pre-rRNAs? Similarly, do *cis*-acting elements in the circular pre-rRNAs play a role for the re-opening and further pre-rRNA processing? What are the dynamics and the half-lives of these intermediates? Which influence do varying growth or stress conditions have on the steady-state levels of the circular pre-rRNAs?

Methodological solutions like Nanopore-based sequencing, RNase H cleavage assays, our *cis*-acting elements reporter assay are at hand to perhaps solve some of these puzzles satisfyingly. Others, like unraveling the RNP context or the RNA folding landscape might require the implementation of new techniques and methods. SHAPE-MaP allows structure probing and analysis of low abundant RNAs *in vivo* (Smola and Weeks 2018). Thus, it could be one valuable option to learn more about the structural context of the circular pre-rRNA. Unfortunately, studies regarding the RNP context might be very tricky in *H. volcanii* as pull-down experiments are often impeded by the high-salt conditions and the abundance and lifetime of pre-ribosomal subspecies is completely unknown. Moreover, cryo-EM studies of pre-ribosomal subunits which have been greatly instrumental in bacteria and eukaryotes, will be challenging due to high salt conditions and purification bottlenecks. Still, technical advancements in the future will likely provide opportunities to examine the intricacies of all aspects of ribosome biogenesis in archaea.

8.3. Commonalities and specificities

One of our main goals has been and still is to provide a comparative perspective on ribosome biogenesis in all three domains of life. The conservation of ribosomal building blocks, RBFs or common principles has been introduced in 3.3. Overall, archaeal ribosome biogenesis appears to represent a mélange of bacteria-like and eukaryotic-like assembly features, besides common and archaea-specific ones. Hereafter, the major commonalities and differences of ribosome assembly in bacteria, eukaryotes and archaea related to this work will be discussed.

The most prominent example we have described here is the presence of circular pre-rRNAs in archaea. This maturation step does not occur during the bacterial or eukaryotic ribosome assembly process and the present work has focused on features of the circular 16S pre-rRNA. Even though the functional relevance of the circularization is still an open question, several possibilities have been discussed above. To resolve the universally conserved folding problem of ribosomal RNA maturation, various strategies might have evolved, one of them could be the formation of circular pre-rRNAs. The use of Nanopore-based sequencing and the 'pan-archaea' primer assay confirmed the presence of this intermediate in a number of archaeal organisms. Nonetheless, exceptions have been described in 5.7 and indicate alternative pre-rRNA maturation. Another example exhibiting variation in archaeal rRNA processing is the before mentioned excision of H98 in Thermococcales. In the end, the rRNA processing pathway does not seem to be universally conserved in all archaeal species.

Another *cis*-acting element we analyzed was the conserved helix B in the 5' leader sequence in the pre-rRNA of *H. volcanii*. The exact contribution to rRNA maturation is still unknown, however it was speculated helix B could take to role of U3 snoRNA in eukaryotes. If this assumption can indeed be verified, it would pose an intriguing example how the same, distinct RNA folding problem, i.e., premature folding of the SSU's central pseudoknot, is prevented and overcome in different ways (*cis*- and *trans*-acting) throughout the domains of Life. Yet, this hypothesis still must be further examined to draw solid conclusions.

One *trans*-acting factor studied in this work, archaeal RNase E/G-like, remembers more of the bacterial rRNA maturation. RNase E and G are well characterized for their contribution to *E. coli* RNA processing, whose activity is not restricted to only ribosomal RNAs. Although structural analysis revealed a certain degree of similarity in the protein's domain architecture compared to the bacterial counterpart, the fusion of a newly added diphosphatase alienates archaeal RNase E/G-like from the classical, bacterial enzyme. In addition, the function of this novel domain remains elusive so far. Moreover, it is unclear whether archaeal RNase E/G-like

targets non-ribosomal RNAs. Conclusively, there is still more effort necessary to identify all *cis*- and *trans*-acting players required for the entire rRNA maturation pathway.

We also started to research regulation of ribosome synthesis by analyzing the effects of rRNA gene dosage in *H. volcanii*. So far, it is unfortunately too early to draw conclusive comparisons with the eukaryotic or bacterial regulatory systems. Further examinations of *E. coli* would also be beneficial to effectively compare rRNA gene dosage effects with our results. The few studies in archaea showed both stringent and relaxed phenotypes (Cimmino, Scoarughi, and Donini 1993; Cellini et al. 2004; Müller et al. 2021). Then, different growth-rate dependencies were reported in several archaeal species (John Chant et al. 1986; DiRuggiero et al. 1993; Müller et al. 2021; Gu et al. 2022). Hence, different levels of ribosome synthesis regulation likely reflect lifestyle specific differences and adaptations in archaea who populate basically every imaginable ecological niche on this planet. Future research in this direction will hopefully clarify the underlying principles of how the production of ribosomal subunits is controlled in archaea (see also discussion in 6.3).

Our analysis of the intracellular repartition of the translational apparatus and localization of selected ribosome biogenesis steps by RNA-FISH microscopy allows a first, careful comparison with the bacterial and eukaryotic cellular organization. Certainly, a crucial distinction between prokaryotes and eukaryotes remains the existence of a membrane engulfed nucleus. Nevertheless, distinct functional aspects of ribosome biology and ribosome biogenesis might be tied to the subcellular organization in all three domains, regardless of the presence of defined organelles (see chapter 7). For instance, different types of distribution of ribosomes and genetic material was reported in bacteria (Lewis, Thaker, and Errington 2000; Borgnia, Subramaniam, and Milne 2008; Montero Llopis et al. 2010; Bakshi et al. 2012; Chai et al. 2014) Just in the same manner, active gene expression was found to be important for intracellular architecture in *E. coli*, *S. acdiocaldarius* and *H. volcanii*, for which it was shown by our analysis and Delmas et al. (Cabrera et al. 2009; Delmas, Duggin, and Allers 2013). Yet, the observed differences in *H. volcanii* and *S. acidocaldarius* indicate a variety of intracellular organization forms in archaea. The dot-like localization pattern of early pre-rRNA species observed in *H. volcanii* strongly resembles a previous analysis in *E. coli* and could indicate co-transcriptional RNA processing events (Malagon 2013). Comparisons with eukaryotes remain difficult due to the great differences. However, exciting observation in *S. solfataricus* suggested the presence of a nucleolar-like structure (Islas-Morales et al. 2023). It will be interesting to see if future studies can provide evidence a role of such structures in the emergence of eukaryotic cells.

Collectively, we could identify several specific and shared traits of ribosome biogenesis in archaea. We tried to put our findings in a broader context to better understand which ways evolution has taken to solve the same problem, that is how to effectively build a ribosome, in different or similar manners.

8.4. ‘Functional phylogenetics’

It is probably no overstatement to claim that the ribosome would have been Darwin’s favorite molecule of all time. (Un)fortunately, he had to content himself with looking at finches’ beaks. Anyhow, in the past decades, the information contained in the sequence and structure of the ribosome has been proven to be a phylogenetic treasure chest and invaluable to define the relationships of species to each other. Importantly, mutations occurring in the ribosomal building blocks during the course of evolution should always be considered from two perspectives. First, what is the effect of alterations on the translational performance? And not to forget, what do these changes imply for the tightly controlled and complex assembly process of ribosomes.

The discovery of the archaea as being a separate domain of Life, quite other than bacteria, is only one of the prominent examples (Fox et al. 1977; Carl R. Woese and Fox 1977; C R Woese, Kandler, and Wheelis 1990). Intriguingly, James Lake was using the same molecule as cornerstone to debate the claims of Woese and his co-workers (Lake et al. 1984; Lake 1988). What is more, the advent of cultivation independent metagenomic studies of microbial communities, using 16S rRNA gene sequences as one of the main markers was a great leap forward for phylogenetic investigations (Jo Handelsman 2004).

Strikingly, in the past few years the description of the Asgardarchaeota has stirred up the debates around the origin of eukaryotes. Many so-called eukaryotic signature proteins (ESPs), have led to the suggestion that Asgards could represent the cradle of the eukaryotic lineage (Spang et al. 2015; Zaremba-Niedzwiedzka et al. 2017). Even though the number of new Asgard members is ever growing, only two, slowly growing representatives could be successfully cultivated so far (Imachi et al. 2020; Y. Liu et al. 2021; Xie et al. 2022; Rodrigues-Oliveira et al. 2022). Hence, biochemical, and functional analyzes remain challenging in these organisms. Nevertheless, besides mere sequence information the biological, function-related meaning of these sequence and/or structure information can be used to refine phylogenetic relationships. We used the organization of the rRNA genes as one example to point out conflicting hypothesis regarding the Asgard-eukaryotes relationship (see chapter 4). In another example of this approach, we focused on subtle differences of the RNA structure of helix 45 in the SSU rRNA (Knüppel et al. 2021; Jüttner and Ferreira-Cerca 2022). Taking these observations into account might also benefit open discussions regarding the origin of halophily in archaea (Jüttner and Ferreira-Cerca 2022). Using functional knowledge about ribosome biogenesis in a phylogenetic context was recently presented as ‘functional phylogenetics’ (Knüppel et al. 2021; Jüttner and Ferreira-Cerca 2022). In a similar way, Michael Lynch and colleagues argued for a conceptual fusion of classical cell biological thinking with evolutionary

perspectives in an article termed ‘Evolutionary cell biology: Two origins, one objective’, (Lynch et al. 2014). For example, biophysical and biochemical laws provided the constraints in which cellular structures have evolved and must be considered in such an evolutionary cell biology approach.

8.5. Conclusions

In the presented work we were able to elucidate different aspects of ribosome biogenesis in archaea. We identified several *cis*- and *trans*-acting elements involved in rRNA maturation, which are in parts specific for the archaeal domain. Furthermore, we provided a broader perspective on the rRNA processing pathway in archaea by using Nanopore-based sequencing and examined the abundance of circular 16S pre-rRNAs in archaea. Our rDNA reporter element assay enabled us to demonstrate the importance of *cis*-acting RNA elements for circular and total rRNA production. By functional characterization of archaeal RNase E/G-like we could identify a novel *trans*-acting ribosome biogenesis factor in *H. volcanii*. Moreover, we laid the foundation to study the intricacy of the regulation of ribosome biogenesis in *H. volcanii*. Lastly, we successfully established RNA-FISH methodology to visualize the intracellular organization of the translation machinery and distinct ribosome biogenesis steps. Eventually, we promote the idea, that research on ribosome biogenesis in archaea provides meaningful insights to better understand the key principles of this process in all forms of Life. On top of that, we are convinced that these insights can help to refine phylogenetic relationships and can advance current debates, for example about the placement of the eukaryotic lineage in the tree of Life.

9. Material & Methods

9.1. Materials

9.1.1. Consumables

All chemicals, antibiotics and other consumables used in this work were purchased at the highest available purity from Sigma-Aldrich, Merck, Fluka, Roth or J.T.Baker, unless otherwise stated. All solutions, buffers, media were prepared with purified H_2O from an Elga Purelab Ultra (18.2 MΩ-cm resistivity). Typically, pH measurements were done at room temperature and adjustments were made with HCl or NaOH, unless stated otherwise.

Table 1: Chemicals and consumables

Material/chemical	Manufacturer
100 bp DNA ladder	New England Biolabs
1 kb DNA ladder	New England Biolabs
2-log DNA ladder	New England Biolabs
Agarose ultrapure	Invitrogen
Biosphere® filter tips	Sarstedt
BM Chemiluminescence Western Blotting Substrate (POD)R	Roche
Disposable plastic cuvettes	Sarstedt
Disposable pipettes (2-50 ml)	Sarstedt
dNTPs Mix (25 mM each)	Agilent Technologies
Extra thick blot paper	Bio-Rad
Falcon tubes (15 ml/50 ml)	Sarstedt
Filter paper 3MM	Whatman
Gel Loading Dye (6x), blue	New England Biolabs
Hoechst 33342	Thermo Fisher Scientific
Immun-Blot PVDF membrane #162-0177	BioRad
Novex® Gel Cassette 1.0 mm	Thermo Fisher Scientific
PCR-tubes and caps	Kisker
Pipette tips (10-1000µl)	Sarstedt
Polypropylene centrifuge tubes (14 x 95 mm)	Beckmann Coulter
Reaction tubes (1.5 ml, 2 ml)	Sarstedt
SYBR Safe DNA Gel Stain	Invitrogen
Zirkonia glas beads (Ø 0.1 nm)	Roth

Table 2: Kits

Name	Manufacturer
Gibson Assembly® Mix	NEB
innuPREP Micro RNA Kit	Analytik Jena
NucleoSpin RNA Kit®	MACHEREY-NAGEL
peqGOLD Plasmid MiniPrep Kit I	VWR life science
QIAquick® PCR purification kit	Qiagen
QIAquick® Gel Extraction Kit	Qiagen
SuperScript™ III Reverse Transcriptase	Invitrogen (by life technologies™)
Zero Blunt ® TOPO PCR Cloning Kit	Invitrogen (by life technologies™)

All restriction enzymes used for this work were purchased from New England Biolabs (NEB). Restriction digest was performed with the most suitable NEB buffer.

Table 3: Enzymes

Enzyme	Manufacturer
Go-Taq	Promega
Phusion HF DNA Polymerase	NEB
RNase H	NEB
RNasin®	Promega
RQ1 RNase-free DNase	Promega
SuperScript™ III Reverse Transcriptase	Invitrogen (by life technologies™)
T4 DNA Ligase	NEB

Table 4: Antibiotics

Antibiotic	Final concentration used
Ampicillin	100 µg/ml
ActinomycinD	5 µg/ml
Chloramphenicol	30 µg/ml
Kanamycin	100 µg/ml
Pactamycin	2.5 – 50 µM
Rifampicin	50 µg/ml
Thiostrepton	2.5 pM

All antibiotics were diluted 1 to 1000 from stock solutions (1000x).

Table 5: Commonly used buffers

Buffer	Ingredients	Final concentration
AE	NaOAc, pH 5.3 EDTA, pH 8.0	50 mM 10 mM
Denhards (50x)	Ficoll (Typ400, Pharmacia) Polyvinylpyrrolidone BSA (FractionV, Sigma)	10 mg/ml 10 mg/ml 10 mg/ml
	Store at -20 °C	
Extraction buffer	NaCl EDTA, pH 8.0 Tris-HCl, pH 8.5 $MgCl_2$ SDS	150 mM 100 mM 50 mM 1 mM 1 %
gDNA extraction lysis buffer	EDTA, pH 8.0 SDS autoclave	100 mM 0.2 %
gDNA extraction ST buffer	NaCl Tris-HCl, pH 7.5 autoclave	1 M 100 mM
HU-sample buffer	SDS Tris-HCl, pH 6.8 EDTA β-Mercaptoethanol (add fresh) Urea Bromophenol Blue	5 % 200 mM 1 mM 2.13 mM 8 M
K1800	Glycerol KCl $MgCl_2$ Tris-HCl, pH 7.5 Imidazol β-Mercaptoethanol	10 % (w/v) 1.8 M 50 mM 20 mM 10 mM 2 mM

K200	Glycerol KCl $MgCl_2$ Tris-HCl, pH 7.5 Imidazol β-Mercaptoethanol	10 % (w/v) 200 mM 5 mM 20 mM 10 mM 2 mM
Hv-buffer	KCl $MgCl_2$ Tris-HCl, pH 7.5 β-Mercaptoethanol	2.8 M 75 mM 10 mM 2 mM
MOPS running buffer (10x)	Sodium Acetate Trihydrate MOPS EDTA, pH 8.0 adjust to pH 7.0 with HCl store in the dark	80 mM 200 mM 10 mM
NaAc solution	NaAcetate * 3 H_2O adjust to pH 5.3 with acetic acid	3 M
PBS (10x)	NaCl KCl KH_2PO_4 Na_2HPO_4 adjust to pH 7.4 with NaOH	1.37 M 27 mM 18 mM 0.1 M
PBS-T (1x)	1x PBS Tween	1x 0.05 % (v/v)
Pre-hybridization buffer for RNA-FISH microscopy	Formamide SSC Dextran sulfate yeast tRNA Salmon sperm DNA Denhards	50 % 4x 10 % 125 µg/ml 500 µg/ml 1x
	store at -20 °C	
	add DTT add RNasin	1mM 0.4 U/ml

Pre-hybridization buffer for Northern blot (prepare freshly)	Formamide SSC SDS Denhards	50 % 5x 0.5 % 5x
10x RNase H buffer	Tris-HCl KCl $MgCl_2$ DTT adjust to pH 8.3 store at 4 °C	500 mM 750 mM 30 mM 100 mM
RNA loading buffer (2x)	Formamide Bromophenol blue	99.95 % 0.05 %
SSC (20x)	NaCl Sodium-Citrate Trihydrate adjust to pH 7.0	3 M 0.3 M
TBE (5x)	Tris Boric Acid EDTA, pH 8.0	445 mM 445 mM 50 mM
TE-buffer		

Table 6: *H. volcanii* transformation buffers

Buffer	Ingredients	Final concentration
for 30 % saltwater see Table 8		
Buffered spheroplasting solution	NaCl KCl Tris-HCl, pH 8.5 Sucrose autoclave for 10 min	1 M 27 mM 50 mM 15 % (w/v)
Unbuffered spheroplasting solution	NaCl KCl Sucrose	1 M 27 mM 15 % (w/v)

	adjust to pH 7.5 with NaOH autoclave for 10 min	
Spheroplast dilution solution	30 % saltwater Sucrose autoclave for 10 min add 0.5 M $CaCl_2$	23 % (v/v) 15 % (w/v) 3.75 mM
Regeneration solution	30 % saltwater 10x YPC Sucrose autoclave for 10 min add 0.5 M $CaCl_2$	18 % (v/v) 1x 15 % (w/v) 3 M
Transformant dilution solution	30 % saltwater Sucrose autoclave for 10 min add 0.5 M $CaCl_2$	18 % 15 % 3 M

Table 7: *E. coli* transformation buffers

Buffer	Ingredients	Final concentration
TfB I	KAc $MnCl_2$ KCl Glycerol adjust to pH 5.8 with 0.2 M acetic acid filter sterilize trough 0.22 µm filter	30 mM 50 mM 100 mM 15 % (w/v)

	store at 4 °C	
Tfb II	MOPS $CaCl_2$ KCl Glycerol adjust to pH 7.0 with NaOH filter sterilize through 0.22 µm filter store at 4 °C	10 mM 75 mM 10 mM 15 % (w/v)

9.1.2. Media

Growth media were made from ingredients purchased from BD Biosciences (Bacto™ Agar, Bacto™ Peptone, Bacto™ Tryptone, Bacto™ Casamino acids and Bacto™ Yeast Extract), Sigma-Aldrich (amino acids, uracil and EZMix™ N-Z-Amine® A). Growth media were autoclaved for 20 min at 120 °C and stored depending on instructions.

Table 8: *Haloferax volcanii* media

Medium	Ingredients	Final concentration
30 % saltwater	NaCl $MgCl_2$ * 6 H_2O $MgSO_4$ * 7 H_2O KCl Tris-HCl, pH 7.5 autoclave for 20 min	4.1 M 0.15 M 0.14 M 94 mM 20 mM
10x YPC	Bacto™ yeast extract Bacto™ peptone Bacto™ casamino acids KOH	5 % (w/v) 1 % (w/v) 1 % (w/v) 17 mM
10x Ca	Bacto™ casamino acids KOH	5 % (w/v) 17 mM

	autoclave for 20 min or filter sterilize trough 0.22 µm filter	
Hv-Min Carbon Source	Lactic acid Succinic acid Glycerol adjust to pH 7.5 with NaOH filter sterilize through 0.45 µm	10 % 9 % 1 %
Hv-Min-Salts	NH_4Cl $CaCl_2$ Trace elements	0.4 M 0.25 M 8.3 % (v/v)
Trace elements	$MnCl_2 * 4 H_2O$ $ZnSO_4 * 7 H_2O$ $FeSO_4 * 7 H_2O$ $CuSO_4 * 5 H_2O$ filter sterilize through 0.45 µm	0.15 M 0.13 mM 0.67 mM 16.7 µM
0.5 M KPO_4 buffer pH 7.0	K_2HPO_4 KH_2PO_4 autoclave for 20 min	 0.3 M 0.2 M
Thiamin & Biotin	Thiamin Biotin autoclave for 20 min	 0.9 mg/ml 0.1 mg/ml
Hv-YPC (complete medium)	200 ml 30 % saltwater 33ml 10x YPC 100 ml H_2O	18 % 1x
	autoclave for 20 minutes	
	2 ml 0.5M $CaCl_2$	3 mM
Hv-Ca (casamino acids medium)	200 ml 30 % saltwater 100 ml H_2O	18 %
	autoclave for 20 min	
	33 ml 10x Ca	
	2 ml 2M $CaCl_2$	3 mM
	300 µl Thiamin & Biotin	
Hv-Ca^+	200 ml 30 % salt water	18 %

(enhanced casamino acid broth)	1 M Tris-HCl pH 7.0 75 ml H_2O	30 mM
	autoclave for 20 minutes	
	33 ml 10x Ca	
	8.5 ml Hv-Min Carbon Source	
	4 ml Hv-Min-Salts	
	650 µl 0.5 M KPO4 buffer pH 7.0	
	300 µl Thiamin & Biotin	
for plates add 0.8 % Agar (w/v) to bottles (333 ml) before autoclaving		
store *H. v.* media in a dark cupboard		

Table 9: *Haloarcula marismortui m*edium

Medium	Ingredients	Final concentration
ATTC-medium:1218	NaCl $MgCl_2$ * 6 H_2O $CaCl_2$ K_2SO_4 Bacto™ peptone Bacto™ yeast extract soluble starch adjust to pH 7.0 autoclave	126 g/l 160 g/l 0.1 g/l 5 g/l 0.1 % 0.1 % 0.2 %

Table 10: *Halorobrum lacusprofundi* medium

Medium	Ingredients	Final concentration
HL-medium (DSMZ Medium 589)	NaCl $MgCl_2$ * 6 H_2O $MgSO_4$ * 7 H_2O KCl $CaCl_2$ * 2 H_2O	181 g/l 75 g/l 7.4 g/l 7.4 g/l 1 g/l

	Na-succinate * 6 H_2O Bacto™ yeast extract Vitamin solution adjust to pH 7.4 autoclave for 20 min	16.7 g/l 0.1 % 1 ml
Vitamin solution	Biotin Vitamin B12 Thiamine-HCl * 2 H2O distilled water Filter-sterilize and add to medium at 55-60 °C	10 mg 10 mg 10 mg 100 ml

Table 11: *Sulfolobus acdiocaldarius* Brock medium (1 L - *Sulfolobus* 88 DMSZ medium)

Ingredients			**Final concentration**
autoclave ~920 ml H_2O			
add 1 ml Brock I	$CaCl_2$ * H_2O autoclave for 20 min		70 g/L
add 10 ml Brock II	$(NH_4)_2SO_4$ $MgSO_4$* 7 H_2O H_2SO_4 autoclave for 20 min		130 g/L 25 g/L 1:1
add 5 ml Brock III	KH_2PO_4 Trace elements sol. H_2SO_4		56 g/L 1x 1:1
	Trace elements solution (2000x)	$MnCl_2$ * 4 H_2O $Na_2B_4O_7$ * 10 H_2O $ZnSO_4$ * 7 H_2O $CuCl_2$ * 2 H_2O $NaMoO_4$ * 2 H_2O $VOSO_4$ * 2 H_2O	3.6 g/L 9 g/L 0.4 g/L 0.1 g/L 60 mg/L 60 mg/L

		$CoSO_4$ * 7 H_2O	20 mg/L
	autoclave for 20 min		
add 1 ml Fe III solution	1000x $FeCl_3$ * H_2O (20 g/L) sterile filtrate through 0.22 µm filter		20 mg/L
add 20 ml NZ-Amine (5 %)	5 % NZ-Amine (w/v) autoclave for 20 min		0.1 % (w/v)
40 ml 5 % Dextrin	5 % Dextrin (w/v) autoclave for 20 min		0.2 % (w/v)
pH 3.5 with H_2SO_4			
add uracil for all *pyrE* mutants			10 µg/ml

Table 12: *Escherichia coli* media

Medium	Ingredients	Final concentration
LB	Bacto™ yeast extract Bacto™ tryptone NaCl stored at 4 °C	0.5 % (w/v) 1 % (w/v) 1 % (w/v)
SOB	Bacto™ yeast extract Bacto™ tryptone NaCl KCl $MgSO_4$ store at 4 °C	0.5 % (w/v) 2.0 % (w/v) 10 mM 2.5 mM 20 mM

9.1.3. Nucleic acids

Oligonucleotides were ordered from Eurofins Genomics and dissolved in ddH_2O to a concentration of 100 pmol/µl and stored at -20 °C. The following accession numbers refer to the database of the Biochemie III department of the University of Regensburg.

Table 13: Oligonucleotides

Oligo name	5' > 3' sequence
oHv023-pTA1228 Seq Fw	CTGAAGTCGGCTCGTGGCGAG
oHv024-pTA1228 Seq Rv	CGGATAACAATTTCACACAG
oHv039-ci16S-fw	CGAATCTGGGCTTCGCAAGG
oHv040-ci16S-RV	GTATGAACTCGTGCAACTAGC
oHv041-ci23S-Fw	CGATAGACTCGGGGTGTACGC
oHv042-ci23S-Rv	CAGCTTGGCACGTCCGTCATC
oHv142-16S mature Fw	GAAACCTTTACACTGCACGC
oHv143-16S mature Rv	CAAGCCACGTGGTTTTCACCGG
oHv144-23S mature Fw	CAACTGCGAAGACTAAACACTC
oHv145-23S mature Rv	CAGTTCTTTCGTCGAGTGACC
oHv151-rDNA2860-Fw	GTCTCCTGGAACGGAGCGTG
oHv152-rDNA4070-Fw	CGTCGACGCTTTAGGAAACACC
oHv154-rDNA4930-Rv	GTTGGGAATGTCACTGTCAGAC
oHv155-rDNA3020-Rv	CAGCGTTCGCTCACGCTACTTG
oHv180-pTA1228seq-US	CACCGACCCGATTCGACCC

oHv181-pTA1228seq-DS	GGGAACAAAAGCTGGAGCTCC
oHv203-16S-3end-18nt-Rv	AGGAGGTGATCCAGCCGC
oHv205_16SrRNA_5' end	ATTCCGGTTGATCCTGCCGG
oHv206_23SrRNA_5' end	CTGTGCCAGCTGGTGGATAG
oHv207-rDNA4099-Fw	CCTTCGCCCCGTCGAATCACC
oHv208-rDNA6008-Rv	GATCGATGCGGCCGCGCGAGAAGTTGAGATCAGCGAGG
oHv254-16S-RV	GTACTTCCCAGGCGGCTCG
oHv297-Delta16S 5´Bulge Fw	GTTAGCCCTAGTAGTTCGGTGTCCGAACGGATGTCACGCGAAC
oHv298-Delta16S 5´Bulge Rv	GTTCGCGTGACATCCGTTCGGACACCGAACTACTAGGGCTAAC
oHv299-Delta16S 3´Bulge Fw	ATGACACCCGTTCGGACACCGAACTACTAGGGCTAACACGG
oHv300-Delta16S 3´Bulge Rv	CCGTGTTAGCCCTAGTAGTTCGGTGTCCGAACGGGTGTCAT
oHv301-Delta23S 5´Bulge Fw	GTGTACGTGCAATCCAGGCGTCTGGACCCGTTCTCCGGGTCAC
oHv302-Delta23S 3´Bulge Rv	GTGACCCGGAGAACGGGTCCAGACGCCTGGATTGCACGTACAC
oHv303-Delta23S 3´Bulge Fw	CCGAGAACGGGTCCAGGCGCCTGGATTGCACGGACACATTGG
oHv304-Delta23S 3´Bulge Rv	CCAATGTGTCCGTGCAATCCAGGCGCCTGGACCCGTTCTCGG
oHv307-RT-23SrepBss-Rv	CGTTACCTCGTTGCGTACACC
oHv308-23Srep-Bss-Fw	ACGAGGTTCATTCATGGGAC

oHv309-23Srep-Bss-Rv	GATAGCAGCCGACCTGTCTC
oHv348_GE_Flag_Nde fw	ATTGCGCATATGAGAGTCCGCGTCCGCGGC
oHv349_GE_Flag_rv	TCATCTTTGTAGTCGATATC
oHv373_Hm16S-ABC-circ 3´Fw	ACAAGGTAGCCGTAGAGGAA
oHv375_Hm23S-ABC-circ 3´Fw	GCTTATCGCAGCTTGGCACG
oHv376_Hm23S-ABC-circ 5´Rv	GTGTGCGCGTCGAGGTAACG
oHv377_Hm16S-A-leader-rv	CGAAGGGTGTTCGAGGACAC
oHv378_Hm16S-BC-leader-rv	GTGGTTGCACTCCGTCGGAAG
oHv379_Hm16S-B-trailer-fw	CTTGGTTGTTGGTCACAA
oHv476_helix repeat 16S 5´_Fw	TAGCCCTAGTAGTTCGGTGGGTGACATCCGAACGGATGTCACGCG
oHv477_helix repeat 16S 5´_Rv	CGCGTGACATCCGTTCGGATGTCACCCACCGAACTACTAGGGCTA
oHv478_helix repeat 16S 3´_Fw	CAATGACACCCGTTCGGACACCCACCTTAGAACTACTAGGGCTAACAC
oHv479_helix repeat 16S 3´_Rv	GTGTTAGCCCTAGTAGTTCTAAGGTGGGTGTCCGAACGGGTGTCATTG
oHv480_open helix 16S 5´_Fw	GATGTTAGCCCTAGTAGTTCAAAAACATCCGAACGGATGTCACGC
oHv481_open helix 16S 5´_Rv	GCGTGACATCCGTTCGGATGTTTTTGAACTACTAGGGCTAACATC
oHv482_processing stem delete 16S 5´_Fw	GCAAGACGGTATCTGATGTTGACCTTTGAACGGTGATTTG

oHv483_processing stem delete 16S 5´_Rv	CAAATCACCGTTCAAAGGTCAACATCAGATACCGTCTTGC
oHv484_processing stem delete 16S 3´_Fw	GTGGCTCACACGCGATCTTCAACACGGGCCCATAGCTCAG
oHv485_processing stem delete 16S 3´_Rv	CTGAGCTATGGGCCCGTGTTGAAGATCGCGTGTGAGCCAC
oHv490_Hm16S_5´spacer 5´B_ABC_Fw	GAGGATTCCACCCCTGCGGTCC
oHV539_Hm_16S-ABC-Rv	TAGCAATGGCCTCCGGCAGG
oHv552_Delta_H1_Fw	CGATACGACGGCCTTAAGTGACACCGCGATTGCAGGGCGA
oHv553_Delta_H1_Rv	TCGCCCTGCAATCGCGGTGTCACTTAAGGCCGTCGTATCG
oHv554_Delta_H2_Fw	GAATGCGAACGACACACCGCGCACCGGACCCGAACCGAACG
oHv555_Delta_H2_Rv	CGTTCGGTTCGGGTCCGGTGCGCGGTGTGTCGTTCGCATTC
oHv556_Delta_A_Fw	TCAACGCGTCCTGCCTCACCGAAGGAAATGAGGATTCCGC
oHv557_Delta_A_Rv	GCGGAATCCTCATTTCCTTCGGTGAGGCAGGACGCGTTGA
oHv558_Delta_B_Fw	TCAGGTCCGAAGGAAATGAGTGATGTTAGCCCTAGTAGTTC
oHv559_Delta_B_Rv	GAACTACTAGGGCTAACATCACTCATTTCCTTCGGACCTGA
oHv560_Delta_C1_Fw	CGAACTCGGACCTTTGAACGCCGCCAACACCCCGCGACCAG
oHv561_Delta_C1_Rv	CTGGTCGCGGGGTGTTGGCGGCGTTCAAAGGTCCGAGTTCG
oHv562_Delta_C2_Fw	CATTCACCCGCCAACACCCCGACCCATTCCGGTTGATCCTG
oHv563_Delta_C2_Rv	CAGGATCAACCGGAATGGGTCGGGGTGTTGGCGGGTGAATG
oHv564_Delta_C3_Fw	GGATCACCTCCTAACGACCGCACACGCGATCTTCCGAGTTC
oHv565_Delta_C3_Rv	GAACTCGGAAGATCGCGTGTGCGGTCGTTAGGAGGTGATCC

oHv580_GE_H324A_fw	GCGACGACGTGGAAATCGGCGCCGGGAAGCCGGACGGTCGGCTC
oHv581_GE_H324A_rv	GAGCCGACCGTCCGGCTTCCCGGCGCCGATTTCCACGTCGTCGC
oHv586_GER4D_R6D_Nde_fw	ATTGCGCATATGAGAGTCGACGTCGACGGCATCTACGCCACCGCGCTC
oHv587_GE_H274A_H275A_fw	GTCGAGACGACGATGCCCGGCGCCGCGCGGACGAAGGCCGCCTCGCAG
oHv588_GE_H274A_H275A_rv	CTGCGAGGCGGCCTTCGTCCGCGCGGCGCCGGGCATCGTCGTCTCGAC
oHv589_GE_D421R_fw	GGTACGTCGACCTCCACGTGCGCGTGGTGAAACACGCCGACGG
oHv590_GE_D421R_rv	CCGTCGGCGTGTTTCACCACGCGCACGTGGAGGTCGACGTACC
oHv591_HvGE delta Nterm 315-stop_Nde fw	ATTGCGCATATGCCGCTGGAAGGCGACGAC
oHv592_HvGE delta Cterm atg-314_Bam_rv	ACTAGTGGATCCCCCTAATATGAATCCGCCGAACTGCGCGGTCACCAC
oHv610_P2cut_reporter split23S_Fw	GCATGGATCGATGCCCTTAAGTACAACAGGGTACTTCGGTGGAATGCGAACGGTGGTAAGCAGTACTCCACTCCG
oHv611_MluI_reporter split23S_Fw	GCATGGACGCGTTGGTAAGCAGTACTCCACTC
oHv612_NotI_reporter split16S_rv	GAGCCATGCGGCCGCGTGTTAGCCCTAGTAGTTCTAAGG
oHv613 16S 5' leader fw	GCAAGACGGTATCTGATGTT
oHv614 16S 3' trailer rv	CTGAGCTATGGGCCCGTGTT
oHv615 23Ssplit fw +tRNA	TTCAGGTCCGAAGGAAATGAGGGCCCATAGCTCAGTGGTA
oHv616 23Ssplit rv +tRNA	TACCACTGAGCTATGGGCCCTCATTTCCTTCGGACCTGAA
oHv617 23Ssplit fw -tRNA	TTCAGGTCCGAAGGAAATGATGGTAAGCAGTACTCCACTC

oHv618 23Ssplit rv - tRNA	GAGTGGAGTACTGCTTACCATCATTTCCTTCGGACCTGAA
oHv692 dC4 up fw	AGTAGTTCGGTGACATCCGAAACGGTGATTTGACAGCATA
oHv693 dC4 up rv	TATGCTGTCAAATCACCGTTTCGGATGTCACCGAACTACT
oHv694 dC4 dw fw	CCGACGGGGTGGCTCACACGACCTTAGAACTACTAGGGCT
oHv695 dC4 dw rv	AGCCCTAGTAGTTCTAAGGTCGTGTGAGCCACCCCGTCGG
oHv768GAfw 6HisProtARNaseGE	AGTGGACGCCAACGGCTCGAATATGAGAGTCCGCGTCCGC
oHv769GArev6HisProtARNaseGE	TTCGATATCAAGCTTATCGATACGTACCCCGACAGCGCCG
oHv787_23S split Pci GA rv	GAGGTCATGCTTCGACATGTTTCGGTTGGAACCAGCTGTT
oHv788_23S split Mlu GA fw	CGATTGCAGGGCGATTCAACTGGTAAGCAGTACTCCACTC
oHv789_16S split NotI GA rv	GATGGTCCAGAGGTGCGGCCGTGTTAGCCCTAGTAGTTC
oHv790_16S split BamHI GA fw	CGGACCACCGATGGCGAAAGCACCTCGAGAAGACGGATCC
oHv797_GEc-term trunc FLAG rv	GTGACCGCGCAGTTCGGCGACTACAAAGACCATGACGGTGATTATAAAGATCATGATATCGACTACAAAGATGACGACGATAAATGAGGATTCATATTAGGGGGATCCACTAGTTCTAGA
oHv798 pTA927 rv	TCTAGAACTAGTGGATCCCC
oHv897_helixB_T37C_fw	AGACGGTATCCGATGTTAGCCC
oHv898_helixB_T37C_rv	GGGCTAACATCGGATACCGTCT
oHv899_helixB_G2A_fw	AAGGAAATGAGAATTCCGCC
oHv900_helixB_G2A_rv	GGCGGAATTCTCATTTCCTT
oHv901_helixB_switched_ends_fw	CCGAAGGAAATGATCTATCCGCCCCTGCGGTACGCCGCAAGACGGTTAGGGATGTTAGCCCTAGT

oHv902_helixB_switched_ends_rv	ACTAGGGCTAACATCCCTAACCGTCTTGCGGCGTACCGCAGGGGCGGATAGATCATTTCCTTCGG
oHv903_helixB_switchmid_fw	CCGAAGGAAATGAGGATTGGCAAAAACGCCATGCGGCGTCCCGCCTATCTGATGTTAGCCCTAGT
oHv904_helixB_switchmid_rv	ACTAGGGCTAACATCAGATAGGCGGGACGCCGCATGGCGTTTTTGCCAATCCTCATTTCCTTCGG
oHv905_helixB_stemtrunc_fw	TCCGAAGGAAATGAGGATTCCGTACGCGGTATCTGATGTTAGCCCTAG
oHv906_helixB_stemtrunc_rv	CTAGGGCTAACATCAGATACCGCGTACGGAATCCTCATTTCCTTCGGA
oHv907_6Aleader_helixB_fw	CGGTTCAGGTCCGAAGGAAAAAAGGATTCCGCCCCTGCGG
oHv908_6Aleader_helixB_rv	CCGCAGGGGCGGAATCCTTTTTTCCTTCGGACCTGAACCG
Sc718	GCAACTTTATCCGCCTCCAT
Sc719	TGAAGCCATACCAAACGACG

Table 14: 5‘-labeled fluorescent oligonucleotides

Oligo name	Dye	5’ > 3’ sequence
oHv305-DY682-16Srep-RV	DY682	GGAAATCCGCCAGCTCAAC
oHv306-DY782-16Srep-RV	DY782	GTACTTCCCAGGCGGCTCG
oHv322-DY682-23Srep-Bss-Fw	DY682	ACGAGGTTCATTCATGGGAC
oHv323-DY782-23Srep-Bss-Rv	DY782	GATAGCAGCCGACCTGTCTC
oHv325-DY782-16S ITS-5end-Rv	DY782	CGTGTGAGCCACCCCGTCGG
oHV637_FISH_16S_Alexa647	Alexa647	CTCCTCCGGTTGTAGTGCTC
oHv674_FISH_16S_Cy5	Cy5	CTCCTCCGGTTGTAGTGCTC
oHv675_FISH_16S_dwn_5´Bulge_Cy5	Cy5	GGGTGTTGGCGGGTGAATGGC
oHv676_FISH_16S_up_5´Bulge_Cy5	Cy5	CCGAACTACTAGGGCTAACATC
oHv677_FISH_23S_Atto488	Atto488	CCTCGGCTGATTGACAGTGCC
oHv678_FISH_circ16S_Cy5	Cy5	CCGTTCGGATAAGGTGTCCG
oHv679_FISH_circ23S_Cy3	Cy3	GGAGAACGGGTCCAGTTTGC
oHv680_FISH_23S_Cy3	Cy3	CCTCGGCTGATTGACAGTGCC
oHv707_PeX_Acp3_910_DY682_Rv	DY682	GAGCTGGTGAGATGTCCGGC

oHv762_DY782_Hv_circ16S	DY782	CCGTTCGGATAAGGTGTCCG
oHv875_FISH_16S_Atto488	Atto488	CTCCTCCGGTTGTAGTGCTC
oHv914_DY782 5' ITS II	DY782	TGTCATTGGTGAACTCGGAA

Table 15: Plasmids

Name	Description	Source
pCR™ II-Blunt-TOPO® (Kan^R)	Commercially available Vector/Cloning Kit from Life Technologies	
pTA-927(Amp^R)	Overexpression vector with *pyrE2* marker and pHV2 origin, derived from pTA230	Lab of Anita Marchfelder; Universirty Ulm (Allers et al. 2010)
pTA-1228 (Amp^R)	Overexpression vector with *pyrE2* marker derived from pTA963	(Brendel et al. 2014)
pTA1228-rDNA	*H. v.* wild type rDNA operon A	(Jüttner et al. 2020)
pTA1228-rDNA-rep	pTA1228-rDNA + reporter mutations A633G [Pcy^R], C734T [EcoRV], C2479 [Cam^R], A2496C [BssS1α]	
pTA1228-rDNA-rep 16S Δ5' bulge	pTA1228-rDNA-rep; *Δ5' bulge 16S rRNA*	
pTA1228-rDNA-rep 16S Δ3' bulge	pTA1228-rDNA-rep; *Δ3' bulge 16S rRNA*	
pTA1228-rDNA-rep 16S Δ bulges	pTA1228-rDNA-rep; *Δ5' bulge 16S rRNA + Δ3' bulge 16S rRNA*	
pTA1228-rDNA-rep 23S Δ5' bulge	pTA1228-rDNA-rep; *Δ5' bulge 23S rRNA*	
pTA1228-rDNA-rep 23S Δ3' bulge	pTA1228-rDNA-rep; *Δ3' bulge 23S rRNA*	
pTA1228-rDNA-rep 23S Δ bulges	pTA1228-rDNA-rep; *Δ5' bulge 23S rRNA + Δ3' bulge 23S rRNA*	
pTA1228-rDNA-rep 16S Δ5' bulge 23S Δ5' bulge	pTA1228-rDNA-rep; *Δ5' bulge 16S rRNA Δ5' bulge 23S rRNA*	
pTA1228-rDNA-rep 16S Δ5' bulge 23S Δ3' bulge	pTA1228-rDNA-rep; *Δ5' bulge 16S rRNA Δ3' bulge 23S rRNA*	
pTA1228-rDNA-rep 16S Δ3' bulge 23S Δ5' bulge	pTA1228-rDNA-rep; *Δ3' bulge 16S rRNA Δ5' bulge 23S rRNA*	
pTA1228-rDNA-rep 16S Δ3' bulge 23S Δ3' bulge	pTA1228-rDNA-rep; *Δ3' bulge 16S rRNA Δ3' bulge 23S rRNA*	
pTA1228-rDNA-rep helix repeat	pTA1228-rDNA-rep; *helix repeat 16S rRNA*	

pTA1228-rDNA-rep open helix	pTA1228-rDNA-rep; *open helix 16S rRNA*	
pTA1228-rDNA-rep stem deletion	pTA1228-rDNA-rep; *processing stem deletion 16S rRNA*	
pTA1228-rDNA-rep Δhelix A'	pTA1228-rDNA-rep; *Δhelix A'*	This study (oHv552/oHv553)
pTA1228-rDNA-rep Δhelix A	pTA1228-rDNA-rep; *Δhelix A*	This study (oHv556/oHv557)
pTA1228-rDNA-rep Δhelix B	pTA1228-rDNA-rep; *Δhelix B*	This study (oHv558/oHv559)
pTA1228-rDNA-rep_helix B_T37C	pTA1228-rDNA-rep; *helix B_T37C*	This study (oHv897/oHv898)
pTA1228-rDNA-rep_helix B_G2A	pTA1228-rDNA-rep; *helix B_G2A*	This study (oHv899/oHv900)
pTA1228-rDNA-rep_helix B_switchend	pTA1228-rDNA-rep; *helix B_switchend*	This study (oHv901/oHv902)
pTA1228-rDNA-rep_helix B_switchmid	pTA1228-rDNA-rep; *helix B_switchmid*	This study (oHv903/oHv904)
pTA1228-rDNA-rep_helix B_stemtrunc	pTA1228-rDNA-rep; *helix B_stemtrunc*	This study (oHv905/oHv906)
pTA1228-rDNA-rep_6Aleader_helix B	pTA1228-rDNA-rep; *6Aleader_helix B*	This study (oHv907/oHv908)
pTA927_RNaseE/G_(N-3xFLAG)	pTA927-*H. v.*-RNaseE/G; N-term 3x Flag-tag	Lab of Anita Marchfelder; Universirty Ulm
pTA927_RNaseE/G_(C-3xFLAG)	pTA927-*H. v.*-RNaseE/G; C-term 3x Flag-tag	Lab of Anita Marchfelder; Universirty Ulm
pTA927_RNaseE/G_H324A (C-3xFLAG)	pTA927-*H. v.*-RNaseE/G_ H324A; C-term 3x Flag-tag	This study oHv580/oHv581
pTA927_RNaseE/G_R4D_R6D (C-3xFLAG)	pTA927-*H. v.*-RNaseE/G_ R4D_R6D; C-term 3x Flag-tag	This study oHv586
pTA927_RNaseE/G_H274_H275A (C-3xFLAG)	pTA927-*H. v.*-RNaseE/G_ H274_H275A; C-term 3x Flag-tag	This study oHv587/oHv588
pTA927_RNaseE/G_D421R (C-3xFLAG)	pTA927-*H. v.*-RNaseE/G_ D421R; C-term 3x Flag-tag	This study oHv589/oHv590
pTA927_RNaseE/G_N-trunc (C-3xFLAG)	pTA927-*H. v.*-RNaseE/G_N-terminal_truncation; C-term 3x Flag-tag	This study oHv591/oHv349

pTA927_RNaseE/G_C-trunc (C-3xFLAG)	pTA927-*H. v.*-RNaseE/G_C-terminal_truncation; C-term 3x Flag-tag	This study oHv348/oHv797
pTA1228-rDNA_split_16S	pTA1228_rDNA_split_16S_rDNA	This study oHv789/oHv790 see figure S1
pTA1228-rDNA_split_23S	pTA1228_rDNA_split_23S_rDNA	This study oHv787/oHv788 see figure S1

9.1.4. Strains

Table 16: Strains

Organism	Strain	Genotype/Source
Escherichia coli	XL1 blue	*recA1 endA1 gyrA96 thi-1 hsdR17 supE44 relA1 lac [*F' *proAB lacI^{q}ZΔM15Tn10(Tet^{r})]*
Escherichia coli	GM2929	F^{-} *dam-13::Tn 9 dcm-6 hsdR2 recF143 mcrA0 mcrB9999 galK2 galT22 ara-14 lacY1 xyl-5 thi-1 tonA31 rpsL136 hisG4 tsx-78 mtl-1 supE44 leuB6 rfbD fhuA13*
Haloferax volcanii	h26	DS70 Derivat Δ*pyrE2* (Allers et al. 2004)
Haloferax volcanii	h119	DS70 derivate Δ*pyrE2* Δ*trpA* Δ*leuB* (Allers et al. 2004)
Haloferax volcanii	ΔE/G-like	DS70 derivate Δ*pyrE2* Δ*trpA* Δ*leuB* based on H119 Δ*HVO_0406* (this study)
Pyrococcus furiosus	DSM 3638	Archaea Center Regensburg (Fiala and Stetter 1986) (https://www.dsmz.de/collection/catalogue/details/culture/DSM-3638)
Sulfolobus acidocaldarius	MW001	Δ*pyrE*; based on DSM639 (Wagner et al. 2012) (https://www.dsmz.de/collection/catalogue/details/culture/DSM-639

Table 17: Additional cell material

Organism	Strain	Source
Archaeoglobus fulgidus	VC-16	Archaea Center Regensburg
Haloarcula marismortui	DSM 3752	DSMZ (https://www.dsmz.de/collection/catalogue/details/culture/DSM-3752)

Halobacterium salinarum	NRC-1	Anita Marchfelder, Universität Ulm
Halorobrum lacusprofundi	ACAM 32	Anita Marchfelder, Universität Ulm
Methanococcus jannaschi	JAL-1	Archaea Center Regensburg
Methanococcus thermolithotrophicus	SN-1	Archaea Center Regensburg
Methanopyrus kandleri	AV-19	Archaea Center Regensburg
Pyrodictium occultum	PL-19	Archaea Center Regensburg
Thermoplasma acdiophilum	122-1B2	Archaea Center Regensburg

9.1.5. Software

Table 18: Software

Software	Producer
Agilent TapeStation Software	Agilent
Gel Documentation Software	Intas
ImageJ	Fiji
Microsoft® Word für Microsoft 365	Microsoft
Microsoft® PowerPoint® für Microsoft 365	Microsoft
Microsoft® Excel® für Microsoft 365 MSO	Microsoft
NanoDrop ND-1000 Operating Software	Peqlab Biotechnologies GmbH
Odyssey Infrared Imaging System Application Software	LI-COR
RStudio	Posit PBC
Serial Cloner 2.6.1	Serial Basics
Zotero	George Mason University, USA

9.2 Methods

9.2.1. Work with *E. coli*

E. coli liquid cultures were incubated at 37 °C in a shaker at 160 rpm unless otherwise stated. If required, antibiotics were added and diluted 1 to 1000 from the stock solutions (see table 4 in 9.1.1). *E. coli* on LB plates was incubated at 37 °C.

9.2.1.1. Making of chemically competent cells

Respective *E. coli* strains (XL1 blue, GM2929) from glycerol stock were incubated in 50 ml SOB-medium with the suitable antibiotic (if required) overnight. The following day OD_{600nm} was measured, 200 ml SOB medium were inoculated to an OD_{600nm} of 0.2 with an appropriate volume and incubated for ~ 1.5 h. At an OD_{600nm} of 0.5, cells were harvested, distributed to four 50 ml falcons, and centrifuged at 4 °C, 4,500 rpm for 10 minutes. Then, the supernatant was discarded, and the pellet resuspended with 15 ml TfbI per 50 ml of culture. After 20 min incubation on ice the cells were once more centrifuged at 4 °C 4,500 rpm for 10 minutes. Supernatant was removed, and the pellets resuspended with 1 ml TfbII per 50 ml tube. After another incubation on ice for 20 min, cells were portioned into 75µl aliquots in 0.5 ml tubes and then stored at -80 °C until use.

9.2.1.2. Transformation of competent cells with DNA by heat shock

For each transformation reaction one aliquot of chemically competent *E. coli* cells was thawed on ice. For re-transformation 10 to 40 ng plasmid DNA or 3 µl of a ligation reaction for transformation were added to 50 µl cells and incubated on ice for around 20 min. Subsequently, the competent cells were heat shocked at 42 °C for 45 sec in a thermoblock. After two more minutes on ice, 500 µl LB medium were added and the cells incubated on a shaker for 60 to 90 min at 37 °C for recovery. Finally, 20 µl to 200 µl were transferred to LB plates with the appropriate antibiotic and the plates were incubated over night at 37 °C. By default, plasmids were amplified in XL1 blue cells. GM2929 cells were only used to prepare unmethylated plasmids for the transformation of *Haloferax volcanii*.

9.2.2. Work with *Haloferax volcanii*

Liquid cultures of *H. volcanii* were grown in YPC, Ca or Ca^{+} medium at 42 °C in Erlenmeyer flasks in a shaker at 160 rpm, unless stated otherwise.

9.2.2.1. Preparation of plates and cultivation

For plate preparation, 6 g agar, 200 ml 30 % saltwater and 100 ml H_2O were mixed in a 500 ml bottle and put into the microwave until the agar had dissolved. Depending on the respective plates (Hv-YPC or Hv-Ca) 33 ml of 10x YPC or 10x Ca were added after the heated solution became clear. Afterwards, the solution was autoclaved for 20 minutes. Then, 2 ml 0.5 M $CaCl_2$ were added as well as 300 µl thiamine and biotin mix (see table 8 in 9.1.2) for Hv-Ca plates after cooling down to ~ 60 °C. For enhanced Ca-plates, the required additives were added (see table 8 in 9.1.2). For each petri dish 30 ml of the solution were poured into plates and stored at 4 °C. *Haloferax volcanii* clones were picked from plates and cultivated in 10 ml to 20 ml of the respective medium at 42 °C under agitation (see 9.2.2).

9.2.2.2. Transformation of *Haloferax volcanii* cells with plasmid DNA

Transformation was performed accordingly to the protocol published by Thorsten Allers and co-workers (Allers et al. 2004). All steps were performed at room temperature, unless stated otherwise. For 3-4 transformations a 10 ml culture of *H. volcanii* cells in YPC medium was set up and incubated at 42 °C overnight. When cells reached an OD_{600nm} around 0.8, they were pelleted via centrifugation (8 min, 6,000 rpm). The pellet was gently resuspended in 2 ml buffered spheroplasting solution. After a second centrifugation step (8min, 6,000 rpm), the pellet was then resuspended very carefully in 600 µl buffered spheroplasting solution and 3x 200 µl were transferred to fresh 2 ml tubes. To ensure the formation of spheroplasts a drop of 20 µl 0.5 M EDTA, pH 8.0 was added on the side of the tube, which was subsequently inverted to mix. During the 10 min incubation time, the plasmid DNA to be transformed was prepared. Each DNA mixture contained 10 µl of ultra-pure, unmethylated DNA (1-2 µg) or 10µl H_2O as a negative control, 15 µl of unbuffered spheroplasting solution and 5 µl of 0.5 M EDTA, pH 8.0. The DNA was added to the cells in the same manner as EDTA before and the samples incubated for 5 min. Meanwhile, 60 % PEG 600 solution was prepared. 320 µl of unbuffered spheroplasting solution and 480 µl PEG 600 were used for 3 transformations. The PEG solution was added in the same way as EDTA and the DNA before, but the tubes were twisted

horizontally to mix gently and then left for 30 min. Now, 1.5 ml of spheroplasting dilution solution were added, inverted to mix and left for 2 min. Following a centrifugation step (6,000 rpm, 8 min) the supernatant was then removed. At this point the formation of spheroplasts should be visible, since *Haloferax volcanii* loses its reddish color during transformation treatment. 2 ml regeneration solution were added without resuspending the pellet and the cells were put in a 42 °C incubator without shaking. After 1.5 to 2 hours, the tubes were transferred to a 42 °C incubator with shaking for 3 to 4 more hours to further regenerate. Finally, the cells were centrifuged (6,000 rpm, 8 min) and the supernatant was removed. With successful recovery of the cell's walls, they should have now regained their reddish color. The pellet was carefully resuspended in 1 ml transformant dilution solution and 100 µl to 250 µl were plated on Hv-Ca+ plates. After a few days single colonies were visible on the plates and clones could be picked for further analysis.

9.2.2.3. Genomic DNA extraction from *H. volcanii* by DNA spooling

About 1 ml of a liquid culture of *H. volcanii* (OD_{600nm} ~0.8) was pelleted at 6,000 rpm for 5 min in a round bottomed tube. The pellet was resuspended in 200 µl of ST buffer (1 M NaCl, 20 mM Tris-HCl) before adding 200 µl lysis solution (100 mM EDTA pH 8.0, 0.2 % SDS) and inverted to mix. The solution was covered with 1 ml EtOH to spool the DNA onto a sterile inoculation loop (white, 1 µl). The DNA was then transferred into a new cup with fresh EtOH to wash the spooled DNA. To pellet the DNA, it was put in the centrifuge for 2 min at 6,000 rpm, before removing the supernatant and let the excess EtOH dry. The DNA was resuspended in 500 µl TE and left to soak for 10 min. 50 µl 3 M sodium acetate (pH 5.2) and 400 µl isopropanol were added and inverted to mix and again centrifuged at 6,000 rpm for 10 min. The pellet was washed in 1 ml 70 % EtOH and the pellet was air-dried before resuspending it in 100 µl TE. To get rid of residual RNA, 1 µl RNase A (30 mg/ml) was added and incubated (shaking) at 45 °C for 1 h. The DNA was kept at 4 °C to resuspend overnight.

9.2.2.4. Growth analysis with spot assay

Standard YPC or Casamino plates were prepared like described above. 100 ml were poured into a rectangular petri dish. For low or high salt conditions medium was prepared with 1.4 M or 4 M NaCl, respectively. Plates were dried at least one day on the bench at RT. *H. volcanii* was grown to 0.4 to 0.6 OD_{600nm} and measured. Different dilutions (10^{-2}, 10^{-3},…,10^{-6} OD_{600nm}) of *H. volcanii* cultures (YPC or Ca^{+}) were prepared in the respective medium and mixed by

vortex. Subsequently, 5µl of each dilution was pipetted as spot on a plate next to a burning Bunsen burner. Importantly, the pipette tip was changed after every spot. The plates were dried until no residual liquid was visible anymore. Afterwards, the plates were incubated at 42 °C or at 30/50 °C for cold/heat shock. The plates were checked after one and two days and the following days.

9.2.3. Work with *H. marismortui*

Liquid cultures of *H. marismortui* were grown in ATTC:1218 medium at 37 °C in Erlenmeyer flasks in a shaker at 160 rpm.

9.2.4. Work with *H. lacusprofundi*

Liquid cultures of *H. lacusprofundi* were grown in HL medium (DSMZ Medium 589) at 30 °C in Erlenmeyer flasks in a shaker at 160 rpm.

9.2.5. Work with *S. acidocaldarius*

Liquid cultures of *S. acidocaldarius* were grown in Brock (*Sulfolobus* 88 DMSZ) medium at 65 °C in Erlenmeyer flasks in a shaker at 160 rpm, unless indicated otherwise.

9.2.6. DNA & cloning work

9.2.6.1. Polymerase Chain Reaction (PCR)

Standard PCR for cloning purposes was done using the Phusion polymerase from NEB according to manufacturer's protocol. Before, annealing temperatures of oligos were calculated using the NEB Tm calculator online tool. Depending on GC content either 5x GC-buffer (high GC) or 5x HF-buffers were used. Elongation time was 30 sec per 1 kb amplicon.

Setup for 50 µl: 10 µl 5x GC/HF-buffer, 1.5 µl DMSO, 1 µl dNTP-mix (10 mM each), 2.5 µl each oligo (10 mM), 0.5 µl Phusion polymerase, 1 µl of DNA template.

Table 19: PCR - standard program

PCR Program		
Step	**Temperature**	**Time**
Heat lid	110 °C	-
Initial denaturation	98 °C	30 sec
Cycles* (20 – 30)	98 °C	30 sec
	65 °C	15 sec
	72 °C	15 sec
Final elongation	72 °C	5 min
Hold	12 °C	∞

* 20-25 cycles were used for *cis*-acting reporter assay, 30 cycles for cloning purposes.

9.2.6.2. Colony-PCR

Colony PCR was performed using Go-Taq polymerase from Promega in a reduced volume of 20 µl according to manufacturer's protocol. For colony PCR of *E. coli* clones from LB plates colonies were scratched off with a 10 µl pipette tip and directly transferred to the prepared PCR reaction. To check *H. volcanii* clones for the *cis*-acting reporter assay 50 µl of liquid *H. volcanii* culture were mixed with 950 µl H_2O and 1 µl of this mix added as template to the prepared PCR reaction.

9.2.6.3. PCR-Purification

For the purification of PCR products, the QIAquick PCR purification kit by Qiagen was used. The kit was used according to manufacturer's protocol.

9.2.6.4. Restriction enzyme digest

gDNA or plasmid DNA was digested by a large variety of restriction enzymes (purchased from NEB) according to manufacturer's manual. The digested DNA was separated by agarose gel electrophoresis. Desired vectors or digested PCR products were excised from gel with a scalpel and extracted with QUIAEX II gel extraction kit from Qiagen.

9.2.6.5. DNA ligation

Following the restriction digest with suitable restriction enzymes, DNA fragments were integrated into the vector. DNA ligation was performed with 1 µl T4 DNA ligase from NEB, 1 µl of the provided ligation buffer (10x) in a total volume of 10 µl and a molar ratio of 3:1 of insert to digested vector. As a control the same reaction was prepared, but instead of the insert 3 µl H_2O were used. The ligation mixture was incubated for 1 h at RT or at 16 ° C overnight. 5 µl of the ligation reaction were taken for transformation into XL1 blue cells.

9.2.6.6. Agarose gel electrophoresis

Agarose gel electrophoresis was used for separation of DNA fragments. Depending on the fragment size 1 % to 2 % gels were prepared dissolving agarose in 1x TBE by microwaving. Once cooled down, SYBR Safe stain (1:20000 dilution) was added and poured into form. Samples were mixed with 6x gel loading dye from NEB and loaded with 100 bp, 1 kb or 2-log marker as reference. Agarose gels ran at around 120 V and read out on a blue light screen.

9.2.6.7. Polyacrylamide gel electrophoresis of DNA

Polyacrylamide gel electrophoresis enables separation of smaller DNA fragments with better resolution than agarose gels. This type of gel was also used for the *cis*-acting reporter assay. Polyacrylamide concentrations: 10 % for 30 – 1000 bp, 12 % for 40 – 200 bp, 14 % for 25 bp – 150 bp (in 1x TBE); 1 % APS (20 % stock solution) and 0.1 % (TEMED) was used to start polymerization. 1x TBE was used as running buffer.

9.2.6.8. Gibson assembly

As alternative to standard cloning procedure the Gibson Assembly® method (NEB) was used. Multiple overlapping DNA fragments can simultaneously be inserted into a vector that is opened by suitable restriction enzymes in a single reaction. Gibson Assembly® master mix contains an exonuclease, DNA polymerase and ligase to efficiently join overlapping DNA fragments. Usually, vector was mixed with a 2- to 3-fold excess of each insert and 2x Gibson Assembly® master mix added in a total volume of 4 µl. After incubation at 50 °C for 15 min the

complete reaction was transformed into XL1blue *E. coli* cells. A detailed protocol for this method is available on the NEB website.

9.2.6.9. TOPO subcloning

For subcloning of PCR fragments Zero Blunt ® TOPO PCR Cloning Kit was used according to manufacturer's protocol. Positive clones were selected on Kanamycin plates and plasmids sent for sequencing.

9.2.6.10. DNA sequencing

For the verification of successful cloning, 400 ng to 800 ng of plasmid were sent to Microsynth for sequencing.

9.2.6.11. DNA/RNA quantification

The Nanodrop-ND1000 by Peqlab was used to measure DNA/RNA quantities at the respective DNA/RNA measuring presets.

9.2.6.12. cDNA synthesis (SS III)

For reverse transcription the SuperScript™ III kit was used. The following ingredients were mixed:

Table 20: cDNA synthesis pipetting scheme

Ingredient	Volume/final concentration
RNA	1 µg – 2 µg
dNTPs (25 mM each)	1 µl
RT primer	2 pmol
Add H_2O to 13 µl total volume	
Incubate 5 min at 65 °C and put on ice	

Add:	
5x first strand synthesis buffer	4 µl
0.1 M DTT	1 µl
RNasin®	1 µl
SuperScript III/ H_2O*	1µl
Incubate 1 h at 55 °C	
Incubate 15 min at 75 °C	

* -RT control was prepared using water instead of SS III.

9.2.6.13. Southern blot analysis

To determine genomic fragments and their changes southern blotting or upward capillary transfer is a simple method to screen for said changes. Overnight digested genomic DNA was separated on a large agarose gel electrophoresis. Subsequently, the gel was washed once with H_2O, and was then incubated 2 x 15 min in denaturing solution (0.5 M NaOH, 1.5 M NaCl). Then, the gel was washed once with water before incubating it again 2 x 15 min in 1M ammonium acetate. The transfer to the positive membrane was done overnight with 1 M ammonium acetate. On the next day the blot was air-dried for 10 min before crosslinking the DNA to the blot on the Fluo_Link (Vilber Lourmat) at 0.3 J/cm2. The blot was stored at 4 °C or used immediately.

For the downstream analysis the blot was pre-hybridized for 1-3 h in 25 ml hybridization buffer (0.5 M Na-phosphate pH 7.2, 7 % SDS). While waiting, the DNA probe was prepared with the RadPrime DNA labeling system (GIBCO BRL). The probe was purified on a G25 spin column (Amersham) at 2,800 rpm. Salmon sperm DNA was added to the probe (final concentration of ss-DNA in hybridization solution should be 100 µg/ml). The sample was then boiled for 10 min, before they were put on ice. The probe was then added to the hybridizing buffer and left to incubate overnight rotating at 65 °C. On the following day the blot was washed with 35 ml Rinse buffer (3x SSC, 0.1 % SDS), following two washes with Wash Buffer #1 (0.3x SSC, 0.1 % SDS) for 15 min at 65 °C. Next two wash steps with Wash Buffer #2 (0.1x SSC, 0.1 % SDS) for 15 min at 65 °C and one last time two washes with Wash Buffer #3 (0.1x SSC, 1.5 % SDS) followed. The blots were then checked for radioactive counts and exposed to a PhosphoImager screen.

9.2.7. RNA work

9.2.7.1. Phenol/chloroform RNA extraction

Cell pellets were resuspended in 500 µl AE buffer and mixed with 500 µl phenol equilibrated in AE Buffer and 50 µl 10 % SDS. Then, the samples were transferred to a 65 °C thermomixer and shaken vigorously (1,400 rpm) for 5 min. Next, they were vortexed and cooled down on ice for 2 min. The mixture was centrifuged at full speed and 4 °C for 2 min before removing 3x 150 µl of the aqueous layer into a fresh cup. The aqueous layer was mixed with 500 µl of phenol equilibrated in AE Buffer and vortexed. Again, the samples were centrifuged as before and 3x 120 µl of the supernatant were mixed with 500 µl Chloroform and vortexed. Again, phase separation was done by centrifugation and 3x 100 µl was then mixed with 2.5 volumes of ice cold EtOH and 1/10 vol of 3 M NaAc pH 5.3 to precipitate the RNA. Finally, samples were incubated at -20 °C for a few hours or overnight. RNA was pelleted by centrifugation for 30 min at full speed and 4 °C. The pellet was air-dried and then dissolved in 50 µl nuclease-free H_2O.

9.2.7.2. DNase Digestion

For further analysis it was essential to get rid of residual DNA contaminations in the phenol/chloroform extracted RNA. Thus, DNase treatment of the probes was performed at 37 °C overnight. Digestion was performed in a total volume of 50 µl containing 1 µl RQ1 DNase, 5 µl 10x RQ1 DNase buffer and 1 µl RNasin®. After the digestion, 750 µl EtOH and 30 µl 3M Na-Acetate (pH 5.3) were added and the samples stored at -20°C for at least one hour to precipitate the RNA. The centrifugation was performed as described before (9.2.7.1) and the dried RNA pellets were resuspended in 50 µl nuclease-free H_2O. The RNA concentration was measured on the Nanodrop ND-1000 at the given presets and the RNA stored at – 20 °C.

9.2.7.3. RNA extraction with extraction kits

Phenol/chloroform RNA extraction from *H. volcanii* cells co-purifies substantial amounts of DNA, which makes a subsequent DNase digestion crucial for many downstream experiments. To easily obtain clean, DNA-free total RNA the innuPREP Micro RNA kit (Analytik Jena) or the NucleoSpin RNA kit® (MACHEREY-NAGEL) were used according to manufacturer's protocol.

9.2.7.4. *Cis*-acting elements reporter assay

The complete procedure of the *cis*-acting elements reporter assay is described in my Master thesis and the corresponding publication (Jüttner 2018; Jüttner et al. 2020). In brief, *H. volcanii* h26 cells were transformed with reporter plasmids and 10 ml to 20 ml liquid cultures inoculated. Ratios between genomic and plasmid rDNA copies were determined by colony PCR with the oligos oHv305/oHv306 (16S rDNA) and oHv322/oHv323. PCR products were EtOH/NaAc precipitated, and restriction digest performed with EcoRV (16S rDNA) or BssS1α (23S rDNA). TBE-PAGE-gel was used to read-out the ratios of uncut vs cut (representing genomic vs plasmid), fluorescently labeled PCR fragments. For RNA expression analysis cells were harvested at mid exponentially phase (0.6-0.8 OD_{600nm}) and RNA phenol/chloroform extracted. After DNase digestion, cDNA synthesis was performed with oHv40 (circular 16S pre-rRNAs), oHv42 (circular 23S pre-rRNAs), oHv252 (total 16S rRNA) or oHv307 (total 23S rRNA). PCR, restriction digest and PAGE was performed similarly and read out at the Li-COR Odyssey Imaging system. ImageJ was used to quantify fluorescent signals.

9.2.7.5. Northern blot analysis of RNAs

For Northern blot analyses 2 µg to 5 µg of total RNA were separated on a denaturing agarose gel. The gel consisting of 1.3 % agarose, 20 ml of 10x MOPS running buffer, 10.8 ml 37 % formaldehyde and 20 µl SYBR Safe was run over night at 35 V for 16 h. After the run, the gel was rinsed with 1L H_2O for 5 minutes on a shaker followed by 20 min in 1L 0.05 M NaOH under mild agitation. Then, two steps of 20 min in 10x SSC on a shaker followed. RNAs were transferred from the denaturing gel onto a charged membrane (Positive MP Biomedicals) using capillary transfer for at least 24 h. Sufficient (at least 1 L) 10x SSC transfer buffer was drawn from a downward reservoir through the gel into a stack of paper towels. The RNAs were carried by the buffer stream from the gel to the positively charged membrane between gel and paper towels. The transfer membrane was dried after the transfer and crosslinked by UV light exposure (0.3 J/cm^2) in a Fluo_Link device. For hybridization of fluorescent probes crosslinked membranes were incubated in a glass tube with 25 ml pre-hybridization buffer for at least 3 hours at 30 °C in a hybridization oven under mild rotation. After pre-hybridization fluorescently labeled oligos (DY682 or DY782) were added and incubated overnight at 30 °C in a hybridization oven under mild rotation. The amount of oligos varied from total RNA load and detected RNA species. For detecting mature rRNAs 1 pmol to 10 pmol, for pre-rRNAs 25 pmol to 100 pmol of the respective oligos were used. After overnight hybridization membranes were rinsed once with 50 ml 2x SSC followed by two washing steps (1. 50 ml of 2x SSC; 2. 50 ml of

1x SSC; 15 min each) at 30 °C in a hybridization oven under mild rotation. Finally, membranes were dried, and image acquisition performed on a Li-Cor Odyssey Image reader.

9.2.7.6. RNase H cleavage assay

Typically, 2 µg to 5 µg of *H. v.* total RNA was incubated with oHv203 and oHv254 (5pmol each) and 1.5µl 10x RNase H buffer for 5 minutes at 65 °C followed by oligo annealing for 10 minutes at 37 °C in a total volume of 14 µl in a PCR cup. 1 µl of NEB RNase H (5 U) was added followed by an incubation of 20 minutes at 37 °C. 15 µl of 2x formamide buffer were added and the reaction stopped at 65 °C for 15 minutes. RNase H cleaved total RNAs were loaded on a denaturing 1.4 % to 1.5 % agarose gel and further analyzed by northern blotting (see above).

9.2.7.7. Agilent 4200 TapeStation system

The Agilent 4200 TapeStation system is a highly sensitive device to measure and analyze DNA or RNA. High sensitivity RNA screen tapes were used for the TapeStation run to analyze 2 ng to 5 ng RNA (per lane) extracted by RNA extraction kit or phenol/chloroform extraction. The experiment was performed exactly as described in the manufacturer's manual. The corresponding Agilent TapeStation software was used for data analysis.

9.2.7.8. Sucrose gradient separation and fractionation

To separate ribosomal particles from cellular components 5 % to 30 % sucrose gradients in K1800 buffer were prepared using the 'SW40 LONG SUCR 5 30' program of the Biocomp Gradient Master 107 IP. Per gradient 50 ml of a *H. volcanii* culture (~0.5 OD_{600nm}) was harvested by centrifugation (3300 g, 8 min). All steps following steps were performed on ice or at 4 °C, unless stated otherwise. The pellet was resuspended in cold 300 µl K1800 buffer and 4 µl RNasin® were added. An equal volume of Zirkonia beads was added and used to lyse the cells in a Precellys Evolution, with Cryolysis cooler (3 runs of 6x 30 s; 6,000 rpm; 30 s pause, 4 °C). The lysate was centrifuged for 10 min at 4000 g at 4 °C and the supernatant further cleared by a second centrifugation step for 30 min at 16000 g at 4 °C. The nucleic acid concentration was measured with the RNA setting at a NanoDrop ND-1000 (PeqLab) and 1 µg of total nucleic acids was loaded per 12 ml sucrose gradient (5 % to 30 %). Then, gradients

were tared precisely the same weight and centrifuged overnight in a Beckman Coulter Optima L-80XP ultracentrifuge in a SW40 swing-out rotor (16 h, 26,000 rpm, 4 °C). Acceleration and brake were both set to maximum. The subsequent fractionation (500 µl fractions) was performed on a ÄKTA (2 ml/min flowrate) using a siFractor (siTOOLs Biotech) adaptor with simultaneous detection of UV_{260nm} profiles. As chase solution 60 % sucrose solution was used to compensate for high weight of K1800 buffer.

9.2.7.9. Nanopore-based sequencing

Oxford Nanopore Technology was used to determine pre-rRNA intermediates in archaea. RNA extraction, library preparation, direct cDNA and RNA sequencing as well as bioinformatical downstream analyses have been performed by Felix Grünberger and are described in the corresponding manuscript (Grünberger et al. 2022). The protocol of RNase H cleavage assays is available in 9.2.7.6 and in the corresponding manuscript.

9.2.8. RNA-FISH Microscopy

9.2.8.1. Poly-L-lysine coating of glass slides

Glass slides were coated with poly-L-lysine for RNA-FISH experiments. 100 µl of poly-L-lysine solution (0.1 % (w/v)) in H_2O, Sigma Aldrich) were added on each well of a diagnostic microscope slide (ER-303B-CE:3 well 14 mm). The slides were air dried for 30 minutes. Afterwards, the residual solution was removed from the wells. Lastly, the glass slides were air dried again at room temperature overnight.

9.2.8.2. RNA fluorescent *in situ* hybridization (RNA-FISH)

The RNA-FISH protocol was developed in cooperation with a Master student, Maximilian Liebl (Liebl 2021). *H. volcanii* and *S. acidocaldarius* cells were grown to 0.2 OD_{600} in the respective rich medium at 42 °C or 65 °C, respectively 2 ml (= 0.4 OD_{600}) of cells were mixed with 113.5 µl 37 % formaldehyde (final concentration 2 %) and incubated for 20 minutes while shaking at 42 °C (*H. v.*) or 65 °C (*S. a.*). Then, 1 µl Hoechst 33342 (10 mg/ml) was added and the samples incubated for another 5 minutes at the respective temperature while shaking. 100 µl 2.5 M glycine were added to stop fixation and incubated at the respective temperature for 5 minutes

while shaking. Next, cells were harvested by centrifugation (3300 g, 8 min), washed with 1x PBS and centrifuged once more (3300 g, 8 min). The cell pellet was resuspended in 80 µl 1x SSC and 10 µl of this cell suspension were transferred per well on the poly-L-lysine coated glass plates. Subsequently, the glass slides were air dried for 30 minutes at RT and washed one time by immersing the slide completely in 1x PBS. Afterwards, slides were air dried at RT again and immediately after being dried out 14 µl pre-hybridization buffer (PHB) were added onto each well. The slides were incubated for 1 h in an airtight humid chamber at 37 °C. The bottom of the chamber was filled with paper towels soaked in 2x SSC buffer. After 1 h, 1 µl of RNA-FISH oligos (10 pmol/µl) were added directly to the PHB followed by another incubation for 3 h at 37 °C in the humid chamber. PHB was completely removed with a pipette and each well was washed three times with 50 µl 2x SSC buffer. Finally, slides were completely dried at RT,12 µl Diamond anti fade solution mounting solution (Invitrogen, Thermo Fisher) were added to each well and covered with a glass coverslip. Slides were dried at least two days before microscopy.

9.2.8.3. Microscopy

By default, image acquisition after RNA-FISH experiments was performed using a Plan-Apochromat 100x / 1.45 NA oil DIC objective on a Keyence BZ-X810 Analyzer fluorescence microscope with a cooled monochrome CCD camera.

9.2.9. Crystallography

Crystallography of archaeal RNase E/G-like from *Sulfolobus acidocaldarius* and *Pyrococcus furiosus* was done by the group of Prof. Dr. Nicolas Leulliot and is described in the PhD thesis of Marlene Vayssieres (Vayssieres 2019).

9.2.10. RNA secondary structure predictions

All RNA secondary structure predictions were performed with the web tools on the ‘ViennaRNA Web Services’ website developed by Gruber and co-workers (Gruber et al. 2008).

9.2.11. Data analysis using RStudio

Plots were designed in RStudio using the '`tidyverse`' package (Wickham et al. 2019).

9.2.12. Statistic Calculations

For the quantification of all obtained images from the reporter assay the ImageJ software was used. The Li-Cor Odyssey Imaging system generates two images from separate measurements. The signals of fluorescently labeled PCR primers were detected, once at 700 nm and once at 800 nm. Then, the intensities of gel bands were determined with ImageJ in two independent measurements for each wavelength, respectively. After correction of these intensities with a background value, the ratios of the intensities corresponding to plasmid and genomic derived RNA, or DNA amounts were calculated. Furthermore, the RNA ratios were normalized with DNA template amounts. The normalization factors were obtained by calculating ratios from previous colony PCR experiments.

10. References

Adam, Panagiotis S., Guillaume Borrel, Céline Brochier-Armanet, and Simonetta Gribaldo. 2017. 'The Growing Tree of Archaea: New Perspectives on Their Diversity, Evolution and Ecology'. *The ISME Journal* 11 (11): 2407–25. https://doi.org/10.1038/ismej.2017.122.

Adesnik, Milton, and Cyrus Levtnthal. 1969. 'Synthesis and Maturation of Ribosomal RNA in Escherichia Coli'. *Journal of Molecular Biology* 46 (2): 281–303. https://doi.org/10.1016/0022-2836(69)90422-7.

Adilakshmi, Tadepalli, Priya Ramaswamy, and Sarah A. Woodson. 2005. 'Protein-Independent Folding Pathway of the 16S RRNA 5′ Domain'. *Journal of Molecular Biology* 351 (3): 508–19. https://doi.org/10.1016/j.jmb.2005.06.020.

Agalarov, Sultan, Marat Yusupov, and Gulnara Yusupova. 2016. 'Reconstitution of Functionally Active Thermus Thermophilus 30S Ribosomal Subunit from Ribosomal 16S RNA and Ribosomal Proteins'. In *Nucleic Acid Crystallography: Methods and Protocols*, edited by Eric Ennifar, 303–14. Methods in Molecular Biology. New York, NY: Springer. https://doi.org/10.1007/978-1-4939-2763-0_19.

Ahn, Hyeonju, Donghyeok Seol, Seoae Cho, Heebal Kim, and Woori Kwak. 2020. 'Enhanced Symbiotic Characteristics in Bacterial Genomes with the Disruption of RRNA Operon'. *Biology* 9 (12): 440. https://doi.org/10.3390/biology9120440.

Aït-Bara, Soraya, and Agamemnon J. Carpousis. 2015. 'RNA Degradosomes in Bacteria and Chloroplasts: Classification, Distribution and Evolution of RNase E Homologs'. *Molecular Microbiology* 97 (6): 1021–1135. https://doi.org/10.1111/mmi.13095.

Akanuma, Genki, Hideaki Nanamiya, Yousuke Natori, Koichi Yano, Shota Suzuki, Shuya Omata, Morio Ishizuka, Yasuhiko Sekine, and Fujio Kawamura. 2012. 'Inactivation of Ribosomal Protein Genes in Bacillus Subtilis Reveals Importance of Each Ribosomal Protein for Cell Proliferation and Cell Differentiation'. *Journal of Bacteriology* 194 (22): 6282–91. https://doi.org/10.1128/JB.01544-12.

Albers, Sonja, Jonathan Ashmore, Thomas Pollard, Anja Spang, and Jizhong Zhou. 2022. 'Origin of Eukaryotes: What Can Be Learned from the First Successfully Isolated Asgard Archaeon'. *Faculty Reviews* 11: 3. https://doi.org/10.12703/r-01-000005.

Albert, Benjamin, Jorge Perez-Fernandez, Isabelle Léger-Silvestre, and Olivier Gadal. 2012. 'Regulation of Ribosomal RNA Production by RNA Polymerase I: Does Elongation Come First?' *Genetics Research International* 2012: 276948. https://doi.org/10.1155/2012/276948.

Alberts, Bruce, Alexander Johnson, Julian Lewis, Martin Raff, Keith Roberts, and Peter Walter. 2002. *Molecular Biology of the Cell*. 4th ed. Garland Science.

Allers, Thorsten, Shahar Barak, Susan Liddell, Kayleigh Wardell, and Moshe Mevarech. 2010. 'Improved Strains and Plasmid Vectors for Conditional Overexpression of His-Tagged Proteins in Haloferax Volcanii'. *Applied and Environmental Microbiology* 76 (6): 1759–69. https://doi.org/10.1128/AEM.02670-09.

Allers, Thorsten, Hien-Ping Ngo, Moshe Mevarech, and Robert G. Lloyd. 2004. 'Development of Additional Selectable Markers for the Halophilic Archaeon Haloferax Volcanii Based on the LeuB and TrpA Genes'. *Applied and Environmental Microbiology* 70 (2): 943–53. https://doi.org/10.1128/AEM.70.2.943-953.2004.

Almeida, Alexandre, Alex L. Mitchell, Miguel Boland, Samuel C. Forster, Gregory B. Gloor, Aleksandra Tarkowska, Trevor D. Lawley, and Robert D. Finn. 2019. 'A New Genomic Blueprint of the Human Gut Microbiota'. *Nature* 568 (7753): 499–504. https://doi.org/10.1038/s41586-019-0965-1.

Altamura, S, E Caprini, M E Sanchez, and P Londei. 1991. 'Early Assembly Proteins of the Large Ribosomal Subunit of the Thermophilic Archaebacterium Sulfolobus. Identification and Binding to Heterologous RRNA Species.' *Journal of Biological Chemistry* 266 (10): 6195–6200. https://doi.org/10.1016/S0021-9258(18)38103-1.

Amann, Gudrun, K. O. Stetter, Enric Llobet-Brossa, Rudolf Amann, and Josefa Antón. 2000. 'Direct Proof for the Presence and Expression of Two 5% Different 16S RRNA Genes in Individual Cells of Haloarcula Marismortui'. *Extremophiles* 4 (6): 373–76. https://doi.org/10.1007/s007920070007.

Ameismeier, Michael, Ivo Zemp, Jasmin van den Heuvel, Matthias Thoms, Otto Berninghausen, Ulrike Kutay, and Roland Beckmann. 2020. 'Structural Basis for the Final Steps of Human 40S Ribosome Maturation'. *Nature* 587 (7835): 683–87. https://doi.org/10.1038/s41586-020-2929-x.

References

Ammar, Ron, Dax Torti, Kyle Tsui, Marinella Gebbia, Tanja Durbic, Gary D Bader, Guri Giaever, and Corey Nislow. 2012. 'Chromatin Is an Ancient Innovation Conserved between Archaea and Eukarya'. Edited by Danny Reinberg. *ELife* 1 (December): e00078. https://doi.org/10.7554/eLife.00078.

Aouad, Monique, Jean-Pierre Flandrois, Frédéric Jauffrit, Manolo Gouy, Simonetta Gribaldo, and Céline Brochier-Armanet. 2022. 'A Divide-and-Conquer Phylogenomic Approach Based on Character Supermatrices Resolves Early Steps in the Evolution of the Archaea'. *BMC Ecology and Evolution* 22 (1): 1. https://doi.org/10.1186/s12862-021-01952-0.

Apirion, D., and A. B. Lassar. 1978. 'A Conditional Lethal Mutant of Escherichia Coli Which Affects the Processing of Ribosomal RNA.' *Journal of Biological Chemistry* 253 (5): 1738–42. https://doi.org/10.1016/S0021-9258(17)34927-X.

Archibald, John M. 2008. 'The Eocyte Hypothesis and the Origin of Eukaryotic Cells'. *Proceedings of the National Academy of Sciences* 105 (51): 20049–50. https://doi.org/10.1073/pnas.0811118106.

———. 2015. 'Endosymbiosis and Eukaryotic Cell Evolution'. *Current Biology* 25 (19): R911–21. https://doi.org/10.1016/j.cub.2015.07.055.

Arraiano, Cecília M., José M. Andrade, Susana Domingues, Inês B. Guinote, Michal Malecki, Rute G. Matos, Ricardo N. Moreira, et al. 2010. 'The Critical Role of RNA Processing and Degradation in the Control of Gene Expression'. *FEMS Microbiology Reviews* 34 (5): 883–923. https://doi.org/10.1111/j.1574-6976.2010.00242.x.

Asai, Tsuneaki, Ciarán Condon, Justina Voulgaris, Dmitry Zaporojets, Binghua Shen, Michaal Al-Omar, Craig Squires, and Catherine L. Squires. 1999. 'Construction and Initial Characterization of Escherichia Coli Strains with Few or No Intact Chromosomal RRNA Operons'. *Journal of Bacteriology* 181 (12): 3803–9. https://doi.org/10.1128/JB.181.12.3803-3809.1999.

Atkinson, Gemma C., Tanel Tenson, and Vasili Hauryliuk. 2011. 'The RelA/SpoT Homolog (RSH) Superfamily: Distribution and Functional Evolution of PpGpp Synthetases and Hydrolases across the Tree of Life'. *PloS One* 6 (8): e23479. https://doi.org/10.1371/journal.pone.0023479.

Audesirk, Gerald, Teresa Audesirk, and Bruce Byers. 2016. *Biology: Life on Earth with Physiology, Global Edition*. 11th ed. Pearson Education Limited.

Avcı, Burak, Jakob Brandt, Dikla Nachmias, Natalie Elia, Mads Albertsen, Thijs J. G. Ettema, Andreas Schramm, and Kasper Urup Kjeldsen. 2022. 'Spatial Separation of Ribosomes and DNA in Asgard Archaeal Cells'. *The ISME Journal* 16 (2): 606–10. https://doi.org/10.1038/s41396-021-01098-3.

Babitzke, P, and S R Kushner. 1991. 'The Ams (Altered MRNA Stability) Protein and Ribonuclease E Are Encoded by the Same Structural Gene of Escherichia Coli.' *Proceedings of the National Academy of Sciences* 88 (1): 1–5. https://doi.org/10.1073/pnas.88.1.1.

Bahram, Mohammad, Sten Anslan, Falk Hildebrand, Peer Bork, and Leho Tedersoo. 2019. 'Newly Designed 16S RRNA Metabarcoding Primers Amplify Diverse and Novel Archaeal Taxa from the Environment'. *Environmental Microbiology Reports* 11 (4): 487–94. https://doi.org/10.1111/1758-2229.12684.

Baka, Erzsébet, Sándor Varga, Cédric Hobel, Roland Wilhelm Knispel, Csaba Fekete, Milán Ivanics, Balázs Kriszt, István Nagy, and József Kukolya. 2013. 'The First Transformation Method for the Thermo-Acidophilic Archaeon Thermoplasma Acidophilum'. *Journal of Microbiological Methods* 95 (2): 145–48. https://doi.org/10.1016/j.mimet.2013.08.006.

Bakshi, Somenath, Albert Siryaporn, Mark Goulian, and James C. Weisshaar. 2012. 'Superresolution Imaging of Ribosomes and RNA Polymerase in Live Escherichia Coli Cells'. *Molecular Microbiology* 85 (1): 21–38. https://doi.org/10.1111/j.1365-2958.2012.08081.x.

Baliga, Nitin S., Richard Bonneau, Marc T. Facciotti, Min Pan, Gustavo Glusman, Eric W. Deutsch, Paul Shannon, et al. 2004. 'Genome Sequence of Haloarcula Marismortui: A Halophilic Archaeon from the Dead Sea'. *Genome Research* 14 (11): 2221–34. https://doi.org/10.1101/gr.2700304.

Bange, Gert, Ditlev E. Brodersen, Anastasia Liuzzi, and Wieland Steinchen. 2021. 'Two P or Not Two P: Understanding Regulation by the Bacterial Second Messengers (p)PpGpp'. *Annual Review of Microbiology* 75 (1): 383–406. https://doi.org/10.1146/annurev-micro-042621-122343.

Baracchini, E, and H Bremer. 1988. 'Stringent and Growth Control of RRNA Synthesis in Escherichia Coli Are Both Mediated by PpGpp.' *Journal of Biological Chemistry* 263 (6): 2597–2602. https://doi.org/10.1016/S0021-9258(18)69108-2.

Baracchini, E., and H. Bremer. 1991. 'Control of RRNA Synthesis in Escherichia Coli at Increased Rrn Gene Dosage. Role of Guanosine Tetraphosphate and Ribosome Feedback'. *Journal of Biological Chemistry* 266 (18): 11753–60. https://doi.org/10.1016/S0021-9258(18)99021-6.

References

Barns, S M, R E Fundyga, M W Jeffries, and N R Pace. 1994. 'Remarkable Archaeal Diversity Detected in a Yellowstone National Park Hot Spring Environment.' *Proceedings of the National Academy of Sciences* 91 (5): 1609–13. https://doi.org/10.1073/pnas.91.5.1609.

Baßler, Jochen, and Ed Hurt. 2019. 'Eukaryotic Ribosome Assembly'. *Annual Review of Biochemistry* 88 (1): 281–306. https://doi.org/10.1146/annurev-biochem-013118-110817.

Baum, David A., and Buzz Baum. 2014. 'An Inside-out Origin for the Eukaryotic Cell'. *BMC Biology* 12 (1): 76. https://doi.org/10.1186/s12915-014-0076-2.

Beauclerk, A. A., H. Hummel, D. J. Holmes, A. Böck, and E. Cundliffe. 1985. 'Studies of the GTPase Domain of Archaebacterial Ribosomes'. *European Journal of Biochemistry* 151 (2): 245–55. https://doi.org/10.1111/j.1432-1033.1985.tb09095.x.

Beltrame, M., Y. Henry, and D. Tollervey. 1994. 'Mutational Analysis of an Essential Binding Site for the U3 SnoRNA in the 5' External Transcribed Spacer of Yeast Pre-RRNA'. *Nucleic Acids Research* 22 (23): 5139–47. https://doi.org/10.1093/nar/22.23.5139.

Beltrame, M., and D. Tollervey. 1992. 'Identification and Functional Analysis of Two U3 Binding Sites on Yeast Pre-Ribosomal RNA'. *The EMBO Journal* 11 (4): 1531–42. https://doi.org/10.1002/j.1460-2075.1992.tb05198.x.

Beltrame, M, and D Tollervey. 1995. 'Base Pairing between U3 and the Pre-Ribosomal RNA Is Required for 18S RRNA Synthesis.' *The EMBO Journal* 14 (17): 4350–56.

Ben-Shem, Adam, Nicolas Garreau de Loubresse, Sergey Melnikov, Lasse Jenner, Gulnara Yusupova, and Marat Yusupov. 2011. 'The Structure of the Eukaryotic Ribosome at 3.0 Å Resolution'. *Science (New York, N.Y.)* 334 (6062): 1524–29. https://doi.org/10.1126/science.1212642.

Berg, Karen L., Craig Squires, and Catherine L. Squires. 1989. 'Ribosomal RNA Operon Anti-Termination: Function of Leader and Spacer Region Box B-Box A Sequences and Their Conservation in Diverse Micro-Organisms'. *Journal of Molecular Biology* 209 (3): 345–58. https://doi.org/10.1016/0022-2836(89)90002-8.

Bernier, Chad R, Anton S Petrov, Nicholas A Kovacs, Petar I Penev, and Loren Dean Williams. 2018. 'Translation: The Universal Structural Core of Life'. *Molecular Biology and Evolution* 35 (8): 2065–76. https://doi.org/10.1093/molbev/msy101.

Bertrand, Edouard, Felicia Houser-Scott, Ann Kendall, Robert H. Singer, and David R. Engelke. 1998. 'Nucleolar Localization of Early TRNA Processing'. *Genes & Development* 12 (16): 2463–68.

Besançon, Willi, and Rolf Wagner. 1999. 'Characterization of Transient RNA-RNA Interactions Important for the Facilitated Structure Formation of Bacterial Ribosomal 16S RNA'. *Nucleic Acids Research* 27 (22): 4353–62. https://doi.org/10.1093/nar/27.22.4353.

Birikmen, Mehmet, Katherine E. Bohnsack, Vinh Tran, Sharvari Somayaji, Markus T. Bohnsack, and Ingo Ebersberger. 2021. 'Tracing Eukaryotic Ribosome Biogenesis Factors Into the Archaeal Domain Sheds Light on the Evolution of Functional Complexity'. *Frontiers in Microbiology* 12. https://www.frontiersin.org/articles/10.3389/fmicb.2021.739000.

Birkedal, Ulf, Bertrand Beckert, Daniel N. Wilson, and Henrik Nielsen. 2020. 'The 23S Ribosomal RNA From Pyrococcus Furiosus Is Circularly Permuted'. *Frontiers in Microbiology* 11. https://www.frontiersin.org/articles/10.3389/fmicb.2020.582022.

Bisson-Filho, Alexandre W., Jenny Zheng, and Ethan Garner. 2018. 'Archaeal Imaging: Leading the Hunt for New Discoveries'. *Molecular Biology of the Cell* 29 (14): 1675–81. https://doi.org/10.1091/mbc.E17-10-0603.

Blaha, Gregor, and Pavel Ivanov. 2004. 'Structure of the Ribosome'. In *Protein Synthesis and Ribosome Structure*, 53–84. John Wiley & Sons, Ltd. https://doi.org/10.1002/3527603433.ch2.

Blaha, Gregor M., and Joseph T. Wade. 2022. 'Transcription-Translation Coupling in Bacteria'. *Annual Review of Genetics* 56 (1): 187–205. https://doi.org/10.1146/annurev-genet-072220-033342.

Bohnsack, Katherine E., Anthony K. Henras, Henrik Nielsen, and Markus T. Bohnsack. 2023. 'Making Ends Meet: A Universal Driver of Large Ribosomal Subunit Biogenesis'. *Trends in Biochemical Sciences* 48 (3): 213–15. https://doi.org/10.1016/j.tibs.2022.09.003.

Boisvert, François-Michel, Silvana van Koningsbruggen, Joaquín Navascués, and Angus I. Lamond. 2007. 'The Multifunctional Nucleolus'. *Nature Reviews Molecular Cell Biology* 8 (7): 574–85. https://doi.org/10.1038/nrm2184.

Borgnia, Mario J., Sriram Subramaniam, and Jacqueline L. S. Milne. 2008. 'Three-Dimensional Imaging of the Highly Bent Architecture of Bdellovibrio Bacteriovorus by Using Cryo-Electron Tomography'. *Journal of Bacteriology* 190 (7): 2588–96. https://doi.org/10.1128/JB.01538-07.

References

Bowman, Jessica C., Anton S. Petrov, Moran Frenkel-Pinter, Petar I. Penev, and Loren Dean Williams. 2020. 'Root of the Tree: The Significance, Evolution, and Origins of the Ribosome'. *Chemical Reviews*, May. https://doi.org/10.1021/acs.chemrev.9b00742.

Bremer, H., and P. Dennis. 2008. 'Feedback Control of Ribosome Function in Escherichia Coli'. *Biochimie* 90 (3): 493–99. https://doi.org/10.1016/j.biochi.2007.10.008.

Brendel, Jutta, Britta Stoll, Sita J. Lange, Kundan Sharma, Christof Lenz, Aris-Edda Stachler, Lisa-Katharina Maier, et al. 2014. 'A Complex of Cas Proteins 5, 6, and 7 Is Required for the Biogenesis and Stability of Clustered Regularly Interspaced Short Palindromic Repeats (CRISPR)-Derived RNAs (CrRNAs) in Haloferax Volcanii*'. *Journal of Biological Chemistry* 289 (10): 7164–77. https://doi.org/10.1074/jbc.M113.508184.

Breuer, Ruth, Jose-Vicente Gomes-Filho, and Lennart Randau. 2021. 'Conservation of Archaeal C/D Box SRNA-Guided RNA Modifications'. *Frontiers in Microbiology* 12. https://www.frontiersin.org/articles/10.3389/fmicb.2021.654029.

Brewer, Tess E., Mads Albertsen, Arwyn Edwards, Rasmus H. Kirkegaard, Eduardo P. C. Rocha, and Noah Fierer. 2020. 'Unlinked RRNA Genes Are Widespread among Bacteria and Archaea'. *The ISME Journal* 14 (2): 597–608. https://doi.org/10.1038/s41396-019-0552-3.

Britton, Robert A., Tingyi Wen, Laura Schaefer, Olivier Pellegrini, William C. Uicker, Nathalie Mathy, Crystal Tobin, Roula Daou, Jacek Szyk, and Ciarán Condon. 2007. 'Maturation of the 5′ End of Bacillus Subtilis 16S RRNA by the Essential Ribonuclease YkqC/RNase J1'. *Molecular Microbiology* 63 (1): 127–38. https://doi.org/10.1111/j.1365-2958.2006.05499.x.

Brown, James W., Charles J. Daniels, John N. Reeve, and Jordan Konisky. 1989. 'Gene Structure, Organization, And Expression In Archaebacteria'. *CRC Critical Reviews in Microbiology* 16 (4): 287–337. https://doi.org/10.3109/10408418909105479.

Bubunenko, Mikhail, Donald L. Court, Abdalla Al Refaii, Shivalika Saxena, Alexey Korepanov, David I. Friedman, Max E. Gottesman, and Jean-Hervé Alix. 2013. 'Nus Transcription Elongation Factors and RNase III Modulate Small Ribosome Subunit Biogenesis in Escherichia Coli'. *Molecular Microbiology* 87 (2): 382–93. https://doi.org/10.1111/mmi.12105.

Bubunenko, Mikhail, Alexey Korepanov, Donald L. Court, Indu Jagannathan, Daniel Dickinson, Biswajoy Roy Chaudhuri, Maria B. Garber, and Gloria M. Culver. 2006. '30S Ribosomal Subunits Can Be Assembled in Vivo without Primary Binding Ribosomal Protein S15'. *RNA* 12 (7): 1229–39. https://doi.org/10.1261/rna.2262106.

Bunner, Anne E., Stefan Nord, P. Mikael Wikström, and James R. Williamson. 2010. 'The Effect of Ribosome Assembly Cofactors on In Vitro 30S Subunit Reconstitution'. *Journal of Molecular Biology* 398 (1): 1–7. https://doi.org/10.1016/j.jmb.2010.02.036.

Burman, Luke G., and Vincent P. Mauro. 2012. 'Analysis of RRNA Processing and Translation in Mammalian Cells Using a Synthetic 18S RRNA Expression System'. *Nucleic Acids Research* 40 (16): 8085–98. https://doi.org/10.1093/nar/gks530.

Cabrera, Julio E., Cedric Cagliero, Selwyn Quan, Catherine L. Squires, and Ding Jun Jin. 2009. 'Active Transcription of RRNA Operons Condenses the Nucleoid in Escherichia Coli: Examining the Effect of Transcription on Nucleoid Structure in the Absence of Transertion'. *Journal of Bacteriology* 191 (13): 4180–85. https://doi.org/10.1128/JB.01707-08.

Cabrera, Julio E., and Ding J. Jin. 2003. 'The Distribution of RNA Polymerase in Escherichia Coli Is Dynamic and Sensitive to Environmental Cues'. *Molecular Microbiology* 50 (5): 1493–1505. https://doi.org/10.1046/j.1365-2958.2003.03805.x.

———. 2006. 'Active Transcription of RRNA Operons Is a Driving Force for the Distribution of RNA Polymerase in Bacteria: Effect of Extrachromosomal Copies of RrnB on the in Vivo Localization of RNA Polymerase'. *Journal of Bacteriology* 188 (11): 4007–14. https://doi.org/10.1128/JB.01893-05.

Caforio, Antonella, Melvin F. Siliakus, Marten Exterkate, Samta Jain, Varsha R. Jumde, Ruben L. H. Andringa, Servé W. M. Kengen, Adriaan J. Minnaard, Arnold J. M. Driessen, and John van der Oost. 2018. 'Converting Escherichia Coli into an Archaebacterium with a Hybrid Heterochiral Membrane'. *Proceedings of the National Academy of Sciences* 115 (14): 3704–9. https://doi.org/10.1073/pnas.1721604115.

Callaghan, Anastasia J, Jukka P Aurikko, Leopold L Ilag, J Günter Grossmann, Vidya Chandran, Karin Kühnel, Leonora Poljak, et al. 2004. 'Studies of the RNA Degradosome-Organizing Domain of the Escherichia Coli Ribonuclease RNase E'. *Journal of Molecular Biology* 340 (5): 965–79. https://doi.org/10.1016/j.jmb.2004.05.046.

Callaghan, Anastasia J., Maria Jose Marcaida, Jonathan A. Stead, Kenneth J. McDowall, William G. Scott, and Ben F. Luisi. 2005. 'Structure of Escherichia Coli RNase E Catalytic Domain and Implications for RNA Turnover'. *Nature* 437 (7062): 1187–91. https://doi.org/10.1038/nature04084.

References

Carpousis, Agamemnon J. 2007. 'The RNA Degradosome of Escherichia Coli: An MRNA-Degrading Machine Assembled on RNase E'. *Annual Review of Microbiology* 61 (1): 71–87. https://doi.org/10.1146/annurev.micro.61.080706.093440.

Carpousis, Agamemnon J., Ben F. Luisi, and Kenneth J. McDowall. 2009. 'Endonucleolytic Initiation of MRNA Decay in Escherichia Coli'. *Progress in Molecular Biology and Translational Science* 85: 91–135. https://doi.org/10.1016/S0079-6603(08)00803-9.

Cashel, M., D. R. Gentry, V. J. Hernandez, and D. Vinella. 1996. 'The Stringent Response'. In *Escherichia Coli and Salmonella: Cellular and Molecular Biology*, 2nd edition. Washington, D.C: ASM Press.

Castellana, Michele, Sophia Hsin-Jung Li, and Ned S. Wingreen. 2016. 'Spatial Organization of Bacterial Transcription and Translation'. *Proceedings of the National Academy of Sciences* 113 (33): 9286–91. https://doi.org/10.1073/pnas.1604995113.

Castelle, Cindy J., and Jillian F. Banfield. 2018. 'Major New Microbial Groups Expand Diversity and Alter Our Understanding of the Tree of Life'. *Cell* 172 (6): 1181–97. https://doi.org/10.1016/j.cell.2018.02.016.

Cellini, Andrea, Gian Luca Scoarughi, Paola Poggiali, Iolanda Santino, Rosa Sessa, Pierluigi Donini, and Carmen Cimmino. 2004. 'Stringent Control in the Archaeal Genus Sulfolobus'. *Research in Microbiology* 155 (2): 98–104. https://doi.org/10.1016/j.resmic.2003.11.006.

Chai, Qian, Bhupender Singh, Kristin Peisker, Nicole Metzendorf, Xueliang Ge, Santanu Dasgupta, and Suparna Sanyal. 2014. 'Organization of Ribosomes and Nucleoids in Escherichia Coli Cells during Growth and in Quiescence *'. *Journal of Biological Chemistry* 289 (16): 11342–52. https://doi.org/10.1074/jbc.M114.557348.

Chant, J., and P. Dennis. 1986. 'Archaebacteria: Transcription and Processing of Ribosomal RNA Sequences in Halobacterium Cutirubrum'. *The EMBO Journal* 5 (5): 1091–97. https://doi.org/10.1002/j.1460-2075.1986.tb04327.x.

Chant, John, Ivy Hui, Deidre De Jong-Wong, Lawrence Shimmin, and Patrick P. Dennis. 1986. 'The Protein Synthesizing Machinery of the Archaebacterium Halobacterium Cutirubrum: Molecular Characterization'. *Systematic and Applied Microbiology* 7 (1): 106–14. https://doi.org/10.1016/S0723-2020(86)80132-1.

Chen, Robert, Sean K. Wang, Julia A. Belk, Laura Amaya, Zhijian Li, Angel Cardenas, Brian T. Abe, Chun-Kan Chen, Paul A. Wender, and Howard Y. Chang. 2022. 'Engineering Circular RNA for Enhanced Protein Production'. *Nature Biotechnology*, July, 1–11. https://doi.org/10.1038/s41587-022-01393-0.

Chen, Wu, Zhensheng Xie, Fuquan Yang, and Keqiong Ye. 2017. 'Stepwise Assembly of the Earliest Precursors of Large Ribosomal Subunits in Yeast'. *Nucleic Acids Research* 45 (11): 6837–47. https://doi.org/10.1093/nar/gkx254.

Cheng, Jingdong, Giuseppe La Venuta, Benjamin Lau, Otto Berninghausen, Roland Beckmann, and Ed Hurt. 2022. 'In Vitro Structural Maturation of an Early Stage Pre-40S Particle Coupled with U3 SnoRNA Release and Central Pseudoknot Formation'. *Nucleic Acids Research* 50 (20): 11916–23. https://doi.org/10.1093/nar/gkac910.

Ciganda, Martin, and Noreen Williams. 2011. 'Eukaryotic 5S RRNA Biogenesis'. *Wiley Interdisciplinary Reviews. RNA* 2 (4): 523–33. https://doi.org/10.1002/wrna.74.

Cimmino, C., G. L. Scoarughi, and P. Donini. 1993. 'Stringency and Relaxation among the Halobacteria'. *Journal of Bacteriology* 175 (20): 6659–62. https://doi.org/10.1128/jb.175.20.6659-6662.1993.

Clouet-d'Orval, Béatrice, Manon Batista, Marie Bouvier, Yves Quentin, Gwennaele Fichant, Anita Marchfelder, and Lisa-Katharina Maier. 2018. 'Insights into RNA-Processing Pathways and Associated RNA-Degrading Enzymes in Archaea'. *FEMS Microbiology Reviews* 42 (5): 579–613. https://doi.org/10.1093/femsre/fuy016.

Cockram, Charlotte, Agnès Thierry, Aurore Gorlas, Roxane Lestini, and Romain Koszul. 2021. 'Euryarchaeal Genomes Are Folded into SMC-Dependent Loops and Domains, but Lack Transcription-Mediated Compartmentalization'. *Molecular Cell* 81 (3): 459-472.e10. https://doi.org/10.1016/j.molcel.2020.12.013.

Cole, J. R., and M. Nomura. 1986. 'Translational Regulation Is Responsible for Growth-Rate-Dependent and Stringent Control of the Synthesis of Ribosomal Proteins L11 and L1 in Escherichia Coli'. *Proceedings of the National Academy of Sciences of the United States of America* 83 (12): 4129–33. https://doi.org/10.1073/pnas.83.12.4129.

Cole, J. R., C. L. Olsson, J. W. Hershey, M. Grunberg-Manago, and M. Nomura. 1987. 'Feedback Regulation of RRNA Synthesis in Escherichia Coli. Requirement for Initiation Factor IF2'. *Journal of Molecular Biology* 198 (3): 383–92. https://doi.org/10.1016/0022-2836(87)90288-9.

Condon, C., S. French, C. Squires, and C. L. Squires. 1993. 'Depletion of Functional Ribosomal RNA Operons in Escherichia Coli Causes Increased Expression of the Remaining Intact Copies'. *The EMBO Journal* 12 (11): 4305–15. https://doi.org/10.1002/j.1460-2075.1993.tb06115.x.

References

Condon, C, D Liveris, C Squires, I Schwartz, and C L Squires. 1995. 'RRNA Operon Multiplicity in Escherichia Coli and the Physiological Implications of Rrn Inactivation.' *Journal of Bacteriology* 177 (14): 4152–56.

Copeland, Herbert Faulkner. 1956. *The Classification of Lower Organisms*. Palo Alto, Calif: Pacific Books. https://www.biodiversitylibrary.org/item/23393.

Cox, Cymon J., Peter G. Foster, Robert P. Hirt, Simon R. Harris, and T. Martin Embley. 2008. 'The Archaebacterial Origin of Eukaryotes'. *Proceedings of the National Academy of Sciences* 105 (51): 20356–61. https://doi.org/10.1073/pnas.0810647105.

Cremer, T., and C. Cremer. 2001. 'Chromosome Territories, Nuclear Architecture and Gene Regulation in Mammalian Cells'. *Nature Reviews Genetics* 2 (4): 292–301. https://doi.org/10.1038/35066075.

Crick, F. H. 1956. 'Ideas on Protein Synthesis (Oct. 1956)'. Wellcome Collection. 1956. https://wellcomecollection.org/works/xmscu3g4.

———. 1958. 'On Protein Synthesis'. *Symposia of the Society for Experimental Biology* 12: 138–63.

Cruz, Jesús de la, Katrin Karbstein, and John L. Woolford. 2015. 'Functions of Ribosomal Proteins in Assembly of Eukaryotic Ribosomes In Vivo'. *Annual Review of Biochemistry* 84 (1): 93–129. https://doi.org/10.1146/annurev-biochem-060614-033917.

Cunha, Violette Da, Morgan Gaia, Daniele Gadelle, Arshan Nasir, and Patrick Forterre. 2017. 'Lokiarchaea Are Close Relatives of Euryarchaeota, Not Bridging the Gap between Prokaryotes and Eukaryotes'. *PLOS Genetics* 13 (6): e1006810. https://doi.org/10.1371/journal.pgen.1006810.

Cunha, Violette Da, Morgan Gaia, Arshan Nasir, and Patrick Forterre. 2018. 'Asgard Archaea Do Not Close the Debate about the Universal Tree of Life Topology'. *PLOS Genetics* 14 (3): e1007215. https://doi.org/10.1371/journal.pgen.1007215.

Czekay, Dominic P., and Ute Kothe. 2021. 'H/ACA Small Ribonucleoproteins: Structural and Functional Comparison Between Archaea and Eukaryotes'. *Frontiers in Microbiology* 12. https://www.frontiersin.org/articles/10.3389/fmicb.2021.654370.

Da Cunha, Violette, Morgan Gaïa, and Patrick Forterre. 2022. 'The Expanding Asgard Archaea and Their Elusive Relationships with Eukarya'. *MLife* 1 (1): 3–12. https://doi.org/10.1002/mlf2.12012.

Dabbs, E. R. 1991. 'Mutants Lacking Individual Ribosomal Proteins as a Tool to Investigate Ribosomal Properties'. *Biochimie* 73 (6): 639–45. https://doi.org/10.1016/0300-9084(91)90043-Z.

Dammann, R., R. Lucchini, T. Koller, and J. M. Sogo. 1993. 'Chromatin Structures and Transcription of RDNA in Yeast Saccharomyces Cerevisiae'. *Nucleic Acids Research* 21 (10): 2331–38. https://doi.org/10.1093/nar/21.10.2331.

Dammel, C. S., and H. F. Noller. 1993. 'A Cold-Sensitive Mutation in 16S RRNA Provides Evidence for Helical Switching in Ribosome Assembly.' *Genes & Development* 7 (4): 660–70. https://doi.org/10.1101/gad.7.4.660.

Danan, Miri, Schraga Schwartz, Sarit Edelheit, and Rotem Sorek. 2012. 'Transcriptome-Wide Discovery of Circular RNAs in Archaea'. *Nucleic Acids Research* 40 (7): 3131–42. https://doi.org/10.1093/nar/gkr1009.

Darzacq, Xavier, Beáta E. Jády, Céline Verheggen, Arnold M. Kiss, Edouard Bertrand, and Tamás Kiss. 2002. 'Cajal Body-Specific Small Nuclear RNAs: A Novel Class of 2′-O-Methylation and Pseudouridylation Guide RNAs'. *The EMBO Journal* 21 (11): 2746–56. https://doi.org/10.1093/emboj/21.11.2746.

Datta, Partha P., Daniel N. Wilson, Masahito Kawazoe, Neil K. Swami, Tatsuya Kaminishi, Manjuli R. Sharma, Timothy M. Booth, et al. 2007. 'Structural Aspects of RbfA Action during Small Ribosomal Subunit Assembly'. *Molecular Cell* 28 (3): 434–45. https://doi.org/10.1016/j.molcel.2007.08.026.

Davies, Bryan W., Caroline Köhrer, Asha I. Jacob, Lyle A. Simmons, Jianyu Zhu, Lourdes M. Aleman, Uttam L. RajBhandary, and Graham C. Walker. 2010. 'Role of Escherichia Coli YbeY, a Highly Conserved Protein, in RRNA Processing'. *Molecular Microbiology* 78 (2): 506–18. https://doi.org/10.1111/j.1365-2958.2010.07351.x.

Davis, Joseph H., Yong Zi Tan, Bridget Carragher, Clinton S. Potter, Dmitry Lyumkis, and James R. Williamson. 2016. 'Modular Assembly of the Bacterial Large Ribosomal Subunit'. *Cell* 167 (6): 1610-1622.e15. https://doi.org/10.1016/j.cell.2016.11.020.

Davis, Joseph H., and James R. Williamson. 2017. 'Structure and Dynamics of Bacterial Ribosome Biogenesis'. *Philosophical Transactions of the Royal Society B: Biological Sciences* 372 (1716): 20160181. https://doi.org/10.1098/rstb.2016.0181.

De Anda, Valerie, Lin-Xing Chen, Nina Dombrowski, Zheng-Shuang Hua, Hong-Chen Jiang, Jillian F. Banfield, Wen-Jun Li, and Brett J. Baker. 2021. 'Brockarchaeota, a Novel Archaeal Phylum with Unique and Versatile Carbon Cycling Pathways'. *Nature Communications* 12 (1): 2404. https://doi.org/10.1038/s41467-021-22736-6.

References

Delmas, Stéphane, Iain G. Duggin, and Thorsten Allers. 2013. 'DNA Damage Induces Nucleoid Compaction via the Mre11-Rad50 Complex in the Archaeon Haloferax Volcanii'. *Molecular Microbiology* 87 (1): 168–79. https://doi.org/10.1111/mmi.12091.

Dennis, P. P., A. G. Russell, and M. Moniz De Sá. 1997. 'Formation of the 5' End Pseudoknot in Small Subunit Ribosomal RNA: Involvement of U3-like Sequences'. *RNA (New York, N.Y.)* 3 (4): 337–43.

Dennis, P. P., S. Ziesche, and S. Mylvaganam. 1998. 'Transcription Analysis of Two Disparate RRNA Operons in the Halophilic Archaeon Haloarcula Marismortui'. *Journal of Bacteriology* 180 (18): 4804–13. https://doi.org/10.1128/JB.180.18.4804-4813.1998.

Dennis, Patrick P., and Masayasu Nomura. 1974. 'Stringent Control of Ribosomal Protein Gene Expression in Escherichia Coli*'. *Proceedings of the National Academy of Sciences* 71 (10): 3819–23. https://doi.org/10.1073/pnas.71.10.3819.

Dennis, Patrick P., Vanessa Tripp, Lauren Lui, Todd Lowe, and Lennart Randau. 2015. 'C/D Box SRNA-Guided 2′-O-Methylation Patterns of Archaeal RRNA Molecules'. *BMC Genomics* 16 (1): 632. https://doi.org/10.1186/s12864-015-1839-z.

Deutscher, Murray P. 2009. 'Chapter 9 Maturation and Degradation of Ribosomal RNA in Bacteria'. In *Progress in Molecular Biology and Translational Science*, 85:369–91. Molecular Biology of RNA Processing and Decay in Prokaryotes. Academic Press. https://doi.org/10.1016/S0079-6603(08)00809-X.

———. 2015. 'Twenty Years of Bacterial RNases and RNA Processing: How We've Matured'. *RNA* 21 (4): 597–600. https://doi.org/10.1261/rna.049692.115.

Dez, Christophe, Carine Froment, Jacqueline Noaillac-Depeyre, Bernard Monsarrat, Michèle Caizergues-Ferrer, and Yves Henry. 2004. 'Npa1p, a Component of Very Early Pre-60S Ribosomal Particles, Associates with a Subset of Small Nucleolar RNPs Required for Peptidyl Transferase Center Modification'. *Molecular and Cellular Biology* 24 (14): 6324–37. https://doi.org/10.1128/MCB.24.14.6324-6337.2004.

Dez, Christophe, Jonathan Houseley, and David Tollervey. 2006. 'Surveillance of Nuclear-Restricted Pre-Ribosomes within a Subnucleolar Region of Saccharomyces Cerevisiae'. *The EMBO Journal* 25 (7): 1534–46. https://doi.org/10.1038/sj.emboj.7601035.

Ding, Jiun-Yan, Pei-Wen Chiang, Mei-Jhu Hong, Mike Dyall-Smith, and Sen-Lin Tang. 2014. 'Complete Genome Sequence of the Extremely Halophilic Archaeon Haloarcula Hispanica Strain N601'. *Genome Announcements* 2 (2): e00178-14. https://doi.org/10.1128/genomeA.00178-14.

DiRuggiero, J., L. A. Achenbach, S. H. Brown, R. M. Kelly, and F. T. Robb. 1993. 'Regulation of Ribosomal RNA Transcription by Growth Rate of the Hyperthermophilic Archaeon, Pyrococcus Furiosus'. *FEMS Microbiology Letters* 111 (2–3): 159–64. https://doi.org/10.1111/j.1574-6968.1993.tb06379.x.

Dombrowski, Nina, Jun-Hoe Lee, Tom A Williams, Pierre Offre, and Anja Spang. 2019. 'Genomic Diversity, Lifestyles and Evolutionary Origins of DPANN Archaea'. *FEMS Microbiology Letters* 366 (2): fnz008. https://doi.org/10.1093/femsle/fnz008.

Dombrowski, Nina, Tom A. Williams, Jiarui Sun, Benjamin J. Woodcroft, Jun-Hoe Lee, Bui Quang Minh, Christian Rinke, and Anja Spang. 2020. 'Undinarchaeota Illuminate DPANN Phylogeny and the Impact of Gene Transfer on Archaeal Evolution'. *Nature Communications* 11 (1): 3939. https://doi.org/10.1038/s41467-020-17408-w.

Durovic, Peter, and Patrick P. Dennis. 1994. 'Separate Pathways for Excision and Processing of 16S and 23S RRNA from the Primary RRNA Operon Transcript from the Hyperthermophilic Archaebacterium Sulfolobus Acldocaldarius: Similarities to Eukaryotic RRNA Processing'. *Molecular Microbiology* 13 (2): 229–42. https://doi.org/10.1111/j.1365-2958.1994.tb00418.x.

Duss, Olivier, Galina A Stepanyuk, Joseph D Puglisi, and James R Williamson. 2019. 'Transient Protein-RNA Interactions Guide Nascent Ribosomal RNA Folding'. *Cell* 179 (6): 1357-1369.e16. https://doi.org/10.1016/j.cell.2019.10.035.

Dutca, Laura M., Jennifer E. G. Gallagher, and Susan J. Baserga. 2011. 'The Initial U3 SnoRNA:Pre-RRNA Base Pairing Interaction Required for Pre-18S RRNA Folding Revealed by in Vivo Chemical Probing'. *Nucleic Acids Research* 39 (12): 5164–80. https://doi.org/10.1093/nar/gkr044.

Dworsky, P., and M. Schaechter. 1973. 'Effect of Rifampin on the Structure and Membrane Attachment of the Nucleoid of Escherichia Coli'. *Journal of Bacteriology* 116 (3): 1364–74.

Ebersberger, Ingo, Stefan Simm, Matthias S. Leisegang, Peter Schmitzberger, Oliver Mirus, Arndt von Haeseler, Markus T. Bohnsack, and Enrico Schleiff. 2014. 'The Evolution of the Ribosome Biogenesis Pathway from a Yeast Perspective'. *Nucleic Acids Research* 42 (3): 1509–23. https://doi.org/10.1093/nar/gkt1137.

Eckert, Iris, and Zasha Weinberg. 2020. 'Discovery of 20 Novel Ribosomal Leader Candidates in Bacteria and Archaea'. *BMC Microbiology* 20 (1): 130. https://doi.org/10.1186/s12866-020-01823-6.

References

Edlind, T D, and P R Chakraborty. 1987. 'Unusual Ribosomal RNA of the Intestinal Parasite Giardia Lamblia.' *Nucleic Acids Research* 15 (19): 7889–7901.

Elela, Sherif Abou, Haller Igel, and Manuel Ares. 1996. 'RNase III Cleaves Eukaryotic Preribosomal RNA at a U3 SnoRNP-Dependent Site'. *Cell* 85 (1): 115–24. https://doi.org/10.1016/S0092-8674(00)81087-9.

Emma Sanchez, M., Paola Londei, and Ricardo Amils. 1996. 'Total Reconstitution of Active Small Ribosomal Subunits of the Extreme Halophilic Archaeon Haloferax Mediterranei'. *Biochimica et Biophysica Acta (BBA) - Protein Structure and Molecular Enzymology* 1292 (1): 140–44. https://doi.org/10.1016/0167-4838(95)00179-4.

Englert, Markus, Kelly Sheppard, Aaron Aslanian, John R. Yates, and Dieter Söll. 2011. 'Archaeal 3'-Phosphate RNA Splicing Ligase Characterization Identifies the Missing Component in TRNA Maturation'. *Proceedings of the National Academy of Sciences of the United States of America* 108 (4): 1290–95. https://doi.org/10.1073/pnas.1018307108.

Escobar-Zepeda, Alejandra, Arturo Vera-Ponce de León, and Alejandro Sanchez-Flores. 2015. 'The Road to Metagenomics: From Microbiology to DNA Sequencing Technologies and Bioinformatics'. *Frontiers in Genetics* 6. https://www.frontiersin.org/articles/10.3389/fgene.2015.00348.

Ettema, Thijs J. G., Ann-Christin Lindås, and Rolf Bernander. 2011. 'An Actin-Based Cytoskeleton in Archaea'. *Molecular Microbiology* 80 (4): 1052–61. https://doi.org/10.1111/j.1365-2958.2011.07635.x.

Fallon, A. M., C. S. Jinks, G. D. Strycharz, and M. Nomura. 1979. 'Regulation of Ribosomal Protein Synthesis in Escherichia Coli by Selective MRNA Inactivation'. *Proceedings of the National Academy of Sciences of the United States of America* 76 (7): 3411–15. https://doi.org/10.1073/pnas.76.7.3411.

Fan, Jun, Hafez El Sayyed, Oliver J. Pambos, Mathew Stracy, Jingwen Kyropoulos, and Achillefs N. Kapanidis. 2022. 'RNA Polymerase Redistribution and Increased Gene Dosage Support Growth in E. Coli Strains with a Minimal Number of Ribosomal RNA Operons'. bioRxiv. https://doi.org/10.1101/2022.02.10.479894.

Fatica, Alessandro, Marlene Oeffinger, Mensur Dlakić, and David Tollervey. 2003. 'Nob1p Is Required for Cleavage of the 3′ End of 18S RRNA'. *Molecular and Cellular Biology* 23 (5): 1798–1807. https://doi.org/10.1128/MCB.23.5.1798-1807.2003.

Feagin, Jean E., Maria Isabel Harrell, Jung C. Lee, Kevin J. Coe, Bryan H. Sands, Jamie J. Cannone, Germaine Tami, Murray N. Schnare, and Robin R. Gutell. 2012. 'The Fragmented Mitochondrial Ribosomal RNAs of Plasmodium Falciparum'. *PLOS ONE* 7 (6): e38320. https://doi.org/10.1371/journal.pone.0038320.

Feng, Yutian, Uri Neri, Sean Gosselin, Artemis S Louyakis, R Thane Papke, Uri Gophna, and Johann Peter Gogarten. 2021. 'The Evolutionary Origins of Extreme Halophilic Archaeal Lineages'. *Genome Biology and Evolution* 13 (8): evab166. https://doi.org/10.1093/gbe/evab166.

Fernández-Pevida, Antonio, Dieter Kressler, and Jesús de la Cruz. 2015. 'Processing of Preribosomal RNA in Saccharomyces Cerevisiae'. *WIREs RNA* 6 (2): 191–209. https://doi.org/10.1002/wrna.1267.

Ferreira-Cerca, Sébastien. 2017. 'Life and Death of Ribosomes in Archaea'. In *RNA Metabolism and Gene Expression in Archaea*, edited by Béatrice Clouet-d'Orval, 129–58. Nucleic Acids and Molecular Biology. Cham: Springer International Publishing. https://doi.org/10.1007/978-3-319-65795-0_6.

Ferreira-Cerca, Sébastien, Irene Kiburu, Emma Thomson, Nicole LaRonde, and Ed Hurt. 2014. 'Dominant Rio1 Kinase/ATPase Catalytic Mutant Induces Trapping of Late Pre-40S Biogenesis Factors in 80S-like Ribosomes'. *Nucleic Acids Research* 42 (13): 8635–47. https://doi.org/10.1093/nar/gku542.

Ferreira-Cerca, Sébastien, Gisela Pöll, Pierre-Emmanuel Gleizes, Herbert Tschochner, and Philipp Milkereit. 2005. 'Roles of Eukaryotic Ribosomal Proteins in Maturation and Transport of Pre-18S RRNA and Ribosome Function'. *Molecular Cell* 20 (2): 263–75. https://doi.org/10.1016/j.molcel.2005.09.005.

Ferreira-Cerca, Sébastien, Gisela Pöll, Holger Kühn, Andreas Neueder, Steffen Jakob, Herbert Tschochner, and Philipp Milkereit. 2007. 'Analysis of the In Vivo Assembly Pathway of Eukaryotic 40S Ribosomal Proteins'. *Molecular Cell* 28 (3): 446–57. https://doi.org/10.1016/j.molcel.2007.09.029.

Fiala, Gerhard, and Karl O. Stetter. 1986. 'Pyrococcus Furiosus Sp. Nov. Represents a Novel Genus of Marine Heterotrophic Archaebacteria Growing Optimally at 100°C'. *Archives of Microbiology* 145 (1): 56–61. https://doi.org/10.1007/BF00413027.

Foster, Peter G., Cymon J. Cox, and T. Martin Embley. 2009. 'The Primary Divisions of Life: A Phylogenomic Approach Employing Composition-Heterogeneous Methods'. *Philosophical Transactions of the Royal Society B: Biological Sciences* 364 (1527): 2197–2207. https://doi.org/10.1098/rstb.2009.0034.

Fox, George E., Linda J. Magrum, William E. Balch, Ralph S. Wolfe, and Carl R. Woese. 1977. 'Classification of Methanogenic Bacteria by 16S Ribosomal RNA Characterization'. *Proceedings of the National Academy of Sciences* 74 (10): 4537–41. https://doi.org/10.1073/pnas.74.10.4537.

Frank, Joachim. 2000. 'The Ribosome – a Macromolecular Machine Par Excellence'. *Chemistry & Biology* 7 (6): R133–41. https://doi.org/10.1016/S1074-5521(00)00127-7.

References

Franzetti, B, B Sohlberg, G Zaccai, and A von Gabain. 1997. 'Biochemical and Serological Evidence for an RNase E-like Activity in Halophilic Archaea'. *Journal of Bacteriology* 179 (4): 1180–85. https://doi.org/10.1128/jb.179.4.1180-1185.1997.

Fuchs, Georg, Thomas Eitinger, Johann Heider, Börries Kemper, and Erika Kothe. 2014. *Allgemeine Mikrobiologie*. 9th ed. Stuttgart: Thieme.

Gaal, T., and R. L. Gourse. 1990. 'Guanosine 3'-Diphosphate 5'-Diphosphate Is Not Required for Growth Rate-Dependent Control of RRNA Synthesis in Escherichia Coli'. *Proceedings of the National Academy of Sciences of the United States of America* 87 (14): 5533–37. https://doi.org/10.1073/pnas.87.14.5533.

Gaal, Tamas, Benjamin P. Bratton, Patricia Sanchez-Vazquez, Alexander Sliwicki, Kristine Sliwicki, Andrew Vegel, Rachel Pannu, and Richard L. Gourse. 2016. 'Colocalization of Distant Chromosomal Loci in Space in E. Coli: A Bacterial Nucleolus'. *Genes & Development* 30 (20): 2272–85. https://doi.org/10.1101/gad.290312.116.

Gamalinda, Michael, Uli Ohmayer, Jelena Jakovljevic, Beril Kumcuoglu, Joshua Woolford, Bertrade Mbom, Lawrence Lin, and John L. Woolford. 2014. 'A Hierarchical Model for Assembly of Eukaryotic 60S Ribosomal Subunit Domains'. *Genes & Development* 28 (2): 198–210. https://doi.org/10.1101/gad.228825.113.

Garrett, Roger. 1999. 'Mechanics of the Ribosome'. *Nature* 400 (6747): 811–12. https://doi.org/10.1038/23573.

Garrett, Roger A., Jacob Daigaard, Niels Larsen, Jorgen Kjems, and Alexander S. Mankin. 1991. 'Archaeal RRNA Operons'. *Trends in Biochemical Sciences* 16 (January): 22–26. https://doi.org/10.1016/0968-0004(91)90011-J.

Gitai, Zemer. 2005. 'The New Bacterial Cell Biology: Moving Parts and Subcellular Architecture'. *Cell* 120 (5): 577–86. https://doi.org/10.1016/j.cell.2005.02.026.

Goodfellow, Sarah J., and Joost C. B. M. Zomerdijk. 2012. 'Basic Mechanisms in RNA Polymerase I Transcription of the Ribosomal RNA Genes'. *Sub-Cellular Biochemistry* 61: 10.1007/978-94-007-4525-4_10. https://doi.org/10.1007/978-94-007-4525-4_10.

Gourse, R. L., H. A. de Boer, and M. Nomura. 1986. 'DNA Determinants of RRNA Synthesis in E. Coli: Growth Rate Dependent Regulation, Feedback Inhibition, Upstream Activation, Antitermination'. *Cell* 44 (1): 197–205. https://doi.org/10.1016/0092-8674(86)90498-8.

Gourse, R. L., and M. Nomura. 1984. 'Level of RRNA, Not TRNA, Synthesis Controls Transcription of RRNA and TRNA Operons in Escherichia Coli'. *Journal of Bacteriology* 160 (3): 1022–26. https://doi.org/10.1128/jb.160.3.1022-1026.1984.

Gourse, R. L., Y. Takebe, R. A. Sharrock, and M. Nomura. 1985. 'Feedback Regulation of RRNA and TRNA Synthesis and Accumulation of Free Ribosomes after Conditional Expression of RRNA Genes'. *Proceedings of the National Academy of Sciences of the United States of America* 82 (4): 1069–73. https://doi.org/10.1073/pnas.82.4.1069.

Gouy, Manolo, and Wen-Hsiung Li. 1989. 'Phylogenetic Analysis Based on RRNA Sequences Supports the Archaebacterial Rather than the Eocyte Tree'. *Nature* 339 (6220): 145–47. https://doi.org/10.1038/339145a0.

Granneman, Sander, Madhusudan R. Nandineni, and Susan J. Baserga. 2005. 'The Putative NTPase Fap7 Mediates Cytoplasmic 20S Pre-RRNA Processing through a Direct Interaction with Rps14'. *Molecular and Cellular Biology* 25 (23): 10352–64. https://doi.org/10.1128/MCB.25.23.10352-10364.2005.

Granneman, Sander, Elisabeth Petfalski, Agata Swiatkowska, and David Tollervey. 2010. 'Cracking Pre-40S Ribosomal Subunit Structure by Systematic Analyses of RNA–Protein Cross-Linking'. *The EMBO Journal* 29 (12): 2026–36. https://doi.org/10.1038/emboj.2010.86.

Grosjean, Henri, Christine Gaspin, Christian Marck, Wayne A. Decatur, and Valérie de Crécy-Lagard. 2008. 'RNomics and Modomics in the Halophilic Archaea Haloferax Volcanii: Identification of RNA Modification Genes'. *BMC Genomics* 9 (1): 470. https://doi.org/10.1186/1471-2164-9-470.

Grossmann, J. G., A. J. Callaghan, M. J. Marcaida, B. F. Luisi, F. H. Alcock, and K. Tokatlidis. 2008. 'Complementing Structural Information of Modular Proteins with Small Angle Neutron Scattering and Contrast Variation'. *European Biophysics Journal* 37 (5): 603–11. https://doi.org/10.1007/s00249-008-0278-z.

Gruber, Andreas R., Ronny Lorenz, Stephan H. Bernhart, Richard Neuböck, and Ivo L. Hofacker. 2008. 'The Vienna RNA Websuite'. *Nucleic Acids Research* 36 (suppl_2): W70–74. https://doi.org/10.1093/nar/gkn188.

Gruber-Vodicka, Harald R., Brandon K. B. Seah, and Elmar Pruesse. 2020. 'PhyloFlash: Rapid Small-Subunit RRNA Profiling and Targeted Assembly from Metagenomes'. *MSystems* 5 (5): e00920-20. https://doi.org/10.1128/mSystems.00920-20.

References

Grummt, Ingrid. 2010. 'Wisely Chosen Paths – Regulation of RRNA Synthesis'. *The FEBS Journal* 277 (22): 4626–39. https://doi.org/10.1111/j.1742-4658.2010.07892.x.

Grummt, Ingrid, and Craig S. Pikaard. 2003. 'Epigenetic Silencing of RNA Polymerase I Transcription'. *Nature Reviews Molecular Cell Biology* 4 (8): 641–49. https://doi.org/10.1038/nrm1171.

Grünberger, Felix, Sébastien Ferreira-Cerca, and Dina Grohmann. 2022. 'Nanopore Sequencing of RNA and CDNA Molecules in Escherichia Coli'. *RNA (New York, N.Y.)* 28 (3): 400–417. https://doi.org/10.1261/rna.078937.121.

Grünberger, Felix, Michael Jüttner, Robert Knüppel, Sébastien Ferreira-Cerca, and Dina Grohmann. 2022. 'Insights into RRNA Processing and Modification Mapping in Archaea Using Nanopore-Based RNA Sequencing'. bioRxiv. https://doi.org/10.1101/2021.06.14.448286.

Grünberger, Felix, Robert Knüppel, Michael Jüttner, Martin Fenk, Andreas Borst, Robert Reichelt, Winfried Hausner, Jörg Soppa, Sébastien Ferreira-Cerca, and Dina Grohmann. 2020. 'Exploring Prokaryotic Transcription, Operon Structures, RRNA Maturation and Modifications Using Nanopore-Based Native RNA Sequencing'. bioRxiv. https://doi.org/10.1101/2019.12.18.880849.

Gu, Wenyu, Albert L. Müller, Jörg S. Deutzmann, James R. Williamson, and Alfred M. Spormann. 2022. 'Growth Rate-Dependent Coordination of Catabolism and Anabolism in the Archaeon Methanococcus Maripaludis under Phosphate Limitation'. *The ISME Journal* 16 (10): 2313–19. https://doi.org/10.1038/s41396-022-01278-9.

Guo, Qiang, Yi Yuan, Yanji Xu, Boya Feng, Liang Liu, Kai Chen, Ming Sun, Zhixiu Yang, Jianlin Lei, and Ning Gao. 2011. 'Structural Basis for the Function of a Small GTPase RsgA on the 30S Ribosomal Subunit Maturation Revealed by Cryoelectron Microscopy'. *Proceedings of the National Academy of Sciences* 108 (32): 13100–105. https://doi.org/10.1073/pnas.1104645108.

Gupta, Neha, and Gloria M. Culver. 2014. 'Multiple in Vivo Pathways for Escherichia Coli Small Ribosomal Subunit Assembly Occur on One Pre-RRNA'. *Nature Structural & Molecular Biology* 21 (10): 937–43. https://doi.org/10.1038/nsmb.2887.

Guthrie, Christine, Hiroko Nashimoto, and Masayasu Nomura. 1969. 'STRUCTURE AND FUNCTION OF E. Coli RIBOSOMES, VIII. COLD-SENSITIVE MUTANTS DEFECTIVE IN RIBOSOME ASSEMBLY*'. *Proceedings of the National Academy of Sciences of the United States of America* 63 (2): 384–91.

Guy, Lionel, and Thijs J. G. Ettema. 2011. 'The Archaeal "TACK" Superphylum and the Origin of Eukaryotes'. *Trends in Microbiology* 19 (12): 580–87. https://doi.org/10.1016/j.tim.2011.09.002.

Guy, Lionel, Jimmy H. Saw, and Thijs J.G. Ettema. 2014. 'The Archaeal Legacy of Eukaryotes: A Phylogenomic Perspective'. *Cold Spring Harbor Perspectives in Biology* 6 (10): a016022. https://doi.org/10.1101/cshperspect.a016022.

Gyorfy, Zsuzsanna, Gabor Draskovits, Viktor Vernyik, Frederick F. Blattner, Tamas Gaal, and Gyorgy Posfai. 2015. 'Engineered Ribosomal RNA Operon Copy-Number Variants of E. Coli Reveal the Evolutionary Trade-Offs Shaping RRNA Operon Number'. *Nucleic Acids Research* 43 (3): 1783–94. https://doi.org/10.1093/nar/gkv040.

Haas, Karina. 2017. 'Untersuchung Des CRISPR-Cas-Systems Und Der RNase G/E in Archaeen'.

Hadjeras, Lydia, Marie Bouvier, Isabelle Canal, Leonora Poljak, Quentin Morin-Ogier, Carine Froment, Odile Burlet-Schlitz, et al. 2023. 'Attachment of the RNA Degradosome to the Bacterial Inner Cytoplasmic Membrane Prevents Wasteful Degradation of RRNA in Ribosome Assembly Intermediates'. *PLOS Biology* 21 (1): e3001942. https://doi.org/10.1371/journal.pbio.3001942.

Hadjiolov, Asen A. 1985. *The Nucleolus and Ribosome Biogenesis*. Vol. 12. Cell Biology Monographs. Vienna: Springer. https://doi.org/10.1007/978-3-7091-8742-5.

Hage, Aziz El, and David Tollervey. 2004. 'A Surfeit of Factors: Why Is Ribosome Assembly So Much More Complicated in Eukaryotes than Bacteria?' *RNA Biology* 1 (1): 9–14. https://doi.org/10.4161/rna.1.1.932.

Hamm, Joshua N., Susanne Erdmann, Emiley A. Eloe-Fadrosh, Allegra Angeloni, Ling Zhong, Christopher Brownlee, Timothy J. Williams, et al. 2019. 'Unexpected Host Dependency of Antarctic Nanohaloarchaeota'. *Proceedings of the National Academy of Sciences* 116 (29): 14661–70. https://doi.org/10.1073/pnas.1905179116.

Hamouche, Lina, Leonora Poljak, and Agamemnon J. Carpousis. 2021. 'Ribosomal RNA Degradation Induced by the Bacterial RNA Polymerase Inhibitor Rifampicin'. *RNA* 27 (8): 946–58. https://doi.org/10.1261/rna.078776.121.

Handelsman, J., M. R. Rondon, S. F. Brady, J. Clardy, and R. M. Goodman. 1998. 'Molecular Biological Access to the Chemistry of Unknown Soil Microbes: A New Frontier for Natural Products'. *Chemistry & Biology* 5 (10): R245-249. https://doi.org/10.1016/s1074-5521(98)90108-9.

References

Handelsman, Jo. 2004. ‘Metagenomics: Application of Genomics to Uncultured Microorganisms’. *Microbiology and Molecular Biology Reviews* 68 (4): 669–85. https://doi.org/10.1128/MMBR.68.4.669-685.2004.

Hartman, Amber L., Cédric Norais, Jonathan H. Badger, Stéphane Delmas, Sam Haldenby, Ramana Madupu, Jeffrey Robinson, et al. 2010. ‘The Complete Genome Sequence of Haloferax Volcanii DS2, a Model Archaeon’. *PLoS ONE* 5 (3): e9605. https://doi.org/10.1371/journal.pone.0009605.

Hartmann, Guido, Karl Otto Honikel, Fritz Knüsel, and Jakob Nüesch. 1967. ‘The Specific Inhibition of the DNA-Directed RNA Synthesis by Rifamycin’. *Biochimica et Biophysica Acta (BBA) - Nucleic Acids and Protein Synthesis* 145 (3): 843–44. https://doi.org/10.1016/0005-2787(67)90147-5.

Hartwell, Leland, Leroy Hood, Michael Goldberg, Ann E. Reynolds, and Lee Silver. 2010. *Genetics: From Genes to Genomes*. 4th edition. New York: McGraw-Hill Education.

Hasegawa, Masami, Naoyuko Iwabe, Yasuo Mukohata, and Takashi Miyata. 1990. ‘Close Evolutionary Relatedness of Archaebacteria, *Methanococcus* and *Halobacterium*, to Eukaryotes Demonstrated by Composite Phylogenetic Trees of Elongation Factors EF-Tu and EF-G: Eocyte Tree Is Unlikely’. *The Japanese Journal of Genetics* 65 (3): 109–14. https://doi.org/10.1266/jjg.65.109.

Hawkins, Michelle, Sunir Malla, Martin J. Blythe, Conrad A. Nieduszynski, and Thorsten Allers. 2013. ‘Accelerated Growth in the Absence of DNA Replication Origins’. *Nature* 503 (7477): 544–47. https://doi.org/10.1038/nature12650.

Hellmich, Ute A., Benjamin L. Weis, Anatoli Lioutikov, Jan Philip Wurm, Marco Kaiser, Nina A. Christ, Katharina Hantke, et al. 2013. ‘Essential Ribosome Assembly Factor Fap7 Regulates a Hierarchy of RNA-Protein Interactions during Small Ribosomal Subunit Biogenesis’. *Proceedings of the National Academy of Sciences of the United States of America* 110 (38): 15253–58. https://doi.org/10.1073/pnas.1306389110.

Henras, A. K., J. Soudet, M. Gérus, S. Lebaron, M. Caizergues-Ferrer, A. Mougin, and Y. Henry. 2008. ‘The Post-Transcriptional Steps of Eukaryotic Ribosome Biogenesis’. *Cellular and Molecular Life Sciences* 65 (15): 2334–59. https://doi.org/10.1007/s00018-008-8027-0.

Henras, Anthony K., Célia Plisson-Chastang, Marie-Françoise O’Donohue, Anirban Chakraborty, and Pierre-Emmanuel Gleizes. 2015. ‘An Overview of Pre-Ribosomal RNA Processing in Eukaryotes’. *WIREs RNA* 6 (2): 225–42. https://doi.org/10.1002/wrna.1269.

Hernandez, V. J., and H. Bremer. 1993. ‘Characterization of RNA and DNA Synthesis in Escherichia Coli Strains Devoid of PpGpp’. *The Journal of Biological Chemistry* 268 (15): 10851–62.

Herold, M, and K H Nierhaus. 1987. ‘Incorporation of Six Additional Proteins to Complete the Assembly Map of the 50 S Subunit from Escherichia Coli Ribosomes.’ *Journal of Biological Chemistry* 262 (18): 8826–33. https://doi.org/10.1016/S0021-9258(18)47489-3.

Hewlett, M J, R F Pettersson, and D Baltimore. 1977. ‘Circular Forms of Uukuniemi Virion RNA: An Electron Microscopic Study.’ *Journal of Virology* 21 (3): 1085–93.

Hiregange, Disha-Gajanan, Andre Rivalta, Tanaya Bose, Elinor Breiner-Goldstein, Sarit Samiya, Giuseppe Cimicata, Liudmila Kulakova, et al. 2022. ‘Cryo-EM Structure of the Ancient Eukaryotic Ribosome from the Human Parasite Giardia Lamblia’. *Nucleic Acids Research* 50 (3): 1770–82. https://doi.org/10.1093/nar/gkac046.

Holben, W E, and E A Morgan. 1984. ‘Antitermination of Transcription from an Escherichia Coli Ribosomal RNA Promoter.’ *Proceedings of the National Academy of Sciences* 81 (21): 6789–93. https://doi.org/10.1073/pnas.81.21.6789.

Holmes, Kristi L., and Gloria M. Culver. 2004. ‘Mapping Structural Differences between 30S Ribosomal Subunit Assembly Intermediates’. *Nature Structural & Molecular Biology* 11 (2): 179–86. https://doi.org/10.1038/nsmb719.

Hölzle, Annette, Susan Fischer, Ruth Heyer, Stefanie Schütz, Martin Zacharias, Paul Walther, Thorsten Allers, and Anita Marchfelder. 2008. ‘Maturation of the 5S RRNA 5′ End Is Catalyzed in Vitro by the Endonuclease TRNase Z in the Archaeon H. Volcanii’. *RNA* 14 (5): 928–37. https://doi.org/10.1261/rna.933208.

Hori, Yutaro, Christoph Engel, and Takehiko Kobayashi. 2023. ‘Regulation of Ribosomal RNA Gene Copy Number, Transcription and Nucleolus Organization in Eukaryotes’. *Nature Reviews Molecular Cell Biology*, February, 1–16. https://doi.org/10.1038/s41580-022-00573-9.

Hsu, M. T., and M. Coca-Prados. 1979. ‘Electron Microscopic Evidence for the Circular Form of RNA in the Cytoplasm of Eukaryotic Cells’. *Nature* 280 (5720): 339–40. https://doi.org/10.1038/280339a0.

Huber, Harald, Michael J. Hohn, Reinhard Rachel, Tanja Fuchs, Verena C. Wimmer, and Karl O. Stetter. 2002. ‘A New Phylum of Archaea Represented by a Nanosized Hyperthermophilic Symbiont’. *Nature* 417 (6884): 63–67. https://doi.org/10.1038/417063a.

References

Huet, J., R. Schnabel, A. Sentenac, and W. Zillig. 1983. 'Archaebacteria and Eukaryotes Possess DNA-Dependent RNA Polymerases of a Common Type'. *The EMBO Journal* 2 (8): 1291–94. https://doi.org/10.1002/j.1460-2075.1983.tb01583.x.

Hughes, J.m., and M. Ares Jr. 1991. 'Depletion of U3 Small Nucleolar RNA Inhibits Cleavage in the 5′ External Transcribed Spacer of Yeast Pre-Ribosomal RNA and Impairs Formation of 18S Ribosomal RNA.' *The EMBO Journal* 10 (13): 4231–39. https://doi.org/10.1002/j.1460-2075.1991.tb05001.x.

Hughes, John M. X. 1996. 'Functional Base-Pairing Interaction Between Highly Conserved Elements of U3 Small Nucleolar RNA and the Small Ribosomal Subunit RNA'. *Journal of Molecular Biology* 259 (4): 645–54. https://doi.org/10.1006/jmbi.1996.0346.

Hui, Monica P., Patricia L. Foley, and Joel G. Belasco. 2014. 'Messenger RNA Degradation in Bacterial Cells'. *Annual Review of Genetics* 48 (1): 537–59. https://doi.org/10.1146/annurev-genet-120213-092340.

Ide, Satoru, Takaaki Miyazaki, Hisaji Maki, and Takehiko Kobayashi. 2010. 'Abundance of Ribosomal RNA Gene Copies Maintains Genome Integrity'. *Science (New York, N.Y.)* 327 (5966): 693–96. https://doi.org/10.1126/science.1179044.

Iida, Tetsushi, and Takehiko Kobayashi. 2019a. 'RNA Polymerase I Activators Count and Adjust Ribosomal RNA Gene Copy Number'. *Molecular Cell* 73 (4): 645-654.e13. https://doi.org/10.1016/j.molcel.2018.11.029.

———. 2019b. 'How Do Cells Count Multi-Copy Genes?: "Musical Chair" Model for Preserving the Number of RDNA Copies'. *Current Genetics* 65 (4): 883–85. https://doi.org/10.1007/s00294-019-00956-0.

Ikeda, Yoshiki, Yasuhiro Okada, Asako Sato, Tamotsu Kanai, Masaru Tomita, Haruyuki Atomi, and Akio Kanai. 2017. 'An Archaeal RNA Binding Protein, FAU-1, Is a Novel Ribonuclease Related to RRNA Stability in Pyrococcus and Thermococcus'. *Scientific Reports* 7 (1): 12674. https://doi.org/10.1038/s41598-017-13062-3.

Imachi, Hiroyuki, Masaru K. Nobu, Nozomi Nakahara, Yuki Morono, Miyuki Ogawara, Yoshihiro Takaki, Yoshinori Takano, et al. 2020. 'Isolation of an Archaeon at the Prokaryote–Eukaryote Interface'. *Nature* 577 (7791): 519–25. https://doi.org/10.1038/s41586-019-1916-6.

Irastortza-Olaziregi, Mikel, and Orna Amster-Choder. 2021. 'Coupled Transcription-Translation in Prokaryotes: An Old Couple With New Surprises'. *Frontiers in Microbiology* 11. https://www.frontiersin.org/articles/10.3389/fmicb.2020.624830.

Irving, Sophie E., Naznin R. Choudhury, and Rebecca M. Corrigan. 2021. 'The Stringent Response and Physiological Roles of (Pp)PGpp in Bacteria'. *Nature Reviews Microbiology* 19 (4): 256–71. https://doi.org/10.1038/s41579-020-00470-y.

Iskakova, Madina, Sean R. Connell, and Knud H. Nierhaus. 2004. 'Regulation of Ribosome Biosynthesis in Escherichia Coli'. In *Protein Synthesis and Ribosome Structure*, 429–48. John Wiley & Sons, Ltd. https://doi.org/10.1002/3527603433.ch11.

Islas-Morales, Parsifal F., Anny Cárdenas, María J. Mosqueira, Luis Felipe Jiménez-García, and Christian R. Voolstra. 2023. 'Ultrastructural and Proteomic Evidence for the Presence of a Putative Nucleolus in an Archaeon'. *Frontiers in Microbiology* 14 (February). https://doi.org/10.3389/fmicb.2023.1075071.

Jaafar, Mariam, Julia Contreras, Carine Dominique, Sara Martín-Villanueva, Régine Capeyrou, Patrice Vitali, Olga Rodríguez-Galán, et al. 2021. 'Association of SnR190 SnoRNA Chaperone with Early Pre-60S Particles Is Regulated by the RNA Helicase Dbp7 in Yeast'. *Nature Communications* 12 (1): 6153. https://doi.org/10.1038/s41467-021-26207-w.

Jacob, Asha Ivy, Caroline Köhrer, Bryan William Davies, Uttam Lal RajBhandary, and Graham Charles Walker. 2013. 'Conserved Bacterial RNase YbeY Plays Key Roles in 70S Ribosome Quality Control and 16S RRNA Maturation'. *Molecular Cell* 49 (3): 427–38. https://doi.org/10.1016/j.molcel.2012.11.025.

Jeganathan, Ajitha, Aida Razi, Brett Thurlow, and Joaquin Ortega. 2015. 'The C-Terminal Helix in the YjeQ Zinc-Finger Domain Catalyzes the Release of RbfA during 30S Ribosome Subunit Assembly'. *RNA* 21 (6): 1203–16. https://doi.org/10.1261/rna.049171.114.

Jiang, Xunqing, and Joel G. Belasco. 2004. 'Catalytic Activation of Multimeric RNase E and RNase G by 5′-Monophosphorylated RNA'. *Proceedings of the National Academy of Sciences* 101 (25): 9211–16. https://doi.org/10.1073/pnas.0401382101.

Jinks-Robertson, Sue, Richard L. Gourse, and Masayasu Nomura. 1983. 'Expression of RRNA and TRNA Genes in Escherichia Coli: Evidence for Feedback Regulation by Products of RRNA Operons'. *Cell* 33 (3): 865–76. https://doi.org/10.1016/0092-8674(83)90029-6.

Joret, Clément, Régine Capeyrou, Kamila Belhabich-Baumas, Célia Plisson-Chastang, Rabea Ghandour, Odile Humbert, Sébastien Fribourg, et al. 2018. 'The Npa1p Complex Chaperones the Assembly of the Earliest Eukaryotic Large Ribosomal Subunit Precursor'. *PLoS Genetics* 14 (8): e1007597. https://doi.org/10.1371/journal.pgen.1007597.

References

Jourdan, Stefanie S., and Kenneth J. McDowall. 2008. 'Sensing of 5′ Monophosphate by Escherichia Coli RNase G Can Significantly Enhance Association with RNA and Stimulate the Decay of Functional MRNA Transcripts in Vivo'. *Molecular Microbiology* 67 (1): 102–15. https://doi.org/10.1111/j.1365-2958.2007.06028.x.

Jüttner, Michael. 2018. 'Function of Circular Pre-Ribosomal RNAs for Ribosome Biogenesis in Archaea'.

Jüttner, Michael, and Sébastien Ferreira-Cerca. 2022. 'Looking through the Lens of the Ribosome Biogenesis Evolutionary History: Possible Implications for Archaeal Phylogeny and Eukaryogenesis'. *Molecular Biology and Evolution* 39 (4): msac054. https://doi.org/10.1093/molbev/msac054.

Jüttner, Michael, Matthias Weiß, Nina Ostheimer, Corinna Reglin, Michael Kern, Robert Knüppel, and Sébastien Ferreira-Cerca. 2020. 'A Versatile Cis-Acting Element Reporter System to Study the Function, Maturation and Stability of Ribosomal RNA Mutants in Archaea'. *Nucleic Acids Research* 48 (4): 2073–90. https://doi.org/10.1093/nar/gkz1156.

Kaczanowska, Magdalena, and Monica Rydén-Aulin. 2007. 'Ribosome Biogenesis and the Translation Process in Escherichia Coli'. *Microbiology and Molecular Biology Reviews* 71 (3): 477–94. https://doi.org/10.1128/MMBR.00013-07.

Kandler, O. 1995. 'Cell Wall Biochemistry in Archaea and Its Phylogenetic Implications'. *Journal of Biological Physics* 20 (1): 165–69. https://doi.org/10.1007/BF00700433.

Kandler, Otto, and Hans Hippe. 1977. 'Lack of Peptidoglycan in the Cell Walls of Methanosarcina Barkeri'. *Archives of Microbiology* 113 (1): 57–60. https://doi.org/10.1007/BF00428580.

Karbstein, Katrin. 2011. 'Inside the 40S Ribosome Assembly Machinery'. *Current Opinion in Chemical Biology* 15 (5): 657–63. https://doi.org/10.1016/j.cbpa.2011.07.023.

Kater, Lukas, Valentin Mitterer, Matthias Thoms, Jingdong Cheng, Otto Berninghausen, Roland Beckmann, and Ed Hurt. 2020. 'Construction of the Central Protuberance and L1 Stalk during 60S Subunit Biogenesis'. *Molecular Cell* 79 (4): 615-628.e5. https://doi.org/10.1016/j.molcel.2020.06.032.

Kater, Lukas, Matthias Thoms, Clara Barrio-Garcia, Jingdong Cheng, Sherif Ismail, Yasar Luqman Ahmed, Gert Bange, et al. 2017. 'Visualizing the Assembly Pathway of Nucleolar Pre-60S Ribosomes'. *Cell* 171 (7): 1599-1610.e14. https://doi.org/10.1016/j.cell.2017.11.039.

Kern, Michael, and Sébastien Ferreira-Cerca. 2022. 'Differential Translation Activity Analysis Using Bioorthogonal Noncanonical Amino Acid Tagging (BONCAT) in Archaea'. *Methods in Molecular Biology (Clifton, N.J.)* 2533: 229–46. https://doi.org/10.1007/978-1-0716-2501-9_14.

Khemici, Vanessa, Leonora Poljak, Ben F. Luisi, and Agamemnon J. Carpousis. 2008. 'The RNase E of Escherichia Coli Is a Membrane-Binding Protein'. *Molecular Microbiology* 70 (4): 799–813. https://doi.org/10.1111/j.1365-2958.2008.06454.x.

Khoshnevis, Sohail, Xin Liu, Maria D. Dattolo, and Katrin Karbstein. 2019. 'Rrp5 Establishes a Checkpoint for 60S Assembly during 40S Maturation'. *RNA (New York, N.Y.)* 25 (9): 1164–76. https://doi.org/10.1261/rna.071225.119.

Kief, D. R., and J. R. Warner. 1981. 'Coordinate Control of Syntheses of Ribosomal Ribonucleic Acid and Ribosomal Proteins during Nutritional Shift-up in Saccharomyces Cerevisiae'. *Molecular and Cellular Biology* 1 (11): 1007–15. https://doi.org/10.1128/mcb.1.11.1007-1015.1981.

King, T C, and D Schlessinger. 1983. 'S1 Nuclease Mapping Analysis of Ribosomal RNA Processing in Wild Type and Processing Deficient Escherichia Coli.' *Journal of Biological Chemistry* 258 (19): 12034–42. https://doi.org/10.1016/S0021-9258(17)44336-5.

Kjems, J., and R. A. Garrett. 1990. 'Secondary Structural Elements Exclusive to the Sequences Flanking Ribosomal RNAs Lend Support to the Monophyletic Nature of the Archaebacteria'. *Journal of Molecular Evolution* 31 (1): 25–32. https://doi.org/10.1007/BF02101789.

Klappenbach, Joel A., John M. Dunbar, and Thomas M. Schmidt. 2000. 'RRNA Operon Copy Number Reflects Ecological Strategies of Bacteria'. *Applied and Environmental Microbiology* 66 (4): 1328–33. https://doi.org/10.1128/AEM.66.4.1328-1333.2000.

Klinge, Sebastian, and John L. Woolford. 2019. 'Ribosome Assembly Coming into Focus'. *Nature Reviews. Molecular Cell Biology* 20 (2): 116–31. https://doi.org/10.1038/s41580-018-0078-y.

Knüppel, Robert, Regitse H Christensen, Fiona C Gray, Dominik Esser, Daniela Strauß, Jan Medenbach, Bettina Siebers, Stuart A MacNeill, Nicole LaRonde, and Sébastien Ferreira-Cerca. 2018. 'Insights into the Evolutionary Conserved Regulation of Rio ATPase Activity'. *Nucleic Acids Research* 46 (3): 1441–56. https://doi.org/10.1093/nar/gkx1236.

Knüppel, Robert, Corinna Kuttenberger, and Sébastien Ferreira-Cerca. 2017. 'Toward Time-Resolved Analysis of RNA Metabolism in Archaea Using 4-Thiouracil'. *Frontiers in Microbiology* 8. https://www.frontiersin.org/articles/10.3389/fmicb.2017.00286.

References

Knüppel, Robert, Christian Trahan, Michael Kern, Alexander Wagner, Felix Grünberger, Winfried Hausner, Tessa E F Quax, Sonja-Verena Albers, Marlene Oeffinger, and Sébastien Ferreira-Cerca. 2021. 'Insights into Synthesis and Function of KsgA/Dim1-Dependent RRNA Modifications in Archaea'. *Nucleic Acids Research* 49 (3): 1662–87. https://doi.org/10.1093/nar/gkaa1268.

Kobayashi, Takehiko. 2011. 'Regulation of Ribosomal RNA Gene Copy Number and Its Role in Modulating Genome Integrity and Evolutionary Adaptability in Yeast'. *Cellular and Molecular Life Sciences* 68 (8): 1395–1403. https://doi.org/10.1007/s00018-010-0613-2.

Kobayashi, Takehiko, Denis J. Heck, Masayasu Nomura, and Takashi Horiuchi. 1998. 'Expansion and Contraction of Ribosomal DNA Repeats in Saccharomyces Cerevisiae: Requirement of Replication Fork Blocking (Fob1) Protein and the Role of RNA Polymerase I'. *Genes & Development* 12 (24): 3821–30.

Kolakofsky, Daniel. 1976. 'Isolation and Characterization of Sendai Virus DI-RNAs'. *Cell* 8 (4): 547–55. https://doi.org/10.1016/0092-8674(76)90223-3.

Kolter, Roberto. 2021. 'The History of Microbiology—A Personal Interpretation'. *Annual Review of Microbiology* 75 (1): 1–17. https://doi.org/10.1146/annurev-micro-033020-020648.

Könneke, Martin, Anne E. Bernhard, José R. de la Torre, Christopher B. Walker, John B. Waterbury, and David A. Stahl. 2005. 'Isolation of an Autotrophic Ammonia-Oxidizing Marine Archaeon'. *Nature* 437 (7058): 543–46. https://doi.org/10.1038/nature03911.

Koonin, Eugene V., and Natalya Yutin. 2014. 'The Dispersed Archaeal Eukaryome and the Complex Archaeal Ancestor of Eukaryotes'. *Cold Spring Harbor Perspectives in Biology* 6 (4): a016188. https://doi.org/10.1101/cshperspect.a016188.

Koslover, Daniel J., Anastasia J. Callaghan, Maria J. Marcaida, Elspeth F. Garman, Monika Martick, William G. Scott, and Ben F. Luisi. 2008. 'The Crystal Structure of the Escherichia Coli RNase E Apoprotein and a Mechanism for RNA Degradation'. *Structure(London, England:1993)* 16 (8–2): 1238–44. https://doi.org/10.1016/j.str.2008.04.017.

Krause, Susanne, Sabrina Gfrerer, Andriko von Kügelgen, Carsten Reuse, Nina Dombrowski, Laura Villanueva, Boyke Bunk, et al. 2022. 'The Importance of Biofilm Formation for Cultivation of a Micrarchaeon and Its Interactions with Its Thermoplasmatales Host'. *Nature Communications* 13 (1): 1735. https://doi.org/10.1038/s41467-022-29263-y.

Kressler, Dieter, Ed Hurt, and Jochen Baßler. 2017. 'A Puzzle of Life: Crafting Ribosomal Subunits'. *Trends in Biochemical Sciences*, Special Issue: Ribosomes & Translation, 42 (8): 640–54. https://doi.org/10.1016/j.tibs.2017.05.005.

Kressler, Dieter, Patrick Linder, and Jesús de la Cruz. 1999. 'Protein Trans-Acting Factors Involved in Ribosome Biogenesis in Saccharomyces Cerevisiae'. *Molecular and Cellular Biology* 19 (12): 7897–7912. https://doi.org/10.1128/MCB.19.12.7897.

Kristensen, Lasse S., Maria S. Andersen, Lotte V. W. Stagsted, Karoline K. Ebbesen, Thomas B. Hansen, and Jørgen Kjems. 2019. 'The Biogenesis, Biology and Characterization of Circular RNAs'. *Nature Reviews Genetics* 20 (11): 675–91. https://doi.org/10.1038/s41576-019-0158-7.

Kudla, Grzegorz, Sander Granneman, Daniela Hahn, Jean D. Beggs, and David Tollervey. 2011. 'Cross-Linking, Ligation, and Sequencing of Hybrids Reveals RNA–RNA Interactions in Yeast'. *Proceedings of the National Academy of Sciences* 108 (24): 10010–15. https://doi.org/10.1073/pnas.1017386108.

Kufel, J., B. Dichtl, and D. Tollervey. 1999. 'Yeast Rnt1p Is Required for Cleavage of the Pre-Ribosomal RNA in the 3' ETS but Not the 5' ETS.' *RNA* 5 (7): 909–17.

Kummer, Eva, and Nenad Ban. 2021. 'Mechanisms and Regulation of Protein Synthesis in Mitochondria'. *Nature Reviews Molecular Cell Biology* 22 (5): 307–25. https://doi.org/10.1038/s41580-021-00332-2.

Kutschera, U. 2016. 'Haeckel's 1866 Tree of Life and the Origin of Eukaryotes'. *Nature Microbiology* 1 (8): 1–1. https://doi.org/10.1038/nmicrobiol.2016.114.

Lafontaine, Denis, Jean Delcour, Anne-Lise Glasser, Jean Desgres, and Jean Vandenhaute. 1994. 'The DIM1 Gene Responsible for the Conserved M62Am62A Dimethylation in the 3′-Terminal Loop of 18 S RRNA Is Essential in Yeast'. *Journal of Molecular Biology* 241 (3): 492–97. https://doi.org/10.1006/jmbi.1994.1525.

Lafontaine, Denis L. J. 2010. 'A "Garbage Can" for Ribosomes: How Eukaryotes Degrade Their Ribosomes'. *Trends in Biochemical Sciences* 35 (5): 267–77. https://doi.org/10.1016/j.tibs.2009.12.006.

Lafontaine, Denis L. J., and David Tollervey. 2001. 'The Function and Synthesis of Ribosomes'. *Nature Reviews Molecular Cell Biology* 2 (7): 514–20. https://doi.org/10.1038/35080045.

Lake, James A. 1988. 'Origin of the Eukaryotic Nucleus Determined by Rate-Invariant Analysis of RRNA Sequences'. *Nature* 331 (6152): 184–86. https://doi.org/10.1038/331184a0.

References

Lake, James A., E Henderson, M Oakes, and M W Clark. 1984. 'Eocytes: A New Ribosome Structure Indicates a Kingdom with a Close Relationship to Eukaryotes.' *Proceedings of the National Academy of Sciences* 81 (12): 3786–90. https://doi.org/10.1073/pnas.81.12.3786.

Lamanna, Allison C., and Katrin Karbstein. 2009. 'Nob1 Binds the Single-Stranded Cleavage Site D at the 3′-End of 18S RRNA with Its PIN Domain'. *Proceedings of the National Academy of Sciences* 106 (34): 14259–64. https://doi.org/10.1073/pnas.0905403106.

LaRonde-LeBlanc, Nicole, and Alexander Wlodawer. 2005. 'The RIO Kinases: An Atypical Protein Kinase Family Required for Ribosome Biogenesis and Cell Cycle Progression'. *Biochimica et Biophysica Acta (BBA) - Proteins and Proteomics*, Inhibitors of Protein Kinases (4th International Conference, Inhibitors of Protein Kinases) and Associated Workshop: Modelling of Specific Molecular Recognition Processes (Warsaw, Poland, June 25-29, 2005), 1754 (1): 14–24. https://doi.org/10.1016/j.bbapap.2005.07.037.

Lebaron, Simon, Carine Froment, Micheline Fromont-Racine, Jean-Christophe Rain, Bernard Monsarrat, Michèle Caizergues-Ferrer, and Yves Henry. 2005. 'The Splicing ATPase Prp43p Is a Component of Multiple Preribosomal Particles'. *Molecular and Cellular Biology* 25 (21): 9269–82. https://doi.org/10.1128/MCB.25.21.9269-9282.2005.

Lebaron, Simon, Åsa Segerstolpe, Sarah L. French, Tatiana Dudnakova, Flavia de lima Alves, Sander Granneman, Juri Rappsilber, Ann L. Beyer, Lars Wieslander, and David Tollervey. 2013. 'Rrp5 Binding at Multiple Sites Coordinates Pre-RRNA Processing and Assembly'. *Molecular Cell* 52 (5): 707–19. https://doi.org/10.1016/j.molcel.2013.10.017.

Lecompte, Odile, Raymond Ripp, Jean-Claude Thierry, Dino Moras, and Olivier Poch. 2002. 'Comparative Analysis of Ribosomal Proteins in Complete Genomes: An Example of Reductive Evolution at the Domain Scale'. *Nucleic Acids Research* 30 (24): 5382–90. https://doi.org/10.1093/nar/gkf693.

Lee, Kangseok, Jonathan A. Bernstein, and Stanley N. Cohen. 2002. 'RNase G Complementation of Rne Null Mutation Identifies Functional Interrelationships with RNase E in Escherichia Coli'. *Molecular Microbiology* 43 (6): 1445–56. https://doi.org/10.1046/j.1365-2958.2002.02848.x.

Lee, Zarraz May-Ping, Carl Bussema, and Thomas M. Schmidt. 2009. 'RrnDB: Documenting the Number of RRNA and TRNA Genes in Bacteria and Archaea'. *Nucleic Acids Research* 37 (Database issue): D489-493. https://doi.org/10.1093/nar/gkn689.

Lennox, James. 2021. 'Aristotle's Biology'. In *The Stanford Encyclopedia of Philosophy*, edited by Edward N. Zalta, Fall 2021. Metaphysics Research Lab, Stanford University. https://plato.stanford.edu/archives/fall2021/entries/aristotle-biology/.

Lewis, P. J., S. D. Thaker, and J. Errington. 2000. 'Compartmentalization of Transcription and Translation in Bacillus Subtilis'. *The EMBO Journal* 19 (4): 710–18. https://doi.org/10.1093/emboj/19.4.710.

Li, Ningning, Yuling Chen, Qiang Guo, Yixiao Zhang, Yi Yuan, Chengying Ma, Haiteng Deng, Jianlin Lei, and Ning Gao. 2013. 'Cryo-EM Structures of the Late-Stage Assembly Intermediates of the Bacterial 50S Ribosomal Subunit'. *Nucleic Acids Research* 41 (14): 7073–83. https://doi.org/10.1093/nar/gkt423.

Li, Zhengqun, Yoshiaki Kinosita, Marta Rodriguez-Franco, Phillip Nußbaum, Frank Braun, Floriane Delpech, Tessa E. F. Quax, and Sonja-Verena Albers. 2019. 'Positioning of the Motility Machinery in Halophilic Archaea'. *MBio* 10 (3): e00377-19. https://doi.org/10.1128/mBio.00377-19.

Li, Zhongwei, Shilpa Pandit, and Murray P. Deutscher. 1999. 'RNase G (CafA Protein) and RNase E Are Both Required for the 5′ Maturation of 16S Ribosomal RNA'. *The EMBO Journal* 18 (10): 2878–85. https://doi.org/10.1093/emboj/18.10.2878.

Liao, Yan, Solenne Ithurbide, Christian Evenhuis, Jan Löwe, and Iain G. Duggin. 2021. 'Cell Division in the Archaeon Haloferax Volcanii Relies on Two FtsZ Proteins with Distinct Functions in Division Ring Assembly and Constriction'. *Nature Microbiology* 6 (5): 594–605. https://doi.org/10.1038/s41564-021-00894-z.

Liebl, Maximilian. 2021. 'Identification and Functional Characterization of Circular Pre-Ribosomal RNA Intermediates in Archaea'.

Lindahl, Lasse. 1975. 'Intermediates and Time Kinetics of the in Vivo Assembly of Escherichia Coli Ribosomes'. *Journal of Molecular Biology* 92 (1): 15–37. https://doi.org/10.1016/0022-2836(75)90089-3.

Liu, Hailong, Zhenfang Wu, Ming Li, Fan Zhang, Huajun Zheng, Jing Han, Jingfang Liu, Jian Zhou, Shengyue Wang, and Hua Xiang. 2011. 'Complete Genome Sequence of Haloarcula Hispanica, a Model Haloarchaeon for Studying Genetics, Metabolism, and Virus-Host Interaction'. *Journal of Bacteriology* 193 (21): 6086–87. https://doi.org/10.1128/JB.05953-11.

Liu, Yang, Kira S. Makarova, Wen-Cong Huang, Yuri I. Wolf, Anastasia N. Nikolskaya, Xinxu Zhang, Mingwei Cai, et al. 2021. 'Expanded Diversity of Asgard Archaea and Their Relationships with Eukaryotes'. *Nature* 593 (7860): 553–57. https://doi.org/10.1038/s41586-021-03494-3.

References

Lodish, Harvey F., Arnold Berk, Chris Kaiser, Monty Krieger, Anthony Bretscher, Hidde L. Ploegh, Kelsey C. Martin, Michael B. Yaffe, and Angelika Amon. 2021. *Molecular Cell Biology*. Ninth edition, Loose-leaf Student edition. Austin: Macmillan Learning. http://public.ebookcentral.proquest.com/choice/publicfullrecord.aspx?p=6499946.

Londei, P., J. Teixidò, M. Acca, P. Cammarano, and R. Amils. 1986. 'Total Reconstitution of Active Large Ribosomal Subunits of the Thermoacidophilic Archaebacterium Sulfolobus Solfataricus'. *Nucleic Acids Research* 14 (5): 2269–85. https://doi.org/10.1093/nar/14.5.2269.

Londei, Paola, and Sébastien Ferreira-Cerca. 2021. 'Ribosome Biogenesis in Archaea'. *Frontiers in Microbiology* 12. https://www.frontiersin.org/articles/10.3389/fmicb.2021.686977.

Long, R. M., D. J. Elliott, F. Stutz, M. Rosbash, and R. H. Singer. 1995. 'Spatial Consequences of Defective Processing of Specific Yeast MRNAs Revealed by Fluorescent in Situ Hybridization'. *RNA (New York, N.Y.)* 1 (10): 1071–78.

Lopez, Francesca B, Antoine Fort, Luca Tadini, Aline V Probst, Marcus McHale, James Friel, Peter Ryder, et al. 2021. 'Gene Dosage Compensation of RRNA Transcript Levels in Arabidopsis Thaliana Lines with Reduced Ribosomal Gene Copy Number'. *The Plant Cell* 33 (4): 1135–50. https://doi.org/10.1093/plcell/koab020.

López-López, A., S. Benlloch, M. Bonfá, F. Rodríguez-Valera, and A. Mira. 2007. 'Intragenomic 16S RDNA Divergence in Haloarcula Marismortui Is an Adaptation to Different Temperatures'. *Journal of Molecular Evolution* 65 (6): 687–96. https://doi.org/10.1007/s00239-007-9047-3.

Lučić, Vladan, Andrew Leis, and Wolfgang Baumeister. 2008. 'Cryo-Electron Tomography of Cells: Connecting Structure and Function'. *Histochemistry and Cell Biology* 130 (2): 185–96. https://doi.org/10.1007/s00418-008-0459-y.

Luidalepp, Hannes, Stefan Berger, Oliver Joss, Tanel Tenson, and Norbert Polacek. 2016. 'Ribosome Shut-Down by 16S RRNA Fragmentation in Stationary-Phase Escherichia Coli'. *Journal of Molecular Biology*, Ribosomes Structure and Mechanisms in Regulation of Protein Synthesis (I), 428 (10, Part B): 2237–47. https://doi.org/10.1016/j.jmb.2016.01.033.

Lykke-Andersen, Jens, Claus Aagaard, Mikhail Semionenkov, and Roger A. Garrett. 1997. 'Archaeal Introns: Splicing, Intercellular Mobility and Evolution'. *Trends in Biochemical Sciences* 22 (9): 326–31. https://doi.org/10.1016/S0968-0004(97)01113-4.

Lynch, Michael, Mark C. Field, Holly V. Goodson, Harmit S. Malik, José B. Pereira-Leal, David S. Roos, Aaron P. Turkewitz, and Shelley Sazer. 2014. 'Evolutionary Cell Biology: Two Origins, One Objective'. *Proceedings of the National Academy of Sciences* 111 (48): 16990–94. https://doi.org/10.1073/pnas.1415861111.

Mackie, George A. 1998. 'Ribonuclease E Is a 5′-End-Dependent Endonuclease'. *Nature* 395 (6703): 720–24. https://doi.org/10.1038/27246.

———. 2013. 'RNase E: At the Interface of Bacterial RNA Processing and Decay'. *Nature Reviews Microbiology* 11 (1): 45–57. https://doi.org/10.1038/nrmicro2930.

Magrum, Linda J., Kenneth R. Luehrsen, and Carl R. Woese. 1978. 'Are Extreme Halophiles Actually "Bacteria"?' *Journal of Molecular Evolution* 11 (1): 1–8. https://doi.org/10.1007/BF01768019.

Maiväli, Ülo, Anton Paier, and Tanel Tenson. 2013. 'When Stable RNA Becomes Unstable: The Degradation of Ribosomes in Bacteria and Beyond'. *Biological Chemistry* 394 (7): 845–55. https://doi.org/10.1515/hsz-2013-0133.

Malagon, Francisco. 2013. 'RNase III Is Required for Localization to the Nucleoid of the 5′ Pre-RRNA Leader and for Optimal Induction of RRNA Synthesis in E. Coli'. *RNA* 19 (9): 1200–1207. https://doi.org/10.1261/rna.038588.113.

Malandrin, L., H. Huber, and R. Bernander. 1999. 'Nucleoid Structure and Partition in Methanococcus Jannaschii: An Archaeon with Multiple Copies of the Chromosome'. *Genetics* 152 (4): 1315–23. https://doi.org/10.1093/genetics/152.4.1315.

Mangiarotti, G., E. Turco, C. Perlo, and F. Altruda. 1975. 'Role of Precursor 16S RNA in Assembly of E. Coli 30S Ribosomes'. *Nature* 253 (5492): 569–71. https://doi.org/10.1038/253569a0.

Mangiarotti, Giorgio, and Sara Chiaberge. 1997. 'Reconstitution of Functional Eukaryotic Ribosomes FromDictyostelium Discoideum Ribosomal Proteins and RNA*'. *Journal of Biological Chemistry* 272 (32): 19682–87. https://doi.org/10.1074/jbc.272.32.19682.

Marcaida, Maria Jose, Mark A. DePristo, Vidya Chandran, Agamemnon J. Carpousis, and Ben F. Luisi. 2006. 'The RNA Degradosome: Life in the Fast Lane of Adaptive Molecular Evolution'. *Trends in Biochemical Sciences* 31 (7): 359–65. https://doi.org/10.1016/j.tibs.2006.05.005.

Marck, Christian, and Henri Grosjean. 2003. 'Identification of BHB Splicing Motifs in Intron-Containing TRNAs from 18 Archaea: Evolutionary Implications'. *RNA* 9 (12): 1516–31. https://doi.org/10.1261/rna.5132503.

References

Márquez, Viter, Thomas Fröhlich, Jean-Paul Armache, Daniel Sohmen, Alexandra Dönhöfer, Aleksandra Mikolajka, Otto Berninghausen, et al. 2011. 'Proteomic Characterization of Archaeal Ribosomes Reveals the Presence of Novel Archaeal-Specific Ribosomal Proteins'. *Journal of Molecular Biology* 405 (5): 1215–32. https://doi.org/10.1016/j.jmb.2010.11.055.

Martijn, Joran, and Thijs J.G. Ettema. 2013. 'From Archaeon to Eukaryote: The Evolutionary Dark Ages of the Eukaryotic Cell'. *Biochemical Society Transactions* 41 (1): 451–57. https://doi.org/10.1042/BST20120292.

Martijn, Joran, Max E. Schön, Anders E. Lind, Julian Vosseberg, Tom A. Williams, Anja Spang, and Thijs J. G. Ettema. 2020. 'Hikarchaeia Demonstrate an Intermediate Stage in the Methanogen-to-Halophile Transition'. *Nature Communications* 11 (1): 5490. https://doi.org/10.1038/s41467-020-19200-2.

Martin, A. 2009. *Encyclopedia of Microbiology. 5*. 3. ed. Amsterdam Heidelberg: Elsevier/Academic Press.

Mascarenhas, Judita, Michael H.W. Weber, and Peter L. Graumann. 2001. 'Specific Polar Localization of Ribosomes in Bacillus Subtilis Depends on Active Transcription'. *EMBO Reports* 2 (8): 685–89. https://doi.org/10.1093/embo-reports/kve160.

Mayr, E. 1998. 'Two Empires or Three?' *Proceedings of the National Academy of Sciences of the United States of America* 95 (17): 9720–23. https://doi.org/10.1073/pnas.95.17.9720.

McDowall, K. J., R. G. Hernandez, S. Lin-Chao, and S. N. Cohen. 1993. 'The Ams-1 and Rne-3071 Temperature-Sensitive Mutations in the Ams Gene Are in Close Proximity to Each Other and Cause Substitutions within a Domain That Resembles a Product of the Escherichia Coli Mre Locus'. *Journal of Bacteriology* 175 (13): 4245–49. https://doi.org/10.1128/jb.175.13.4245-4249.1993.

Melnikov, Sergey, Adam Ben-Shem, Nicolas Garreau de Loubresse, Lasse Jenner, Gulnara Yusupova, and Marat Yusupov. 2012. 'One Core, Two Shells: Bacterial and Eukaryotic Ribosomes'. *Nature Structural & Molecular Biology* 19 (6): 560–67. https://doi.org/10.1038/nsmb.2313.

Miller, O. L., and Barbara R. Beatty. 1969. 'Visualization of Nucleolar Genes'. *Science* 164 (3882): 955–57. https://doi.org/10.1126/science.164.3882.955.

Miller, O. L., B. A. Hamkalo, and C. A. Thomas. 1970. 'Visualization of Bacterial Genes in Action'. *Science (New York, N.Y.)* 169 (3943): 392–95. https://doi.org/10.1126/science.169.3943.392.

Misteli, Tom. 2001. 'The Concept of Self-Organization in Cellular Architecture'. *Journal of Cell Biology* 155 (2): 181–86. https://doi.org/10.1083/jcb.200108110.

Mizushima, Shoji, and Masayasu Nomura. 1970. 'Assembly Mapping of 30S Ribosomal Proteins from E. Coli'. *Nature* 226 (5252): 1214–18. https://doi.org/10.1038/2261214a0.

Mohammadzadeh, Rokhsareh, Alexander Mahnert, Stefanie Duller, and Christine Moissl-Eichinger. 2022. 'Archaeal Key-Residents within the Human Microbiome: Characteristics, Interactions and Involvement in Health and Disease'. *Current Opinion in Microbiology* 67 (June): 102146. https://doi.org/10.1016/j.mib.2022.102146.

Montero Llopis, Paula, Audrey F. Jackson, Oleksii Sliusarenko, Ivan Surovtsev, Jennifer Heinritz, Thierry Emonet, and Christine Jacobs-Wagner. 2010. 'Spatial Organization of the Flow of Genetic Information in Bacteria'. *Nature* 466 (7302): 77–81. https://doi.org/10.1038/nature09152.

Mori, Hiro, Carol Dammel, Elisa Becker, Kathleen Triman, and Harry F. Noller. 1990. 'Single Base Alterations Upstream of the E. Coli 16S RRNA Coding Region Result in Temperature-Sensitive 16S RRNA Expression'. *Biochimica et Biophysica Acta (BBA) - Gene Structure and Expression* 1050 (1): 323–27. https://doi.org/10.1016/0167-4781(90)90189-9.

Moss, T., F. Langlois, T. Gagnon-Kugler, and V. Stefanovsky. 2007. 'A Housekeeper with Power of Attorney: The RRNA Genes in Ribosome Biogenesis'. *Cellular and Molecular Life Sciences* 64 (1): 29–49. https://doi.org/10.1007/s00018-006-6278-1.

Moss, Tom, and Victor Y. Stefanovsky. 2002. 'At the Center of Eukaryotic Life'. *Cell* 109 (5): 545–48. https://doi.org/10.1016/S0092-8674(02)00761-4.

Mudd, E. A., H. M. Krisch, and C. F. Higgins. 1990. 'RNase E, an Endoribonuclease, Has a General Role in the Chemical Decay of Escherichia Coli MRNA: Evidence That Rne and Ams Are the Same Genetic Locus'. *Molecular Microbiology* 4 (12): 2127–35. https://doi.org/10.1111/j.1365-2958.1990.tb00574.x.

Mulder, Anke M., Craig Yoshioka, Andrea H. Beck, Anne E. Bunner, Ronald A. Milligan, Clinton S. Potter, Bridget Carragher, and James R. Williamson. 2010. 'Visualizing Ribosome Biogenesis: Parallel Assembly Pathways for the 30S Subunit'. *Science* 330 (6004): 673–77. https://doi.org/10.1126/science.1193220.

Mullakhanbhai, Moiz F., and Helge Larsen. 1975. 'Halobacterium Volcanii Spec. Nov., a Dead Sea Halobacterium with a Moderate Salt Requirement'. *Archives of Microbiology* 104 (1): 207–14. https://doi.org/10.1007/BF00447326.

Müller, Albert L., Wenyu Gu, Vadim Patsalo, Jörg S. Deutzmann, James R. Williamson, and Alfred M. Spormann. 2021. 'An Alternative Resource Allocation Strategy in the Chemolithoautotrophic Archaeon

Methanococcus Maripaludis'. *Proceedings of the National Academy of Sciences of the United States of America* 118 (16): e2025854118. https://doi.org/10.1073/pnas.2025854118.

Musters, W., K. Boon, C. A. van der Sande, H. van Heerikhuizen, and R. J. Planta. 1990. 'Functional Analysis of Transcribed Spacers of Yeast Ribosomal DNA'. *The EMBO Journal* 9 (12): 3989–96. https://doi.org/10.1002/j.1460-2075.1990.tb07620.x.

Musters, W., J. Venema, G. van der Linden, H. van Heerikhuizen, J. Klootwijk, and R. J. Planta. 1989. 'A System for the Analysis of Yeast Ribosomal DNA Mutations'. *Molecular and Cellular Biology* 9 (2): 551–59. https://doi.org/10.1128/mcb.9.2.551-559.1989.

Mylvaganam, S., and P. P. Dennis. 1992. 'Sequence Heterogeneity between the Two Genes Encoding 16S RRNA from the Halophilic Archaebacterium Haloarcula Marismortui'. *Genetics* 130 (3): 399–410. https://doi.org/10.1093/genetics/130.3.399.

Narvaez, C. Cowgill de, and H. W. Schaup. 1979. 'In Vivo Transcriptionally Coupled Assembly of Escherichia Coli Ribosomal Subunits'. *Journal of Molecular Biology* 134 (1): 1–22. https://doi.org/10.1016/0022-2836(79)90411-X.

Nasir, Arshan, Fizza Mughal, and Gustavo Caetano-Anollés. 2021. 'The Tree of Life Describes a Tripartite Cellular World'. *BioEssays* 43 (6): 2000343. https://doi.org/10.1002/bies.202000343.

Neidhardt, F. C., and B. Magasanik. 1960. 'Studies on the Role of Ribonucleic Acid in the Growth of Bacteria'. *Biochimica Et Biophysica Acta* 42 (July): 99–116. https://doi.org/10.1016/0006-3002(60)90757-5.

Neves, Nuno, Wanda Viegas, and Craig S. Pikaard. 2005. 'Nucleolar Dominance and RRNA Gene Dosage Control: A Paradigm for Transcriptional Regulation via an Epigenetic On/Off Switch'. In *Annual Plant Reviews Volume 19: Plant Epigenetics*, 201–22. John Wiley & Sons, Ltd. https://doi.org/10.1002/9780470988626.ch7.

Nierhaus, K. H., and F. Dohme. 1974. 'Total Reconstitution of Functionally Active 50S Ribosomal Subunits from Escherichia Coli'. *Proceedings of the National Academy of Sciences of the United States of America* 71 (12): 4713–17. https://doi.org/10.1073/pnas.71.12.4713.

Nierhaus, Knud H., and Denis L. Lafontaine. 2004. 'Ribosome Assembly'. In *Protein Synthesis and Ribosome Structure*, 85–143. John Wiley & Sons, Ltd. https://doi.org/10.1002/3527603433.ch3.

Nikolaeva, Daria D, Mikhail S Gelfand, and Sofya K Garushyants. 2021. 'Simplification of Ribosomes in Bacteria with Tiny Genomes'. *Molecular Biology and Evolution* 38 (1): 58–66. https://doi.org/10.1093/molbev/msaa184.

Nikolay, Rainer, Tarek Hilal, Bo Qin, Thorsten Mielke, Jörg Bürger, Justus Loerke, Kathrin Textoris-Taube, Knud H. Nierhaus, and Christian M. T. Spahn. 2018. 'Structural Visualization of the Formation and Activation of the 50S Ribosomal Subunit during In Vitro Reconstitution'. *Molecular Cell* 70 (5): 881-893.e3. https://doi.org/10.1016/j.molcel.2018.05.003.

Nomura, M. 2001. 'Ribosomal RNA Genes, RNA Polymerases, Nucleolar Structures, and Synthesis of RRNA in the Yeast Saccharomyces Cerevisiae'. *Cold Spring Harbor Symposia on Quantitative Biology* 66: 555–65. https://doi.org/10.1101/sqb.2001.66.555.

Nomura, M., and V. A. Erdmann. 1970. 'Reconstitution of 50S Ribosomal Subunits from Dissociated Molecular Components'. *Nature* 228 (5273): 744–48. https://doi.org/10.1038/228744a0.

Nomura, Masayasu. 1999. 'Regulation of Ribosome Biosynthesis in Escherichia Coli and Saccharomyces Cerevisiae: Diversity and Common Principles'. *Journal of Bacteriology* 181 (22): 6857–64. https://doi.org/10.1128/JB.181.22.6857-6864.1999.

Nowotny, V, and K H Nierhaus. 1982. 'Initiator Proteins for the Assembly of the 50S Subunit from Escherichia Coli Ribosomes.' *Proceedings of the National Academy of Sciences of the United States of America* 79 (23): 7238–42.

Nußbaum, Phillip, Maren Gerstner, Marie Dingethal, Celine Erb, and Sonja-Verena Albers. 2021. 'The Archaeal Protein SepF Is Essential for Cell Division in Haloferax Volcanii'. *Nature Communications* 12 (1): 3469. https://doi.org/10.1038/s41467-021-23686-9.

Oakes, M., J.P. Aris, J.S. Brockenbrough, H. Wai, L. Vu, and M. Nomura. 1998. 'Mutational Analysis of the Structure and Localization of the Nucleolus in the Yeast Saccharomyces Cerevisiae'. *Journal of Cell Biology* 143 (1): 23–34. https://doi.org/10.1083/jcb.143.1.23.

Oerum, Stephanie, Tom Dendooven, Marjorie Catala, Laetitia Gilet, Clément Dégut, Aude Trinquier, Maxime Bourguet, et al. 2020. 'Structures of B. Subtilis Maturation RNases Captured on 50S Ribosome with Pre-RRNAs'. *Molecular Cell* 80 (2): 227-236.e5. https://doi.org/10.1016/j.molcel.2020.09.008.

Ohtani, Naoto, Natsumi Saito, Masaru Tomita, Mitsuhiro Itaya, and Aya Itoh. 2005. 'The SCO2299 Gene from Streptomyces Coelicolor A3(2) Encodes a Bifunctional Enzyme Consisting of an RNase H Domain and an

Acid Phosphatase Domain'. *The FEBS Journal* 272 (11): 2828–37. https://doi.org/10.1111/j.1742-4658.2005.04704.x.

Ono, Mayumi, and Michihiko Kuwano. 1979. 'A Conditional Lethal Mutation in an Escherichia Coli Strain with a Longer Chemical Lifetime of Messenger RNA'. *Journal of Molecular Biology* 129 (3): 343–57. https://doi.org/10.1016/0022-2836(79)90500-X.

Ow, Maria C., Tariq Perwez, and Sidney R. Kushner. 2003. 'RNase G of Escherichia Coli Exhibits Only Limited Functional Overlap with Its Essential Homologue, RNase E'. *Molecular Microbiology* 49 (3): 607–22. https://doi.org/10.1046/j.1365-2958.2003.03587.x.

Pace, N. R. 1997. 'A Molecular View of Microbial Diversity and the Biosphere'. *Science (New York, N.Y.)* 276 (5313): 734–40. https://doi.org/10.1126/science.276.5313.734.

Pace, Norman R., David A. Stahl, David J. Lane, and Gary J. Olsen. 1986. 'The Analysis of Natural Microbial Populations by Ribosomal RNA Sequences'. *Advances in Microbial Ecology*, 1–55. https://doi.org/10.1007/978-1-4757-0611-6_1.

Paier, Anton, Margus Leppik, Aksel Soosaar, Tanel Tenson, and Ülo Maiväli. 2015. 'The Effects of Disruptions in Ribosomal Active Sites and in Intersubunit Contacts on Ribosomal Degradation in Escherichia Coli'. *Scientific Reports* 5 (1): 1–8. https://doi.org/10.1038/srep07712.

Pardon, B, and R Wagner. 1995. 'The Escherichia Coli Ribosomal RNA Leader Nut Region Interacts Specifically with Mature 16S RNA.' *Nucleic Acids Research* 23 (6): 932–41.

Parks, Donovan H., Maria Chuvochina, David W. Waite, Christian Rinke, Adam Skarshewski, Pierre-Alain Chaumeil, and Philip Hugenholtz. 2018. 'A Standardized Bacterial Taxonomy Based on Genome Phylogeny Substantially Revises the Tree of Life'. *Nature Biotechnology* 36 (10): 996–1004. https://doi.org/10.1038/nbt.4229.

Pasolli, Edoardo, Francesco Asnicar, Serena Manara, Moreno Zolfo, Nicolai Karcher, Federica Armanini, Francesco Beghini, et al. 2019. 'Extensive Unexplored Human Microbiome Diversity Revealed by Over 150,000 Genomes from Metagenomes Spanning Age, Geography, and Lifestyle'. *Cell* 176 (3): 649-662.e20. https://doi.org/10.1016/j.cell.2019.01.001.

Paterlini, Marta. 2007. 'There Shall Be Order. The Legacy of Linnaeus in the Age of Molecular Biology'. *EMBO Reports* 8 (9): 814–16. https://doi.org/10.1038/sj.embor.7401061.

Pelve, Erik A., Ann-Christin Lindås, Willm Martens-Habbena, José R. de la Torre, David A. Stahl, and Rolf Bernander. 2011. 'Cdv-Based Cell Division and Cell Cycle Organization in the Thaumarchaeon Nitrosopumilus Maritimus'. *Molecular Microbiology* 82 (3): 555–66. https://doi.org/10.1111/j.1365-2958.2011.07834.x.

Penev, Petar I, Sara Fakhretaha-Aval, Vaishnavi J Patel, Jamie J Cannone, Robin R Gutell, Anton S Petrov, Loren Dean Williams, and Jennifer B Glass. 2020. 'Supersized Ribosomal RNA Expansion Segments in Asgard Archaea'. *Genome Biology and Evolution* 12 (10): 1694–1710. https://doi.org/10.1093/gbe/evaa170.

Pertschy, Brigitte, Claudia Schneider, Marén Gnädig, Thorsten Schäfer, David Tollervey, and Ed Hurt. 2009. 'RNA Helicase Prp43 and Its Co-Factor Pfa1 Promote 20 to 18 S RRNA Processing Catalyzed by the Endonuclease Nob1'. *Journal of Biological Chemistry* 284 (50): 35079–91. https://doi.org/10.1074/jbc.M109.040774.

Petrov, Anton S., Chad R. Bernier, Burak Gulen, Chris C. Waterbury, Eli Hershkovits, Chiaolong Hsiao, Stephen C. Harvey, et al. 2014. 'Secondary Structures of RRNAs from All Three Domains of Life'. *PLOS ONE* 9 (2): e88222. https://doi.org/10.1371/journal.pone.0088222.

Petrov, Anton S., Chad R. Bernier, Eli Hershkovits, Yuzhen Xue, Chris C. Waterbury, Chiaolong Hsiao, Victor G. Stepanov, et al. 2013. 'Secondary Structure and Domain Architecture of the 23S and 5S RRNAs'. *Nucleic Acids Research* 41 (15): 7522–35. https://doi.org/10.1093/nar/gkt513.

Pettersson, R F, and C H von Bonsdorff. 1975. 'Ribonucleoproteins of Uukuniemi Virus Are Circular.' *Journal of Virology* 15 (2): 386–92.

Peyretaillade, Eric, Corinne Biderre, Pierre Peyret, Francis Duffieux, Guy Méténier, Manolo Gouy, Bernard Michot, and Christian P. Vivarès. 1998. 'Microsporidian Encephalitozoon Cuniculi , a Unicellular Eukaryote with an Unusual Chromosomal Dispersion of Ribosomal Genes and a LSU RRNA Reduced to the Universal Core'. *Nucleic Acids Research* 26 (15): 3513–20. https://doi.org/10.1093/nar/26.15.3513.

Piir, Kerli, Anton Paier, Aivar Liiv, Tanel Tenson, and Ülo Maiväli. 2011. 'Ribosome Degradation in Growing Bacteria'. *EMBO Reports* 12 (5): 458–62. https://doi.org/10.1038/embor.2011.47.

Podar, Mircea, Iain Anderson, Kira S. Makarova, James G. Elkins, Natalia Ivanova, Mark A. Wall, Athanasios Lykidis, et al. 2008. 'A Genomic Analysis of the Archaeal System Ignicoccus Hospitalis-Nanoarchaeum Equitans'. *Genome Biology* 9 (11): R158. https://doi.org/10.1186/gb-2008-9-11-r158.

References

Pöll, Gisela, Tobias Braun, Jelena Jakovljevic, Andreas Neueder, Steffen Jakob, John L. Woolford Jr, Herbert Tschochner, and Philipp Milkereit. 2009. 'RRNA Maturation in Yeast Cells Depleted of Large Ribosomal Subunit Proteins'. *PLOS ONE* 4 (12): e8249. https://doi.org/10.1371/journal.pone.0008249.

Pöll, Gisela, Michael Pilsl, Joachim Griesenbeck, Herbert Tschochner, and Philipp Milkereit. 2021. 'Analysis of Subunit Folding Contribution of Three Yeast Large Ribosomal Subunit Proteins Required for Stabilisation and Processing of Intermediate Nuclear RRNA Precursors'. *PLOS ONE* 16 (11): e0252497. https://doi.org/10.1371/journal.pone.0252497.

Poot, Raymond A., Sjoerd H. E. van den Worm, Cornelis W. A. Pleij, and Jan van Duin. 1998. 'Base Complementarity in Helix 2 of the Central Pseudoknot in 16S RRNA Is Essential for Ribosome Functioning'. *Nucleic Acids Research* 26 (2): 549–53. https://doi.org/10.1093/nar/26.2.549.

Popławski, A, and R Bernander. 1997. 'Nucleoid Structure and Distribution in Thermophilic Archaea.' *Journal of Bacteriology* 179 (24): 7625–30.

Portnoy, Victoria, and Gadi Schuster. 2006. 'RNA Polyadenylation and Degradation in Different Archaea; Roles of the Exosome and RNase R'. *Nucleic Acids Research* 34 (20): 5923–31. https://doi.org/10.1093/nar/gkl763.

Potrykus, Katarzyna, and Michael Cashel. 2008. '(P)PpGpp: Still Magical?' *Annual Review of Microbiology* 62 (1): 35–51. https://doi.org/10.1146/annurev.micro.62.081307.162903.

Powers, Ted, Gary Daubresse, and Harry F. Noller. 1993. 'Dynamics of In Vitro Assembly of 16 S RRNA into 30 S Ribosomal Subunits'. *Journal of Molecular Biology* 232 (2): 362–74. https://doi.org/10.1006/jmbi.1993.1396.

Preston, C M, K Y Wu, T F Molinski, and E F DeLong. 1996. 'A Psychrophilic Crenarchaeon Inhabits a Marine Sponge: Cenarchaeum Symbiosum Gen. Nov., Sp. Nov.' *Proceedings of the National Academy of Sciences* 93 (13): 6241–46. https://doi.org/10.1073/pnas.93.13.6241.

Pulschen, Andre Arashiro, Delyan R. Mutavchiev, Siân Culley, Kim Nadine Sebastian, Jacques Roubinet, Marc Roubinet, Gabriel Tarrason Risa, et al. 2020. 'Live Imaging of a Hyperthermophilic Archaeon Reveals Distinct Roles for Two ESCRT-III Homologs in Ensuring a Robust and Symmetric Division'. *Current Biology: CB* 30 (14): 2852-2859.e4. https://doi.org/10.1016/j.cub.2020.05.021.

Purusharth, Rajyaguru Ichchhashankar, Bollapalli Madhuri, and Malay Kumar Ray. 2007. 'Exoribonuclease R in Pseudomonas Syringae Is Essential for Growth at Low Temperature and Plays a Novel Role in the 3' End Processing of 16 and 5 S Ribosomal RNA'. *The Journal of Biological Chemistry* 282 (22): 16267–77. https://doi.org/10.1074/jbc.M605588200.

Qi, Lei, Jie Li, Jia Jia, Lei Yue, and Xiuzhu Dong. 2020. 'Comprehensive Analysis of the Pre-Ribosomal RNA Maturation Pathway in a Methanoarchaeon Exposes the Conserved Circularization and Linearization Mode in Archaea'. *RNA Biology* 17 (10): 1427–41. https://doi.org/10.1080/15476286.2020.1771946.

Qin, Bo, Simon M. Lauer, Annika Balke, Carlos H. Vieira-Vieira, Jörg Bürger, Thorsten Mielke, Matthias Selbach, Patrick Scheerer, Christian M. T. Spahn, and Rainer Nikolay. 2023. 'Cryo-EM Captures Early Ribosome Assembly in Action'. *Nature Communications* 14 (1): 898. https://doi.org/10.1038/s41467-023-36607-9.

Qu, Liang, Zongyi Yi, Yong Shen, Liangru Lin, Feng Chen, Yiyuan Xu, Zeguang Wu, et al. 2022. 'Circular RNA Vaccines against SARS-CoV-2 and Emerging Variants'. *Cell* 185 (10): 1728-1744.e16. https://doi.org/10.1016/j.cell.2022.03.044.

Ramakrishnan, V, and P. B Moore. 2001. 'Atomic Structures at Last: The Ribosome in 2000'. *Current Opinion in Structural Biology* 11 (2): 144–54. https://doi.org/10.1016/S0959-440X(00)00184-6.

Ranasinghe, Rohan T., Martin R. Challand, Kristina A. Ganzinger, Benjamin W. Lewis, Charlotte Softley, Wolfgang H. Schmied, Mathew H. Horrocks, et al. 2018. 'Detecting RNA Base Methylations in Single Cells by in Situ Hybridization'. *Nature Communications* 9 (February): 655. https://doi.org/10.1038/s41467-017-02714-7.

Razi, Aida, Robert A. Britton, and Joaquin Ortega. 2017. 'The Impact of Recent Improvements in Cryo-Electron Microscopy Technology on the Understanding of Bacterial Ribosome Assembly'. *Nucleic Acids Research* 45 (3): 1027–40. https://doi.org/10.1093/nar/gkw1231.

Redder, Peter. 2016. 'How Does Sub-Cellular Localization Affect the Fate of Bacterial MRNA?' *Current Genetics* 62 (4): 687–90. https://doi.org/10.1007/s00294-016-0587-1.

Redko, Yulia, David H. Bechhofer, and Ciarán Condon. 2008. 'Mini-III, an Unusual Member of the RNase III Family of Enzymes, Catalyses 23S Ribosomal RNA Maturation in B. Subtilis'. *Molecular Microbiology* 68 (5): 1096–1106. https://doi.org/10.1111/j.1365-2958.2008.06207.x.

Ree, Heesoo K., and Robert A. Zimmermann. 1990. 'Organization and Expression of the 16S, 23S and 5S Ribosomal RNA Genes from the Archaebacterium Thermoplasma Acidophilum'. *Nucleic Acids Research* 18 (15): 4471–78. https://doi.org/10.1093/nar/18.15.4471.

Reid, Gordon McGregor. 2009. 'Carolus Linnaeus (1707–1778): His Life, Philosophy and Science and Its Relationship to Modern Biology and Medicine'. *TAXON* 58 (1): 18–31. https://doi.org/10.1002/tax.581005.

References

Reistad, R. 1972. 'Cell Wall of an Extremely Halophilic Coccus'. *Archiv Für Mikrobiologie* 82 (1): 24–30. https://doi.org/10.1007/BF00424926.

Reistad, Ragnhild. 1975. 'Amino Sugar and Amino Acid Constituents of the Cell Walls of the Extremely Halophilic Cocci'. *Archives of Microbiology* 102 (1): 71–73. https://doi.org/10.1007/BF00428348.

Rheinberger, Hans-Jörg. 2004. 'A History of Protein Biosynthesis and Ribosome Research'. In *Protein Synthesis and Ribosome Structure*, 1–51. John Wiley & Sons, Ltd. https://doi.org/10.1002/3527603433.ch1.

Richards, Jamie, and Joel G. Belasco. 2016. 'Distinct Requirements for 5′-Monophosphate-Assisted RNA Cleavage by Escherichia Coli RNase E and RNase G *'. *Journal of Biological Chemistry* 291 (10): 5038–48. https://doi.org/10.1074/jbc.M115.702555.

Rinke, Christian, Patrick Schwientek, Alexander Sczyrba, Natalia N. Ivanova, Iain J. Anderson, Jan-Fang Cheng, Aaron Darling, et al. 2013. 'Insights into the Phylogeny and Coding Potential of Microbial Dark Matter'. *Nature* 499 (7459): 431–37. https://doi.org/10.1038/nature12352.

Rivera, Maria C., and James A. Lake. 1992. 'Evidence That Eukaryotes and Eocyte Prokaryotes Are Immediate Relatives'. *Science* 257 (5066): 74–76. https://doi.org/10.1126/science.1621096.

Rodgers, Margaret L., and Sarah A. Woodson. 2019. 'Transcription Increases the Cooperativity of Ribonucleoprotein Assembly'. *Cell* 179 (6): 1370-1381.e12. https://doi.org/10.1016/j.cell.2019.11.007.

Rodrigues-Oliveira, Thiago, Florian Wollweber, Rafael I. Ponce-Toledo, Jingwei Xu, Simon K.-M. R. Rittmann, Andreas Klingl, Martin Pilhofer, and Christa Schleper. 2022. 'Actin Cytoskeleton and Complex Cell Architecture in an Asgard Archaeon'. *Nature*, December, 1–8. https://doi.org/10.1038/s41586-022-05550-y.

Röhl, R., and K. H. Nierhaus. 1982. 'Assembly Map of the Large Subunit (50S) of Escherichia Coli Ribosomes'. *Proceedings of the National Academy of Sciences of the United States of America* 79 (3): 729–33. https://doi.org/10.1073/pnas.79.3.729.

Roller, Benjamin R. K., Steven F. Stoddard, and Thomas M. Schmidt. 2016. 'Exploiting RRNA Operon Copy Number to Investigate Bacterial Reproductive Strategies'. *Nature Microbiology* 1 (11): 1–7. https://doi.org/10.1038/nmicrobiol.2016.160.

Roppelt, Verena, Cédric F.V. Hobel, Sonja V. Albers, Christian Lassek, Heinz Schwarz, Gabriele Klug, and Elena Evguenieva-Hackenberg. 2010. 'The Archaeal Exosome Localizes to the Membrane'. *FEBS Letters* 584 (13): 2791–95. https://doi.org/10.1016/j.febslet.2010.05.013.

Russell, A. G., H. Ebhardt, and P. P. Dennis. 1999. 'Substrate Requirements for a Novel Archaeal Endonuclease That Cleaves within the 5' External Transcribed Spacer of Sulfolobus Acidocaldarius Precursor RRNA'. *Genetics* 152 (4): 1373–85. https://doi.org/10.1093/genetics/152.4.1373.

Russell, Jackie, and Joost C.B.M. Zomerdijk. 2006. 'The RNA Polymerase I Transcription Machinery'. Edited by Stefan G.E. Roberts, Robert O.J. Weinzierl, and Robert J. White. *Biochemical Society Symposia* 73 (January): 203–16. https://doi.org/10.1042/bss0730203.

Sagan, Lynn. 1967. 'On the Origin of Mitosing Cells'. *Journal of Theoretical Biology* 14 (3): 225-IN6. https://doi.org/10.1016/0022-5193(67)90079-3.

Sahonero-Canavesi, Diana X., Melvin F. Siliakus, Alejandro Abdala Asbun, Michel Koenen, F. A. Bastiaan von Meijenfeldt, Sjef Boeren, Nicole J. Bale, et al. 2022. 'Disentangling the Lipid Divide: Identification of Key Enzymes for the Biosynthesis of Membrane-Spanning and Ether Lipids in Bacteria'. *Science Advances* 8 (50): eabq8652. https://doi.org/10.1126/sciadv.abq8652.

Sakai, Hiroyuki D., Naswandi Nur, Shingo Kato, Masahiro Yuki, Michiru Shimizu, Takashi Itoh, Moriya Ohkuma, Antonius Suwanto, and Norio Kurosawa. 2022. 'Insight into the Symbiotic Lifestyle of DPANN Archaea Revealed by Cultivation and Genome Analyses'. *Proceedings of the National Academy of Sciences* 119 (3): e2115449119. https://doi.org/10.1073/pnas.2115449119.

Salim, Devika, and Jennifer L. Gerton. 2019. 'Ribosomal DNA Instability and Genome Adaptability'. *Chromosome Research* 27 (1): 73–87. https://doi.org/10.1007/s10577-018-9599-7.

Sanamrad, Arash, Fredrik Persson, Ebba G. Lundius, David Fange, Arvid H. Gynnå, and Johan Elf. 2014. 'Single-Particle Tracking Reveals That Free Ribosomal Subunits Are Not Excluded from the Escherichia Coli Nucleoid'. *Proceedings of the National Academy of Sciences* 111 (31): 11413–18. https://doi.org/10.1073/pnas.1411558111.

Sánchez, Emma, and Ricardo Amils. 1995. 'Absolute Requirement of Ammonium Sulfate for Reconstitution of Active 70s Ribosomes from the Extreme Halophilic Archaeon Haloferax Mediterranei'. *European Journal of Biochemistry* 233 (3): 809–14. https://doi.org/10.1111/j.1432-1033.1995.809_3.x.

Sande, C. A. van der, M. Kwa, R. W. van Nues, H. van Heerikhuizen, H. A. Raué, and R. J. Planta. 1992. 'Functional Analysis of Internal Transcribed Spacer 2 of Saccharomyces Cerevisiae Ribosomal DNA'. *Journal of Molecular Biology* 223 (4): 899–910. https://doi.org/10.1016/0022-2836(92)90251-e.

References

Sanders, Travis J., Craig J. Marshall, and Thomas J. Santangelo. 2019. 'The Role of Archaeal Chromatin in Transcription.' *Journal of Molecular Biology* 431 (20): 4103–15. https://doi.org/10.1016/j.jmb.2019.05.006.

Sanger, H L, G Klotz, D Riesner, H J Gross, and A K Kleinschmidt. 1976. 'Viroids Are Single-Stranded Covalently Closed Circular RNA Molecules Existing as Highly Base-Paired Rod-like Structures.' *Proceedings of the National Academy of Sciences* 73 (11): 3852–56. https://doi.org/10.1073/pnas.73.11.3852.

Sanghai, Zahra Assur, Linamarie Miller, Kelly R. Molloy, Jonas Barandun, Mirjam Hunziker, Malik Chaker-Margot, Junjie Wang, Brian T. Chait, and Sebastian Klinge. 2018. 'Modular Assembly of the Nucleolar Pre-60S Ribosomal Subunit'. *Nature* 556 (7699): 126–29. https://doi.org/10.1038/nature26156.

Sapp, Jan. 2005. 'The Prokaryote-Eukaryote Dichotomy: Meanings and Mythology'. *Microbiology and Molecular Biology Reviews* 69 (2): 292–305. https://doi.org/10.1128/MMBR.69.2.292-305.2005.

Sarmientos, P, and M Cashel. 1983. 'Carbon Starvation and Growth Rate-Dependent Regulation of the Escherichia Coli Ribosomal RNA Promoters: Differential Control of Dual Promoters.' *Proceedings of the National Academy of Sciences* 80 (22): 7010–13. https://doi.org/10.1073/pnas.80.22.7010.

Sashital, Dipali G, Candacia A Greeman, Dmitry Lyumkis, Clinton S Potter, Bridget Carragher, and James R Williamson. 2014. 'A Combined Quantitative Mass Spectrometry and Electron Microscopy Analysis of Ribosomal 30S Subunit Assembly in E. Coli'. Edited by Nahum Sonenberg. *ELife* 3 (October): e04491. https://doi.org/10.7554/eLife.04491.

Sato, Yu, Taketomo Fujiwara, and Hiroyuki Kimura. 2017. 'Expression and Function of Different Guanine-Plus-Cytosine Content 16S RRNA Genes in Haloarcula Hispanica at Different Temperatures'. *Frontiers in Microbiology* 8. https://www.frontiersin.org/articles/10.3389/fmicb.2017.00482.

Sato, Yu, and Hiroyuki Kimura. 2019. 'Temperature-Dependent Expression of Different Guanine-plus-Cytosine Content 16S RRNA Genes in Haloarcula Strains of the Class Halobacteria'. *Antonie van Leeuwenhoek* 112 (2): 187–201. https://doi.org/10.1007/s10482-018-1144-3.

Schaechter, M., O. MaalØe, and N. O.YR 1958 Kjeldgaard. 1958. 'Dependency on Medium and Temperature of Cell Size and Chemical Composition during Balanced Growth of Salmonella Typhimurium'. *Microbiology* 19 (3): 592–606. https://doi.org/10.1099/00221287-19-3-592.

Schimper, Andreas Franz Wilhelm. 1883. 'Ueber die Entwickelung der Chlorophyllkörner und Farbkörper'. *Botanische Zeitung* 41 (7): Sp. 105-Sp. 160.

Schneider, David A, Wilma Ross, and Richard L Gourse. 2003. 'Control of RRNA Expression in Escherichia Coli'. *Current Opinion in Microbiology* 6 (2): 151–56. https://doi.org/10.1016/S1369-5274(03)00038-9.

Schneider, David Alan. 2012. 'RNA Polymerase I Activity Is Regulated at Multiple Steps in the Transcription Cycle: Recent Insights into Factors That Influence Transcription Elongation'. *Gene* 493 (2): 176–84. https://doi.org/10.1016/j.gene.2011.08.006.

Scholz, Scott A., Rucheng Diao, Michael B. Wolfe, Elayne M. Fivenson, Xiaoxia Nina Lin, and Peter L. Freddolino. 2019. 'High-Resolution Mapping of the Escherichia Coli Chromosome Reveals Positions of High and Low Transcription'. *Cell Systems* 8 (3): 212-225.e9. https://doi.org/10.1016/j.cels.2019.02.004.

Schwank, Katrin, Till L. V. Bornemann, Nina Dombrowski, Anja Spang, Jillian F. Banfield, and Alexander J. Probst. 2019. 'An Archaeal Symbiont-Host Association from the Deep Terrestrial Subsurface'. *The ISME Journal* 13 (8): 2135–39. https://doi.org/10.1038/s41396-019-0421-0.

Schwarz, Thandi Sarah, Sarah J. Berkemer, Stephan H. Bernhart, Matthias Weiß, Sébastien Ferreira-Cerca, Peter F. Stadler, and Anita Marchfelder. 2020. 'Splicing Endonuclease Is an Important Player in RRNA and TRNA Maturation in Archaea'. *Frontiers in Microbiology* 11 (November). https://doi.org/10.18725/OPARU-35837.

Shajani, Zahra, Michael T. Sykes, and James R. Williamson. 2011. 'Assembly of Bacterial Ribosomes'. *Annual Review of Biochemistry* 80 (1): 501–26. https://doi.org/10.1146/annurev-biochem-062608-160432.

Sharrock, R A, R L Gourse, and M Nomura. 1985. 'Defective Antitermination of RRNA Transcription and Derepression of RRNA and TRNA Synthesis in the NusB5 Mutant of Escherichia Coli.' *Proceedings of the National Academy of Sciences of the United States of America* 82 (16): 5275–79.

Shimada, T. 1992. 'Distribution of Split 5.8S Ribosomal RNA in Diptera'. *Insect Molecular Biology* 1 (1): 45–49. https://doi.org/10.1111/j.1365-2583.1993.tb00076.x.

Shoji, Shinichiro, Corey M. Dambacher, Zahra Shajani, James R. Williamson, and Peter G. Schultz. 2011. 'Systematic Chromosomal Deletion of Bacterial Ribosomal Protein Genes'. *Journal of Molecular Biology* 413 (4): 751–61. https://doi.org/10.1016/j.jmb.2011.09.004.

Siehnel, R. J., and E. A. Morgan. 1985. 'Unbalanced RRNA Gene Dosage and Its Effects on RRNA and Ribosomal-Protein Synthesis'. *Journal of Bacteriology*, August. https://doi.org/10.1128/jb.163.2.476-486.1985.

References

Silva, Roshali T. de, Mohd F. Abdul-Halim, Dorothea A. Pittrich, Hannah J. Brown, Mechthild Pohlschroder, and Iain G. Duggin. 2021. 'Improved Growth and Morphological Plasticity of Haloferax Volcanii'. *Microbiology* 167 (2): 001012. https://doi.org/10.1099/mic.0.001012.

Sloan, Katherine E., Ahmed S. Warda, Sunny Sharma, Karl-Dieter Entian, Denis L. J. Lafontaine, and Markus T. Bohnsack. 2017. 'Tuning the Ribosome: The Influence of RRNA Modification on Eukaryotic Ribosome Biogenesis and Function'. *RNA Biology* 14 (9): 1138–52. https://doi.org/10.1080/15476286.2016.1259781.

Smola, Matthew J., and Kevin M. Weeks. 2018. 'In-Cell RNA Structure Probing with SHAPE-MaP'. *Nature Protocols* 13 (6): 1181–95. https://doi.org/10.1038/nprot.2018.010.

Sobell, H M. 1985. 'Actinomycin and DNA Transcription.' *Proceedings of the National Academy of Sciences* 82 (16): 5328–31. https://doi.org/10.1073/pnas.82.16.5328.

Spang, Anja, Laura Eme, Jimmy H. Saw, Eva F. Caceres, Katarzyna Zaremba-Niedzwiedzka, Jonathan Lombard, Lionel Guy, and Thijs J. G. Ettema. 2018. 'Asgard Archaea Are the Closest Prokaryotic Relatives of Eukaryotes'. *PLOS Genetics* 14 (3): e1007080. https://doi.org/10.1371/journal.pgen.1007080.

Spang, Anja, Jimmy H. Saw, Steffen L. Jørgensen, Katarzyna Zaremba-Niedzwiedzka, Joran Martijn, Anders E. Lind, Roel van Eijk, Christa Schleper, Lionel Guy, and Thijs J. G. Ettema. 2015. 'Complex Archaea That Bridge the Gap between Prokaryotes and Eukaryotes'. *Nature* 521 (7551): 173–79. https://doi.org/10.1038/nature14447.

Squires, C L, J Greenblatt, J Li, C Condon, and C L Squires. 1993. 'Ribosomal RNA Antitermination in Vitro: Requirement for Nus Factors and One or More Unidentified Cellular Components.' *Proceedings of the National Academy of Sciences of the United States of America* 90 (3): 970–74.

Srivastava, A. K., and D. Schlessinger. 1990. 'Mechanism and Regulation of Bacterial Ribosomal RNA Processing'. *Annual Review of Microbiology* 44: 105–29. https://doi.org/10.1146/annurev.mi.44.100190.000541.

Stanier, R. Y., and C. B. Van Niel. 1962. 'The Concept of a Bacterium'. *Archiv Fur Mikrobiologie* 42: 17–35. https://doi.org/10.1007/BF00425185.

Stark, M. J., R. L. Gourse, and A. E. Dahlberg. 1982. 'Site-Directed Mutagenesis of Ribosomal RNA. Analysis of Ribosomal RNA Deletion Mutants Using Maxicells'. *Journal of Molecular Biology* 159 (3): 417–39. https://doi.org/10.1016/0022-2836(82)90292-3.

Steffen, Kristan K, Mark A McCormick, Kim M Pham, Vivian L MacKay, Joe R Delaney, Christopher J Murakami, Matt Kaeberlein, and Brian K Kennedy. 2012. 'Ribosome Deficiency Protects Against ER Stress in Saccharomyces Cerevisiae'. *Genetics* 191 (1): 107–18. https://doi.org/10.1534/genetics.111.136549.

Stein, J L, T L Marsh, K Y Wu, H Shizuya, and E F DeLong. 1996. 'Characterization of Uncultivated Prokaryotes: Isolation and Analysis of a 40-Kilobase-Pair Genome Fragment from a Planktonic Marine Archaeon'. *Journal of Bacteriology* 178 (3): 591–99. https://doi.org/10.1128/jb.178.3.591-599.1996.

Stepanov, Victor G., and George E. Fox. 2021. 'Expansion Segments in Bacterial and Archaeal 5S Ribosomal RNAs'. *RNA* 27 (2): 133–50. https://doi.org/10.1261/rna.077123.120.

Stetter, K. O., H. König, and E. Stackebrandt. 1983. 'Pyrodictium Gen. Nov., a New Genus of Submarine Disc-Shaped Sulphur Reducing Archaebacteria Growing Optimally at 105°C'. *Systematic and Applied Microbiology* 4 (4): 535–51. https://doi.org/10.1016/S0723-2020(83)80011-3.

Stetter, Karl O. 1982. 'Ultrathin Mycelia-Forming Organisms from Submarine Volcanic Areas Having an Optimum Growth Temperature of 105 °C'. *Nature* 300 (5889): 258–60. https://doi.org/10.1038/300258a0.

———. 2006. 'History of Discovery of the First Hyperthermophiles'. *Extremophiles* 10 (5): 357–62. https://doi.org/10.1007/s00792-006-0012-7.

Stevenson, Bradley S., and Thomas M. Schmidt. 1998. 'Growth Rate-Dependent Accumulation of RNA from Plasmid-Borne RRNA Operons in Escherichia Coli'. *Journal of Bacteriology* 180 (7): 1970–72. https://doi.org/10.1128/JB.180.7.1970-1972.1998.

Sulthana, Shaheen, Georgeta N. Basturea, and Murray P. Deutscher. 2016. 'Elucidation of Pathways of Ribosomal RNA Degradation: An Essential Role for RNase E'. *RNA* 22 (8): 1163–71. https://doi.org/10.1261/rna.056275.116.

Sulthana, Shaheen, and Murray P. Deutscher. 2013. 'Multiple Exoribonucleases Catalyze Maturation of the 3′ Terminus of 16S Ribosomal RNA (RRNA)*'. *Journal of Biological Chemistry* 288 (18): 12574–79. https://doi.org/10.1074/jbc.C113.459172.

Sunagawa, Shinichi, Luis Pedro Coelho, Samuel Chaffron, Jens Roat Kultima, Karine Labadie, Guillem Salazar, Bardya Djahanschiri, et al. 2015. 'Structure and Function of the Global Ocean Microbiome'. *Science* 348 (6237): 1261359. https://doi.org/10.1126/science.1261359.

Symonová, Radka. 2019. 'Integrative RDNAomics—Importance of the Oldest Repetitive Fraction of the Eukaryote Genome'. *Genes* 10 (5): 345. https://doi.org/10.3390/genes10050345.

References

Takemata, Naomichi, and Stephen D. Bell. 2021. 'Multi-Scale Architecture of Archaeal Chromosomes'. *Molecular Cell* 81 (3): 473-487.e6. https://doi.org/10.1016/j.molcel.2020.12.001.

Takemata, Naomichi, Rachel Y. Samson, and Stephen D. Bell. 2019. 'Physical and Functional Compartmentalization of Archaeal Chromosomes'. *Cell* 179 (1): 165-179.e18. https://doi.org/10.1016/j.cell.2019.08.036.

Tamarit, Daniel, Eva F. Caceres, Mart Krupovic, Reindert Nijland, Laura Eme, Nicholas P. Robinson, and Thijs J. G. Ettema. 2022. 'A Closed Candidatus Odinarchaeum Chromosome Exposes Asgard Archaeal Viruses'. *Nature Microbiology* 7 (7): 948–52. https://doi.org/10.1038/s41564-022-01122-y.

Tang, Thean Hock, Timofey S. Rozhdestvensky, Béatrice Clouet d'Orval, Marie-Line Bortolin, Harald Huber, Bruno Charpentier, Christiane Branlant, Jean-Pierre Bachellerie, Jürgen Brosius, and Alexander Hüttenhofer. 2002. 'RNomics in Archaea Reveals a Further Link between Splicing of Archaeal Introns and RRNA Processing'. *Nucleic Acids Research* 30 (4): 921–30. https://doi.org/10.1093/nar/30.4.921.

Tenson, Tanel, and Alexander Mankin. 2006. 'Antibiotics and the Ribosome'. *Molecular Microbiology* 59 (6): 1664–77. https://doi.org/10.1111/j.1365-2958.2006.05063.x.

Thomm, Michael, and Winfried Hausner. 1993. 'Genes for Stable RNAs and Their Expression in Archaea'. In *Genetics and Molecular Biology of Anaerobic Bacteria*, edited by Madaleine Sebald, 36–53. Brock/Springer Series in Contemporary Bioscience. New York, NY: Springer. https://doi.org/10.1007/978-1-4615-7087-5_3.

Thompson, Katharine J., Jeff Zong, and George A. Mackie. 2015. 'Altering the Divalent Metal Ion Preference of RNase E'. *Journal of Bacteriology* 197 (3): 477–82. https://doi.org/10.1128/JB.02372-14.

Thompson, L D, and C J Daniels. 1990. 'Recognition of Exon-Intron Boundaries by the Halobacterium Volcanii TRNA Intron Endonuclease.' *Journal of Biological Chemistry* 265 (30): 18104–11. https://doi.org/10.1016/S0021-9258(17)44723-5.

Thomson, Emma, Sébastien Ferreira-Cerca, and Ed Hurt. 2013. 'Eukaryotic Ribosome Biogenesis at a Glance'. *Journal of Cell Science* 126 (21): 4815–21. https://doi.org/10.1242/jcs.111948.

Times, Richard D. Lyons; Special to The New York. 1977. 'Scientists Discover a Form of Life That Predates Higher Organisms'. *The New York Times*, 3 November 1977, sec. Archives. https://www.nytimes.com/1977/11/03/archives/scientists-discover-a-form-of-life-that-predates-higher-organisms.html.

Tirumalai, Madhan R., Jason T. Kaelber, Donghyun R. Park, Quyen Tran, and George E. Fox. 2020. 'Cryo-Electron Microscopy Visualization of a Large Insertion in the 5S Ribosomal RNA of the Extremely Halophilic Archaeon Halococcus Morrhuae'. *FEBS Open Bio* 10 (10): 1938–46. https://doi.org/10.1002/2211-5463.12962.

Tobiasson, Victor, Ieva Berzina, and Alexey Amunts. 2022. 'Structure of a Mitochondrial Ribosome with Fragmented RRNA in Complex with Membrane-Targeting Elements'. *Nature Communications* 13 (1): 6132. https://doi.org/10.1038/s41467-022-33582-5.

Torres-Machorro, Ana Lilia, Roberto Hernández, Ana María Cevallos, and Imelda López-Villaseñor. 2010. 'Ribosomal RNA Genes in Eukaryotic Microorganisms: Witnesses of Phylogeny?' *FEMS Microbiology Reviews* 34 (1): 59–86. https://doi.org/10.1111/j.1574-6976.2009.00196.x.

Trapman, J., J. Retèl, and R. J. Planta. 1975. 'Ribosomal Precursor Particles from Yeast'. *Experimental Cell Research* 90 (1): 95–104. https://doi.org/10.1016/0014-4827(75)90361-4.

Traub, P., and M. Nomura. 1968. 'Structure and Function of E. Coli Ribosomes. V. Reconstitution of Functionally Active 30S Ribosomal Particles from RNA and Proteins'. *Proceedings of the National Academy of Sciences of the United States of America* 59 (3): 777–84. https://doi.org/10.1073/pnas.59.3.777.

Tu, Daqi, Gregor Blaha, Peter B. Moore, and Thomas A. Steitz. 2005. 'Gene Replacement in Haloarcula Marismortui: Construction of a Strain with Two of Its Three Chromosomal RRNA Operons Deleted'. *Extremophiles* 9 (6): 427–35. https://doi.org/10.1007/s00792-005-0459-y.

Tu, Jenn, and Wolfram Zillig. 1982. 'Organization of RRNA Structural Genes in the Archaebacterium Thermoplasma Acidophilum'. *Nucleic Acids Research* 10 (22): 7231–45. https://doi.org/10.1093/nar/10.22.7231.

Tucker, Sarah, Alexa Vitins, and Craig S Pikaard. 2010. 'Nucleolar Dominance and Ribosomal RNA Gene Silencing'. *Current Opinion in Cell Biology*, Nucleus and gene expression, 22 (3): 351–56. https://doi.org/10.1016/j.ceb.2010.03.009.

Turkowyd, Bartosz, Sandra Schreiber, Julia Wörtz, Ella Shtifman Segal, Moshe Mevarech, Iain G. Duggin, Anita Marchfelder, and Ulrike Endesfelder. 2020. 'Establishing Live-Cell Single-Molecule Localization Microscopy Imaging and Single-Particle Tracking in the Archaeon Haloferax Volcanii'. *Frontiers in Microbiology* 11. https://www.frontiersin.org/articles/10.3389/fmicb.2020.583010.

References

Turowski, Tomasz W., Simon Lebaron, Elodie Zhang, Lauri Peil, Tatiana Dudnakova, Elisabeth Petfalski, Sander Granneman, Juri Rappsilber, and David Tollervey. 2014. 'Rio1 Mediates ATP-Dependent Final Maturation of 40S Ribosomal Subunits'. *Nucleic Acids Research* 42 (19): 12189–99. https://doi.org/10.1093/nar/gku878.

Tyagi, Sanjay, and Fred Russell Kramer. 1996. 'Molecular Beacons: Probes That Fluoresce upon Hybridization'. *Nature Biotechnology* 14 (3): 303–8. https://doi.org/10.1038/nbt0396-303.

Van Valen, Leigh M., and Virginia C. Maiorana. 1980. 'The Archaebacteria and Eukaryotic Origins'. *Nature* 287 (5779): 248–50. https://doi.org/10.1038/287248a0.

Vayssieres, Marlene. 2019. 'Etudes Structurales et Fonctionnelles de La Biogenèse de La Petite Sous-Unité Du Ribosome'. Paris, France.

Veith, Thomas, Roman Martin, Jan P. Wurm, Benjamin L. Weis, Elke Duchardt-Ferner, Charlotta Safferthal, Raoul Hennig, et al. 2012. 'Structural and Functional Analysis of the Archaeal Endonuclease Nob1'. *Nucleic Acids Research* 40 (7): 3259–74. https://doi.org/10.1093/nar/gkr1186.

Veldman, G. M., J. Klootwijk, H. van Heerikhuizen, and R. J. Planta. 1981. 'The Nucleotide Sequence of the Intergenic Region between the 5.8S and 26S RRNA Genes of the Yeast Ribosomal RNA Operon. Possible Implications for the Interaction between 5.8S and 26S RRNA and the Processing of the Primary Transcript'. *Nucleic Acids Research* 9 (19): 4847–62. https://doi.org/10.1093/nar/9.19.4847.

Venema, Jaap, Rudi J. Planta, and Hendrik A. Raué. 1998. 'In Vivo Mutational Analysis of Ribosomal RNA in Saccharomyces Cerevisiae'. In *Protein Synthesis: Methods and Protocols*, edited by Robin Martin, 257–70. Methods in Molecular Biology. Totowa, NJ: Springer New York. https://doi.org/10.1385/0-89603-397-X:257.

Venema, Jaap, and David Tollervey. 1995. 'Processing of Pre-Ribosomal RNA in Saccharomyces Cerevisiae'. *Yeast* 11 (16): 1629–50. https://doi.org/10.1002/yea.320111607.

Vercruysse, Maarten, Caroline Köhrer, Yang Shen, Sandra Proulx, Anubrata Ghosal, Bryan W. Davies, Uttam L. RajBhandary, and Graham C. Walker. 2016. 'Identification of YbeY-Protein Interactions Involved in 16S RRNA Maturation and Stress Regulation in Escherichia Coli'. *MBio* 7 (6): e01785-16. https://doi.org/10.1128/mBio.01785-16.

Villanueva, Laura, F. A. Bastiaan von Meijenfeldt, Alexander B. Westbye, Subhash Yadav, Ellen C. Hopmans, Bas E. Dutilh, and Jaap S. Sinninghe Damsté. 2021. 'Bridging the Membrane Lipid Divide: Bacteria of the FCB Group Superphylum Have the Potential to Synthesize Archaeal Ether Lipids'. *The ISME Journal* 15 (1): 168–82. https://doi.org/10.1038/s41396-020-00772-2.

Vossbrinck, C. R., J. V. Maddox, S. Friedman, B. A. Debrunner-Vossbrinck, and C. R. Woese. 1987. 'Ribosomal RNA Sequence Suggests Microsporidia Are Extremely Ancient Eukaryotes'. *Nature* 326 (6111): 411–14. https://doi.org/10.1038/326411a0.

Vossbrinck, Charles R., and Carl R. Woese. 1986. 'Eukaryotic Ribosomes That Lack a 5.8S RNA'. *Nature* 320 (6059): 287–88. https://doi.org/10.1038/320287a0.

Voulgaris, Justina, Sarah French, Richard L. Gourse, Craig Squires, and Catherine L. Squires. 1999. 'Increased Rrn Gene Dosage Causes Intermittent Transcription of RRNA in Escherichia Coli'. *Journal of Bacteriology* 181 (14): 4170–75. https://doi.org/10.1128/JB.181.14.4170-4175.1999.

Voulgaris, Justina, Dmitry Pokholok, W. Mike Holmes, Craig Squires, and Catherine L. Squires. 2000. 'The Feedback Response of Escherichia Coli RRNA Synthesis Is Not Identical to the Mechanism of Growth Rate-Dependent Control'. *Journal of Bacteriology* 182 (2): 536–39. https://doi.org/10.1128/JB.182.2.536-539.2000.

Wagner, Michaela, Marleen van Wolferen, Alexander Wagner, Kerstin Lassak, Benjamin Meyer, Julia Reimann, and Sonja-Verena Albers. 2012. 'Versatile Genetic Tool Box for the Crenarchaeote Sulfolobus Acidocaldarius'. *Frontiers in Microbiology* 3. https://www.frontiersin.org/articles/10.3389/fmicb.2012.00214.

Wai, Hobert H., Loan Vu, Melanie Oakes, and Masayasu Nomura. 2000. 'Complete Deletion of Yeast Chromosomal RDNA Repeats and Integration of a New RDNA Repeat: Use of RDNA Deletion Strains for Functional Analysis of RDNA Promoter Elements in Vivo'. *Nucleic Acids Research* 28 (18): 3524–34. https://doi.org/10.1093/nar/28.18.3524.

Walter, Justin D., Margaret Hunter, Melanie Cobb, Geoff Traeger, and P. Clint Spiegel. 2012. 'Thiostrepton Inhibits Stable 70S Ribosome Binding and Ribosome-Dependent GTPase Activation of Elongation Factor G and Elongation Factor 4'. *Nucleic Acids Research* 40 (1): 360–70. https://doi.org/10.1093/nar/gkr623.

Waltz, Florent, Thalia Salinas-Giegé, Robert Englmeier, Herrade Meichel, Heddy Soufari, Lauriane Kuhn, Stefan Pfeffer, et al. 2021. 'How to Build a Ribosome from RNA Fragments in Chlamydomonas Mitochondria'. *Nature Communications* 12 (1): 7176. https://doi.org/10.1038/s41467-021-27200-z.

References

Warner, J. R. 1989. ‘Synthesis of Ribosomes in Saccharomyces Cerevisiae’. *Microbiological Reviews* 53 (2): 256–71. https://doi.org/10.1128/mr.53.2.256-271.1989.

———. 1999. ‘The Economics of Ribosome Biosynthesis in Yeast’. *Trends in Biochemical Sciences* 24 (11): 437–40. https://doi.org/10.1016/s0968-0004(99)01460-7.

Waters, Elizabeth, Michael J. Hohn, Ivan Ahel, David E. Graham, Mark D. Adams, Mary Barnstead, Karen Y. Beeson, et al. 2003. ‘The Genome of Nanoarchaeum Equitans: Insights into Early Archaeal Evolution and Derived Parasitism’. *Proceedings of the National Academy of Sciences of the United States of America* 100 (22): 12984–88. https://doi.org/10.1073/pnas.1735403100.

Watson, Traci. 2019. ‘The Trickster Microbes That Are Shaking up the Tree of Life’. *Nature* 569 (7756): 322–24. https://doi.org/10.1038/d41586-019-01496-w.

Weixlbaumer, Albert, Felix Grünberger, Finn Werner, and Dina Grohmann. 2021. ‘Coupling of Transcription and Translation in Archaea: Cues From the Bacterial World’. *Frontiers in Microbiology* 12. https://www.frontiersin.org/articles/10.3389/fmicb.2021.661827.

Weng, Xiaoli, Christopher H. Bohrer, Kelsey Bettridge, Arvin Cesar Lagda, Cedric Cagliero, Ding Jun Jin, and Jie Xiao. 2019. ‘Spatial Organization of RNA Polymerase and Its Relationship with Transcription in Escherichia Coli’. *Proceedings of the National Academy of Sciences of the United States of America* 116 (40): 20115–23. https://doi.org/10.1073/pnas.1903968116.

Whittaker, R. H. 1969. ‘New Concepts of Kingdoms or Organisms. Evolutionary Relations Are Better Represented by New Classifications than by the Traditional Two Kingdoms’. *Science (New York, N.Y.)* 163 (3863): 150–60. https://doi.org/10.1126/science.163.3863.150.

Wickham, Hadley, Mara Averick, Jennifer Bryan, Winston Chang, Lucy D’Agostino McGowan, Romain François, Garrett Grolemund, et al. 2019. ‘Welcome to the Tidyverse’. *Journal of Open Source Software* 4 (43): 1686. https://doi.org/10.21105/joss.01686.

Williams, Bryony A. P., Robert P. Hirt, John M. Lucocq, and T. Martin Embley. 2002. ‘A Mitochondrial Remnant in the Microsporidian Trachipleistophora Hominis’. *Nature* 418 (6900): 865–69. https://doi.org/10.1038/nature00949.

Williams, Tom A., Peter G. Foster, Tom M. W. Nye, Cymon J. Cox, and T. Martin Embley. 2012. ‘A Congruent Phylogenomic Signal Places Eukaryotes within the Archaea’. *Proceedings of the Royal Society B: Biological Sciences* 279 (1749): 4870–79. https://doi.org/10.1098/rspb.2012.1795.

Williams, Tom A, Dominik Schrempf, Gergely J Szöllősi, Cymon J Cox, Peter G Foster, and T Martin Embley. 2021. ‘Inferring the Deep Past from Molecular Data’. *Genome Biology and Evolution* 13 (5): evab067. https://doi.org/10.1093/gbe/evab067.

Wilson, Daniel N. 2014. ‘Ribosome-Targeting Antibiotics and Mechanisms of Bacterial Resistance’. *Nature Reviews Microbiology* 12 (1): 35–48. https://doi.org/10.1038/nrmicro3155.

Witharana, Chamindri, Verena Roppelt, Günther Lochnit, Gabriele Klug, and Elena Evguenieva-Hackenberg. 2012. ‘Heterogeneous Complexes of the RNA Exosome in Sulfolobus Solfataricus’. *Biochimie* 94 (7): 1578–87. https://doi.org/10.1016/j.biochi.2012.03.026.

Woese, C R, O Kandler, and M L Wheelis. 1990. ‘Towards a Natural System of Organisms: Proposal for the Domains Archaea, Bacteria, and Eucarya.’ *Proceedings of the National Academy of Sciences of the United States of America* 87 (12): 4576–79.

Woese, C. R., L. J. Magrum, and G. E. Fox. 1978. ‘Archaebacteria’. *Journal of Molecular Evolution* 11 (3): 245–52. https://doi.org/10.1007/BF01734485.

Woese, Carl R., and George E. Fox. 1977. ‘Phylogenetic Structure of the Prokaryotic Domain: The Primary Kingdoms’. *Proceedings of the National Academy of Sciences* 74 (11): 5088–90. https://doi.org/10.1073/pnas.74.11.5088.

Woese, Carl R., and Ramesh Gupta. 1981. ‘Are Archaebacteria Merely Derived “Prokaryotes”?’ *Nature* 289 (5793): 95–96. https://doi.org/10.1038/289095a0.

Wolfe, Ralph S. 2014. ‘The Archaea: A Personal Overview of the Formative Years’. In *The Prokaryotes: Other Major Lineages of Bacteria and The Archaea*, edited by Eugene Rosenberg, Edward F. DeLong, Stephen Lory, Erko Stackebrandt, and Fabiano Thompson, 3–8. Berlin, Heidelberg: Springer. https://doi.org/10.1007/978-3-642-38954-2_391.

Woolford, John L, Jr., and Susan J Baserga. 2013. ‘Ribosome Biogenesis in the Yeast Saccharomyces Cerevisiae’. *Genetics* 195 (3): 643–81. https://doi.org/10.1534/genetics.113.153197.

Wurm, Jan Philip, Britta Meyer, Ute Bahr, Martin Held, Olga Frolow, Peter Kötter, Joachim W. Engels, et al. 2010. ‘The Ribosome Assembly Factor Nep1 Responsible for Bowen-Conradi Syndrome Is a Pseudouridine-N1-Specific Methyltransferase’. *Nucleic Acids Research* 38 (7): 2387–98. https://doi.org/10.1093/nar/gkp1189.

References

Xie, Ruize, Yinzhao Wang, Danyue Huang, Jialin Hou, Liuyang Li, Haining Hu, Xiaoxiao Zhao, and Fengping Wang. 2022. 'Expanding Asgard Members in the Domain of Archaea Sheds New Light on the Origin of Eukaryotes'. *Science China Life Sciences* 65 (4): 818–29. https://doi.org/10.1007/s11427-021-1969-6.

Yamagishi, Masahiro, Herman A. de Boer, and Masayasu Nomura. 1987. 'Feedback Regulation of RRNA Synthesis: A Mutational Alteration in the Anti-Shine-Dalgarno Region of the 16 S RRNA Gene Abolishes Regulation'. *Journal of Molecular Biology* 198 (3): 547–50. https://doi.org/10.1016/0022-2836(87)90299-3.

Yates, J. L., A. E. Arfsten, and M. Nomura. 1980. 'In Vitro Expression of Escherichia Coli Ribosomal Protein Genes: Autogenous Inhibition of Translation'. *Proceedings of the National Academy of Sciences of the United States of America* 77 (4): 1837–41. https://doi.org/10.1073/pnas.77.4.1837.

Yip, W. S. Vincent, Nicholas G. Vincent, and Susan J. Baserga. 2013. 'Ribonucleoproteins in Archaeal Pre-RRNA Processing and Modification'. *Archaea* 2013 (March): 614735. https://doi.org/10.1155/2013/614735.

Youngman, Elaine M., and Rachel Green. 2005. 'Affinity Purification of in Vivo-Assembled Ribosomes for in Vitro Biochemical Analysis'. *Methods (San Diego, Calif.)* 36 (3): 305–12. https://doi.org/10.1016/j.ymeth.2005.04.007.

Yuan, Cheng, Jikai Lei, James Cole, and Yanni Sun. 2015. 'Reconstructing 16S RRNA Genes in Metagenomic Data'. *Bioinformatics* 31 (12): i35–43. https://doi.org/10.1093/bioinformatics/btv231.

Yun, Ji-Hyun, Hye Seon Song, Seong Woon Roh, Mi-Ja Jung, Pil Soo Kim, and Jin-Woo Bae. 2015. 'Complete Genome Sequence of Haloarcula Sp. CBA1115 Isolated from Non-Purified Solar Salts'. *Marine Genomics* 23 (October): 19–21. https://doi.org/10.1016/j.margen.2015.03.012.

Yutin, Natalya, and Eugene V. Koonin. 2012. 'Archaeal Origin of Tubulin'. *Biology Direct* 7 (1): 10. https://doi.org/10.1186/1745-6150-7-10.

Yutin, Natalya, Pere Puigbò, Eugene V. Koonin, and Yuri I. Wolf. 2012. 'Phylogenomics of Prokaryotic Ribosomal Proteins'. *PloS One* 7 (5): e36972. https://doi.org/10.1371/journal.pone.0036972.

Zaremba-Niedzwiedzka, Katarzyna, Eva F. Caceres, Jimmy H. Saw, Disa Bäckström, Lina Juzokaite, Emmelien Vancaester, Kiley W. Seitz, et al. 2017. 'Asgard Archaea Illuminate the Origin of Eukaryotic Cellular Complexity'. *Nature* 541 (7637): 353–58. https://doi.org/10.1038/nature21031.

Zillig, Wolfram, Karl O. Stetter, and Davorin Janeković. 1979. 'DNA-Dependent RNA Polymerase from the Archaebacterium Sulfolobus Acidocaldarius'. *European Journal of Biochemistry* 96 (3): 597–604. https://doi.org/10.1111/j.1432-1033.1979.tb13074.x.

Zillig, Wolfram, Karl O. Stetter, and Michael Tobien. 1978. 'DNA-Dependent RNA Polymerase from Halobacterium Halobium'. *European Journal of Biochemistry* 91 (1): 193–99. https://doi.org/10.1111/j.1432-1033.1978.tb20951.x.

Zimmerman, Steven B. 2002. 'Toroidal Nucleoids in Escherichia Coli Exposed to Chloramphenicol'. *Journal of Structural Biology* 138 (3): 199–206. https://doi.org/10.1016/s1047-8477(02)00036-9.

11. List of Figures

List of Figures

12. List of Tables

13. List of Abbreviations

Table 21: Abbreviations

Abbreviation	Definition
bhb	bulge-helix-bulge
cDNA	complementary DNA
CPK	central pseudoknot
DPANN	Diapherotrites, Parvarchaeota, Aenigmarchaeota, Nanoarchaeota and Nanohaloarchaeota
ESP	eukaryotic signature protein
LSU	large ribosomal subunit
mRNA	messenger RNA
OD_{600nm}	optical density at 600 nm
ONT	Oxford Nanopore Technology
PAGE	polyacrylamide gel electrophoresis
PCR	polymerase chain reaction
pre-	precursor
RBF	ribosome biogenesis factor
RNA-FISH	RNA fluorescence *in situ* hybridization
RNAP	RNA-polymerase
r-protein	ribosomal protein
rDNA	ribosomal DNA
rRNA	ribosomal RNA
RT	reverse transcription
snoRNA	small nucleolar RNA
SSU	small ribosomal subunit
TACK	Thaumarchaeota, Aigarchaeota, Crenarchaeota and Korarchaeota
tRNA	transfer RNA

14. Supplemental Figures

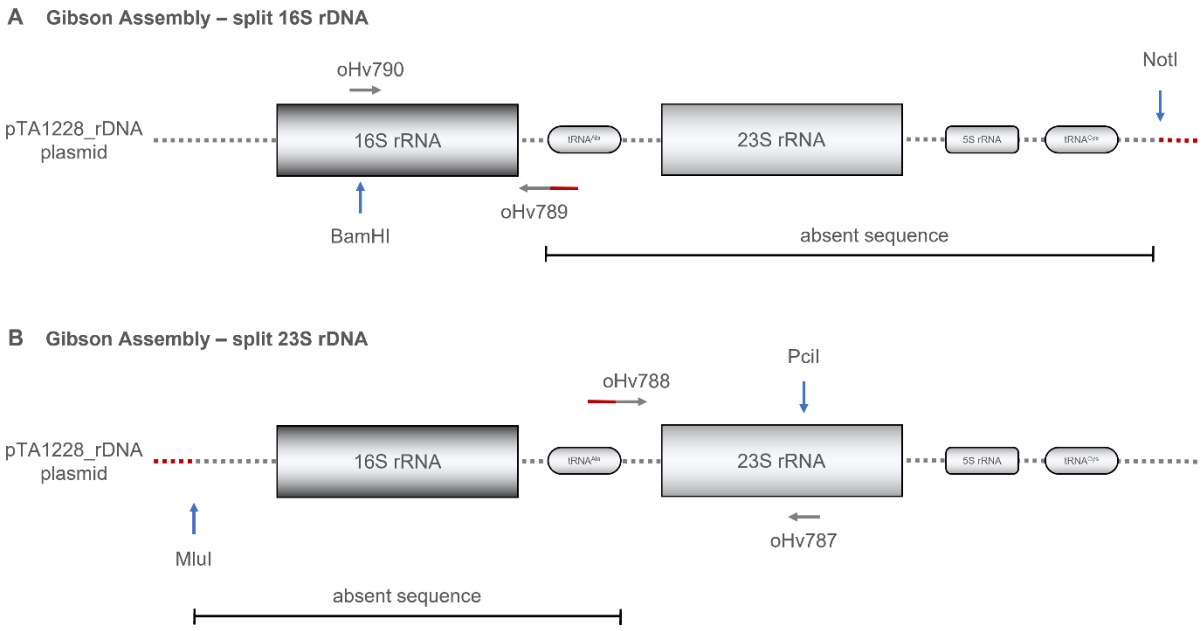

Figure S1: Cloning strategy for generation split rDNA constructs using Gibson Assembly. The outline how split 16S and 23S rDNA plasmids were designed is depicted. Split constructs were based on the pTA228_rDNA plasmid. Oligos used for PCR are indicated in grey, cleavage sites of restriction enzymes in blue. Gibson assembly requires overlapping sequences of vector and inserts, which are indicated in red.

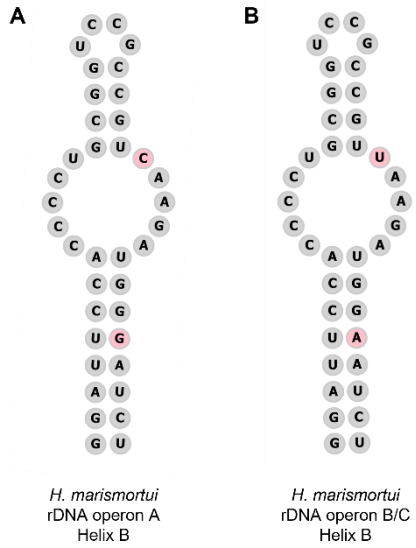

Figure S2: RNA secondary structures of *H. marismortui* helix B from rDNA operon A, B and C. The secondary RNA structure of helix B in all three operons of *H. marismortui* was predicted using ViennaRNA Web Services website (Gruber et al. 2008). The sequence differences of helix B from rDNA operon A (**A**) and from rDNA operon B and C (**B**) are highlighted in red. Note that helix B sequences from rDNA operon B and C are identical.

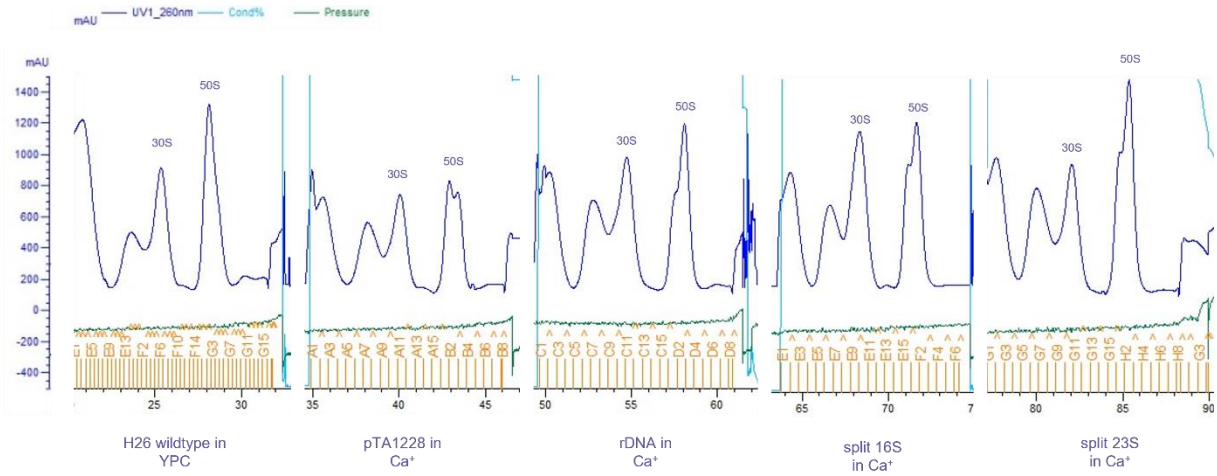

Figure S3: Sucrose gradient fractionation of rRNA gene dosage constructs. The UV_{260nm} profiles (dark blue line) from h26 wildtype (grown in YPC full medium), pTA1228 empty plasmid control, rDNA plasmid, split 16S rDNA and split 23S rDNA constructs are shown. The 30S and 50S peaks are annotated and were identified by Northern blot analysis of the respective fractions. Note that the ratio of the 30S and 50S peaks change in dependency of the respective transformed plasmid. This experiment was only performed once without replicates.

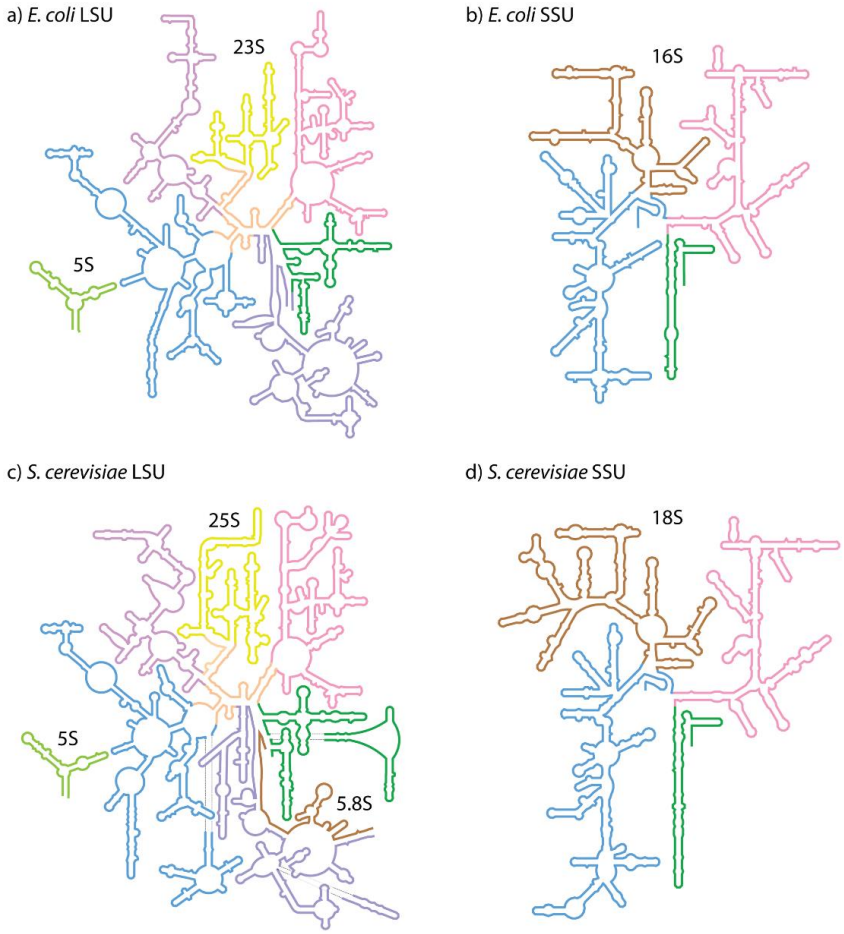

Figure S4: Secondary structures of ribosomal SSU and LSU RNAs in bacteria and eukaryotes. (**a** & **c**) LSU domains are colored in orange (0), purple (I), blue (II), magenta (III), yellow (IV), pink (V) and green (VI). In eukaryotes 5.8S, colored in brown, is reminiscent of prokaryotic 5' end of 23S. 5S is colored in light green. (**b** & **d**) SSU domains are colored in blue (5' domain), brown (central domain), pink (3' major) and green (3' minor). From Petrov et al. 2014.

15. Publications

2023

Manuscript in preparation:

Marlène Vayssières[#], Michael Jüttner[#], et al.,

'Structure-function analysis of an archaeal-specific ribonuclease involved in 16S pre-rRNA maturation'

[#] co-first authors

Felix Grünberger, Michael Jüttner, Robert Knüppel, Sébastien Ferreira-Cerca, and Dina Grohmann
'Nanopore-based RNA sequencing deciphers the formation, processing, and modification steps of rRNA intermediates in archaea '
RNA 2023 Aug;29(8):1255-1273.
https://doi.org/10.1261/rna.079636.123

2022

Michael Jüttner and Sébastien Ferreira-Cerca
'A Comparative Perspective on Ribosome Biogenesis: Unity and Diversity Across the Tree of Life'
Methods in *Molecular Biology (Clifton, N.J.)* 2533: 3–22.
https://doi.org/10.1007/978-1-0716-2501-9_1

Michael Jüttner and Sébastien Ferreira-Cerca
'Ribosomen Biogenese in Archaeen'
Biospektrum 28(5): 478-80.
https://doi.org/10.1007/s12268-022-1815-5

Michael Jüttner and Sébastien Ferreira-Cerca
'Looking through the Lens of the Ribosome Biogenesis Evolutionary History: Possible Implications for Archaeal Phylogeny and Eukaryogenesis'
Molecular Biology and Evolution 39 (4): msac054
https://doi.org/10.1093/molbev/msac054

2020

Michael Jüttner, Matthias Weiß, Nina Ostheimer, Corinna Reglin, Michael Kern, Robert Knüppel, and Sébastien Ferreira-Cerca
'A Versatile Cis-Acting Element Reporter System to Study the Function, Maturation and Stability of Ribosomal RNA Mutants in Archaea'

Nucleic Acids Research 48 (4): 2073–90
https://doi.org/10.1093/nar/gkz1156

2019

Knüppel, Robert, Martin Fenk, Michael Jüttner, and Sébastien Ferreira-Cerca
'In Vivo RNA Chemical Footprinting Analysis in Archaea'
Methods in Molecular Biology (Clifton, N.J.) 2106: 193–208
https://doi.org/10.1007/978-1-0716-0231-7_12.

16. Danksagung

Zuerst möchte ich mich bei meinem Betreuer und Doktorvater Sébastien bedanken. Als ich dein Labor damals als halbwegs frustrierter Masterstudent betreten habe, hatte ich nicht vor überhaupt eine Doktorarbeit zu machen, aber here we are. Mit deiner ansteckenden Art hast du es geschafft mich (und nicht nur mich) für die Laborarbeit, unsere biologischen Fragestellungen und Wissenschaft im Allgemeinen zu begeistern. Danke für die Motivation, Inspiration, Unterstützung, die Geduld, und das Vertrauen, das du mir immer entgegengebracht hast! Ich habe so viel von dir und mit dir lernen können (nicht nur über Ribosomen Biogenese in Archaeen) und hatte auch noch sehr viel Spaß dabei. Ich bin mir sicher, dass diese Doktorarbeit ohne dich nur halb so viel Freude bereitet hätte (und vermutlich wesentlich schlechter gelaufen wäre…). Du hattest immer ein offenes Ohr und warst für jede noch so lange Diskussion spätabends im Labor zu haben (Sorry Danni…). Auch wenn wir dich jetzt an Frankreich verloren haben, freut es mich sehr, dass du die Möglichkeit bekommen hast, noch viele nachfolgende Generationen ausbilden und deine Begeisterung für Wissenschaft übertragen kannst! Bleib so wie du bist (nur manchmal vielleicht etwas weniger arbeiten/mehr streiken): der beste Betreuer, den man sich wünschen kann! Alles Gute im neuen Job und vielen Dank für die fantastische Zeit!

Ich will mich außerdem bei Herbert Tschochner dafür bedanken, dass ich meine Doktorarbeit am Lehrstuhl für Biochemie machen durfte. Und natürlich für das Mentorat beim ausgiebigen Studium der steilen Wissenschaften wie der (Mehrseillängen-)Kletterei oder Skitouren gehen. Danke, fürs Zeigen der vielen Klettergebiete und das Erweitern meines Bergsport-Horizonts! Das Superschneehuhn in der Schweiz (und hoffentlich andere Touren) wartet noch darauf von uns bezwungen zu werden.

Ich möchte mich herzlich bei Anita Marchfelder und Brigitte Pertschy bedanken, dafür dass sie das Mentorat meiner Doktorarbeit übernommen haben und mich begleitet, beraten und unterstützt haben!

Vielen Dank an die Gutachter meiner Doktorarbeit und den Prüfungsausschuss bestehend aus Anita Marchfelder, Remco Sprangers, Winfried Hausner, Herbert Tschochner und Sébastien.

Bei Dina Grohmann möchte ich mich für die erfolgreiche Zusammenarbeit bedanken.

Danke auch an Kinga und Caro für euer unglaubliches Engagement und die sehr nette Zusammenarbeit!

Ich möchte mich herzlich bei Philipp Milkereit, meinem Pandemie-bedingten Büronachbarn, für die Unterstützung und sehr lehrreichen, spannenden Diskussionen über Wissenschaft(s-Politik) bedanken. Der gleiche gilt für Achim ‚supidupi' Griesenbeck, der immer ein offenes Ohr für alle hat und jedem mit Rat, Tat und unendlich viel positiver Energie zur Seite steht.

Unserer Sekretärin Frau Gabriele Meier und allen SFB-Sekretärinnen (Elli, Birgit, & Tanja) möchte ich für die reibungslose Organisation aller Verwaltungsangelegenheiten am Lehrstuhl danken.

Danksagung

Was wäre ein Lehrstuhl ohne die technische Assistenz? Vielen Dank an Gisela, Kristin und Tobi, dass ihr uns Doktoranden den Rücken freihaltet, immer hilfsbereit seid und jede zum tausendsten Mal gestellte Frage noch beantwortet. Danke an Gisela für die überragende Kuchen-Verpflegung, danke an Cpt. Tobi für die gemeinsamen Segel- und Kletterabendteuer und danke an Kristin für die vielen gegenseitigen Therapiegespräche!

Als nächstes möchte ich meinen vielen Leidensgenossen dafür danken, dass ihr diese Zeit so viel besser gemacht habt! Zuerst sei die „alte Garde" (Schmiddi, Christopher, Fabian und Robert) erwähnt, die ein fantastisches Miteinander vorgelebt und viele gemeinsame Aktivitäten angeregt hat. Dann danke ich Catha, Nicolas und Sebastian die mit mir zwei Krisen gleichzeitig (Doktorarbeit und Pandemie) durchgemacht haben! Danke für die lustige Zeit, die sportlichen Aktivitäten, immer unterhaltsamen und interessanten Gespräche, den Spaß auf der Konferenz in der Schweiz und die gegenseitige Unterstützung! Haltet noch gut durch und viel Erfolg auf den letzten Metern!

Ein besonderer Dank geht auch an alle ehemaligen Mitglieder der Archaea Gringos, vor allem Robert, Max, Tom und Jakob. Danke Robert für die super Zeit im Labor (die goldenen alten Zeiten, von denen alle sprechen), dass du mich mit ausgebildet hast (musikalisch, wissenschaftlich, kulturell, usw.) und ein guter Freund bist! Außerdem danke an meine drei Lieblingsstudenten, aus denen inzwischen auch gute Freunde geworden sind!

A special thanks goes also to my fellow archaea PhD colleague Nicolas, the best co-worker with incredibly positive energy!

Bei Felix will ich mich auch für die hervorragende und langjährige Zusammenarbeit innerhalb und außerhalb der Uni bedanken!

Dann will ich mich auch bei allen anderen Mitgliedern des Lehrstuhls für Biochemie III für die schöne Zeit bedanken. Vor allem bei Simon, der immer sehr hilfreich und kompetent beraten hat!

Thanks to all of the PhD students of the 'Meister' department! It was a great time with you guys (not only at the Kicker!).

Sicherheitshalber bedanke ich mich noch bei allen die ich jetzt vergessen habe (war keine Absicht!).

Zu guter Letzt will ich mich vor allem bei meiner lieben Familie für die jahrelange Unterstützung in allen Lebenslagen bedanken!!